



Universiteit
Leiden

The Netherlands

Endothelial plasticity in cardiovascular development : role of growth factors VEGF and PDGF

Akker, N.M.S. van den

Citation

Akker, N. M. S. van den. (2008, April 16). *Endothelial plasticity in cardiovascular development : role of growth factors VEGF and PDGF*. Retrieved from <https://hdl.handle.net/1887/12700>

Version: Corrected Publisher's Version

License: [Licence agreement concerning inclusion of doctoral thesis in the Institutional Repository of the University of Leiden](#)

Downloaded from: <https://hdl.handle.net/1887/12700>

Note: To cite this publication please use the final published version (if applicable).

Endothelial Plasticity in Cardiovascular Development

Role of Growth Factors VEGF and PDGF

Nynke M.S. van den Akker

Colofon

Cover Image: Front: “Antennae galaxies’ fertile marriage”; This Hubble image of the Antennae galaxies is the sharpest yet of this merging pair of galaxies. As the two galaxies smash together, thousands of millions of stars are born, mostly in groups and clusters of stars. The brightest and most compact of these are called super star clusters. Copyright: NASA, ESA, and B. Whitmore (Space Telescope Science Institute).
Back: Photo of a *Vegf120/120* mouse embryo of 11.5 days of development.

Endothelial Plasticity in Cardiovascular Development

Role of Growth Factors VEGF and PDGF

Nynke Margaretha Sophie van den Akker

Thesis Leiden University Medical Center

©2008 Nynke M.S. van den Akker

All rights reserved. No part of this book may be reproduced or transmitted, in any form or by any means, without written permission of the author.

ISBN 978-90-9022792-4

Printed by Gildeprint Drukkerijen B.V. - www.gildeprint.nl

Endothelial Plasticity in Cardiovascular Development

Role of Growth Factors VEGF and PDGF

Proefschrift

ter verkrijging van
de graad van Doctor aan de Universiteit Leiden,
op gezag van Rector Magnificus Prof. Mr. P.F. van der Heijden,
volgens besluit van het College voor Promoties
te verdedigen op woensdag 16 april 2008
klokke 16.15 uur

door

Nynke Margaretha Sophie van den Akker
geboren te Zoeterwoude
in 1981

Promotiecommissie

Promotores	Prof. Dr. A.C. Gittenberger-de Groot Prof Dr. R.E. Poelmann
Referent	Prof. Dr. J. Waltenberger (Universiteit Maastricht)
Overige leden	Prof. Dr. A. van der Laarse Prof. Dr. P. ten Dijke

The work presented in this thesis was carried out at the Department of Anatomy and Embryology of the Leiden University Medical Center and was supported by a grant of the Netherlands Heart Foundation (2001B057).

Financial support of the Netherlands Heart Foundation and of the “J.E. Jurriaanse Stichting” for the publication of this thesis is gratefully acknowledged.

Our hopes and expectations
Black holes and revelations

-From the song 'Starlight' by Muse-

Contents

Chapter 1	General Introduction	9
Part I:	<i>VEGF in Cardiovascular Development and Endothelial Differentiation</i>	37
Chapter 2	Tetralogy of Fallot and Alterations in VEGF and Notch-signaling in Mouse Embryos Solely Expressing the VEGF120 Isoform <i>Circulation Research 2007;100:842-849</i> Appendix	39 58
Chapter 3	Developmental Coronary Maturation is Disturbed by Aberrant Cardiac VEGF-expression and Notch-signaling <i>Cardiovascular Research, 2008, In Press</i> Appendix	65 86
Part II:	<i>PDGF in Cardiovascular Development</i>	91
Chapter 4	Platelet-Derived Growth Factors in the Developing Avian Heart and Maturing Coronary Vasculature <i>Developmental Dynamics 2005;233:1579-1588</i>	93
Chapter 5	PDGF-B-signaling is Important for Murine Cardiac Development; Its Role in Developing Atrioventricular Valves, Coronaries, and Cardiac Innervation <i>Developmental Dynamics, 2008, In Press</i>	111

Part III:	<i>Nuchal Translucency and Endothelial Differentiation</i>	131
Chapter 6	Abnormal Lymphatic Development in Trisomy 16 Mouse Embryos Precedes Nuchal Edema <i>Developmental Dynamics 2004;230:378-384</i>	133
Chapter 7	Jugular Lymphatic Maldevelopment in Turner Syndrome and Trisomy 21: Different Anomalies Leading to Nuchal Edema <i>Reproductive Sciences, 2008, In Press</i>	149
Chapter 8	Nuchal Edema and Venous-lymphatic Phenotype Disturbance in Human Fetuses and Mouse Embryos with Aneuploidy <i>Journal of the Society for Gynecological Investigation 2006;13:209-216</i>	167
Chapter 9	General Discussion	185
	List of Abbreviations	213
	Summary	216
	Samenvatting	219
	Curriculum Vitae	223
	Acknowledgements	224
	List of Publications	226

Chapter 1

General Introduction

General Introduction

The emergence of endothelial cells

The endothelium in vascular growth and function

VEGF-signaling in vascular development

Notch-signaling in endothelial differentiation

PDGF-signaling in arteriogenesis

Normal and abnormal cardiac and coronary development

Cushion development

Cardiac neural crest-development

Development of the second heart field

Epicardial and coronary development

Lymphatic development

Factors in (ab)normal lymphatic development

Prenatal diagnostic value of (ab)normal lymphatic performance

Chapter Outline

The emergence of endothelial cells

The cardiovascular system is the first recognizable and functional organ system within the developing embryo and correct development of this highly structured multicellular system is inevitable for both embryogenesis and later life in vertebrates¹⁻³. Its development starts with the formation of foci of hemangioblastic cells, called blood islands, in the extraembryonic yolk sac^{2;4;5}. Within these blood islands, differentiation between a hematopoietic and an angioblastic subpopulation takes place^{6;7} (Figure 1a-c). The hematopoietic cells will give rise to blood cells⁷, while the angioblasts, i.e. vascular endothelial cells (ECs) that do not yet contain a lumen⁶, provide primitive vessels through vasculogenesis. Individual angioblasts aggregate and elongate into cords. These cords will become organized into capillary-like networks upon which they will form a lumen⁸ (Figure 1c,d). In later stages, this vascular network will expand by proliferation and sprouting of ECs, a process which is called angiogenesis⁶ (Figure 1e). It has been a point of discussion whether the vasculature in the embryo proper is solely derived through angiogenesis from the (earlier arising) extra-embryonic vasculature, or whether vasculogenesis itself can also occur in the intra-embryonic tissue. Reagan^{8;9} demonstrated that the latter option is true.

Not surprisingly, the first vascular structures to arise through vasculogenesis within the embryo are the progenitors which will form the endocardium of the heart^{10;11}. These endocardial precursors develop in the bilateral cardiogenic plates within the splanchnic mesoderm, the primary heart field, together with the cells that will later form the cardiomyocytes (promyocardium)¹². These lateral plates fuse, starting at their midpoint and progressing bidirectionally until the primary heart tube is formed¹³. This cardiac tube has to loop and segment properly during organogenesis in order to form the final four-chambered heart¹ (further discussed below).

It has been debated which embryonic plate gives rise to the endothelial population, but it has become clear that all intra-embryonic ECs are mesoderm-derived⁵. However, correct spatiotemporal interaction of the endoderm with the developing vasculature is of vast importance¹⁴.

Next to the heart and systemic vasculature (i.e. arterial and venous), the lymphatic system emerges somewhat later during development. It primarily arises by budding from the venous system^{15;16} and partly through lymphvasculogenesis and lymphangiogenesis¹⁷ (further discussed below).

The endothelium in vascular growth and function

By means of the above mentioned processes of vasculogenesis and angiogenesis, the entire embryo becomes 'populated' with a vascular endothelial network that will remodel and differentiate in response to various spatiotemporal-specific cues (Figure 1). Discrimination between subpopulations of ECs can be made on basis of direction and forces of blood flow (arterial vs. venous), of large and small vessels and of the area of the embryo/body in which they reside¹⁸.

These subpopulations acquire a different morphology and differentiation (i.e. expression patterns) in order to execute their specific functions. For example, while ECs in the aorta, which mainly transports blood, are up to 1 μm thick, ECs in capillaries, where exchange of gas and nutrients with the surrounding tissue takes place, can even be thinner than 0.1 μm ¹⁹. Furthermore, in organs such as lung and heart the capillary endothelial layer is continuous and non-fenestrated, enabling only water and small solutes to pass the endothelium. In contrast, the endothelium in the liver sinusoids is discontinuous, containing large fenestrations (100 to 200 nm) and gaps within one cell, concomitant with its sieve function (for example mediating transport of medium-sized chylomicrons from blood to hepatocytes)^{19;20}. Next to these morphological differences, more and more knowledge on differential expression patterns is emerging²¹⁻²⁷. For example, arterial EC-specific expression of ephrinB2 in combination with venous EC-specific expression of EphB4 is essential for establishing a functional hierarchical vascular network²⁴.

Recruitment of pericytes and/or vascular smooth muscle cells (vSMCs) towards the endothelium and subsequent differentiation of these cells has to take place (Figure 1f) upon vasculogenesis and angiogenesis. Diversity between different vascular networks is obvious, as arteries develop a thick medial layer when compared with veins, while the capillary component only becomes (partly) covered by supporting pericytes⁶. When specifically the arterial medial differentiation is referred to, this is called arteriogenesis.

Interaction between different germ layers and cell types is essential for obtaining a correctly functioning and properly differentiated cardiovascular system. Communications between these layers, cells and cell types is orchestrated by countless proteins and signaling cascades, of which many have been extensively investigated. In this thesis, we narrow our scope down by focusing on three key (groups of) pathways being the VEGF, Notch and PDGF-families.

VEGF-signaling in vascular development

For over a decade, the role of vascular endothelial growth factor-A (VEGF-A or VEGF) in cardiovascular development has been appreciated due to its strong vasculogenic and angiogenic effects^{28;29}. Next to VEGF-A, three other mammalian VEGF-family members (VEGF-B, -C and -D), viral VEGFs (VEGF-E) and snake venom VEGFs

(VEGF-F) have been discovered. Three VEGF-receptors (VEGFR-1, -2 and -3) are known so far, of which VEGFR-1 and VEGFR-2 bind VEGF and are expressed by ECs. Besides VEGF, also VEGF-B and VEGF-F can bind to VEGFR-1, while VEGF-C, VEGF-D, VEGF-E and VEGF-F can bind to VEGFR-2 (reviewed in^{30;31}). VEGFR-3 can solely bind VEGF-C and VEGF-D. Additionally, Neuropilin-1 (NP-1), NP-2 and heparin/heparan-sulphate are identified to function as coreceptors^{32;33}. During embryogenesis, the importance of VEGF-signaling is underscored by the early embryonic lethality of *Vegf*^{+/-}, *Vegfr-1*^{-/-} and *Vegfr-2*^{-/-} mouse embryos, due to severe impairment of vascular development³⁴ (reviewed in^{30;35}). Most likely, during embryogenesis the angiogenic effect of VEGF is exerted through signaling via VEGFR-2, while VEGFR-1 is thought to play a role as a decoy receptor^{28;31;36;37}. During adulthood, however, VEGFR-1-mediated signaling, either ligand-independent or through binding of a VEGF-homologue called Placenta Growth Factor (PlGF), is involved in processes such as cancer metastasis and atherosclerosis^{37;38}.

The VEGF-gene consists of 8 exons and, due to alternative mRNA splicing, can give rise to at least 6 different isoforms. The biological range and effect differ per VEGF-isoform as exon 6 codes for the heparin/heparan sulphate binding region and exon 7 for the NP-binding domain³⁹. The three main isoforms in human are VEGF121, VEGF165 and VEGF189, which are represented by VEGF120, VEGF164 and VEGF188, respectively, in mouse. All VEGF-isoforms bind VEGFR-2, but the presence of a coreceptor during presentation of the ligand to its receptor is probably involved in regulating the specific effects of signaling^{40;41}. Only VEGF121 is unable to bind to heparin/heparan sulphate and to induce VEGFR-2/NP-1 complexes^{39;40;42}, suggesting different functional characteristics between isoforms.

VEGF-signaling already exerts its effect during the onset of the development of the endothelial precursor from the hemangioblast, as within the blood islands, all cells initially express VEGFR-2. This becomes restricted to the angioblastic subpopulation, whereas the hematopoietic cells lose their VEGFR-2-expression^{5;6}. Subsequently, stimulation of the VEGF-signaling pathway within ECs has mainly been described to result in endothelial migration, proliferation and branching morphogenesis (i.e. angiogenesis; reviewed in^{28;31;35}), but recent evidence also suggests a role for VEGF-signaling in EC-differentiation^{23;43}.

Another member of the VEGF-family, known for its role in lymphatic vascular development (discussed further below), is VEGF-C. When *Vegf-c* is knocked out in mice, its effect is embryonic lethal due to lack of lymphatic vessels and subsequent severe edema⁴⁴. VEGF-C mainly signals through VEGFR-3⁴⁵. VEGFR-3-signaling is likely to be not only involved in lymphatic, but also in cardiovascular development as *Vegfr-3*^{-/-} mouse embryos die from abnormal vascular development⁴⁶. Inversely, VEGFR-2 signaling is also important for lymphatic development by promoting lymphangiogenesis⁴⁷. This suggests that, although VEGFR-2 is mainly known for its role in angiogenesis and VEGFR-3 in lymphangiogenesis, during embryogenesis these two pathways are important for both processes.

In this thesis, the *Vegf120/120* mouse model that solely expresses the VEGF120-isoform, the murine homologue of human VEGF121, was used to further explore the effect of VEGF on cardiovascular development. These embryos lack the larger, heparin and NP-binding isoforms^{32;33} and show impaired angiogenesis^{42;48} and altered retinal arterio-venous differentiation⁴⁹ but also develop cardiac malformations such as Tetralogy of Fallot (TOF)⁵⁰ (a combination of a ventricular septal defect (VSD), stenosis of the pulmonary trunk (PT), dextropositioning of the ascending aorta and, secondarily, hyperplasia of the right ventricular myocardium⁵¹).

Notch-signaling in endothelial differentiation

The role of Notch-signaling pathways in many aspects of cardiovascular development is ultimately demonstrated by mouse mutants that develop congenital cardiac malformations and show severe abnormalities in remodeling of the primitive vasculature⁵²⁻⁵⁶. Notch-receptors (Notch-1, -2, -3 and -4) and their ligands (Jagged1, Jagged2 and Delta-like (Dll)1, Dll3 and Dll4⁵⁷) are all membrane-bound and as such considered to play a role in cell-cell interaction (reviewed in^{58;59}).

Upon activation of a Notch-receptor, its intracellular part is cleaved, thereby releasing the intracellular domain of Notch (NICD), which translocates to the nucleus. There, NICD binds to the DNA-binding protein CSL to act as a transcriptional coactivator⁵⁸. This complex upregulates the expression of primary target genes such as hairy and enhancer of split (Hes) and HES-related repressor protein (HERP or Hey)^{58;60}.

It has recently become clear that, next to cleavage of the Notch-receptor upon binding one of its ligands (forward signaling), Jagged1 and Dll1 can also be cleaved and induce an intracellular signaling pathway upon binding to Notch (reverse signaling) supporting their role in cell-cell interactions⁶¹⁻⁶⁴.

The Notch-specific transcription factors Hes and Hey can either activate or repress expression of many other genes involved in cardiovascular development (reviewed in⁶⁵). One example is the arterial EC-specific protein ephrinB2, which is upregulated by this pathway, while expression of its venous-specific receptor EphB4 is repressed, implying a role for Notch-signaling in differentiation of endothelial cells²³. Additionally, Notch-signaling has been reported in vSMC-development, although both stimulating and inhibiting roles have been described⁶⁶⁻⁶⁸. Our knowledge on Notch-signaling in (ab)normal vascular development has increased markedly within the last few years and many reviews have emerged^{57;58;69;70}.

A link between VEGF-signaling and the Notch-pathway has recently been reported⁷⁰. A negative feedback loop on VEGF-signaling is activated through Notch-signaling as activation of VEGFR-2 on specifically arterial endothelial cells induces Notch-1 and Notch-4^{43;71}, while Notch-signaling can downregulate VEGFR-2-expression.

PDGF-signaling in arteriogenesis

Another family of proteins involved in cardiovascular development is that of the platelet-derived growth factors (PDGFs). The vertebrate VEGF and PDGF-families are highly related and have presumably evolved from a common ancestor^{72;73}. To date, four PDGF-ligands, called PDGF-A, -B, and the more recently discovered PDGF-C and -D, have been defined both in mouse and human. The functional protein is a dimer and except for the PDGF-AB-heterodimer only homodimers can be formed⁷⁴. Two receptors are known, which can form either homo- or heterodimers upon ligand-binding: PDGFR- α , which can bind to PDGF-A, -B and -C, and PDGFR- β that is able to bind PDGF-B and -D. Mainly signaling through PDGFR- β has been implicated in vascular development and especially in arteriogenesis⁷². PDGF-B produced by ECs is a chemoattractant for mesenchymal PDGFR- β positive cells that support the vasculature by differentiating into vSMCs or pericytes during embryogenesis⁷⁵. This is supported by the phenotype of both (endothelial-specific) *Pdgf-b*^{-/-} and *Pdgfr- β* ^{-/-} mouse embryos, in which extreme loss of pericyte-covering of the vasculature leads to microaneurysmata⁷⁵⁻⁷⁸. Following arteriogenesis, PDGF-B-induced signaling remains essential for vascular homeostasis. Mice carrying a mutation in the *Pdgf-b* gene, causing a loss of its heparin-binding domain, show recruitment towards, but later on detachment from ECs of vSMCs^{79;80}. Additionally, recent data is pointing towards a role for PDGFR- β -signaling in vasculogenesis⁸¹ and angiogenesis⁸², implying a broader role of this pathway in vascular development than previously assumed.

PDGF-A/PDGFR- α -signaling has been reported to play a more important role in epithelial-mesenchymal than in endothelial-mesenchymal interactions^{72;73}. However, a role for PDGFR- α -signaling in vascular development seems likely as signaling of PDGFR- α by stimulation with PDGF-C stimulates angiogenesis⁸³. Additionally, fewer vSMCs are observed in the aortic arch of mouse embryos carrying a mutation that involves the *Pdgfr- α* gene (the so-called *Patch*-mutation).

To further explore the role of PDGF in cardiovascular development, several animal models were used in this thesis. First, pro-epicardial quail-chicken chimeras were generated to link protein expression patterns of PDGF-A and -B and their receptors PDGFR- α and - β to the derivatives of the pro-epicardial organ, the epicardium-derived cells (see further below)⁸⁴. Second, *Pdgf-b*^{-/-} and *Pdgfr- β* ^{-/-} mouse embryos were investigated. These two mouse models show highly overlapping abnormalities, such as unstable, leaky vessels and a dilated heart, VSDs and underdeveloped coronary arteries⁷⁶⁻⁷⁸. The cardiac and coronary anomalies in these models were analyzed thoroughly and explored for the relationship between the abnormalities and several cellular populations within the developing heart.

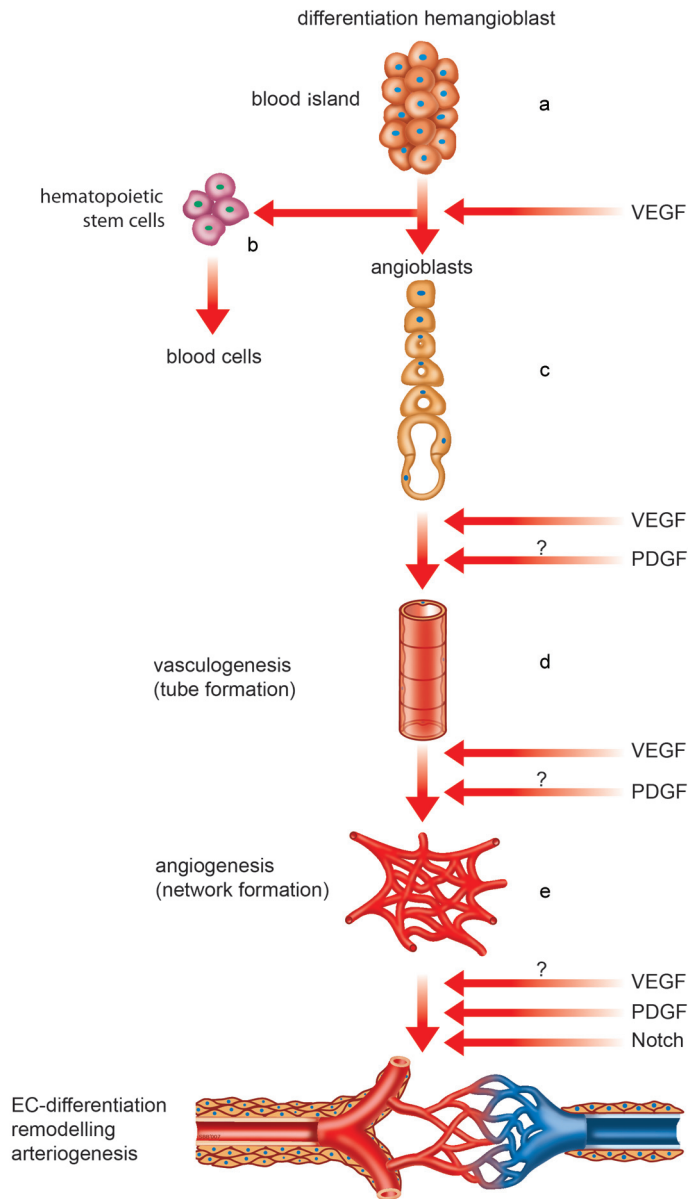


Figure 1. Vascular development. Foci of hemangioblastic cells are formed during early embryonic development (a). Hemangioblasts differentiate into hematopoietic stem cells, which subsequently give rise to blood cells (b), and into angioblasts (c). Angioblasts aggregate into cord-like structures (c) upon which they form a lumen by intercellular fusion of intracellular vacuolae (i.e. vasculogenesis; d). Through proliferation and outgrowth of endothelial cells, a process called angiogenesis, a primitive vascular network is formed (e). This network will undergo extensive differentiation and remodeling upon which a mature vascular bed is formed (f). In which processes VEGF, Notch and PDGF (might; indicated by a question mark) play a role is indicated at the right.

Normal and abnormal cardiac and coronary development

The primitive cardiac tube arises very early during development. This tube consists at first of an endocardial and a myocardial layer with cardiac jelly in between, and has to loop and segment properly to form the final four-chambered heart^{1;85-87}. During these processes, correct formation of the cardiac endocardial cushions as well as proper invasion into the heart of several cellular populations plays an important role (Figure 2). These populations are the cardiac neural crest cells (cNCCs), the anterior heart field (AHF) and posterior heart field (PHF), with the latter including the pro-epicardial organ (PEO). The AHF and PHF together are called the second heart field (SHF).

Cushion development

Cushion development is crucial for many cardiac developmental processes. The endocardial cells covering both the outflow tract (OFT) and atrioventricular cushions (Figure 2) undergo epithelial-to-mesenchymal transformation (EMT) to populate the acellular cardiac jelly of the primitive cushions⁸⁵. In OFT-development, proper cushion development is indispensable for OFT-septation and semilunar valve development^{85;88}. In these processes, the contribution of cNCCs is necessary^{89;90}.

Atrioventricular cushion development is important in septation of the left and right ventricle and the formation of mitral and tricuspid valves⁸⁸. In the transformation of atrioventricular cushions into valves, epicardium-derived cells (EPDCs; see also below) that migrate into the cushions are involved^{91;92}.

One of the factors involved in cushion-EMT is VEGF. Both stimulating^{93;94} and inhibiting^{95;96} effects of VEGF on endocardial cushion EMT have been described, leading to the hypothesis that VEGF has to be expressed within a 'physiologic window' to properly fulfill its role in cushion development⁹⁷. Additionally, VEGF-signaling can upregulate Notch-expression^{43;71} and, concomitantly, loss of VEGF-signaling leads to loss of notch1b-expression during cardiac valve formation in zebrafish⁹⁴. Subsequently, Notch-signaling has been described to stimulate endocardial cushion EMT^{98;99}, implicating a role for Notch-signaling in cushion development as well. This idea is further acknowledged by research demonstrating that both naturally occurring mutations in members of the VEGF and Notch-signaling pathway in humans, as well as mutations in these pathways in mouse models lead to the development of cardiac malformations likely related to abnormal cushion-development, such as valve dysfunction or to OFT-abnormalities as seen in Tetralogy of Fallot or Alagille-syndrome^{50;53;54;56-58;98;100-109}.

A role for PDGF in cushion-development might exist indirectly, as PDGFR- α -signaling is important in cNCC-development¹¹⁰ and PDGFR- β -signaling might play a role in EPDC-development and recruitment¹¹¹ (both discussed further below).

Cardiac neural crest-development

Cardiac NCCs contribute, besides their role in the development of the OFT-cushions as discussed above, to the remodeling of the aortic arch, to the ingrowth of coronary arteries into the aorta and to the development of the cardiac conduction system and cardiac innervation^{89;90;112-115}. Also, the cNCCs in the OFT modulate the local development of the AHF^{116;117} (Figure 2).

Mouse mutants lacking the VEGF164-isoform form OFT-malformations, but altered cNCC-migration or differentiation could not be detected⁵⁰. Therefore, VEGF-signaling is assumably not essential for cNCC-development, although minor modulating functions cannot be excluded⁵⁰.

In contrast, Notch-signaling has been implicated in various neural crest-related developmental processes¹¹⁸⁻¹²⁰. Its specific role in cNCC-development has to date only been linked to the vSMC-subpopulation of cNCCs contributing to the media of the aortic arch⁶⁷. Possible further roles of Notch-signaling in the performance of cNCCs have to be explored.

PDGFR-signaling, mainly through PDGFR- α , is crucial for accurate cNCC-performance by acting as a non-neuronal neural crest-cell growth/survival stimulus¹¹⁰. The role for PDGFR- β -signaling is less clear¹²¹.

Development of the second heart field

Both at the OFT and the inflow tract (IFT), a subpopulation of the dorsal mesoderm called the second heart field (SHF) contributes to the developing heart^{122;123} (Figure 2). Tracing studies have indicated that cells derived from the AHF (addition at the OFT) contribute to the myocardium of the interventricular septum (IVS), the right ventricle and the (right-ventricular) OFT^{122;124;125}. Its contribution specifically to the OFT-myocardium is also referred to as secondary heart field¹²⁶. Research regarding its contribution through the IFT (PHF) has more recently been performed^{123;127} and this population contributes most likely to the formation of the PEO (Mahtab et al, unpublished observations) as well as to the IFT-myocardium, including the cardiac pacemaking and possibly the conduction system¹²³.

Although a direct effect of VEGF-signaling in cardiomyocytes on their differentiation has never been described, it is supported by literature that cardiomyocytes can express VEGFR-2¹²⁸. Additionally, as hypoxia-induced VEGF-expression is important in development of the (AHF-derived) OFT-myocardium^{129;130}, the idea that VEGF-signaling plays a role in SHF-development is reasonable, although not fully proven. The same applies to Notch and PDGF-signaling in which an effect of these pathways on developing cardiomyocytes is known or expected^{131;132} and abnormalities that could be related to abnormal SHF-performance are present in mutant embryos^{55;56;133}.

Epicardial and coronary development

The PEO is, being regarded as a subset of the PHF, derived from the dorsal mesoderm (Figure 2). Instead of direct migration of cells through the dorsal mesocardium into the heart, protrusions of the PEO cross the pericardial cavity where they make contact with the bare myocardium of the heart tube. After contacting the myocardium of the atrioventricular canal, cells spread over the entire heart, forming the epicardium (Figure 2)¹³⁴. The epicardium, in turn, gives rise to the EPDCs via EMT^{91;135;136}. These EPDCs form the subepicardial layer and migrate into the heart. They give rise to the interstitial fibroblasts of the myocardial wall and as such are involved in the development of the fibrous heart skeleton. Also, they are implicated in proper development of the atrioventricular valves and Purkinje fibers and give rise to the vSMCs and adventitial fibroblasts of the coronary vessel wall (reviewed in^{137;138}).

The primitive coronary network develops by subepicardial vasculogenesis and subsequent angiogenesis^{84;139}. The origin of the ECs is a subject for debate, but most likely hemangioblasts brought to the heart through the PEO are its precursors^{84;139;140}. The primitive endothelial network becomes connected to the systemic circulation by ingrowth into the right atrium (venous pole)¹⁴¹ and into the aorta (arterial pole)^{114;142;143}. Upon ingrowth into the aorta, where the two definitive coronary orifices are formed, the coronary system remodels and arteriogenesis of the coronary arteries takes place by recruitment and local differentiation of EPDCs into vSMCs and adventitial fibroblasts¹³⁵. It should be noted that, in mouse, it has been described that not only the EPDC-population but also the cNCCs contribute to the medial wall of the proximal coronary arteries¹⁴⁴.

A role for VEGF-signaling in the development of the epicardium, EPDCs and the coronary system is expected. VEGF has been proposed to be involved in coronary vasculogenesis, angiogenesis¹⁴⁵ and also arteriogenesis¹⁴⁶. The latter effect could partially be attained through an effect of VEGF-signaling on epicardial development by means of induction of epicardial EMT¹³⁶.

For Notch-signaling in epicardial development, no direct evidence is currently available. However, this pathway is important in EMT of endocardial cushions (as discussed above). Therefore, it can be speculated that it might also play a role in epicardial EMT. Furthermore, as Notch-signaling is involved in many aspects of vascular development, a role in embryonic coronary development seems warranted.

Also PDGF-signaling, especially through PDGFR- β , is crucial for vascular development and it can therefore be assumed to be important in coronary development as well. Furthermore, as PDGF-B can induce epicardial EMT *in vitro*¹¹¹, it might have a broader effect on epicardium-related heart development.

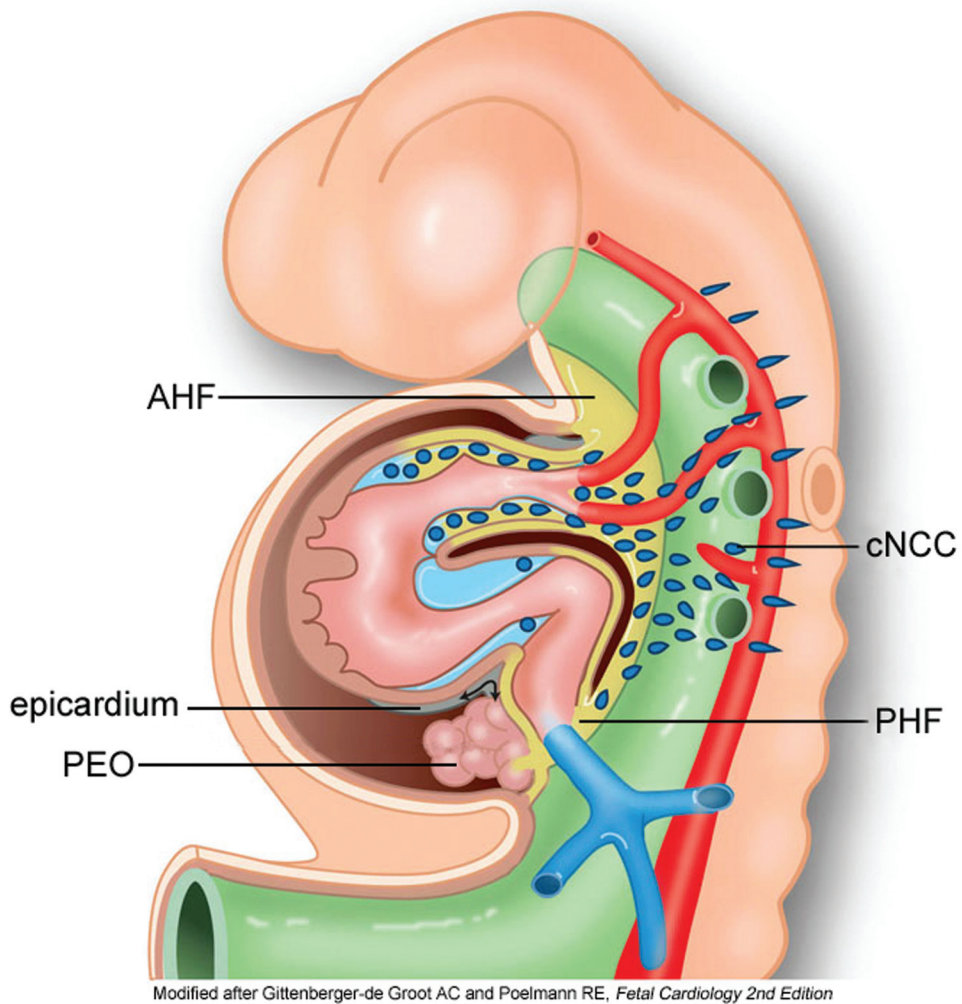


Figure 2. Cardiac development. Several developmental processes and cellular populations contribute to heart development. First, a primary heart tube is formed (indicated in brown). Also, endocardial cushions are formed (indicated in blue), both in the outflow tract area and in the atrioventricular canal. Cardiac neural crest cells (cNCC; dark blue cells) migrate from the neural tube into the outflow and inflow tract of the heart. Also, myocardium is added from the dorsal mesoderm to both the outflow and inflow tract of the heart, called the second heart field (indicated in yellow). The subset contributing to the outflow tract is called the anterior heart field (AHF) and that contributing to the inflow tract the posterior heart field (PHF). Finally, a subpopulation of the PHF, called the pro-epicardial organ (PEO), contributes to the heart by outgrowth of cells covering the heart tube (i.e. the epicardium).

Lymphatic development

The lymphatic system develops somewhat later during development compared with the blood vascular system. At first, in the nuchal region two structures called jugular lymphatic sacs (JLSs) appear, laterally from the internal jugular veins (IJVs). They arise secondarily from the venous system by fusion of buds emerging from the IJVs^{15;16} (Figure 3a-d). Sabin¹⁵ described that, in early phases, the JLSs and IJVs are connected through valves, suggesting a way of drainage of lymphatic fluid into the systemic circulation before a functional thoracic duct (i.e. the main adult lymphatic drainage site) is present. Apart from the neck region, this process occurs at several other locations within the embryo. Additionally, the thoracic duct develops from primordia derived from the intercostal veins¹⁴⁷ and eventually will drain into the left IJV¹⁵. When this contact is established, the JLSs will reorganize into lymph nodes¹⁵ (Figure 3e) as its drainage-function has become redundant.

Next to formation of lymphatic vessels out of veins, lymphvasculogenesis and lymphangiogenesis takes place¹⁷. The combination of these processes leads to the formation of a lymphatic network throughout the body. Interestingly, recent observations show that the lymphangioblasts forming cardiac lymphatic vessels do not reach the heart through the PEO (like the coronary blood vascular system), but most likely immigrate directly into the heart¹⁴⁰.

Factors in (ab)normal lymphatic development

Crucial for the selection of venous ECs within the IJV and for subsequent budding and lymphatic EC-differentiation is the homeobox transcription factor Prox-1¹⁴⁸⁻¹⁵². In addition, as mentioned before, both VEGFR-2 and, predominantly, VEGFR-3-signaling are key pathways in lymphangiogenesis and lymphatic EC (LEC)-differentiation^{31;45;153-155}. Two other proteins, LYVE-1 and Podoplanin, are both described to be specifically expressed by LECs and are therefore often used as LEC-markers. A role for LYVE-1 in lymphatic performance has been suggested because it can function as a receptor for hyaluronan, a high turn-over extracellular matrix glycosaminoglycan which, upon uptake by the lymphatic vasculature, is degraded in lymph nodes¹⁵⁶. Nevertheless, *Lyve-1*^{-/-} mice are viable and fertile and no developmental (lymphatic) abnormalities could be found¹⁵⁷. In contrast, *Hyaluronan*^{-/-} mouse embryos die in utero¹⁵⁸. A direct functional role for Podoplanin in lymphatic development has not been found⁴⁵, but when the *Podoplanin*-gene is knocked out, lymphatic malformations are observed at birth¹⁵⁹, supporting an important role in lymphatic development.

Prenatal diagnostic value of (ab)normal lymphatic performance

Prenatal screening for chromosomal abnormalities comprises a risk-calculation based on maternal age, maternal serum-levels of free β -human chorionic gonadotropin (β -hCG) and of pregnancy-associated plasma protein-A (PAPP-A) and finally on measurement of nuchal translucency (NT)^{160;161}. NT is an ultrasonographical measurement of fluid collection in the fetal neck and a NT >95th percentile is usually associated with chromosomal abnormalities (reviewed in¹⁶²). The etiology of both normal and increased NT is not fully understood, but an association with abnormalities in JLS-development has been made¹⁶³. In fetuses with increased NT, distension of the JLS together with massive nuchal edema (NE) was found upon post-mortem morphologic and microscopic examination¹⁶³. A common underlying cause for abnormal lymphatic development in aneuploid fetuses is, momentarily, still lacking.

To explore the relation between increased NT, NE and lymphatic development, we investigated both human fetuses and mouse embryos. A mouse model for human trisomy 21, or Down syndrome¹⁶⁴; the trisomy 16 mouse model¹⁶⁵ was used and compared with human trisomy 18, 21 and Turner syndrome fetuses¹⁶⁶.

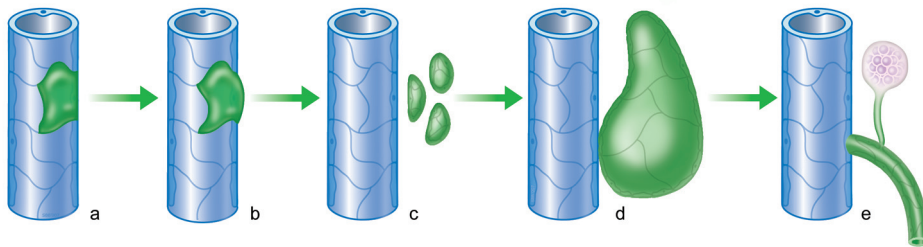


Figure 3. Lymphatic development. During embryonic development, lymphatic drainage transiently depends on the jugular lymphatic sacs (JLSs). These structures develop secondarily from the internal jugular veins (IJVs). First, endothelial cells of the lateral side of the IJVs gain lymphatic characteristics (green cells in a). These selected cells bud from the IJV (b) and form small vesicles (c) that fuse and as such form the JLSs (d). After formation of the definitive lymphatic drainage-site (the thoracic duct; green vessel in e), the JLSs reorganize into lymphatic nodes (purple cells in e).

Chapter Outline

Chapter 1 gives background information regarding blood vascular, cardiac and lymphatic development. The growth factors VEGF, Notch and PDGF are introduced and their possible role in cardiovascular development is defined.

Chapter 2 reports on the effect of sole expression of the small VEGF120-isoform on murine cardiogenesis. Our main focus is aberrant OFT-development, as OFT-abnormalities have earlier been described in this mouse model. Alterations in signaling pathways in right ventricular OFT cushion and myocardial structures are hypothesized to lead to the abnormalities observed.

Chapter 3 addresses the point that altered VEGF-signaling, due to a disturbed VEGF-gradient within the developing heart of *Vegf120/120* mouse embryos, will affect coronary development. To illustrate these effects, coronary patterning, endothelial differentiation and arteriogenesis are explored in normal and mutant mouse embryos.

Chapter 4 describes the cardiac expression patterns of PDGF-A, PDGF-B, PDGFR- α and PDGFR- β during the late phases of cardiac septation and coronary arteriogenesis in the avian embryo. The colocalization of these proteins with the (sub)epicardium and EPDCs is studied using pro-epicardial quail-chicken chimeras.

Chapter 5 shows the effect of PDGF-B/PDGFR- β signaling on heart development using both *Pdgf-b*^{-/-} and *Pdgfr- β* ^{-/-} mouse embryos. Cardiovascular malformations in these two models are examined at several time-points of development and related to cellular lineages involved in cardiogenesis.

Chapter 6 describes the different developmental stages of the JLSs in both murine trisomy 16 mouse embryos and wild-type littermates. The possible link between abnormal embryonic lymphatic and LEC-development and increased NT as seen in human fetuses with trisomy 21 is explored.

Chapter 7 provides a comparison between increased NT/NE in human fetuses with trisomy 21 and Turner syndrome. We speculate that the NE observed in both pathologies is similar but caused by different lymphatic developmental anomalies.

Chapter 8 concerns abnormal lymphatic development and increased NT/NE in the trisomy 16 mouse model in combination with observations in human aneuploid fetuses. Abnormalities in endothelial differentiation of the primitive lymphatic network are investigated as a possible underlying cause.

Chapter 9 provides a general discussion on the effects of VEGF and PDGF on (mal)development of the heart, on endothelial plasticity and on vascular maturation. The effect of aberrations in endothelial differentiation on the development of pathologies such as congenital coronary malformations or fetal NE is pointed out.

References

1. Gittenberger-De Groot AC, Bartelings MM, DeRuiter MC, Poelmann RE. Normal cardiac development. In: Ultrasound and the fetal heart. Wladimiroff JW, Pilu G, eds. 1996. The Parthenon Publishing Group, New York - London.
2. Wilting J, Christ B. Embryonic angiogenesis: a review. *Naturwissenschaften*. 1996;83:153-164.
3. Red-Horse K, Crawford Y, Shojaei F, Ferrara N. Endothelium-microenvironment interactions in the developing embryo and in the adult. *Dev Cell*. 2007;12:181-194.
4. Sabin FR. Preliminary note on the differentiation of angioblasts and the method by which they produce blood-vessels, blood-plasma and red blood-cells as seen in the living chick. 1917. *J Hematother Stem Cell Res*. 2002;11:5-7.
5. Ferguson JE, III, Kelley RW, Patterson C. Mechanisms of endothelial differentiation in embryonic vasculogenesis. *Arterioscler Thromb Vasc Biol*. 2005;25:2246-2254.
6. Risau W. Mechanisms of angiogenesis. *Nature*. 1997;386:671-674.
7. Eichmann A, Pardanaud L, Yuan L, Moyon D. Vasculogenesis and the search for the hemangioblast. *J Hematother Stem Cell Res*. 2002;11:207-214.
8. Drake CJ. Embryonic and adult vasculogenesis. *Birth Defects Res C Embryo Today*. 2003;69:73-82.
9. Reagan FP. Vascularization phenomenon in fragments of embryonic bodies completely isolated from yolk sac blastoderm. *Anat Rec*. 1915;9:329-341.
10. Drake CJ, Fleming PA. Vasculogenesis in the day 6.5 to 9.5 mouse embryo. *Blood*. 2000;95:1671-1679.
11. Dzierzak E. Ontogenic emergence of definitive hematopoietic stem cells. *Curr Opin Hematol*. 2003;10:229-234.
12. DeRuiter MC, Poelmann RE, VanderPlas-de V, I, Mentink MM, Gittenberger-De Groot AC. The development of the myocardium and endocardium in mouse embryos. Fusion of two heart tubes? *Anat Embryol (Berl)*. 1992;185:461-473.
13. Moreno-Rodriguez RA, Krug EL, Reyes L, Villavicencio L, Mjaatvedt CH, Markwald RR. Bidirectional fusion of the heart-forming fields in the developing chick embryo. *Dev Dyn*. 2006;235:191-202.
14. Dyer MA, Farrington SM, Mohn D, Munday JR, Baron MH. Indian hedgehog activates hematopoiesis and vasculogenesis and can respectify prospective neurectodermal cell fate in the mouse embryo. *Development*. 2001;128:1717-1730.
15. Sabin FR. The lymphatic system in human embryos, with a consideration of the morphology of the system as a whole. *Am J Anat*. 1909;9:43-91.
16. Oliver G. Lymphatic vasculature development. *Nat Rev Immunol*. 2004;4:35-45.
17. Wilting J, Aref Y, Huang R, Tomarev SI, Schweigerer L, Christ B, Valasek P, Papoutsis M. Dual origin of avian lymphatics. *Dev Biol*. 2006;292:165-173.

18. Cleaver O, Melton DA. Endothelial signaling during development. *Nat Med.* 2003;9:661-668.
19. Aird WC. Phenotypic heterogeneity of the endothelium: I. Structure, function, and mechanisms. *Circ Res.* 2007;100:158-173.
20. Aird WC. Phenotypic heterogeneity of the endothelium: II. Representative vascular beds. *Circ Res.* 2007;100:174-190.
21. Chi JT, Chang HY, Haraldsen G, Jahnsen FL, Troyanskaya OG, Chang DS, Wang Z, Rockson SG, van de RM, Botstein D, Brown PO. Endothelial cell diversity revealed by global expression profiling. *Proc Natl Acad Sci U S A.* 2003;100:10623-10628.
22. You LR, Lin FJ, Lee CT, Demayo FJ, Tsai MJ, Tsai SY. Suppression of Notch signalling by the COUP-TFII transcription factor regulates vein identity. *Nature.* 2005;435:98-104.
23. Hainaud P, Contreres JO, Villemain A, Liu LX, Plouet J, Tobelem G, Dupuy E. The Role of the Vascular Endothelial Growth Factor-Delta-like 4 Ligand/Notch4-Ephrin B2 Cascade in Tumor Vessel Remodeling and Endothelial Cell Functions. *Cancer Res.* 2006;66:8501-8510.
24. Hirashima M, Suda T. Differentiation of arterial and venous endothelial cells and vascular morphogenesis. *Endothelium.* 2006;13:137-145.
25. Amatschek S, Kriehuber E, Bauer W, Reininger B, Meraner P, Wolpl A, Schweifer N, Haslinger C, Stingl G, Maurer D. Blood and lymphatic endothelial cell-specific differentiation programs are stringently controlled by the tissue environment. *Blood.* 2007;109:4777-4785.
26. Yamashita JK. Differentiation of arterial, venous, and lymphatic endothelial cells from vascular progenitors. *Trends Cardiovasc Med.* 2007;17:59-63.
27. Yano K, Gale D, Massberg S, Cheruvu PK, Monahan-Earley R, Morgan ES, Haig D, von Andrian UH, Dvorak AM, Aird WC. Phenotypic heterogeneity is an evolutionarily conserved feature of the endothelium. *Blood.* 2007;109:613-615.
28. Ferrara N, Gerber HP, LeCouter J. The biology of VEGF and its receptors. *Nat Med.* 2003;9:669-676.
29. Carmeliet P. Mechanisms of angiogenesis and arteriogenesis. *Nat Med.* 2000;6:389-395.
30. Yla-Herttuala S, Rissanen TT, Vajanto I, Hartikainen J. Vascular endothelial growth factors: biology and current status of clinical applications in cardiovascular medicine. *J Am Coll Cardiol.* 2007;49:1015-1026.
31. Shibuya M, Claesson-Welsh L. Signal transduction by VEGF receptors in regulation of angiogenesis and lymphangiogenesis. *Exp Cell Res.* 2006;312:549-560.
32. Houck KA, Leung DW, Rowland AM, Winer J, Ferrara N. Dual regulation of vascular endothelial growth factor bioavailability by genetic and proteolytic mechanisms. *J Biol Chem.* 1992;267:26031-26037.
33. Soker S, Takashima S, Miao HQ, Neufeld G, Klagsbrun M. Neuropilin-1 is expressed by endothelial and tumor cells as an isoform-specific receptor for vascular endothelial growth factor. *Cell.* 1998;92:735-745.
34. Shalaby F, Ho J, Stanford WL, Fischer KD, Schuh AC, Schwartz L, Bernstein A, Rossant J. A requirement for Flk1 in primitive and definitive hematopoiesis and vasculogenesis. *Cell.* 1997;89:981-990.

35. Olsson AK, Dimberg A, Kreuger J, Claesson-Welsh L. VEGF receptor signalling - in control of vascular function. *Nat Rev Mol Cell Biol.* 2006;7:359-371.
36. Roberts DM, Kearney JB, Johnson JH, Rosenberg MP, Kumar R, Bautch VL. The vascular endothelial growth factor (VEGF) receptor Flt-1 (VEGFR-1) modulates Flk-1 (VEGFR-2) signaling during blood vessel formation. *Am J Pathol.* 2004;164:1531-1535.
37. Shibuya M. Vascular endothelial growth factor receptor-1 (VEGFR-1/Flt-1): a dual regulator for angiogenesis. *Angiogenesis.* 2006;9:225-230.
38. Autiero M, Waltenberger J, Communi D, Kranz A, Moons L, Lambrechts D, Kroll J, Plaisance S, De Mol M, Bono F, Kliche S, Fellbrich G, Ballmer-Hofer K, Maglione D, Mayr-Beyrle U, Dewerchin M, Dombrowski S, Stanimirovic D, Van Hummelen P, Dehio C, Hicklin DJ, Persico G, Herbert JM, Communi D, Shibuya M, Collen D, Conway EM, Carmeliet P. Role of PlGF in the intra- and intermolecular cross talk between the VEGF receptors Flt1 and Flk1. *Nat Med.* 2003;9:936-943.
39. Robinson CJ, Stringer SE. The splice variants of vascular endothelial growth factor (VEGF) and their receptors. *J Cell Sci.* 2001;114:853-865.
40. Pan Q, Chanthery Y, Wu Y, Rahtore N, Tong RK, Peale F, Bagri A, Tessier-Lavigne M, Koch AW, Watts RJ. Neuropilin-1 binds to VEGF121 and regulates endothelial cell migration and sprouting. *J Biol Chem.* 2007;282:24049-24056.
41. Shraga-Heled N, Kessler O, Prahst C, Kroll J, Augustin H, Neufeld G. Neuropilin-1 and neuropilin-2 enhance VEGF121 stimulated signal transduction by the VEGFR-2 receptor. *FASEB J.* 2007;21:915-926.
42. Carmeliet P, Ng YS, Nuyens D, Theilmeier G, Brusselmans K, Cornelissen I, Ehler E, Kakkar VV, Stalmans I, Mattot V, Perriard JC, Dewerchin M, Flameng W, Nagy A, Lupu F, Moons L, Collen D, D'Amore PA, Shima DT. Impaired myocardial angiogenesis and ischemic cardiomyopathy in mice lacking the vascular endothelial growth factor isoforms VEGF164 and VEGF188. *Nat Med.* 1999;5:495-502.
43. Lawson ND, Vogel AM, Weinstein BM. sonic hedgehog and vascular endothelial growth factor act upstream of the Notch pathway during arterial endothelial differentiation. *Dev Cell.* 2002;3:127-136.
44. Karkkainen MJ, Haiko P, Sainio K, Partanen J, Taipale J, Petrova TV, Jeltsch M, Jackson DG, Talikka M, Rauvala H, Betsholtz C, Alitalo K. Vascular endothelial growth factor C is required for sprouting of the first lymphatic vessels from embryonic veins. *Nat Immunol.* 2004;5:74-80.
45. Karkkainen MJ, Alitalo K. Lymphatic endothelial regulation, lymphoedema, and lymph node metastasis. *Semin Cell Dev Biol.* 2002;13:9-18.
46. Dumont DJ, Jussila L, Taipale J, Lymboussaki A, Mustonen T, Pajusola K, Breitman M, Alitalo K. Cardiovascular failure in mouse embryos deficient in VEGF receptor-3. *Science.* 1998;282:946-949.
47. Nagy JA, Vasile E, Feng D, Sundberg C, Brown LF, Detmar MJ, Lawitts JA, Benjamin L, Tan X, Manseau EJ, Dvorak AM, Dvorak HF. Vascular permeability factor/vascular endothelial growth factor induces lymphangiogenesis as well as angiogenesis. *J Exp Med.* 2002;196:1497-1506.
48. Maes C, Carmeliet P, Moermans K, Stockmans I, Smets N, Collen D, Bouillon R, Carmeliet G. Impaired angiogenesis and endochondral bone formation in mice lacking the vascular endothelial growth factor isoforms VEGF164 and VEGF188. *Mech Dev.* 2002;111:61-73.

49. Stalmans I, Ng YS, Rohan R, Fruttiger M, Bouche A, Yuce A, Fujisawa H, Hermans B, Shani M, Jansen S, Hicklin D, Anderson DJ, Gardiner T, Hammes HP, Moons L, Dewerchin M, Collen D, Carmeliet P, D'Amore PA. Arteriolar and venular patterning in retinas of mice selectively expressing VEGF isoforms. *J Clin Invest.* 2002;109:327-336.
50. Stalmans I, Lambrechts D, De Smet F, Jansen S, Wang J, Maity S, Kneer P, von der OM, Swillen A, Maes C, Gewillig M, Molin DG, Hellings P, Boetel T, Haardt M, Compennolle V, Dewerchin M, Plaisance S, Vlietinck R, Emanuel B, Gittenberger-De Groot AC, Scambler P, Morrow B, Driscoll DA, Moons L, Esguerra CV, Carmeliet G, Behn-Krappa A, Devriendt K, Collen D, Conway SJ, Carmeliet P. VEGF: a modifier of the del22q11 (DiGeorge) syndrome? *Nat Med.* 2003;9:173-182.
51. Bartelings MM, Gittenberger-De Groot AC. Morphogenetic considerations on congenital malformations of the outflow tract. Part 1: Common arterial trunk and tetralogy of Fallot. *Int J Cardiol.* 1991;32:213-230.
52. Krebs LT, Xue Y, Norton CR, Shutter JR, Maguire M, Sundberg JP, Gallahan D, Closson V, Kitajewski J, Callahan R, Smith GH, Stark KL, Gridley T. Notch signaling is essential for vascular morphogenesis in mice. *Genes Dev.* 2000;14:1343-1352.
53. McCright B, Lozier J, Gridley T. A mouse model of Alagille syndrome: Notch2 as a genetic modifier of Jag1 haploinsufficiency. *Development.* 2002;129:1075-1082.
54. Donovan J, Kordylewska A, Jan YN, Utset MF. Tetralogy of fallot and other congenital heart defects in Hey2 mutant mice. *Curr Biol.* 2002;12:1605-1610.
55. Fischer A, Schumacher N, Maier M, Sendtner M, Gessler M. The Notch target genes Hey1 and Hey2 are required for embryonic vascular development. *Genes Dev.* 2004;18:901-911.
56. Fischer A, Klamt B, Schumacher N, Glaeser C, Hansmann I, Fenge H, Gessler M. Phenotypic variability in Hey2 *-/-* mice and absence of HEY2 mutations in patients with congenital heart defects or Alagille syndrome. *Mamm Genome.* 2004;15:711-716.
57. Shawber CJ, Kitajewski J. Notch function in the vasculature: insights from zebrafish, mouse and man. *Bioessays.* 2004;26:225-234.
58. Iso T, Hamamori Y, Kedes L. Notch signaling in vascular development. *Arterioscler Thromb Vasc Biol.* 2003;23:543-553.
59. Lai EC. Notch signaling: control of cell communication and cell fate. *Development.* 2004;131:965-973.
60. Davis RL, Turner DL. Vertebrate hairy and Enhancer of split related proteins: transcriptional repressors regulating cellular differentiation and embryonic patterning. *Oncogene.* 2001;20:8342-8357.
61. Ascano JM, Beverly LJ, Capobianco AJ. The C-terminal PDZ-ligand of JAGGED1 is essential for cellular transformation. *J Biol Chem.* 2003;278:8771-8779.
62. Bland CE, Kimberly P, Rand MD. Notch-induced proteolysis and nuclear localization of the Delta ligand. *J Biol Chem.* 2003;278:13607-13610.
63. Kolev V, Kacer D, Trifonova R, Small D, Duarte M, Soldi R, Graziani I, Sideleva O, Larman B, Maciag T, Prudovsky I. The intracellular domain of Notch ligand Delta1 induces cell growth arrest. *FEBS Lett.* 2005;579:5798-5802.

64. Hiratochi M, Nagase H, Kuramochi Y, Koh CS, Ohkawara T, Nakayama K. The Delta intracellular domain mediates TGF-beta/Activin signaling through binding to Smads and has an important bi-directional function in the Notch-Delta signaling pathway. *Nucleic Acids Res.* 2007;35:912-922.
65. Iso T, Kedes L, Hamamori Y. HES and HERP families: multiple effectors of the Notch signaling pathway. *J Cell Physiol.* 2003;194:237-255.
66. Limbourg A, Ploom M, Elligsen D, Sorensen I, Ziegelhoeffer T, Gossler A, Drexler H, Limbourg FP. Notch ligand Delta-like 1 is essential for postnatal arteriogenesis. *Circ Res.* 2007;100:363-371.
67. High FA, Zhang M, Proweller A, Tu L, Parmacek MS, Pear WS, Epstein JA. An essential role for Notch in neural crest during cardiovascular development and smooth muscle differentiation. *J Clin Invest.* 2007;117:353-363.
68. Morrow D, Scheller A, Birney YA, Sweeney C, Guha S, Cummins PM, Murphy R, Walls D, Redmond EM, Cahill PA. Notch-mediated CBF-1/RBP-J{kappa}-dependent regulation of human vascular smooth muscle cell phenotype in vitro. *Am J Physiol Cell Physiol.* 2005;289:C1188-C1196.
69. Anderson LM, Gibbons GH. Notch: a mastermind of vascular morphogenesis. *J Clin Invest.* 2007;117:299-302.
70. Hofmann JJ, Iruela-Arispe ML. Notch signaling in blood vessels - Who is talking to whom about what? *Circ Res.* 2007;100:1556-1568.
71. Liu ZJ, Shirakawa T, Li Y, Soma A, Oka M, Dotto GP, Fairman RM, Velazquez OC, Herlyn M. Regulation of Notch1 and Dll4 by vascular endothelial growth factor in arterial endothelial cells: implications for modulating arteriogenesis and angiogenesis. *Mol Cell Biol.* 2003;23:14-25.
72. Betsholtz C. Biology of platelet-derived growth factors in development. *Birth Defects Res C Embryo Today.* 2003;69:272-285.
73. Hoch RV, Soriano P. Roles of PDGF in animal development. *Development.* 2003;130:4769-4784.
74. Heldin CH, Eriksson U, Ostman A. New members of the platelet-derived growth factor family of mitogens. *Arch Biochem Biophys.* 2002;398:284-290.
75. Lindahl P, Johansson BR, Leveen P, Betsholtz C. Pericyte loss and microaneurysm formation in PDGF-B-deficient mice. *Science.* 1997;277:242-245.
76. Leveen P, Pekny M, Gebre-Medhin S, Swolin B, Larsson E, Betsholtz C. Mice deficient for PDGF B show renal, cardiovascular, and hematological abnormalities. *Genes Dev.* 1994;8:1875-1887.
77. Hellstrom M, Kalen M, Lindahl P, Abramsson A, Betsholtz C. Role of PDGF-B and PDGFR-beta in recruitment of vascular smooth muscle cells and pericytes during embryonic blood vessel formation in the mouse. *Development.* 1999;126:3047-3055.
78. Bjarnegard M, Enge M, Norlin J, Gustafsdottir S, Fredriksson S, Abramsson A, Takemoto M, Gustafsson E, Fassler R, Betsholtz C. Endothelium-specific ablation of PDGFB leads to pericyte loss and glomerular, cardiac and placental abnormalities. *Development.* 2004;131:1847-1857.
79. Lindblom P, Gerhardt H, Liebner S, Abramsson A, Enge M, Hellstrom M, Backstrom G, Fredriksson S, Landegren U, Nystrom HC, Bergstrom G, Dejana E, Ostman A, Lindahl P, Betsholtz C. Endothelial PDGF-B retention is required for proper investment of pericytes in the microvessel wall. *Genes Dev.* 2003;17:1835-1840.

80. Nystrom HC, Lindblom P, Wickman A, Andersson I, Norlin J, Faldt J, Lindahl P, Skott O, Bjarnegard M, Fitzgerald SM, Caidahl K, Gan LM, Betsholtz C, Bergstrom G. Platelet-derived growth factor B retention is essential for development of normal structure and function of conduit vessels and capillaries. *Cardiovasc Res.* 2006;71:557-565.
81. Rolny C, Nilsson I, Magnusson P, Armulik A, Jakobsson L, Wentzel P, Lindblom P, Norlin J, Betsholtz C, Heuchel R, Welsh M, Claesson-Welsh L. Platelet-derived growth factor receptor-beta promotes early endothelial cell differentiation. *Blood.* 2006;108:1877-1886.
82. Ulrica MP, Looman C, Ahgren A, Wu Y, Claesson-Welsh L, Heuchel RL. Platelet-Derived Growth Factor Receptor- β Constitutive Activity Promotes Angiogenesis In Vivo and In Vitro. *Arterioscler Thromb Vasc Biol.* 2007.
83. Cao R, Brakenhielm E, Li X, Pietras K, Widenfalk J, Ostman A, Eriksson U, Cao Y. Angiogenesis stimulated by PDGF-CC, a novel member in the PDGF family, involves activation of PDGFR-alpha and -alpha receptors. *FASEB J.* 2002;16:1575-1583.
84. Poelmann RE, GittenbergerdeGroot AC, Mentink MMT, Bokenkamp R, Hogers B. Development of the Cardiac Coronary Vascular Endothelium, Studied with Antiendothelial Antibodies, in Chicken-Quail Chimeras. *Circ Res.* 1993;73:559-568.
85. Markwald RR, Fitzharris TP, Manasek FJ. Structural development of endocardial cushions. *Am J Anat.* 1977;148:85-119.
86. Markwald R, Eisenberg C, Eisenberg L, Trusk T, Sugi Y. Epithelial-mesenchymal transformations in early avian heart development. *Acta Anat (Basel).* 1996;156:173-186.
87. Gittenberger-De Groot AC, Bartelings MM, DeRuiter MC, Poelmann RE. Basics of cardiac development for the understanding of congenital heart malformations. *Pediatr Res.* 2005;57:169-176.
88. Eisenberg LM, Markwald RR. Molecular regulation of atrioventricular valvuloseptal morphogenesis. *Circ Res.* 1995;77:1-6.
89. Kirby ML, Gale TF, Stewart DE. Neural crest cells contribute to normal aorticopulmonary septation. *Science.* 1983;220:1059-1061.
90. Poelmann RE, Mikawa T, Gittenberger-De Groot AC. Neural crest cells in outflow tract septation of the embryonic chicken heart: Differentiation and apoptosis. *Dev Dyn.* 1998;212:373-384.
91. Gittenberger-De Groot AC, Vrancken Peeters MP, Mentink MM, Gourdie RG, Poelmann RE. Epicardium-derived cells contribute a novel population to the myocardial wall and the atrioventricular cushions. *Circ Res.* 1998;82:1043-1052.
92. Gittenberger-De Groot AC, Vrancken Peeters MP, Bergwerff M, Mentink MM, Poelmann RE. Epicardial outgrowth inhibition leads to compensatory mesothelial outflow tract collar and abnormal cardiac septation and coronary formation. *Circ Res.* 2000;87:969-971.
93. Enciso JM, Gratzinger D, Camenisch TD, Canosa S, Pinter E, Madri JA. Elevated glucose inhibits VEGF-A-mediated endocardial cushion formation: modulation by PECAM-1 and MMP-2. *J Cell Biol.* 2003;160:605-615.
94. Lee YM, Cope JJ, Ackermann GE, Goishi K, Armstrong EJ, Paw BH, Bischoff J. Vascular endothelial growth factor receptor signaling is required for cardiac valve formation in zebrafish. *Dev Dyn.* 2006;235:29-37.

95. Dor Y, Camenisch TD, Itin A, Fishman GI, McDonald JA, Carmeliet P, Keshet E. A novel role for VEGF in endocardial cushion formation and its potential contribution to congenital heart defects. *Development*. 2001;128:1531-1538.
96. Dor Y, Klewer SE, McDonald JA, Keshet E, Camenisch TD. VEGF modulates early heart valve formation. *Anat Rec A Discov Mol Cell Evol Biol*. 2003;271:202-208.
97. Armstrong EJ, Bischoff J. Heart valve development: endothelial cell signaling and differentiation. *Circ Res*. 2004;95:459-470.
98. Timmerman LA, Grego-Bessa J, Raya A, Bertran E, Perez-Pomares JM, Diez J, Aranda S, Palomo S, McCormick F, Izpisua-Belmonte JC, de la Pompa JL. Notch promotes epithelial-mesenchymal transition during cardiac development and oncogenic transformation. *Genes Dev*. 2004;18:99-115.
99. Noseda M, McLean G, Niessen K, Chang L, Pollet I, Montpetit R, Shahidi R, Dorovini-Zis K, Li L, Beckstead B, Durand RE, Hoodless PA, Karsan A. Notch activation results in phenotypic and functional changes consistent with endothelial-to-mesenchymal transformation. *Circ Res*. 2004;94:910-917.
100. Kitsukawa T, Shimono A, Kawakami A, Kondoh H, Fujisawa H. Overexpression of a membrane protein, neuropilin, in chimeric mice causes anomalies in the cardiovascular system, nervous system and limbs. *Development*. 1995;121:4309-4318.
101. Kawasaki T, Kitsukawa T, Bekku Y, Matsuda Y, Sanbo M, Yagi T, Fujisawa H. A requirement for neuropilin-1 in embryonic vessel formation. *Development*. 1999;126:4895-4902.
102. Miquerol L, Langille BL, Nagy A. Embryonic development is disrupted by modest increases in vascular endothelial growth factor gene expression. *Development*. 2000;127:3941-3946.
103. Eldadah ZA, Hamosh A, Biery NJ, Montgomery RA, Duke M, Elkins R, Dietz HC. Familial Tetralogy of Fallot caused by mutation in the jagged1 gene. *Hum Mol Genet*. 2001;10:163-169.
104. Le Caignec C, Lefevre M, Schott JJ, Chaventre A, Gayet M, Calais C, Moisan JP. Familial deafness, congenital heart defects, and posterior embryotoxon caused by cysteine substitution in the first epidermal-growth-factor-like domain of jagged 1. *Am J Hum Genet*. 2002;71:180-186.
105. McElhinney DB, Krantz ID, Bason L, Piccoli DA, Emerick KM, Spinner NB, Goldmuntz E. Analysis of cardiovascular phenotype and genotype-phenotype correlation in individuals with a JAG1 mutation and/or Alagille syndrome. *Circulation*. 2002;106:2567-2574.
106. Lu F, Morrissette JJ, Spinner NB. Conditional JAG1 mutation shows the developing heart is more sensitive than developing liver to JAG1 dosage. *Am J Hum Genet*. 2003;72:1065-1070.
107. Kokubo H, Miyagawa-Tomita S, Tomimatsu H, Nakashima Y, Nakazawa M, Saga Y, Johnson RL. Targeted disruption of *hesr2* results in atrioventricular valve anomalies that lead to heart dysfunction. *Circ Res*. 2004;95:540-547.
108. Lambrechts D, Devriendt K, Driscoll DA, Goldmuntz E, Gewillig M, Vlietinck R, Collen D, Carmeliet P. Low expression VEGF haplotype increases the risk for tetralogy of Fallot: a family based association study. *J Med Genet*. 2005;42:519-522.
109. Washington S, I, Byrd NA, Abu-Issa R, Goddeeris MM, Anderson R, Morris J, Yamamura K, Klingensmith J, Meyers EN. Sonic hedgehog is required for cardiac outflow tract and neural crest cell development. *Dev Biol*. 2005;283:357-372.

110. Morrison-Graham K, Schatteman GC, Bork T, Bowen-Pope DF, Weston JA. A PDGF receptor mutation in the mouse (Patch) perturbs the development of a non-neuronal subset of neural crest-derived cells. *Development*. 1992;115:133-142.
111. Lu J, Landerholm TE, Wei JS, Dong XR, Wu SP, Liu X, Nagata K, Inagaki M, Majesky MW. Coronary smooth muscle differentiation from proepicardial cells requires rhoA-mediated actin reorganization and p160 rho-kinase activity. *Dev Biol*. 2001;240:404-418.
112. Poelmann RE, Jongbloed MR, Molin DG, Fekkes ML, Wang Z, Fishman GI, Doetschman T, Azhar M, Gittenberger-De Groot AC. The neural crest is contiguous with the cardiac conduction system in the mouse embryo: a role in induction? *Anat Embryol (Berl)*. 2004;208:389-393.
113. Poelmann RE, Gittenberger-De Groot AC. A subpopulation of apoptosis-prone cardiac neural crest cells targets to the venous pole: Multiple functions in heart development. *Dev Biol*. 1999;207:271-286.
114. Gittenberger-De Groot AC, Bartelings MM, Bogers AJ, Boot MJ, Poelmann RE. The embryology of the common arterial trunk. *Progress in Pediatric Cardiology*. 2002;15:1-8.
115. Epstein JA, Li J, Lang D, Chen F, Brown CB, Jin F, Lu MM, Thomas M, Liu E, Wessels A, Lo CW. Migration of cardiac neural crest cells in Splotch embryos. *Development*. 2000;127:1869-1878.
116. Yelbuz TM, Waldo KL, Kumiski DH, Stadt HA, Wolfe RR, Leatherbury L, Kirby ML. Shortened outflow tract leads to altered cardiac looping after neural crest ablation. *Circulation*. 2002;106:504-510.
117. Waldo KL, Hutson MR, Stadt HA, Zdanowicz M, Zdanowicz J, Kirby ML. Cardiac neural crest is necessary for normal addition of the myocardium to the arterial pole from the secondary heart field. *Dev Biol*. 2005;281:66-77.
118. Christiansen JH, Coles EG, Wilkinson DG. Molecular control of neural crest formation, migration and differentiation. *Curr Opin Cell Biol*. 2000;12:719-724.
119. Huang X, Saint-Jeannet JP. Induction of the neural crest and the opportunities of life on the edge. *Dev Biol*. 2004;275:1-11.
120. Cornell RA, Eisen JS. Notch in the pathway: the roles of Notch signaling in neural crest development. *Semin Cell Dev Biol*. 2005;16:663-672.
121. Richarte AM, Mead HB, Tallquist MD. Cooperation between the PDGF receptors in cardiac neural crest cell migration. *Dev Biol*. 2007;306:785-796.
122. Kelly RG. Molecular inroads into the anterior heart field. *Trends Cardiovasc Med*. 2005;15:51-56.
123. Gittenberger-De Groot AC, Mahtab EA, Hahurij ND, Wisse LJ, DeRuiter MC, Wijffels MC, Poelmann RE. Nkx2.5-negative myocardium of the posterior heart field and its correlation with podoplanin expression in cells from the developing cardiac pacemaking and conduction system. *Anat Rec (Hoboken)*. 2007;290:115-122.
124. Mjaatvedt CH, Nakaoka T, Moreno-Rodriguez R, Norris RA, Kern MJ, Eisenberg CA, Turner D, Markwald RR. The outflow tract of the heart is recruited from a novel heart-forming field. *Dev Biol*. 2001;238:97-109.
125. Verzi MP, McCulley DJ, De Val S, Dodou E, Black BL. The right ventricle, outflow tract, and ventricular septum comprise a restricted expression domain within the secondary/anterior heart field. *Dev Biol*. 2005.

126. Waldo KL, Hutson MR, Ward CC, Zdanowicz M, Stadt HA, Kumiski D, Abu-Issa R, Kirby ML. Secondary heart field contributes myocardium and smooth muscle to the arterial pole of the developing heart. *Dev Biol.* 2005;281:78-90.
127. Blaschke RJ, Hahurij ND, Kuijper S, Just S, Wisse LJ, Deissler K, Maxelon T, Anastassiadis K, Spitzer J, Hardt SE, Scholer H, Feitsma H, Rottbauer W, Blum M, Meijlink F, Rappold G, Gittenberger-De Groot AC. Targeted mutation reveals essential functions of the homeodomain transcription factor Shox2 in sinoatrial and pacemaking development. *Circulation.* 2007;115:1830-1838.
128. Sugishita Y, Takahashi T, Shimizu T, Yao A, Kinugawa K, Sugishita K, Harada K, Matsui H, Nagai R. Expression of genes encoding vascular endothelial growth factor and its Flk-1 receptor in the chick embryonic heart. *J Mol Cell Cardiol.* 2000;32:1039-1051.
129. Sugishita Y, Leifer DW, Agani F, Watanabe M, Fisher SA. Hypoxia-responsive signaling regulates the apoptosis-dependent remodeling of the embryonic avian cardiac outflow tract. *Dev Biol.* 2004;273:285-296.
130. Sugishita Y, Watanabe M, Fisher SA. Role of myocardial hypoxia in the remodeling of the embryonic avian cardiac outflow tract. *Dev Biol.* 2004;267:294-308.
131. Watanabe Y, Kokubo H, Miyagawa-Tomita S, Endo M, Igarashi K, Aisaki KI, Kanno J, Saga Y. Activation of Notch1 signaling in cardiogenic mesoderm induces abnormal heart morphogenesis in mouse. *Development.* 2006;133:1625-1634.
132. Hsieh PC, Davis ME, Gannon J, MacGillivray C, Lee RT. Controlled delivery of PDGF-BB for myocardial protection using injectable self-assembling peptide nanofibers. *J Clin Invest.* 2006;116:237-248.
133. Schattteman GC, Motley ST, Effmann EL, Bowen-Pope DF. Platelet-derived growth factor receptor alpha subunit deleted Patch mouse exhibits severe cardiovascular dysmorphogenesis. *Teratology.* 1995;51:351-366.
134. Vrancken Peeters MP, Mentink MM, Poelmann RE, Gittenberger-De Groot AC. Cytokeratins as a marker for epicardial formation in the quail embryo. *Anat Embryol (Berl).* 1995;191:503-508.
135. Vrancken Peeters MP, Gittenberger-De Groot AC, Mentink MM, Poelmann RE. Smooth muscle cells and fibroblasts of the coronary arteries derive from epithelial-mesenchymal transformation of the epicardium. *Anat Embryol (Berl).* 1999;199:367-378.
136. Morabito CJ, Dettman RW, Kattan J, Collier JM, Bristow J. Positive and negative regulation of epicardial-mesenchymal transformation during avian heart development. *Dev Biol.* 2001;234:204-215.
137. Winter EM, Gittenberger-De Groot AC. Cardiovascular development: towards biomedical applicability : Epicardium-derived cells in cardiogenesis and cardiac regeneration. *Cell Mol Life Sci.* 2007;64:692-703.
138. Lie-Venema H, Van Den Akker NMS, Bax NA, Winter EM, Maas S, Kerkarainen T, Hoeben RC, DeRuiter MC, Poelmann RE, Gittenberger-De Groot AC. Origin, fate and function of epicardium-derived cells (EPDCs) in normal and abnormal cardiac development. *ScientificWorldJournal.* 2007;7:1777-1798.
139. Lie-Venema H, Eralp I, Maas S, Gittenberger-De Groot AC, Poelmann RE, DeRuiter MC. Myocardial heterogeneity in permissiveness for epicardium-derived cells and endothelial precursor cells along the developing heart tube at the onset of coronary vascularization. *Anat Rec A Discov Mol Cell Evol Biol.* 2005;282:120-129.

140. Wilting J, Buttler K, Schulte I, Papoutsi M, Schweigerer L, Manner J. The proepicardium delivers hemangioblasts but not lymphangioblasts to the developing heart. *Dev Biol.* 2007;305:451-459.
141. Vrancken Peeters MP, Gittenberger-De Groot AC, Mentink MM, Hungerford JE, Little CD, Poelmann RE. Differences in development of coronary arteries and veins. *Cardiovasc Res.* 1997;36:101-110.
142. Vrancken Peeters MP, Gittenberger-De Groot AC, Mentink MM, Hungerford JE, Little CD, Poelmann RE. The development of the coronary vessels and their differentiation into arteries and veins in the embryonic quail heart. *Dev Dyn.* 1997;208:338-348.
143. Bogers AJ, Gittenberger-De Groot AC, Poelmann RE, Peault BM, Huysmans HA. Development of the origin of the coronary arteries, a matter of ingrowth or outgrowth? *Anat Embryol (Berl).* 1989;180:437-441.
144. Jiang X, Rowitch DH, Soriano P, McMahon AP, Sucov HM. Fate of the mammalian cardiac neural crest. *Development.* 2000;127:1607-1616.
145. Tomanek RJ, Ratajska A, Kitten GT, Yue X, Sandra A. Vascular endothelial growth factor expression coincides with coronary vasculogenesis and angiogenesis. *Dev Dyn.* 1999;215:54-61.
146. Tomanek RJ, Ishii Y, Holifield JS, Sjogren CL, Hansen HK, Mikawa T. VEGF family members regulate myocardial tubulogenesis and coronary artery formation in the embryo. *Circ Res.* 2006;98:947-953.
147. Miller AM. Histogenesis and morphogenesis of the thoracic duct in the chick; development of blood cells and their passage to the blood stream via the thoracic duct. *Am J Anat.* 1913;15:131-198.
148. Wigle JT, Oliver G. Prox1 function is required for the development of the murine lymphatic system. *Cell.* 1999;98:769-778.
149. Wigle JT, Harvey N, Detmar M, Lagutina I, Grosveld G, Gunn MD, Jackson DG, Oliver G. An essential role for Prox1 in the induction of the lymphatic endothelial cell phenotype. *EMBO J.* 2002;21:1505-1513.
150. Hong YK, Harvey N, Noh YH, Schacht V, Hirakawa S, Detmar M, Oliver G. Prox1 is a master control gene in the program specifying lymphatic endothelial cell fate. *Dev Dyn.* 2002;225:351-357.
151. Hong YK, Detmar M. Prox1, master regulator of the lymphatic vasculature phenotype. *Cell Tissue Res.* 2003;314:85-92.
152. Petrova TV, Makinen T, Makela TP, Saarela J, Virtanen I, Ferrell RE, Finegold DN, Kerjaschki D, Yla-Herttuala S, Alitalo K. Lymphatic endothelial reprogramming of vascular endothelial cells by the Prox-1 homeobox transcription factor. *EMBO J.* 2002;21:4593-4599.
153. Makinen T, Veikkola T, Mustjoki S, Karpanen T, Catimel B, Nice EC, Wise L, Mercer A, Kowalski H, Kerjaschki D, Stacker SA, Achen MG, Alitalo K. Isolated lymphatic endothelial cells transduce growth, survival and migratory signals via the VEGF-C/D receptor VEGFR-3. *EMBO J.* 2001;20:4762-4773.
154. Karpanen T, Makinen T. Regulation of lymphangiogenesis--from cell fate determination to vessel remodeling. *Exp Cell Res.* 2006;312:575-583.
155. Goldman J, Rutkowski JM, Shields JD, Pasquier MC, Cui Y, Schmokel HG, Willey S, Hicklin DJ, Pytowski B, Swartz MA. Cooperative and redundant roles of VEGFR-2 and VEGFR-3 signaling in adult lymphangiogenesis. *FASEB J.* 2007;21:1003-1012.

156. Banerji S, Ni J, Wang SX, Clasper S, Su J, Tammi R, Jones M, Jackson DG. LYVE-1, a new homologue of the CD44 glycoprotein, is a lymph-specific receptor for hyaluronan. *J Cell Biol.* 1999;144:789-801.
157. Gale NW, Prevo R, Espinosa J, Ferguson DJ, Dominguez MG, Yancopoulos GD, Thurston G, Jackson DG. Normal lymphatic development and function in mice deficient for the lymphatic hyaluronan receptor LYVE-1. *Mol Cell Biol.* 2007;27:595-604.
158. McDonald JA, Brehm-Gibson T, Camenisch T, Spicer AP. Molecular cloning and gene targeting of hyaluronan synthase-2 reveals a critical role in development of the cardiovascular system in the mouse. *Glycobiology.* 1998;8:1142-1143.
159. Schacht V, Ramirez MI, Hong YK, Hirakawa S, Feng D, Harvey N, Williams M, Dvorak AM, Dvorak HF, Oliver G, Detmar M. T1alpha/podoplanin deficiency disrupts normal lymphatic vasculature formation and causes lymphedema. *EMBO J.* 2003;22:3546-3556.
160. Snijders RJ, Noble P, Sebire N, Souka A, Nicolaides KH. UK multicentre project on assessment of risk of trisomy 21 by maternal age and fetal nuchal-translucency thickness at 10-14 weeks of gestation. Fetal Medicine Foundation First Trimester Screening Group. *Lancet.* 1998;352:343-346.
161. Nicolaides KH, Spencer K, Avgidou K, Faiola S, Falcon O. Multicenter study of first-trimester screening for trisomy 21 in 75 821 pregnancies: results and estimation of the potential impact of individual risk-orientated two-stage first-trimester screening. *Ultrasound Obstet Gynecol.* 2005;25:221-226.
162. Haak MC, Van Vugt JM. Pathophysiology of increased nuchal translucency: a review of the literature. *Hum Reprod Update.* 2003;9:175-184.
163. Haak MC, Bartelings MM, Jackson DG, Webb S, Van Vugt JM, Gittenberger-De Groot AC. Increased nuchal translucency is associated with jugular lymphatic distension. *Hum Reprod.* 2002;17:1086-1092.
164. Sheppard C, Platt LD. Nuchal translucency and first trimester risk assessment: a systematic review. *Ultrasound Q.* 2007;23:107-116.
165. Miyabara S, Gropp A, Winking H. Trisomy 16 in the mouse fetus associated with generalized edema and cardiovascular and urinary tract anomalies. *Teratology.* 1982;25:369-380.
166. Gravholt CH. Epidemiological, endocrine and metabolic features in Turner syndrome. *Eur J Endocrinol.* 2004;151:657-687.

Part I

*VEGF in Cardiovascular Development and Endothelial
Differentiation*

Chapter 2

Tetralogy of Fallot and Alterations in VEGF and Notch-signaling in Mouse Embryos Solely Expressing the VEGF120 Isoform

Nynke M.S. van den Akker¹, Daniël G.M. Molin^{1,3}, Patricia P.W.M. Peters³, Saskia Maas¹, Lambertus J. Wisse¹, Ronald van Bremp², Conny J. van Munsteren¹, Margot M. Bartelings¹, Robert E. Poelmann¹, Peter Carmeliet^{4,5}, Adriana C. Gittenberger-de Groot¹

¹Department of Anatomy and Embryology, and ²Department of Pediatric Intensive Care Leiden University Medical Center, Leiden, The Netherlands; ³Department of Physiology, CARIM, Maastricht University, Maastricht, The Netherlands; ⁴Center for Transgene Technology and Gene Therapy, KU Leuven; ⁵Department of Transgene Technology and Gene Therapy, VIB, Leuven, Belgium.

Modified after Circulation Research, 2007;100:842-849.

Tetralogy of Fallot and Alterations in VEGF and Notch-signaling in Mouse Embryos Solely Expressing the VEGF120 Isoform

Abstract

The importance of VEGF and subsequent Notch-signaling in cardiac outflow tract development is generally recognised. Although genetic heterogeneity and mutations of these genes in both humans and mouse models relate to a high susceptibility to develop outflow tract malformations such as Tetralogy of Fallot and peripheral pulmonary stenosis, no etiology has been proposed so far. Using immunohistochemistry, in situ hybridisation and RT-qPCR on embryonic hearts, we have shown spatiotemporal increase and abnormal patterning of *Vegf*, VEGF and (phosphorylated) VEGFR-2, (cleaved) Notch1 and Jagged2 in the outflow tract of *Vegf120/120* mouse embryos. This coincides with hyperplasia of specifically the outflow tract cushions and a high degree of subpulmonary myocardial apoptosis that, in later stages, manifest as pulmonary stenosis and ventricular septal defects. We postulate that increase of VEGF and Notch-signaling during right ventricular outflow tract development can lead to abnormal development of both cushion and myocardial structures. Defective right ventricular outflow tract development as presented provides new insight in the etiology of Tetralogy of Fallot.

Introduction

The importance of Vascular Endothelial Growth Factor-A (VEGF) for angiogenesis is ultimately demonstrated by the early embryonic death of both VEGF heterozygous and VEGF receptor (VEGFR)-2 homozygous knockout mice^{1,2}. Recent data point towards a critical role for VEGF during cardiac development as well. It has been shown in humans that a low expression VEGF haplotype correlates with increased risk for Tetralogy of Fallot (TOF), a congenital heart disease consisting of a ventricular septal defect (VSD), pulmonary stenosis and dextroposition of the aorta^{3,4}. Furthermore, the VEGF165 isoform has been postulated as a modifier of the cardiovascular phenotype in the human DiGeorge syndrome⁵. In addition, mouse models in which genes of proteins involved in VEGF-signaling are mutated show comparable cardiac malformations⁶⁻⁹.

During cardiac development, the early outflow tract (OFT) has to be divided into the aortic and pulmonary OFT with proper alignment to the left and right ventricle, respectively. Here, the development of both the endocardial cushions and the adjacent myocardium is crucial. Within this process the cushions have to be populated by cells predominantly recruited from the cushion endocardium through epithelial-mesenchymal transformation (EMT). A role for VEGF in atrioventricular cushion EMT has been shown, albeit both stimulating^{10,11} and inhibiting¹². This lead to the hypothesis that VEGF has to be expressed within a 'physiological window' during cushion development¹³.

The myocardium of the pulmonary OFT, derived from the secondary heart field (SHF), is a distinct population added to the arterial pole after the initial heart tube is formed¹⁴. SHF addition is critical for OFT development as ablation of the SHF in chicken embryos leads to cardiac malformations such as TOF, in which anomalous OFT development is obvious^{15,16}. Furthermore, upregulated by hypoxia, VEGF seems to play a role in this part of OFT development¹⁷.

VEGF-signaling can upregulate members of the Jagged/Delta-like/Notch-family^{18,19}. *JAGGED1*-mutations in humans are correlated with TOF or pulmonary stenosis²⁰⁻²². Involvement of other members of Notch-signaling in cardiac development has been demonstrated by several mouse mutants²³⁻²⁵. Notch has also been described to stimulate endocardial cushion EMT^{23,26}, implying a potential effect of VEGF on cushion development via Notch-signaling.

To investigate the role of VEGF and Notch-signaling, we made use of the earlier described *Vegf120/120* mouse model^{5,27}. We demonstrate that *Vegf120/120* mouse embryos, which solely express the VEGF120 isoform, are highly susceptible for development of TOF. We hypothesise that this is most likely attributal to spatiotemporal elevations of VEGF and Notch-signaling, mainly seen in the SHF-derived right ventricular OFT myocardium.

Materials and Methods

Mouse embryos and tissue processing

All animal experiments were approved by the Animal Ethics Committee of the Leiden University and performed according to the *Guide for the Care and Use of Laboratory Animals* published by the NIH. An extensive description of mouse experiments can be found in the appendix of this chapter.

Immunohistochemistry

Paraffin sections of 5 μ M were incubated overnight with primary antibody, after which sections were incubated with secondary antibody. For the detection of apoptosis, the TUNEL-kit was used (1684817, Roche/Boehringer Mannheim, Basel, Switzerland). An extensive description of the technique and of the antibodies used can be found in the appendix of this chapter.

In situ hybridisation

Sense and anti-sense 35 S-radiolabeled *Vegf-A* cRNA probes were transcribed using a 451-bp clone encoding for the mouse *Vegf120* isoform (pVEGF2; kindly provided by Dr. G. Breier, University of Technology, Dresden, Germany). Radioactive in situ hybridisation (ISH) was performed²⁸. A brief description can be found online.

RT-qPCR

RNA was isolated using the RNeasy mini kit (QIAGEN). All samples were normalized for input based on β -actin and *Gapdh*. Data analyses were performed using an Excel spreadsheet based on geNorm (Relative expression with error propagation)²⁹. Statistic significance was tested using randomization testing as provided in the REST2005 program³⁰. Samples with a probability (p)-value of <0.05 were regarded to be significant different between the groups. Primer sequences and detailed description of the technique appear in the appendix of this chapter (Table A2).

3D-reconstruction

3D-reconstructions were performed as described³¹. In short, micrographs were made of every seventh section of embryonic day (E)12.5 and E19.5 hearts of wild-type embryos and *Vegf120/120* littermates. The micrographs were converted to 3D using AMIRA-software (Template Graphics Software Inc., San Diego, USA).

Results

Morphology

Right ventricular OFT development is impaired

At E10.5 the development of the common OFT of *Vegf120/120* embryos was comparable with wild-type littermates. In E11.5 to E13.5 mutants we could observe hyperplasia of the proximal OFT cushions (Figure 1a,e; Table 1). More striking, in all of these embryos a large apoptotic ring surrounded the right ventricular OFT as observed using Mayer's hematoxylin³² (Table 1) as well as with TUNEL-staining, specifically located in the subpulmonary myocardium up to the level of the developing pulmonary valves (Figure 1b-d,f-h). Stenosis of the right ventricular OFT concomitant with hypoplasia of the pulmonary trunk or pulmonary arteries was apparent in several cases (Figure 1c,g; Table 1).

At E14.5 to E19.5, right ventricular OFT abnormalities varied from stenosis of the left pulmonary artery at the level of branching from the pulmonary trunk (Figure 1i,m) to stenosis of the right ventricular OFT, which was always accompanied by hypoplasia of the pulmonary trunk (Table 2). In cases with severe OFT stenosis almost complete atresia of the pulmonary trunk was seen (Figure 1j,n).

Pulmonary OFT and aortic arch defects

All pharyngeal arch arteries were present in *Vegf120/120* embryos of E10.5, excluding anomalous Anlage. Already at E11.5, associated with pulmonary OFT stenosis, atresia of the ductus arteriosus (DA) was observed in 2/4 embryos. From E14.5 onwards, an atretic strand or absence of the DA was seen (Figure 1k,o) and coincided in 8/9 cases with pulmonary OFT stenosis (Table 2). Other aortic arch malformations observed from E14.5 onwards were right or double aortic arch with right dominance and a right DA (Figure 1l,p; Table 2) or hypoplasia of the aortic arch (5/31). Pulmonary-systemic collateral arteries from the dorsal aorta to the lungs were found in embryos with pulmonary stenosis and absence of the DA at later stages of development (data not shown).

Table 1. Outflow abnormalities in Vegf120/120 embryos of E11.5 to E13.5.

Cardiac Anomaly	No/total	%	
Apoptosis subpulmonary myocardium	14/14	100	Abbreviations: PT/PA = pulmonary trunk / pulmonary artery(ies); RV-OFT = right ventricular outflow tract. *These 6 out of 14 embryos represent all of E11.5 to E13.5 with stenosis of the right ventricular OFT.
Hyperplasia OFT cushions	8/14	57	
only	3/14	21	
+ malposition OFT cushions	5/14	36	
Hypoplasia PT/PA	9/14	64	
only	3/14	21	
+ stenosis RV-OFT *	6/14	43	
+ hyperplasia OFT cushions	2/14	14	

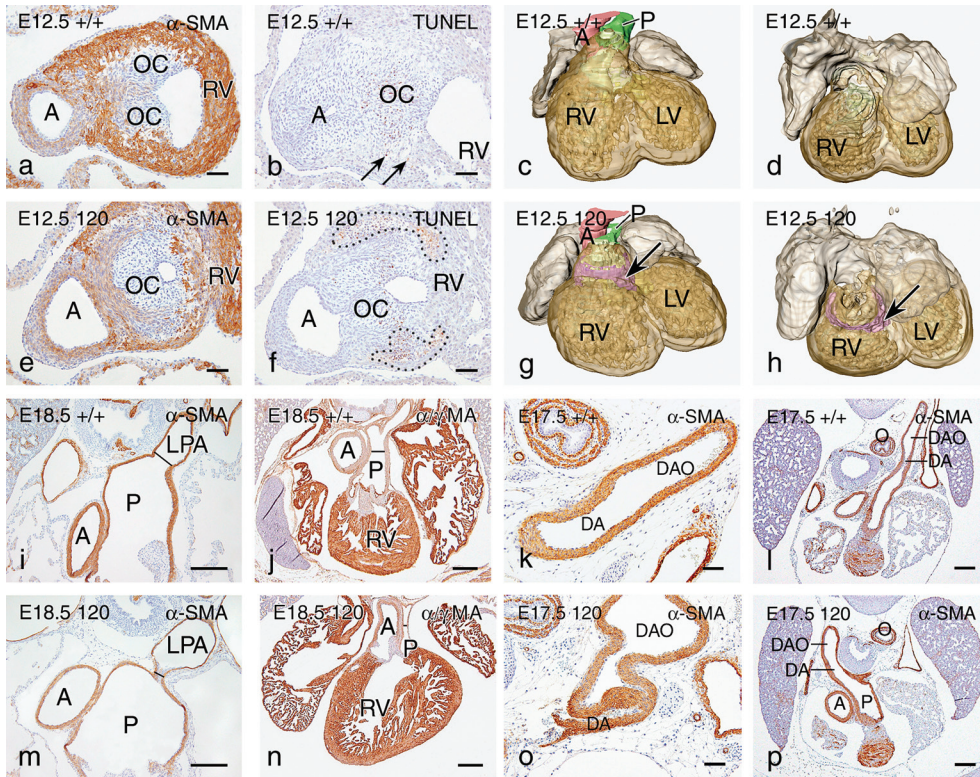


Figure 1. Outflow tract (OFT) and aortic arch malformations in *Vegf120/120* mouse embryos. The stainings performed are indicated in the upper right corner. Wild-type (+/+) and *Vegf120/120* (120) are compared as indicated, together with the age in embryonic days (E). During OFT development an increased volume of the mesenchyme of the OFT cushions (OC) is observed (a,e). Apoptosis of the subpulmonary myocardium is seen (b, dotted areas f). Figure c,d,g and h are 3D-reconstructions of anti- α/γ muscle actin (α/γ MA) stained sections. The pink structure is the ascending aorta (A) and the green structure the pulmonary trunk (P), which is stenotic in the *Vegf120/120* embryo. The purple area indicated with the arrow is apoptotic subpulmonary myocardium. Severe stenosis of the left pulmonary artery (LPA) was seen (lines in i,m) or even almost complete obliteration of the P (lines in j,n). Both atresia of the ductus arteriosus (DA; k,o) and a right DA (l vs p), coinciding with a right aortic arch, could be observed. Abbreviations: α -SMA = α -smooth muscle actin; DAO = dorsal aorta; LV = left ventricle; O = oesophagus; RV = right ventricle; TUNEL = Terminal deoxynucleotidyl Transferase Biotin-dUTP Nick End Labeling. Scale bar = 60 μ m (a,b,e,f,k,o) or 200 μ m (i,j,l,m,n,p).

Other cardiac anomalies

Correct looping of the early heart tube is crucial for proper cardiac septation. In half of the E10.5 to E11.5 *Vegf120/120* embryos looping was diminished (Figure 2a,d), leading to a wider inner curvature and a ventral displacement of the OFT. *Vegf120/120* embryos of E11.5 to E13.5 showed malposition of the OFT cushions together with ventral displacement of the OFT (Table 1), which at later stages (E14.5 to E19.5) was concomitant with subaortic ventricular septal defects (VSDs) (Figure 2b,e; Table 2).

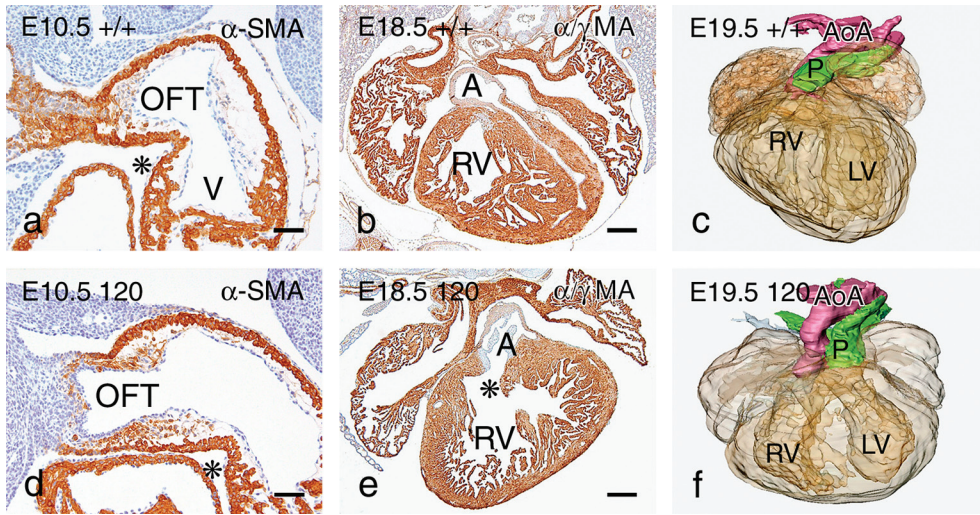


Figure 2. Heart malformations in *Vegf120/120* embryos. Stainings performed are indicated. Wild-type (+/+) and *Vegf120/120* (120) are compared, together with age in embryonic days (E). Abnormal outflow tract (OFT) looping was observed in mutant embryos (asterisk in a and in d). Subaortic ventricular septal defect was encountered in older mutant embryos (b and asterisk in e) as was dextroposition of the ascending aorta (A) and side-by-side positioning of the OFT (c,f). Panels c and f are 3D-reconstructions of α/γ MA stained sections. The pink structure is the aortic arch (AoA) and the green structure is the pulmonary trunk. Abbreviations: α -SMA = α -smooth muscle actin; α/γ muscle actin = α/γ MA; LV = left ventricle; P = pulmonary trunk; RV = right ventricle; V = ventricle. Scale bar = 60 μ m (a,d) or 200 μ m (b,e).

Significant dextroposition of the aorta and a subaortic VSD, referred to as a double outlet right ventricle (DORV) (Table 2), went along with a side-by-side positioning of the great arteries (Figure 2c,f). Often, a combination of a subaortic VSD, dextroposition of the aorta and right ventricular OFT stenosis, TOF, was found (Table 2).

Signaling

Vegf120 mRNA levels are increased and patterning is abnormal

To determine the mRNA levels of the different *Vegf*-isoforms during normal cardiac development, isoform-specific qPCR on normal hearts of E14.5, E16.5 and E18.5 was performed. In this time span, *Vegf120* was least prominent compared with the larger isoforms, although a temporal increase was seen at E16.5 (Figure 3a). When comparing total *Vegf* mRNA levels of wild-type to *Vegf120/120* hearts, no significant difference was found (Figure 3b). However, when only the expression of the *Vegf120* isoform was compared, a 6-16 times increase was seen in the *Vegf120/120* hearts, being most prominent at E16.5 (Figure 3c).

Table 2. TOF related abnormalities in *Vegf120/120* embryos of E14.5 to E19.5.

Cardiac Anomaly	No/Total	%
VSD	13/31	42
subaortic	11/31	35
+ muscular	2/31	6
muscular only	2/31	6
subaortic VSD + dextroposition aorta (=DORV)	10/31	32
+ stenosis RV-OFT (=TOF)	9/31	29
Hypoplasia PT/PA	19/31	61
only	9/31	29
+ stenosis RV-OFT *	10/31	32
+ atresia DA †	8/31	26
Right AoA	4/31	13
only	3/31	10
+ TOF	1/31	3
Double AoA	2/31	6
only	1/31	3
+ subaortic VSD	1/31	3
Thin myocardium	17/31	55

Abbreviations: AoA = aortic arch; DA = ductus arteriosus; DORV = double outlet right ventricle; PT/PA = pulmonary trunk / pulmonary artery(ies); RV-OFT = right ventricular outflow tract; TOF = Tetralogy of Fallot; VSD = ventricular septal defect. * These 10/31 embryos represent all E14.5 to E19.5 with stenosis of the right ventricular OFT. † In addition, one embryo with isolated DA atresia was found.

Spatiotemporal changes in *Vegf* mRNA patterning were investigated in *Vegf120/120* embryonic hearts, using radioactive ISH. Between E10.5 and E14.5, high expression was observed in the OFT myocardium at the level of the OFT cushions, whereas very low expression was seen in the endocardium of the OFT cushions of wild-type embryos (Figure 4a,b,d,e). Increased *Vegf* mRNA signal in the endocardial cells of the OFT cushions was found in *Vegf120/120* embryos of E10.5, while the level in the OFT myocardium was comparable between genotypes at this age (Figure 4d). In *Vegf120/120* embryos of E14.5, a highly increased *Vegf*-signal was seen in the subpulmonary myocardium (Figure 4e), up to the level of the OFT valves when compared with wild-type littermates (Figure 4b). In wild-type embryos of E16.5 the highest expression was present at the borderline of compact to trabecular myocardium (data not shown). At E18.5, only scattered *Vegf* expression was observed (Figure 4c). In *Vegf120/120* hearts of E16.5 to E18.5, the OFT myocardial signal was higher (data not shown) and the expression at the borderline of compact to trabecular myocardium was markedly increased (Figure 4f).

Increased expression of VEGF, (phosphorylated) VEGFR-2, (cleaved-)Notch1 and Jagged2 in the OFT

In accordance with the ISH data, VEGF levels were increased in the endothelium of the OFT cushions at E10.5 (Figure 5a,e). In older embryos (E13.5 and older), the VEGF protein expression was equally distributed throughout wild-type myocardium, while the staining intensity was higher in the trabeculae compared with the compact myocardium in *Vegf120/120* embryos (data not shown). In wild-type embryos of E10.5, VEGFR-2 expression was present throughout the myocardium and in the endocardium of the OFT. Expression in these cell types was higher in the *Vegf120/120* embryos (Figure 5b,f). Although in wild-types of E18.5 and older the myocardial VEGFR-2 signal had disappeared, the mutants still expressed low levels of VEGFR-2 in the myocardium (data not shown). Furthermore, in the subpulmonary myocardium, in the region of the apoptotic area an increase in expression of phosphorylated VEGFR-2 expression was observed, indicating locally high levels of VEGF-signaling in *Vegf120/120* mouse embryos of E11.5 to E14.5 (Figure 5j,m).

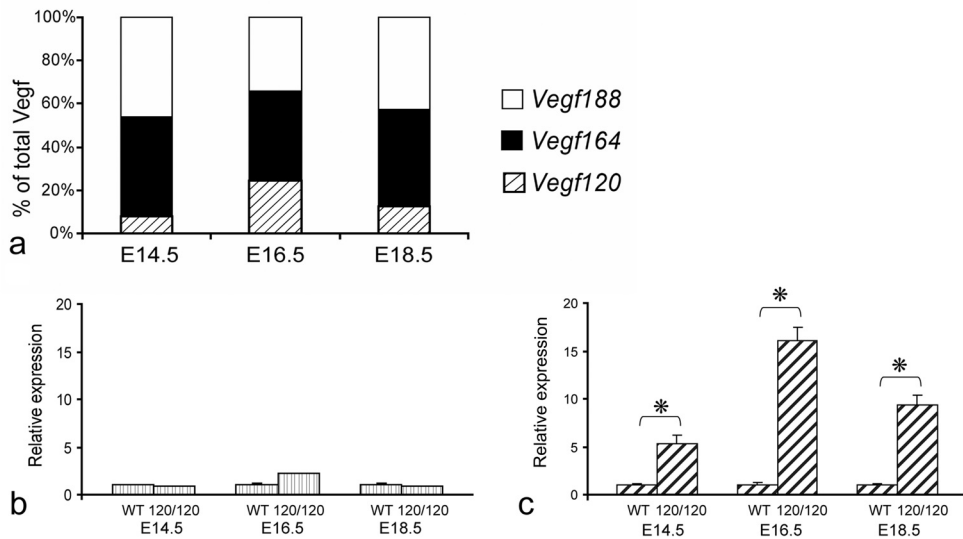


Figure 3. Vegf mRNA distribution in wild-type and Vegf120/120 embryonic hearts. In hearts of wild-type embryos of E14.5, E16.5 and E18.5, *Vegf* isoform specific qPCR shows that the *Vegf164* isoform is most abundantly present (a), while the *Vegf120* isoform is least present. No significant differences are found in total *Vegf* mRNA levels (b), but the expression levels of *Vegf120* isoform are significantly elevated in mutant as compared with wild-type embryos (c). * = $p < 0.05$.

Spatiotemporally coinciding with *Vegf*, VEGF and VEGFR-2 expression, we observed both Notch1 expression and presence of cleaved- (activated) Notch1 in the OFT endocardium of *Vegf*^{+/+} embryos of E10.5 (Figure 5c,d). In *Vegf*^{120/120} mutants of E10.5 an increased number of endocardial and mesenchymal cells revealed Notch1 expression and presence of cleaved-Notch1 while no differences were seen for the myocardial expression (Figure 5g,h). Expression patterns of Notch2 were unaltered between both genotypes. In wild-type embryos of E11.5 to E15.5, Jagged2 expression was present at low levels in the subpulmonary OFT myocardium (Figure 5k). Jagged2 expression in the mutants embryos was more prominent (Figure 5n), especially for the apoptotic subpulmonary myocardium (Figure 1f-h). This increase in Jagged2 expression colocalised with increase of phosphorylated VEGFR-2 expression and higher levels of cleaved-Notch1 when compared with wild-type littermates (Figure 5i,j,l,m). Also, increased level of Jagged1 in the OFT myocardium was obvious in *Vegf*^{120/120} embryos (data not shown) while again no differences in Notch2-expression were seen.

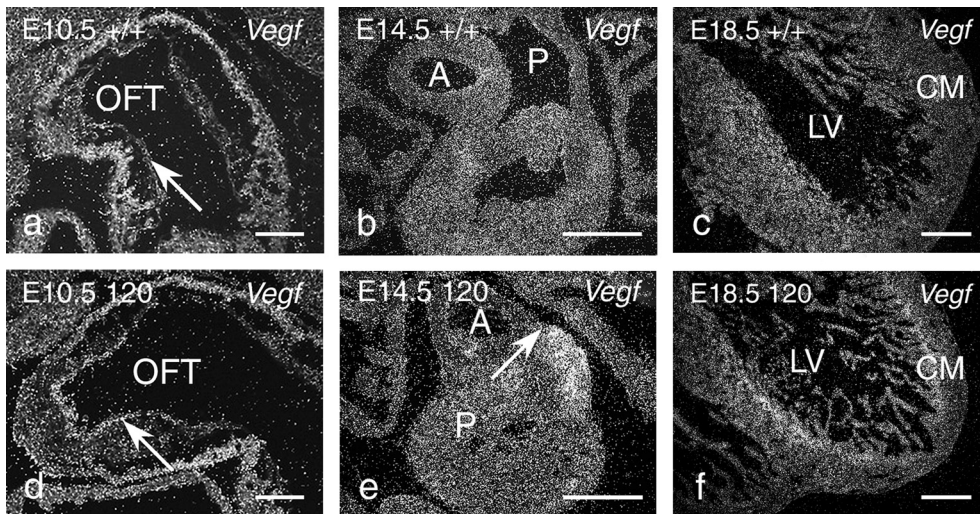


Figure 4. Vegf mRNA expression patterns in wild-type and Vegf120/120 embryonic hearts. All sections show Vegf mRNA expression using radioactive in situ hybridisation. Wild-type and *Vegf*^{120/120} are compared as indicated, together with age in embryonic days (E). At E10.5, an increase in endocardial *Vegf* mRNA expression was found in the outflow tract (OFT; compare arrows in a and d) while myocardial expression was comparable between genotypes. At E14.5, an increase in *Vegf* expression was seen in the subpulmonary myocardium (Figure b and e). At E18.5, an increase in expression was found between the compact myocardium (CM) and the trabecular myocardium of the mutant embryos (compare f and c). Abbreviations: A = ascending aorta; LV = left ventricle; P = pulmonary trunk. Scale bar = 60 μm (a,d) or 200 μm (b,c,e,f).

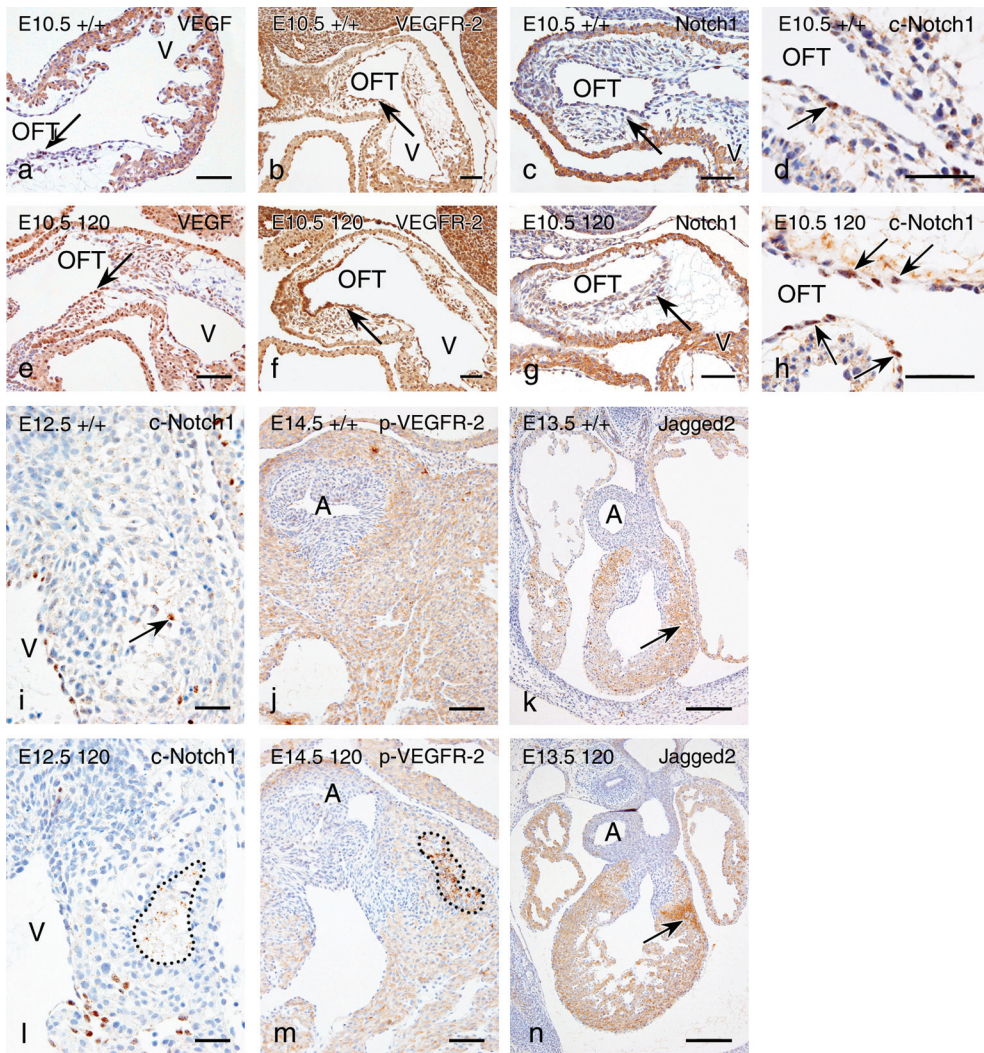


Figure 5. Increased expression of VEGF, (phosphorylated) VEGFR-2, (cleaved-) Notch1 and Jagged2 in Vegf120/120 embryonic hearts. The stainings performed are indicated and age-matched wild-type (+/+) and Vegf120/120 (120) are compared as indicated in the upper left corner. In the developing OFT an increase in endocardial VEGF expression (arrows in a and e) combined with an increased endocardial VEGFR-2 expression (arrows in b and f) and more Notch1 positive cells in the endocardium and mesenchymal cells (arrows in c and g) in the OFT cushions is shown. Furthermore, more cells staining for cleaved-Notch1 (c-Notch1) are seen in the endocardium (d,h). In the subpulmonary myocardium an increase in expression of c-Notch1 (arrow in i versus dotted line in l), phosphorylated VEGFR-2 (p-VEGFR-2; j and dotted line in m) and of Jagged2 was seen (arrows in k and n). Abbreviations: see Figure 1; V = ventricle. Scale bar = 60 μ m (a-i,l), 90 μ m (j,m) or 200 μ m (k,n).

Discussion

It has been shown in humans that mutations in the *VEGF* gene³³, its promoter³ or in *JAGGED1*²⁰⁻²² increase the risk to develop congenital heart disease such as TOF and pulmonary stenosis. In order to unravel the role of VEGF in normal and abnormal OFT development, we investigated several stages of heart development in wild-type and *Vegf120/120* mouse embryos, that have been reported with TOF⁵. We found that spatiotemporal increase of VEGF and subsequent Notch-signaling coincides with hyperplasia of the OFT cushions and abnormally high levels of apoptosis in the subpulmonary myocardium. In addition, abnormal size and positioning of the OFT cushions as found in our model are associated with cardiac looping defects, VSD and malpositioning of the great arteries^{34;35}. Also changes in endocardial VEGF-signaling has been shown to cause heart bending defects³⁶. The anomalies in pulmonary outflow tract morphogenesis as exemplified in the *Vegf120/120* mutants can contribute to the development of TOF, consisting of right ventricular OFT stenosis, dextroposition of the aorta and subaortic VSD.

Alterations in Vegf-expression in Vegf120/120 mutants

Although cardiac levels of total *Vegf* mRNA do not differ between *Vegf120/120* and wild-type embryos, expression levels of the *Vegf120* isoform are markedly higher in mutants. As during normal cardiac development VEGF120 is the least prominent isoform (Figure 3a and ³⁷), an adverse effect of overexpression in *Vegf120/120* embryos should be considered. Furthermore, this mouse model lacks the heparin- and NP-1-binding VEGF-isoforms (i.e. VEGF164 and VEGF188) and hence a lack of NP-1-mediated VEGFR-2-signaling is expected³⁸. However, we observe increased levels of *Vegf* (Figure 4e) and of phosphorylated VEGFR-2 (Figure 5m) in the subpulmonary cardiomyocytes, indicating locally increased instead of decreased signaling. Based on qPCR data (Figure 3a) and ISH comprising all isoforms (Figure 4b) it is expected that in wild-type embryos the non-soluble VEGF164 isoform is dominant in the subpulmonary myocardium. In the *Vegf120/120* embryos only the soluble VEGF120 isoform is expressed. This could initially result in decreased signaling followed by altered feedback mechanisms in *Vegf*-expression, which then lead to the extreme increase of *Vegf120*-levels (Figure 3c, 4e). However, as little is known about feedback mechanisms regulating *Vegf*-expression, this remains elusive at this point.

VEGF and Notch-signaling in abnormal cushion development

VEGF-signaling has been described to play a role in OFT cushion development¹⁰⁻¹³. Although these processes largely take place before E10.5 we still find expression levels of VEGF and VEGFR-2 in the endocardium and the mesenchyme of the OFT cushions of normal embryos (Figure 5a,b,e,f) and favor a role of VEGF-signaling in cushion expansion as well. VEGF has been reported to increase Notch1-expression^{18;19}, which in its turn stimulates endocardial EMT^{13;23;26}. In agreement with the low VEGF/

VEGFR-2 levels, Notch1 was weakly present in wild-type OFT endocardium of E10.5. In contrast, the *Vegf120/120* mutants of this age showed ectopic *Vegf* expression and increased VEGF/VEGFR-2 protein levels for the OFT endocardium. A high Notch1 and cleaved- (activated) Notch1 expression was also observed in the cushion endocardium as well as in the mesenchyme of these embryos. These data imply that VEGF⁴⁰ and subsequent Notch-signaling is disturbed in the mutant and seems to be prolonged. Potentially these disturbances will exert an effect on cushion EMT and could relate to OFT cushion hyperplasia and associated cardiac malformations as observed in the *Vegf120/120* embryos.

The positive effect of VEGF on cushion EMT in our model seems to contradict the finding that myocardial overexpression of VEGF has an inhibiting effect on atrioventricular endocardial cushion EMT and growth¹². Functional differences between VEGF120 (as overexpressed in our mouse model) and the human VEGF165 (as used in research performed by Dor et al¹²) might partially explain these differences. Furthermore, in our research the overexpression was observed in both the endothelium and myocardium of the OFT cushions, whereas no disturbed VEGF expression was apparent for the atrioventricular cushions. Moreover, our data, as well as earlier research using this mouse model⁵, do not present inflow anomalies. This difference between OFT and atrioventricular cushions implies a distinct function or sensitivity for VEGF in OFT versus atrioventricular cushion development and endothelial versus myocardial expression.

Apoptosis of subpulmonary myocardium colocalises with increased Notch-signaling

During mouse and chicken development, apoptosis of subaortic cardiomyocytes has been described as a normal phenomenon essential for proper OFT-remodeling^{39;41}. In addition, it has been described in chicken embryos that aforementioned apoptosis is associated with hypoxia-induced expression of VEGF³⁹. In this research we show that the subpulmonary *Vegf*-expression coincides with high phosphorylated VEGFR-2 and Jagged2 expression of cardiomyocytes. Although only a very small number of apoptotic cells is seen in the OFT myocardium of wild-type embryos, which is in agreement with earlier observations⁴¹, *Vegf120/120* mutants show remarkable large ring-like apoptotic areas in the subpulmonary myocardium. These areas spatiotemporally overlap with elevated levels of *Vegf*, phosphorylated VEGFR-2, cleaved-Notch1 and Jagged2. This indicates that increased VEGF and Notch-signaling is present in the subpulmonary myocardium of *Vegf120/120* embryos. It has been described that stimulation of Notch1 by Jagged2 can result in apoptosis^{42;43} and the observed increase in Notch-signaling in the subpulmonary myocardium as indicated by cleaved-Notch1 and Jagged2 could account for the pathological levels of apoptosis found in the *Vegf120/120* model. Thus, we conclude that VEGF-signaling is protective for the subpulmonary cardiomyocytes, as suggested by Sugishita et al³⁹, within a physiological window; when signaling-levels are too low or too high (as in the *Vegf120/120* mouse model), the cardiomyocytes will undergo (Notch-mediated) apoptosis leading to congenital heart malformations.

In humans, changes in NOTCH-signaling by mutations in the *JAGGED1* gene can lead to congenital cardiac malformations such as TOF²⁰⁻²². However, little is known about the alterations in signaling under these conditions. It can be speculated that in these cases decreased JAGGED1 function favors JAGGED2 related signaling, leading to a comparable condition as in our mouse model. This is only speculative as little information is available at present regarding the differences in affinities and/or intracellular pathways between the combinations of Notch-ligands and receptors. However, as we show that spatiotemporal changes in VEGF and Notch-signaling are associated with the development of cardiac abnormalities, we think that our model does provide further insight in the embryonic development of right ventricular OFT anomalies with a potential function for VEGF and Notch-signaling.

It should be mentioned that the affected subpulmonary myocardium has been linked to the SHF^{14;44;45}. Recent data suggests that this myocardium is a distinct population critically involved in proper positioning of the large OFT vessels⁴⁶. Furthermore, increasing evidence is pointing towards a link between alterations in SHF development and the etiology of OFT anomalies including TOF^{15;16;44}. We postulate that this SHF derived subpulmonary myocardium is highly sensitive for VEGF and Notch-signaling. The high levels of apoptosis in this myocardial population probably lead to hypoplasia of the pulmonary trunk and the often observed right ventricular OFT stenosis. The occurrence of this phenotype in our model is likely aggravated by the manifestation of the earlier discussed cushion hyperplasia. Furthermore, ablation of this SHF-derived myocardium, in our case by apoptosis, might lead to alterations in proper positioning of the OFT vessels leading to dextroposition of the aorta.

Abnormalities of the pulmonary arteries and aortic arch

The development of vascular anomalies has been linked to altered blood flow⁴⁷ and as such can develop secondary to cardiac outflow defects. The high frequencies of pulmonary vascular defects (i.e. hypoplasia and atresia of the DA and pulmonary arteries) in the *Vegf120/120* mutant along with right ventricular OFT obstruction is in agreement with this assumption. The severe pulmonary outflow or -arterial stenosis will impair blood flow to the lungs. We suggest that this leads to local hypoxia and development of collateral vessels originating from the dorsal aorta as observed in our mouse model as well as in human neonates with severe pulmonary stenosis⁴⁸.

The *Vegf120/120* mouse model has been described as a model with overt cardiovascular defects found in patients with DiGeorge syndrome (i.e. TOF, common arterial trunk and aortic arch interruption type-B). However, the occurrence of aortic arch malformations in this research seems to differ slightly from earlier published data on this model³. This might be explained by the differences in time points analysed between both studies. As in this research, embryos at several different time points of development were investigated (E10.5 to E19.5 versus E14.5/neonates), the number of anomalies encountered here might be underestimated due to ongoing development.

Conclusions

We conclude that during normal heart development, VEGF and subsequent Notch-signaling must be tightly controlled, especially in the SHF-derived myocardium of the right ventricular OFT. In the *Vegf120/120* mice, local increase of VEGF-signaling in this region leads, likely via changes in the Notch-pathway, to hyperplasia of the OFT cushions and apoptosis of the SHF-derived subpulmonary myocardium. This working model might explain the development of TOF in the human population as found in individuals with *VEGF* and *JAGGED1*-mutations and 22q11-deletions²⁰⁻²².

Acknowledgements

The authors would like to thank Jan Lens for preparation of the Figures.

References

1. Carmeliet P, Ferreira V, Breier G, Pollefeyt S, Kieckens L, Gertsenstein M, Fahrigr M, Vandenhoeck A, Harpal K, Eberhardt C, Declercq C, Pawling J, Moons L, Collen D, Risau W, Nagy A. Abnormal blood vessel development and lethality in embryos lacking a single VEGF allele. *Nature*. 1996;380:435-439.
2. Shalaby F, Ho J, Stanford WL, Fischer KD, Schuh AC, Schwartz L, Bernstein A, Rossant J. A requirement for Flk1 in primitive and definitive hematopoiesis and vasculogenesis. *Cell*. 1997;89:981-990.
3. Lambrechts D, Devriendt K, Driscoll DA, Goldmuntz E, Gewillig M, Vlietinck R, Collen D, Carmeliet P. Low expression VEGF haplotype increases the risk for tetralogy of Fallot: a family based association study. *J Med Genet*. 2005;42:519-522.
4. Bartelings, M. M. and Gittenberger-De Groot, A. C. Morphogenetic considerations on congenital malformations of the outflow tract. Part 1: Common arterial trunk and tetralogy of Fallot. *Int J Cardiol*. 32(2), 213-230. 1991.
5. Stalmans I, Lambrechts D, De Smet F, Jansen S, Wang J, Maity S, Kneer P, von der OM, Swillen A, Maes C, Gewillig M, Molin DG, Hellings P, Boetel T, Haardt M, Compennolle V, Dewerchin M, Plaisance S, Vlietinck R, Emanuel B, Gittenberger-De Groot AC, Scambler P, Morrow B, Driscoll DA, Moons L, Esguerra CV, Carmeliet G, Behn-Krappa A, Devriendt K, Collen D, Conway SJ, Carmeliet P. VEGF: a modifier of the del22q11 (DiGeorge) syndrome? *Nat Med*. 2003;9:173-182.
6. Kawasaki T, Kitsukawa T, Bekku Y, Matsuda Y, Sanbo M, Yagi T, Fujisawa H. A requirement for neuropilin-1 in embryonic vessel formation. *Development*. 1999;126:4895-4902.
7. Washington S, I, Byrd NA, Abu-Issa R, Goddeeris MM, Anderson R, Morris J, Yamamura K, Klingensmith J, Meyers EN. Sonic hedgehog is required for cardiac outflow tract and neural crest cell development. *Dev Biol*. 2005;283:357-372.
8. Kitsukawa T, Shimono A, Kawakami A, Kondoh H, Fujisawa H. Overexpression of a membrane protein, neuropilin, in chimeric mice causes anomalies in the cardiovascular system, nervous system and limbs. *Development*. 1995;121:4309-4318.
9. Miquerol L, Langille BL, Nagy A. Embryonic development is disrupted by modest increases in vascular endothelial growth factor gene expression. *Development*. 2000;127:3941-3946.
10. Enciso JM, Gratzinger D, Camenisch TD, Canosa S, Pinter E, Madri JA. Elevated glucose inhibits VEGF-A-mediated endocardial cushion formation: modulation by PECAM-1 and MMP-2. *J Cell Biol*. 2003;160:605-615.
11. Lee YM, Cope JJ, Ackermann GE, Goishi K, Armstrong EJ, Paw BH, Bischoff J. Vascular endothelial growth factor receptor signaling is required for cardiac valve formation in zebrafish. *Dev Dyn*. 2006;235:29-37.
12. Dor Y, Camenisch TD, Itin A, Fishman GI, McDonald JA, Carmeliet P, Keshet E. A novel role for VEGF in endocardial cushion formation and its potential contribution to congenital heart defects. *Development*. 2001;128:1531-1538.
13. Armstrong EJ, Bischoff J. Heart valve development: endothelial cell signaling and differentiation. *Circ Res*. 2004;95:459-470.
14. Kelly RG. Molecular inroads into the anterior heart field. *Trends Cardiovasc Med*. 2005;15:51-56.

15. Ward C, Stadt H, Hutson M, Kirby ML. Ablation of the secondary heart field leads to tetralogy of Fallot and pulmonary atresia. *Dev Biol.* 2005;284:72-83.
16. Yelbuz TM, Waldo KL, Kumiski DH, Stadt HA, Wolfe RR, Leatherbury L, Kirby ML. Shortened outflow tract leads to altered cardiac looping after neural crest ablation. *Circulation.* 2002;106:504-510.
17. Sugishita Y, Watanabe M, Fisher SA. Role of myocardial hypoxia in the remodeling of the embryonic avian cardiac outflow tract. *Dev Biol.* 2004;267:294-308.
18. Lawson ND, Vogel AM, Weinstein BM. sonic hedgehog and vascular endothelial growth factor act upstream of the Notch pathway during arterial endothelial differentiation. *Dev Cell.* 2002;3:127-136.
19. Liu ZJ, Shirakawa T, Li Y, Soma A, Oka M, Dotto GP, Fairman RM, Velazquez OC, Herlyn M. Regulation of Notch1 and Dll4 by vascular endothelial growth factor in arterial endothelial cells: implications for modulating arteriogenesis and angiogenesis. *Mol Cell Biol.* 2003;23:14-25.
20. Eldadah ZA, Hamosh A, Biery NJ, Montgomery RA, Duke M, Elkins R, Dietz HC. Familial Tetralogy of Fallot caused by mutation in the jagged1 gene. *Hum Mol Genet.* 2001;10:163-169.
21. McElhinney DB, Krantz ID, Bason L, Piccoli DA, Emerick KM, Spinner NB, Goldmuntz E. Analysis of cardiovascular phenotype and genotype-phenotype correlation in individuals with a JAG1 mutation and/or Alagille syndrome. *Circulation.* 2002;106:2567-2574.
22. Le Caignec C, Lefevre M, Schott JJ, Chaventre A, Gayet M, Calais C, Moisan JP. Familial deafness, congenital heart defects, and posterior embryotoxon caused by cysteine substitution in the first epidermal-growth-factor-like domain of jagged 1. *Am J Hum Genet.* 2002;71:180-186.
23. Timmerman LA, Grego-Bessa J, Raya A, Bertran E, Perez-Pomares JM, Diez J, Aranda S, Palomo S, McCormick F, Izpisua-Belmonte JC, de la Pompa JL. Notch promotes epithelial-mesenchymal transition during cardiac development and oncogenic transformation. *Genes Dev.* 2004;18:99-115.
24. Iso T, Hamamori Y, Kedes L. Notch signaling in vascular development. *Arterioscler Thromb Vasc Biol.* 2003;23:543-553.
25. McCright B, Lozier J, Gridley T. A mouse model of Alagille syndrome: Notch2 as a genetic modifier of Jag1 haploinsufficiency. *Development.* 2002;129:1075-1082.
26. Nosedá M, McLean G, Niessen K, Chang L, Pollet I, Montpetit R, Shahidi R, Dorovini-Zis K, Li L, Beckstead B, Durand RE, Hoodless PA, Karsan A. Notch activation results in phenotypic and functional changes consistent with endothelial-to-mesenchymal transformation. *Circ Res.* 2004;94:910-917.
27. Carmeliet P, Ng YS, Nuyens D, Theilmeier G, Brusselmans K, Cornelissen I, Ehler E, Kakkav VV, Stalmans I, Mattot V, Perriard JC, Dewerchin M, Flameng W, Nagy A, Lupu F, Moons L, Collen D, D'Amore PA, Shima DT. Impaired myocardial angiogenesis and ischemic cardiomyopathy in mice lacking the vascular endothelial growth factor isoforms VEGF164 and VEGF188. *Nat Med.* 1999;5:495-502.
28. Hierck BP, Poelmann RE, van Iperen L, Brouwer A, Gittenberger-De Groot AC. Differential expression of alpha-6 and other subunits of laminin binding integrins during development of the murine heart. *Dev Dyn.* 1996;206:100-111.
29. Vandesompele J, De Preter K, Pattyn F, Poppe B, Van Roy N, De Paepe A, Speleman F. Accurate normalization of real-time quantitative RT-PCR data by geometric averaging of multiple internal control genes. *Genome Biol.* 2002;3:research0034.1-0034.11.

30. Pfaffl MW, Horgan GW, Dempfle L. Relative expression software tool (REST) for group-wise comparison and statistical analysis of relative expression results in real-time PCR. *Nucleic Acids Res.* 2002;30:e36p1-10.
31. Gittenberger-De Groot AC, Van Den Akker NM, Bartelings MM, Webb S, Van Vugt JM, Haak MC. Abnormal lymphatic development in trisomy 16 mouse embryos precedes nuchal edema. *Dev Dyn.* 2004;230:378-384.
32. Molin DG, DeRuiter MC, Wisse LJ, Azhar M, Doetschman T, Poelmann RE, Gittenberger-De Groot AC. Altered apoptosis pattern during pharyngeal arch artery remodelling is associated with aortic arch malformations in Tgfbeta2 knock-out mice. *Cardiovasc Res.* 2002;56:312-322.
33. Vannay A, Vasarhelyi B, Kornyei M, Treszl A, Kozma G, Gyorffy B, Tulassay T, Sulyok E. Single-nucleotide polymorphisms of VEGF gene are associated with risk of congenital valvuloseptal heart defects. *Am Heart J.* 2006;151:878-881.
34. Eisenberg LM, Markwald RR. Molecular regulation of atrioventricular valvuloseptal morphogenesis. *Circ Res.* 1995;77:1-6.
35. Gittenberger-De Groot AC, Bartelings MM, DeRuiter MC, Poelmann RE. Basics of cardiac development for the understanding of congenital heart malformations. *Pediatr Res.* 2005;57:169-176.
36. Drake CJ, Wessels A, Trusk T, Little CD. Elevated vascular endothelial cell growth factor affects mesocardial morphogenesis and inhibits normal heart bending. *Dev Dyn.* 2006;235:10-18.
37. Ng YS, Rohan R, Sunday ME, Demello DE, D'Amore PA. Differential expression of VEGF isoforms in mouse during development and in the adult. *Dev Dyn.* 2001;220:112-121.
38. Mac GF, Popel AS. Differential binding of VEGF isoforms to VEGF receptor 2 in the presence of neuropilin-1: a computational model. *Am J Physiol Heart Circ Physiol.* 2005;288:H2851-H2860.
39. Sugishita Y, Leifer DW, Agani F, Watanabe M, Fisher SA. Hypoxia-responsive signaling regulates the apoptosis-dependent remodeling of the embryonic avian cardiac outflow tract. *Dev Biol.* 2004;273:285-296.
40. Zachary I. VEGF signalling: integration and multi-tasking in endothelial cell biology. *Biochem Soc Trans.* 2003;31:1171-1177.
41. Sharma PR, Anderson RH, Copp AJ, Henderson DJ. Spatiotemporal analysis of programmed cell death during mouse cardiac septation. *Anat Rec A Discov Mol Cell Evol Biol.* 2004;277:355-369.
42. Francis JC, Radtke F, Logan MP. Notch1 signals through Jagged2 to regulate apoptosis in the apical ectodermal ridge of the developing limb bud. *Dev Dyn.* 2005;234:1006-1015.
43. Pan Y, Liu Z, Shen J, Kopan R. Notch1 and 2 cooperate in limb ectoderm to receive an early Jagged2 signal regulating interdigital apoptosis. *Dev Biol.* 2005;286:472-482.
44. Waldo KL, Hutson MR, Ward CC, Zdanowicz M, Stadt HA, Kumiski D, Abu-Issa R, Kirby ML. Secondary heart field contributes myocardium and smooth muscle to the arterial pole of the developing heart. *Dev Biol.* 2005;281:78-90.
45. Mjaatvedt CH, Nakaoka T, Moreno-Rodriguez R, Norris RA, Kern MJ, Eisenberg CA, Turner D, Markwald RR. The outflow tract of the heart is recruited from a novel heart-forming field. *Dev Biol.* 2001;238:97-109.

46. Bajolle F, Zaffran S, Kelly RG, Hadchouel J, Bonnet D, Brown NA, Buckingham ME. Rotation of the myocardial wall of the outflow tract is implicated in the normal positioning of the great arteries. *Circ Res.* 2006;98:421-428.
47. Hogers B, DeRuiter MC, Gittenberger-De Groot AC, Poelmann RE. Unilateral vitelline vein ligation alters intracardiac blood flow patterns and morphogenesis in the chick embryo. *Circ Res.* 1997;80:473-481.
48. DeRuiter MC, Gittenberger-De Groot AC, Poelmann RE, VanIperen L, Mentink MM. Development of the pharyngeal arch system related to the pulmonary and bronchial vessels in the avian embryo. With a concept on systemic-pulmonary collateral artery formation. *Circulation.* 1993;87:1306-1319.

Appendix

Materials and Methods

Mouse embryos and tissue processing

All animal experiments were approved by the Animal Ethics Committee of the Leiden University and performed according to the *Guide for the Care and Use of Laboratory Animals* published by the NIH. *Vegf*^{+/+} mice were crossed to obtain *Vegf*^{120/120} embryos and *Vegf*^{+/+} wild-type littermates. The morning of the vaginal plug was stated embryonic day (E)0.5. Pregnant females were sacrificed by cervical dislocation. The embryos were isolated and either snap-frozen in liquid nitrogen or fixed in 4% paraformaldehyde/phosphate-buffered saline (0.1 Mol/L, pH 7.4), dehydrated and embedded in paraffin. In total, 34 *Vegf*^{+/+} and 47 *Vegf*^{120/120} embryos ranging from E10.5 to E19.5 were embedded in paraffin and used for microscopic analyses. Of the snap-frozen embryos (12 *Vegf*^{+/+} and 13 *Vegf*^{120/120} embryos of E14.5, E16.5 or E18.5) hearts were dissected and veins and great arteries were removed and stored in RNAlaterice (Ambion, Cambridgeshire, UK) at -80 °C before use for RT-qPCR.

Immunohistochemistry

Paraffin sections of 5 µm were deparaffinated and antigen retrieval was performed by heating the sections (12 minutes to 98° C) in citric acid buffer (0.01 Mol/L, pH 6.0) in several cases (Table A1). Inhibition of endogenous peroxidase was performed by incubating the sections for 20 minutes in PBS with 0.3% H₂O₂. Incubation with primary antibody (Table A1) was performed overnight, after which sections were incubated for 1 hour with peroxidase-labeled antibody (rabbit-anti-mouse; P0260, DAKO, Glostrup, Denmark) or biotin-labeled secondary antibody (goat-anti-rabbit (BA-1000), horse-anti-mouse (BA-2000) and horse-anti-goat (BA-9500), all Vector Labs, Burlingame, USA). In case of the cleaved Notch1 staining, the CSA-II kit (K1497, DAKO, Glostrup, Denmark) was used for amplification. When using biotin-labeled antibody, additional incubation with the Vectastain ABC staining kit (PK-6100, Vector Labs, Burlingame, USA) was performed for 45 minutes. For the detection of apoptosis, the Terminal deoxynucleotidyl Transferase Biotin-dUTP Nick End Labeling (TUNEL)-kit was used according to manual (1684817, Roche/Boehringer Mannheim, Basel, Switzerland), followed by anti-FITC antibody (1772465, Roche/Boehringer Mannheim, Basel, Switzerland). Visualisation was performed with the DAB-procedure and Mayer's hematoxylin was used as a counterstaining. The sections were mounted with Entellan (1.07961.0100, Merck, Darmstadt, Germany). Differences between genotypes were scored as such when this was shown per immunostaining at least in 3 different embryos per genotype per age-group. An extensive description of the primary antibodies used is listed in Table A1. When omitting the primary antibodies, no signal was detected. In case of the Notch1 and Jagged2 antibodies, additional characterisation was performed using preincubation of the primary antibody with competing peptide, which led to loss of signal (see Figure A1).

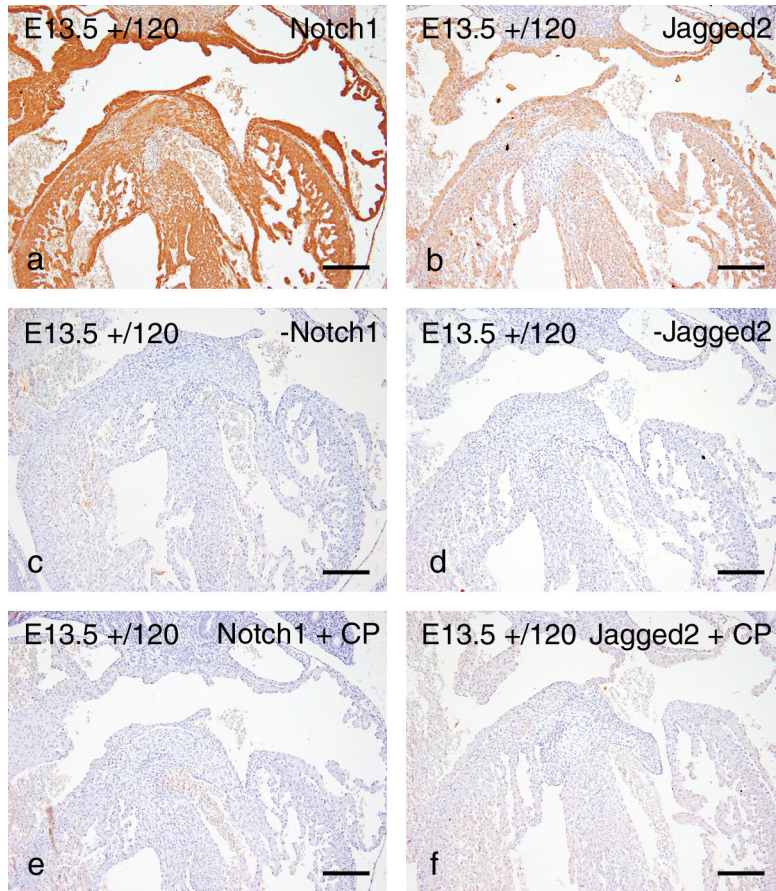


Figure A1. Characterisation of the anti-Notch1 and anti-Jagged2 antibodies using competing peptides. The stainings performed are indicated in the upper right corner. All stainings have been performed on a *Vegf*^{+/120} mouse embryo of E13.5. The staining is performed according to the protocols described. Figure a and b are the positive controls while Figure c and d show sections in which the primary antibody has been omitted. Figure e and f present sections incubated with primary antibody preincubated with 75x competing peptide (CP). Scale bar = 200 μ m.

In situ hybridisation

Sense and anti-sense ³⁵S-radiolabeled *Vegf-A* RNA probes were transcribed using a 451-bp clone encoding for the mouse *Vegf120*-isoform (pVEGF2; kindly provided by Dr. G. Breier, University of Technology, Dresden, Germany). To obtain sense and antisense ³⁵S-labeled riboprobes, the clones were linearized and transcribed with T7 or T3 RNA-polymerase, respectively. Radioactive in situ hybridisation (ISH) was performed¹. In brief, after hybridisation, sections were dehydrated in graded ethanol, air-dried, coated with Ilford G5 emulsion (ILFORD, Ltd., Mobberly, England), and exposed (14 days at 4 °C). Subsequently, the slides were developed in Kodak D19 developing solution (Kodak, Chalon s. Saone, France) for 4 minutes at room temperature, rinsed in distilled water, and fixed in Ilford Hypam fixative (ILFORD, Ltd.). Sections were briefly counterstained with Mayer's hematoxylin, dehydrated, and mounted with Malinol (Schmid & Co, Stuttgart-Untertürkheim, Germany). The sections were examined by light microscopy using darkfield optics.

RT-qPCR

Prior to total RNA isolation the tissues were disrupted using a micro-pestle (Kleinfeld Labortechnik, Gehrden, Germany) in Qiagen RLT buffer (Qiagen, Hilden, Germany). After samples were homogenized total RNA was isolated using the RNeasy mini kit (QIAGEN). Samples with sufficient RNA quality (OD_{260/280} > 1.9 and a RIN >7.5) were approved for analysis. A total of 100 ng total RNA sample was subjected to reverse transcription (RT). RT-qPCR was performed by using Superscript™III Platinum Two-step qRT-PCR kit and SYBR green (Invitrogen, Paisley, UK) with a primer concentration of 10 μM. Primers were designed with Oligoperfect™ Designer (Invitrogen), Primer3 and Mfold (<http://www.idtdna.com/scitools/Applications/mfold/>) and synthesized by Eurogentec (Seraing, Belgium). qPCR reactions were run on a MyiQ Single-Color Real-Time PCR Detection System (Bio-Rad, Veenendaal, the Netherlands). All samples were normalized for input based on two normalizing genes, *β-actin* and *Gapdh*. The qPCR efficiency of all primers was tested and included in the data analysis. Data analyses were performed using an Excel spreadsheet based on geNorm (Relative expression with error propagation)². Statistic significance was tested using randomization testing as provided in the REST2005 program³. Samples with a p-value <0.05 were regarded to be significant different between the groups. Primer sequences are shown in Table S2.

Table A1. Characteristics of primary antibodies used for immunohistochemistry.

Antibody	Cat. no. (company)	Antigen retrieval	ABC	CSA-II kit (DAKO)	Reference
α -SMA (1A4)	A2547 (Sigma-Aldrich, Missouri, USA)	Yes	No	No	Skalli et al ⁴
VEGFR-2	AF644 (R&D Systems, Minneapolis, USA)	Yes	Yes	No	rndsystems.com
p-VEGFR-2	Sc-16628 (Santa Cruz, Santa Cruz, USA)	No	Yes	No	Becker et al ⁵
Notch1	sc-6014-R (Santa Cruz, Santa Cruz, USA)	No	Yes	No	Sestan et al ⁶
cleaved Notch1	2421 (Cell Signaling, Beverly, MA, USA)	Yes	No	Yes	Tanaka et al ⁷
Notch2	sc-5545 (Santa Cruz, Santa Cruz, USA)	No	Yes	No	Okuyama et al ⁸
Jagged1	sc-6011 (Santa Cruz, Santa Cruz, USA)	Yes	Yes	No	Sestan et al ⁶
Jagged2	sc-8158 (Santa Cruz, Santa Cruz, USA)	No	Yes	No	Rivolta et al ⁹
VEGF	sc-507 (Santa Cruz, Santa Cruz, USA)	No	Yes	No	Seo et al ¹⁰
α γ -MA (HHF35)	M0635 (DAKO, Glostrup, Denmark)	No	Yes	No	Tsukada et al ¹¹

Table A2. Primer sequences used for RT-qPCR.

Gene	Forward	Reverse
<i>β-actin</i> (NM_007393)	5'- actctatgtgggacgag -3'	5'- ccagatcttccatgctg -3'
<i>Gapdh</i> (BC083149)	5'- aagtgagattgtccatc -3'	5'- cgtgagggagtcatactgg -3'
<i>Vegfa</i> (ENSMUST00000071648)	5'- gtcagagacaatcacca -3'	5'- catctctgtgctgtaggaa -3'
<i>Vegf120</i>	5'- aaagccagacataggagag -3'	5'- ggcttgacattttctgg -3'
<i>Vegf164</i>	5'- gaacaagccagaaatcacctg -3'	5'- cgagctgtrtttgcaggaa -3'
<i>Vegf188</i>	5'- ggtttaaatcctggagcgttca -3'	5'- cgagctgtrtttgcaggaa -3'

References

1. Hierck BP, Poelmann RE, van Iperen L, Brouwer A, Gittenberger-De Groot AC. Differential expression of alpha-6 and other subunits of laminin binding integrins during development of the murine heart. *Dev Dyn.* 1996;206:100-111.
2. Vandesompele J, De Preter K, Pattyn F, Poppe B, Van Roy N, De Paepe A, Speleman F. Accurate normalization of real-time quantitative RT-PCR data by geometric averaging of multiple internal control genes. *Genome Biol.* 2002;3:research0034.1-0043.11.
3. Pfaffl MW, Horgan GW, Dempfle L. Relative expression software tool (REST) for group-wise comparison and statistical analysis of relative expression results in real-time PCR. *Nucleic Acids Res.* 2002;30:e36p1-10.
4. Skalli O, Ropraz P, Trzeciak A, Benzouana G, Gillessen D, Gabbiani G. A monoclonal antibody against alpha-smooth muscle actin: a new probe for smooth muscle differentiation. *J Cell Biol.* 1986;103:2787-2796.
5. Becker PM, Waltenberger J, Yachechko R, Mirzapooiazova T, Sham JS, Lee CG, Elias JA, Verin AD. Neuropilin-1 regulates vascular endothelial growth factor-mediated endothelial permeability. *Circ Res.* 2005;96:1257-1265.
6. Sestan N, Artavanis-Tsakonas S, Rakic P. Contact-dependent inhibition of cortical neurite growth mediated by notch signaling. *Science.* 1999;286:741-746.
7. Tanaka M, Marunouchi T. Immunohistochemical localization of Notch receptors and their ligands in the postnatally developing rat cerebellum. *Neurosci Lett.* 2003;353:87-90.
8. Okuyama R, Nguyen BC, Talora C, Ogawa E, Tommasi d, V, Lioumi M, Chiorino G, Tagami H, Woo M, Dotto GP. High commitment of embryonic keratinocytes to terminal differentiation through a Notch1-caspase 3 regulatory mechanism. *Dev Cell.* 2004;6:551-562.
9. Rivolta MN, Halsall A, Johnson CM, Tones MA, Holley MC. Transcript profiling of functionally related groups of genes during conditional differentiation of a mammalian cochlear hair cell line. *Genome Res.* 2002;12:1091-1099.
10. Seo MS, Okamoto N, Viores MA, Viores SA, Hackett SF, Yamada H, Yamada E, Derevjani NL, LaRochelle W, Zack DJ, Campochiaro PA. Photoreceptor-specific expression of platelet-derived growth factor-B results in traction retinal detachment. *Am J Pathol.* 2000;157:995-1005.
11. Tsukada T, Tippens D, Gordon D, Ross R, Gown AM. HHF35, a muscle-actin-specific monoclonal antibody. I. Immunocytochemical and biochemical characterization. *Am J Pathol.* 1987;126:51-60.

Chapter 3

Developmental Coronary Maturation is Disturbed by Aberrant Cardiac VEGF-expression and Notch-signaling

Nynke M.S. van den Akker¹, Vincenza Caolo², Lambertus J. Wisse¹, Patricia P.W.M. Peters², Robert E. Poelmann¹, Peter Carmeliet^{3,4}, Daniël G.M. Molin^{1,2}, Adriana C. Gittenberger-de Groot¹

¹Department of Anatomy and Embryology, Leiden University Medical Center, Leiden, The Netherlands; ²Department of Physiology, CARIM, Maastricht University, Maastricht, The Netherlands; ³Center for Transgene Technology and Gene Therapy, KU Leuven, Leuven, Belgium; ⁴Department of Transgene Technology and Gene Therapy, VIB, Leuven, Belgium.

Modified after Cardiovascular Research, 2008, In Press.

Developmental Coronary Maturation is Disturbed by Aberrant Cardiac VEGF-expression and Notch-signaling

Abstract

Currently, many potential cardiac revascularization therapies target the vascular endothelial growth factor (VEGF)-pathway, with variable success. Knowledge regarding the role of the VEGF/Notch/ephrinB2-cascade in (ab)normal coronary development will provide information on the subtle balance of VEGF-signaling in coronary maturation and might enhance our therapeutic possibilities. The effect of VEGF-isoforms on coronary development was explored in vivo using immunohistochemistry and RT-qPCR on *Vegf120/120* mouse embryos, solely expressing VEGF120. In vitro, human arterial coronary endothelial cells were treated with VEGF121 or VEGF165 upon which RT-qPCR was performed. In vivo, mutant coronary arterial endothelium showed a decrease in protein expression of arterial markers such as cleaved Notch1, Delta-like4 and ephrinB2 concomitant with an increase of venous markers such as chicken ovalbumin upstream promoter transcription factor II. The venous endothelium showed the opposite effect, which was confirmed on mRNA-level. In vitro, mRNA-expression of arterial markers highly depended on the VEGF-isoform used, with VEGF165 having the strongest effect. Also, coronary arteriogenesis was anomalous in the mouse embryos with decreased arterial and increased venous medial development as shown by staining for smooth muscle α -actin, Delta-like1 and Notch3. We demonstrate that VEGF-isoform related spatiotemporal cardiac alterations in the VEGF/Notch/ephrinB2-cascade lead to disturbed coronary development. This knowledge can contribute to optimizing therapies targeting VEGF-signaling by enabling balancing between angiogenesis and vascular maturation.

Introduction

Morphological diversity between different populations of endothelial cells (ECs) has long been recognized to relate to functional variation and as such proper physiology. More recently, differential expression profiles between arterial, microcirculatory, venous and lymphatic endothelial populations have been described¹, further underscoring endothelial diversity. Both intrinsic and microenvironmental differences are instructive for these endothelial characteristics². Abnormalities can lead to endothelial dysfunction and subsequent pathogenesis, as found for maternal diabetes-related fetal endothelial dysfunction³, increased nuchal translucency⁴, and tumor angiogenesis⁵ but also for coronary atherosclerosis⁶ and adult venous bypass graft disease⁷.

Numerous factors associate with endothelial functioning in processes such as vasculogenesis, angiogenesis and arteriogenesis, with one of the key factors being vascular endothelial growth factor (VEGF)⁸. Therefore, it is not surprising that many potential therapies for ischemic cardiovascular disease target VEGF, although clinical success is less than expected⁸. VEGF exerts its main effects through binding to the VEGF receptor VEGFR-2⁸. Its coreceptor neuropilin-1 (NP-1) can enhance this effect⁹. VEGF-signaling can upregulate members of the Delta-like/Jagged/Notch-family, proteins highly important in cardiovascular development^{10;11}. Several members of this family are specifically expressed by arterial ECs, including Notch1, Notch4 and Delta-like4 (Dll4)¹². Upon stimulation of the Notch-receptor, its cytoplasmic domain becomes cleaved and translocated to the nucleus. There, it forms a complex with other nuclear proteins, which upregulates transcription of Notch-signaling specific transcription factors (i.e. Hes, Hey). These can enhance arterial EC-specific ephrinB2-expression¹⁰, suggesting a role for the VEGF/Notch/ephrinB2-cascade in arterial differentiation¹¹.

The development of the coronary vasculature is of eminent importance for the final phases of cardiogenesis. Disbalance in these processes might lead to a dysfunctional vascular bed which will predispose for coronary diseases. Coronary development starts with the occurrence of a subepicardially located primitive endothelial network. This becomes connected to the systemic circulation downstream to the right atrium and upstream to the ascending aorta through coronary orifices at the level of the left and right sinus of the semilunar valves¹³. After connection to the circulation is established, arterial differentiation of the most proximal ECs becomes obvious and, subsequently, arteriogenesis is stimulated by inducing vascular smooth muscle cell (vSMC) migration and differentiation^{13;14}. In the coronary system, vSMCs are mainly recruited from the population of epicardium-derived cells (EPDCs), which arises through epithelial-to-mesenchymal transformation of cells of the epicardium¹⁵. In addition, microcirculatory and venous endothelial differentiation and remodeling of the primitive endothelial network into a fully functional coronary system will take place.

We recently described the *Vegf120/120* mouse model that solely expresses the non-heparin binding isoform VEGF120. Structural cardiac abnormalities such as Tetralogy of Fallot (TOF) were found concomitant with alterations in VEGF and Notch-signaling^{16;17}.

This mouse model presents postnatally with impaired myocardial angiogenesis¹⁸ and altered retinal arterio-venous differentiation¹⁹. In this paper, we show that changes in spatiotemporal distribution of VEGF and Notch-signaling -due to altered VEGF-isoform expression in *Vegf120/120* embryos- lead to anomalous coronary EC differentiation and disturbed arteriogenesis.

Materials and Methods

Mouse Experiments

All animal experiments were approved by the Animal Ethics Committee of the Leiden University and executed according to the *Guide for the Care and Use of Laboratory Animals* published by the US National Institute of Health (NIH Publication No. 85-23, revised 1996). For an extensive description of mouse experiments see¹⁷.

Immunohistochemistry, in situ hybridisation and microscopy

Immunohistochemistry was performed as described¹⁷. In short, immunohistochemistry was carried out on sections of 5 µm of 4% PFA/0.01 Mol/L phosphate buffered fixed, paraffin embedded tissue. Antigen retrieval was achieved either by heating the sections (12 minutes to 98° C) in citric acid buffer (0.01 Mol/L, pH 6.0) or by incubating them for 6 minutes in 0.1 mg/mL Pronase E (1.07433.0001, Merck, Darmstadt, Germany) in PBS. Visualization was performed with the DAB-procedure and Mayer's hematoxylin was used as a counterstaining. Differences between genotypes were scored per immunostaining in at least 3 different embryos per genotype per age-group (i.e. E10.5-E14.5 or E15.5-E19.5) that were processed within one and the same experiment. The primary antibodies were checked for false positive signals. An extensive description of the primary antibodies used is listed in Table A1. The anti-Notch4-antibodies listed in Table A1 were tested to bind aspecific to the material used and therefore no characteristics were mentioned. For in situ hybridisation, sense and anti-sense ³⁵S-radiolabelled *Vegf-A* RNA probes were transcribed using a 451-bp clone encoding for the mouse *Vegf-120* isoform (pVEGF2; kindly provided by Dr. G. Breier, University of Technology, Dresden, Germany). Micrographs were made using an Olympus AX70-microscope fitted with Olympus UPlanApo-objectives (Olympus, Tokyo, Japan). The camera used was an Olympus DP12 and micrographs were fitted into a panel using Adobe Photoshop CS2 (Adobe, San Jose, USA).

3D-reconstructions

3D-reconstructions were performed as described⁴. In short, micrographs were made of E18.5 wild-type and *Vegf120/120* hearts and converted to 3D using ResolveRT™-software (Template Graphics Software Inc., San Diego, USA).

Morphometry

For morphometry, VEGFR-2 stained sections of 8 embryos (4 *Vegf*^{+/+} and 4 *Vegf120/120*; E17.5-E19.5) were used. To calculate the total heart volume and the ratio myocardial to vascular volume, we performed volume measurements for total heart volume, myocardium and coronary veins/microvasculature using the Cavalieri method²². Statistical analysis was performed using a Mann-Whitney test with SPSS 11.0 (SPSS Inc., Chicago, USA) software.

Cell culture

Human coronary artery endothelial cells (HCAECs) were obtained from Cambrex (Verviers, Belgium) and cultured according to the protocol of the manufacturer. Cells at passage 9 were seeded at a density of 3500 cells/cm² and cultured to a 70% subconfluent monolayer in EGM-2-MV BulletKit without bFGF and VEGF165 supplemented with 5% Fetal Bovine Serum (Cambrex). Subsequently, HCAECs were stimulated for 24 hours with 100 ng/mL recombinant human VEGF165 or VEGF121 (ReliaTech GmbH, Braunschweig, Germany). Cells were harvested according to the manufacturer's protocol using a trypsin/EDTA and a Trypsin neutralization solution (Cambrex). Cell number was determined using trypan blue dye and the Neubauer improved chamber method. mRNA was isolated as described below. Per sample, 100,000-140,000 cells were harvested. Samples stimulated with either VEGF165 or VEGF121 provided higher cell numbers than unstimulated samples (cultured without VEGF).

RT-qPCR

Total RNA from triplicate HCAEC cultures or from cardiac tissue of E18.5 wild-type and *Vegf120/120* embryos (n=3 per group) was isolated by using the RNeasy micro-kit Qiagen with DNase treatment (Qiagen, GmbH, Hilden, Germany). Sample with sufficient RNA quality (OD260/280>1.9, RIN>7.5) and content were approved for analysis. A total of 100 ng total RNA per sample was subjected to reverse transcription (RT). qPCR was performed by using SuperscriptTMIII Platinum Two-step qRT-PCR kit with SYBR green (Invitrogen, Paisley, UK) and primer concentration of 10 μM. qPCR reactions were run on a MyiQ Single-Color Real time PCR detection System (Bio-Rad, Veenendaal, the Netherlands). Primers were designed with oligoperfectTM Designer (Invitrogen), Primer3 and Mfold (<http://www.idtdna.com/scitools/Application/mfold/>) and were synthesized by Eurogentec (Seraing, Belgium). All primers used met the requested qPCR efficiency (between 80-105%) and were found to be gene-specific. Primer sequences are found in Table A2. Data analysis was performed using a Microsoft Excel spreadsheet based on the qBase program²¹. Statistic significance was determined by applying one-way ANOVA/Tukey (SigmaStat v2.03, Systat Software, San Jose, USA) testing. Sample with a probability value (p) <0.05 were regarded to be significant different between groups. HCAEC samples were normalized for input based on both *β-ACTIN* and *GADPH*-values. For the E18.5 embryos normalization was based on the pan-endothelial marker *Tie2*. No significant differences were found for *Tie2* between wild-type and *Vegf120/120* littermates as determined after normalization for *β-actin* and *Gapdh* expression (correction for cDNA input). Using immunohistochemistry, no altered myocardial expression of the genes investigated was found. Myocardial Notch4-expression was not determined due to aspecific binding of the antibodies tested (see Table A1), however, Notch4 has been reported to be highly selective for ECs during development²².

Results

Anomalous coronary morphology in Vegf120/120 mouse embryos

In line with literature on murine coronary development²³, the first appearance of coronary ECs and vessels was seen at E11.5 when using an α -VEGFR-2-staining for visualization of the ECs. We observed that at this stage, primitive coronaries already connected (in)directly to the right atrium in all embryos, suggesting normal coronary development in mutant embryos (Figures 1A-B,E,H). However, abnormally large coronary veins were discerned in 22/33 early-stage (E11.5-E13.5) mutant cases (Figure 1A-B,F-G).

In wild-type embryos, two definitive coronary orifices, originating from the left and right aortic sinus respectively, were observed in 24/24 cases of E15.5 and older. In contrast, only 15/28 *Vegf120/120* embryos of these stages presented with 2 coronary orifices, whereas others showed solely one (2/28), three (7/28) or in one case four orifices (1/28 and Table 1). After formation of the coronary orifices, maturation of coronary arteries was obvious in normal embryos. In 22/28 mutant embryos between E15.5 and E19.5, arteriogenesis was severely impaired (Table 1; Figure 1C-D). Half of the mutant embryos showed abnormalities in anatomy of the primary coronary branches (Table 1; Figure 1C-D), with the main artery supplying the interventricular septum (IVS) either having its own coronary orifice and/or originating from the left instead of the right sinus, which is normal²⁴. All embryos in which the IVS-branch originated (in)directly from the left sinus were previously diagnosed with TOF (5/28)¹⁷. For a more detailed description of the abnormalities in coronary branching patterns we refer to the appendix of this chapter.

In 50% of E15.5-E19.5 *Vegf120/120* embryos (14/28) enlarged coronary veins (Table 1; Figure 1J-K), already evident at earlier stages, and enlarged cardiac lymphatics (16/28; Table 1; Figure 1L-M), visualized using staining for LYVE-1 of which expression is specific for lymphatic ECs, were encountered. Also, in late stage embryos, ventriculo-coronary arterial communications (VCACs) and/or coronary arterio-venous shunts were evident (Table 1; Figure 1N,O). Arterio-venous shunts between the aortic arch and vena cava superior were found in 3 cases (all E19.5; Figure 1P).

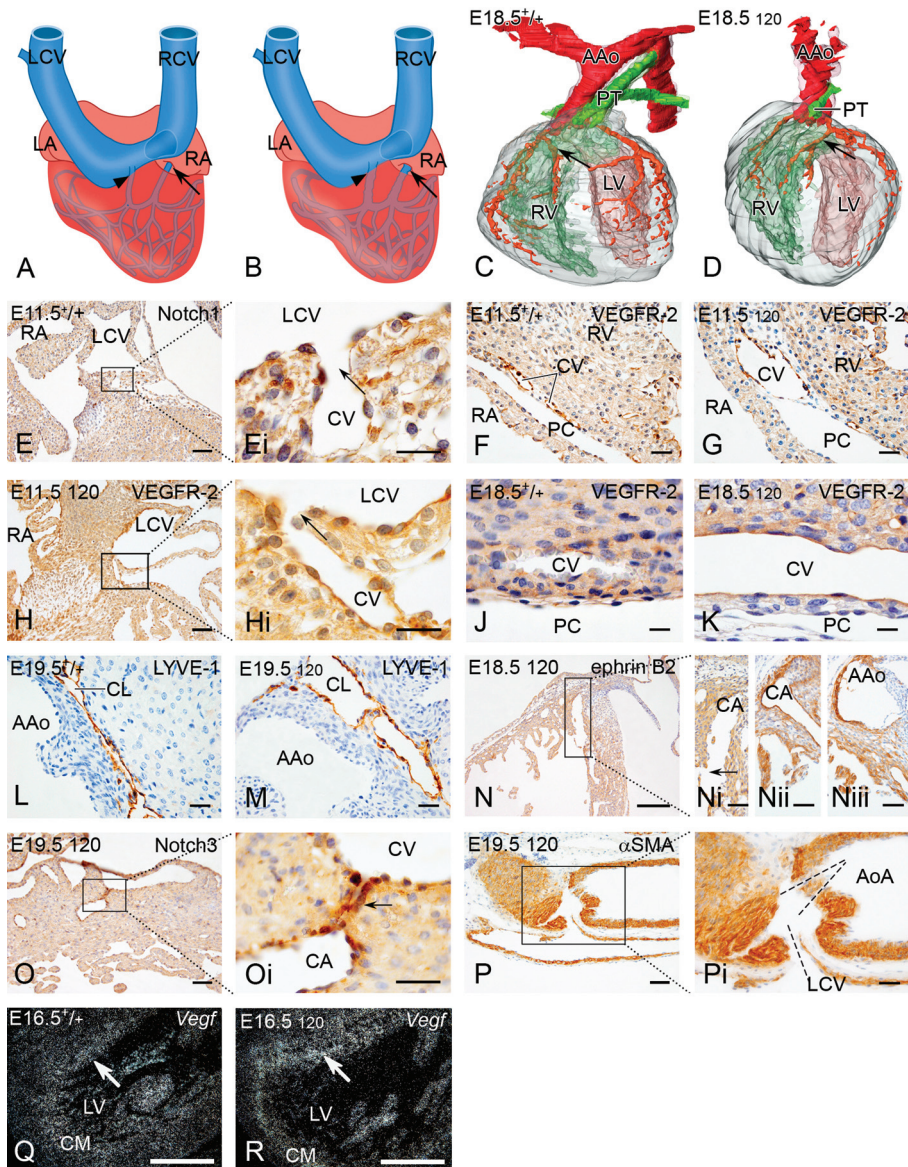
Table 1. Coronary abnormalities in Vegf120/120 embryos of E15.5-E19.5.

Coronary Anomaly	No/Total	%
Abnormal number of coronary orifices	10/28	36
< 2	2/28	7
> 2	8/28	29
Small coronary arteries	22/28	79
Abnormal origin IVS-branch	14/28	50
Large coronary veins	14/28	50
Large cardiac lymphatics	16/28	57
Increased microvascular density	17/28	61
VCAC	10/28	36

IVS = interventricular septum; VCAC = ventriculo-coronary artery communication

Spatiotemporal distribution of Vegf in normal and mutant embryonic hearts

During early cardiac development (E10.5-E14.5), the distribution of *Vegf*-expression has been described before¹⁷ and is likely mainly related to myocardial and to a lesser extent to coronary development. In later stages (E16.5 and older) the predominant area of *Vegf*-expression was confined to the borderline of compact to trabecular myocardium, overlapping with the region where prominent coronary angiogenesis and arteriogenesis takes place at this stage²⁵. *Vegf*-levels in this area were increased in *Vegf120/120* embryos (Figure 1Q-R).



Loss of coronary venous endothelial differentiation in Vegf120/120 embryos

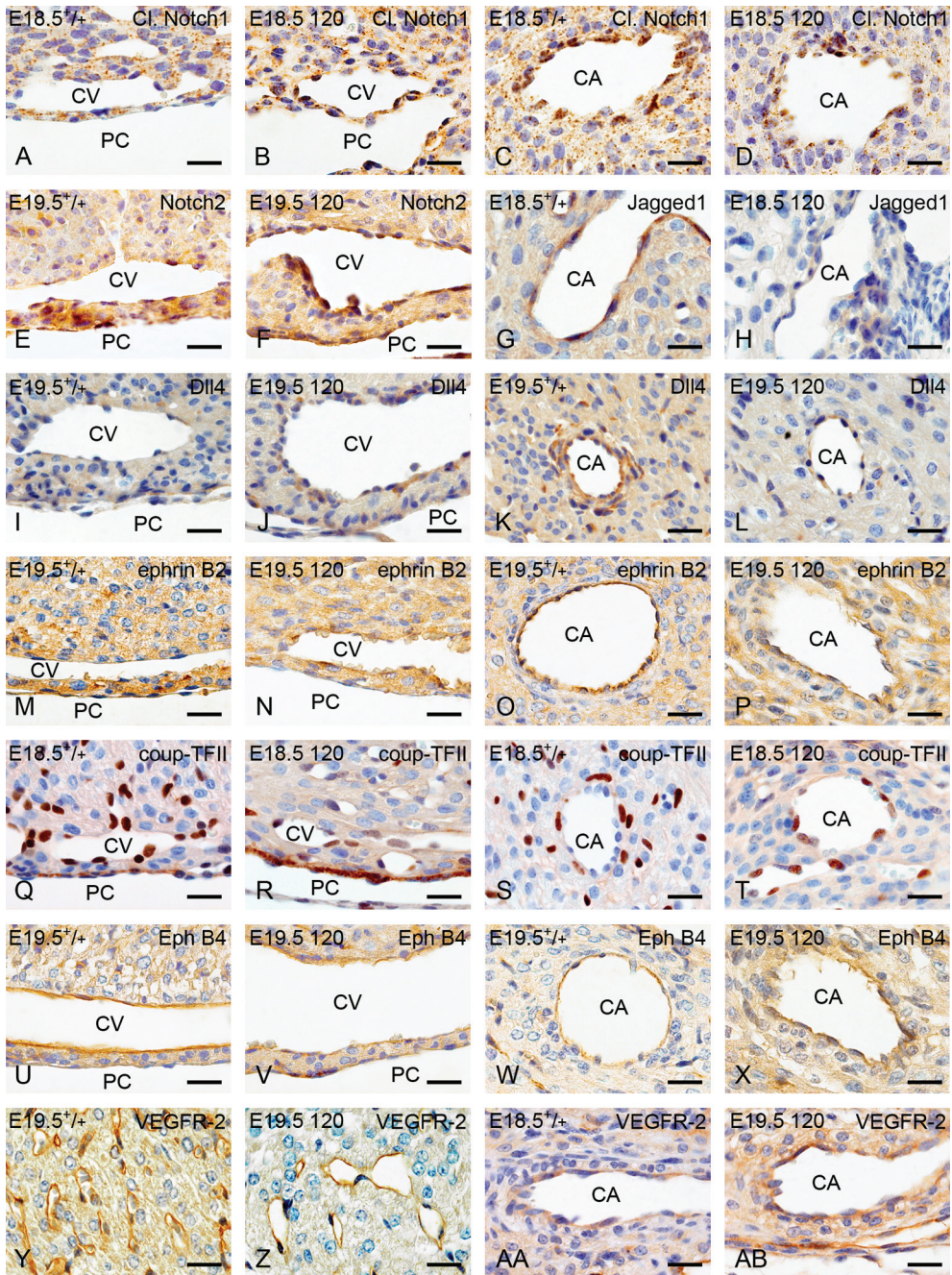
Besides morphological differences in mutant veins, abnormal differentiation of coronary venous ECs was clearly distinguishable from E15.5 onwards (Table A3). High expression per EC of VEGFR-2 was still seen at later stages of development (Figure 1J-K), together with anomalous expression of arterial markers including cleaved (nuclear/activated) Notch1, Notch2, Dll4 and ephrinB2 (Figure 2A-B,E-F,I-J,M-N), suggesting increased VEGF and Notch-signaling per EC. Expression of the venous EC-markers chicken ovalbumin upstream promoter transcription factor II (COUP-TFII) and EphB4 (Figure 2Q-R,U-V) was clearly reduced in mutant coronary venous ECs.

RT-qPCR, normalized for endothelial-specific *Tie2*-expression, was performed on whole hearts of either wild-type mouse embryos or *Vegf120/120* littermates of E18.5. A significant increase of *Notch1*, *Notch4* and *Hes1* mRNA-levels could be found (Figure 3A). Furthermore, a significant decrease in *Ephb4* mRNA was obvious, while a positive trend was noticed for expression of *Dll4* and *Hey1* (Figure 3A).

Abnormalities in mutant coronary microvasculature

Not only the coronary veins, but also the capillaries were enlarged and dilated in *Vegf120/120* embryos (Figure 2Y-Z). To quantify these differences morphometry was performed on late-stage embryos. Total heart volumes did not differ significantly between groups (data not shown). The ratio myocardial to coronary vascular volume was significantly decreased in mutant mouse embryos with a p-value of 0.021 (Figure 3B). The differentiation of microvascular ECs in *Vegf120/120* mouse embryos, however, was indistinguishable from normal.

← *Figure 1. Abnormal coronary and aortic arch morphology and Vegf-distribution in Vegf120/120 embryos.* Wild-type (+/+) and mutants (120) are compared (upper left corner, age in embryonic days (E)) with the staining indicated upper right. At E11.5, a direct (arrow) and an indirect via the left cardinal vein (LCV; arrowhead) connection between the coronary system and the right atrium (RA) are seen in +/+ and 120 embryos (schematic drawings in A and B, respectively). The indirect connection is also shown in E (+/+) and H (120) and arrows in Ei and Hi. The stainings indicated in E and H do not correspond, as differentially stained sections had to be chosen due to the fact that the connection can only be seen in a very small area of the embryos. Mutant coronary arteries are smaller and reveal abnormal morphology of the main branches (arrows in C-D), especially in embryos with TOF (D). Both the aortic arch (AoA) and coronary arteries are shown in red, the pulmonary trunk (PT) in green. At E11.5, an increase in size of the coronary veins (CV) is seen in mutant embryos (compare F and G). This is maintained throughout development (J-K). An increase in size of cardiac lymphatics (CL), as visualized using a staining for the lymphatic EC-specific marker LYVE-1, is obvious (L-M). In mutant embryos, ventriculo-coronary artery connections (VCAC), visualized using an ephrinB2-staining (N-Niii; with Nii being a consecutive section of Ni stained for α SMA and Niii a section 35 μ m caudal from Nii) and arterio-venous shunts in both the coronary system visualized using a Notch3-staining (O and arrow in Oi) and the AoA (P and dotted lines in Pi) were seen. Locally increased levels of *Vegf*-mRNA are observed in mutant embryos (arrows in Q-R). Abbreviations: AAo = ascending aorta; CA = coronary artery; CM = compact myocardium; LA = left atrium; LV = left ventricle; PC = pericardial cavity; RCV = right cardinal vein; RV = right ventricle. Scale bar = 60 μ m (E,H,Ni-P); 20 μ m (Ei,Hi,Oi); 30 μ m (F-G,J-K,L-M); 200 μ m (N,Pi,Q-R).



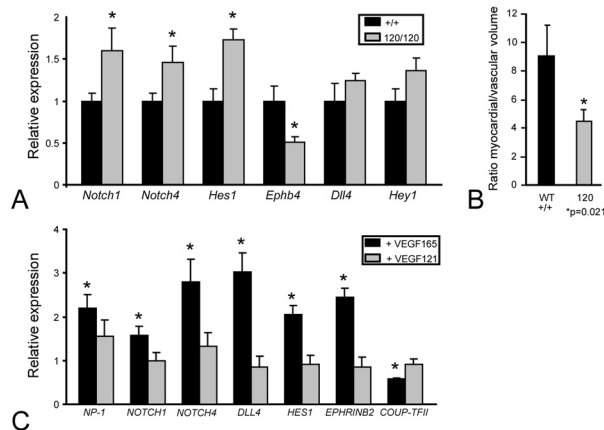


Figure 3. Quantification of alterations in mRNA expression *in vivo* and *in vitro* with regard to VEGF-isoforms and abnormalities in microvascular density in *Vegf120/120* embryos. A significant (*) increase in *Notch1*, *Notch4* and *Hes1*, a significant decrease in *Ephb4* and a trend in increase of *Dll4* and *Hey1* mRNA expression is seen when performing RT-qPCR normalized for *Tie2* on mRNA isolated from wild-type (+/+) and mutant (120) hearts of E18.5 (A). Using morphometry, a significant difference ($p = 0.021$) in myocardial/vascular volume is found (B). When human coronary arterial ECs (HCAECs) are cultured with VEGF165 or VEGF121, it is obvious that VEGF165 can while VEGF121 cannot significantly increase expression of arterial markers (*NP-1*, *NOTCH1*, *NOTCH4*, *DLL4*, *HES1* and *EPHRINB2*) and decrease expression of the venous marker *COUP-TFII* when compared with HCAECs cultured without VEGF (of which expression is set to 1) (C).

*Coronary arterial endothelial differentiation is impaired in *Vegf120/120* embryos*

In mutant embryos of E15.5 and older, obvious differences in differentiation of coronary arterial ECs were observed (Table A3). Protein expression levels indicative for arterial maturation, including cleaved Notch1, Jagged1, Dll4, and ephrinB2 (Figure 2C-D,G-H,K-L,O-P) were lower per EC, suggesting decreased Notch-signaling. Increased expression per EC of the venous markers COUP-TFII and EphB4 (Figure 2S-T,W-X) was observed. Due to lack of Notch4-specific antibodies its expression profiles could not be determined (see information in the appendix of this chapter). Although arterial endothelial VEGFR-2-expression normally decreased upon induction of Notch-signaling²⁶, this decrease was much less prominent in mutant embryos (Figure 2AA-AB).

← **Figure 2.** *Abnormal EC-differentiation and microvascular morphology in *Vegf120/120* embryos.* Stainings performed are indicated in the upper right corner and the genotype (+/+ wild-type and 120 mutant) and age in embryonic days (E) upper left. ECs of the mutant coronary veins (CV) showed an increase in staining per cell for arterial markers cleaved Notch1 (A-B), Notch2 (E-F), Dll4 (I-J) and ephrinB2 (M-N) and a decrease for the venous markers COUP-TFII (Q-R) and EphB4 (U-V). Increased capillary size is seen (Y-Z). ECs of the coronary arteries (CA) show decreased expression of cleaved Notch1 (C-D), Jagged1 (G-H), Dll4 (K-L) and ephrinB2 (O-P) concomitant with an increase in COUP-TFII (S-T), EphB4 (W-X) and VEGFR-2-expression (AA-AB). Abbreviations: Cl. Notch1 = cleaved Notch1; PC = pericardial cavity. Scale bars = 20 μ m.

To determine whether differences in arterial marker expression were VEGF-isoform related, expression of differentiation-specific markers (i.e. arterial; *NP-1*, *NOTCH1*, *NOTCH4*, *DLL4*, *HES1*, *EPHRINB2* and venous; *COUP-TFII*) was analyzed in HCAECs in vitro. RT-qPCR on HCAECs cultured with or without VEGF165 or VEGF121 showed that VEGF121 was much less able to affect expression than VEGF165. VEGF165 significantly induced expression levels of arterial markers and decreased expression of *COUP-TFII* (Figure 3C).

Abnormal arteriogenesis is evident in Vegf120/120 mouse embryos

Anomalous coronary endothelial differentiation observed in mutant mouse embryos was concomitant with abnormal arteriogenesis. Coronary arteries of mutant embryos of E15.5 and older showed a decrease in medial development with a reduction in number of medial cells and abnormal morphologic and differentiation characteristics as evident by staining for the SMC-marker α SMA (Figure 4A-B). The spatiotemporal protein expression of NP-1, Dll1, Jagged2 and Notch3 was analyzed and a decrease in number of cells positive for these markers was seen in the medial layer of the coronary arteries of mutant embryos (Figures 4E-F,I-J,M-N,Q-R). In contrast, the coronary veins of mutant embryos were surrounded by a larger number of α SMA positive cells when compared with wild-type littermates (Figure 4C-D). These cells were also positive for the SMC-related markers NP-1, Dll1 and Jagged2 (Figures 4G-H,K-L,O-P). Additionally, the pericyte-coverage of the coronary microvasculature as determined by Notch3-staining showed a marked decrease in number of positive cells in mutant mouse embryos (Figure 4S-T).

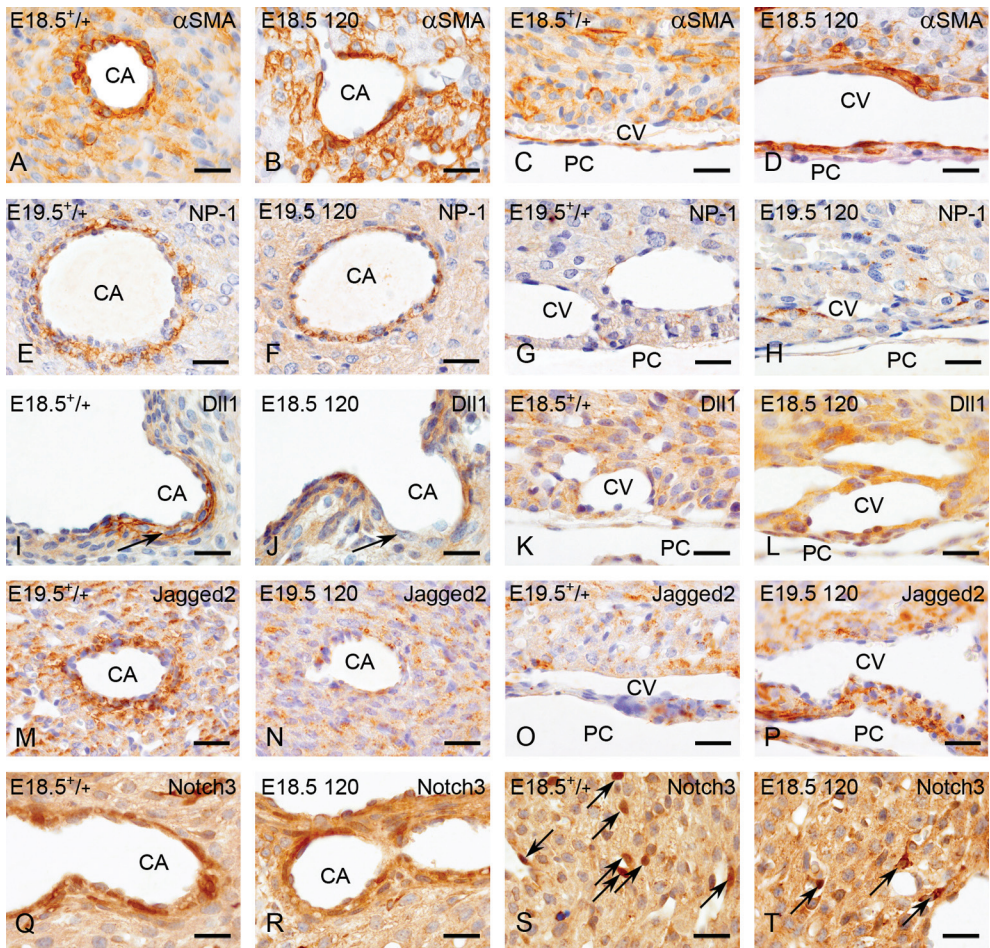


Figure 4. Abnormal coronary arteriogenesis in *Vegf120/120* embryos. The expression of several different markers (upper right) in vSMCs/pericytes was compared between wild-type (+/+) and mutants (120; upper left together with embryonic age in days (E)). A decrease in medial cells expressing α SMA (A-B), NP-1 (E-F), Dll1 (I-J), Jagged2 (M,N) and Notch3 (I-J) is obvious in the coronary arteries media (CA) of mutants while an increase of α SMA (C-D), NP-1 (G-H), Dll1 (K-L) and Jagged2-positive cells (O-P) surrounds the coronary veins (CV). A decrease in number of Notch3-positive pericytes is seen in mutant coronary microvasculature (K-L). Abbreviation: PC = pericardial cavity. Scale bars = 20 μ m.

Discussion

The loss of the *Vegf164* and *Vegf188* isoforms in *Vegf120/120* mutants results in spatiotemporal alterations in VEGF and Notch-signaling in the heart. These alterations coincide with abnormalities in coronary endothelial differentiation and subsequent arteriogenesis. The data provide us with further insight on the role of both VEGF-isoform and spatiotemporal VEGF-distribution on coronary differentiation and maturation.

Anomalous endothelial differentiation of the Vegf120/120 coronary system

VEGF-signaling influences vasculogenesis and angiogenesis, but also arterial endothelial differentiation^{11;27}. VEGF-signaling in ECs can upregulate expression of members of the Notch-signaling family, which instructs ephrinB2-expression and defines arterial differentiation^{11;27}. In venous ECs, expression of these proteins is inhibited by the vein-specific transcription factor COUP-TFII, thereby favoring EphB4-expression and venous differentiation²⁸. We show in vitro that addition of VEGF165, but not of VEGF121, leads to significant decrease in COUP-TFII-expression in human coronary arterial ECs, indicating a possible mechanism through which VEGF-signaling might favor arterial endothelial differentiation. The exact pathway by which VEGF-signaling regulates COUP-TFII-expression remains to be elucidated.

The main isoform expressed during normal murine cardiac development is *Vegf164*¹⁷. VEGF164 has a proximate bioactivity to its place of production due to high heparin-binding capacities²⁹ (Figure 1Q and 5A,C,E). We show that cardiac *Vegf*-production in vivo overlaps in later stages (\geq E16.5) with the region where coronary arteries develop (i.e. deep in the myocardium of the ventricular free walls in the mouse). We consider that this spatial distribution will result in relatively high levels of VEGF and subsequent Notch-signaling in ECs localized in the region of the developing coronary arteries due to 1) high local levels of VEGF, combined with 2) amplification of signaling levels by artery-specific NP-1²⁸ (Figure 5C). This is reflected in vivo by inhibition of COUP-TFII and induction of Dll4, cleaved Notch1 and ephrinB2 staining in coronary arterial ECs in late embryonic stages, suggesting increased Notch-signaling, and (potentially Notch-induced²⁶) reduced VEGFR-2 expression. In contrast, veins develop subepicardially and therefore, venous ECs are mainly subjected to the less expressed and more diffuse VEGF120-isoform, with resulting low levels of Notch-signaling as indicated by low cleaved Notch1 and high COUP-TFII and EphB4-staining in wild-type embryos. In combination with the fact that venous ECs do not express NP-1²⁸, this leads to the assumption that coronary venous ECs experience lower levels of VEGF and Notch-signaling (Figure 5E). This spatiotemporal determination of arterial and venous specification also corresponds with the situation in zebrafish. Here, VEGF-expression is induced in the somites next to the notochord, which is located directly caudal from the dorsal aorta. The posterial cardinal vein is positioned more ventrally, so further away from the place of VEGF-production²⁷.

In *Vegf120/120* mouse embryos, only the highly soluble non-heparin-binding VEGF120 isoform is produced²⁹. This will affect the VEGF-gradient in the myocardium giving relative low levels of VEGF in the area of the coronary arteries and higher levels around the coronary veins (Figure 5B,D,F). Because of this, combined with the fact that VEGF120 cannot induce formation of the signaling potent NP-1/VEGFR-2 complexes³⁰, lower VEGF and Notch-signaling levels are expected in the ECs in the area of the coronary arteries (Figure 5D), and higher levels in the ECs of the coronary veins (Figure 5F). This might result in the alterations in EC-differentiation observed in these embryos. Besides altered differentiation, a severe decrease in coronary arterial size coincides with an increase in venous size. As VEGF is involved in endothelial proliferation and vascular fusion³¹, locally increased *Vegf*-expression in the venous region could lead to enlarged veins as observed in the mutant mouse embryos. Therefore, we speculate that the RT-qPCR data normalized for endothelial input on embryonic hearts indicate mainly venous expression. This underscores that VEGF-signaling in venous ECs might induce expression of arterial markers such as *Notch1* and *Notch4*. Unfortunately, we could not confirm alterations in Notch4 protein-expression as the anti-Notch4-antibodies tested bind aspecific (Table A1).

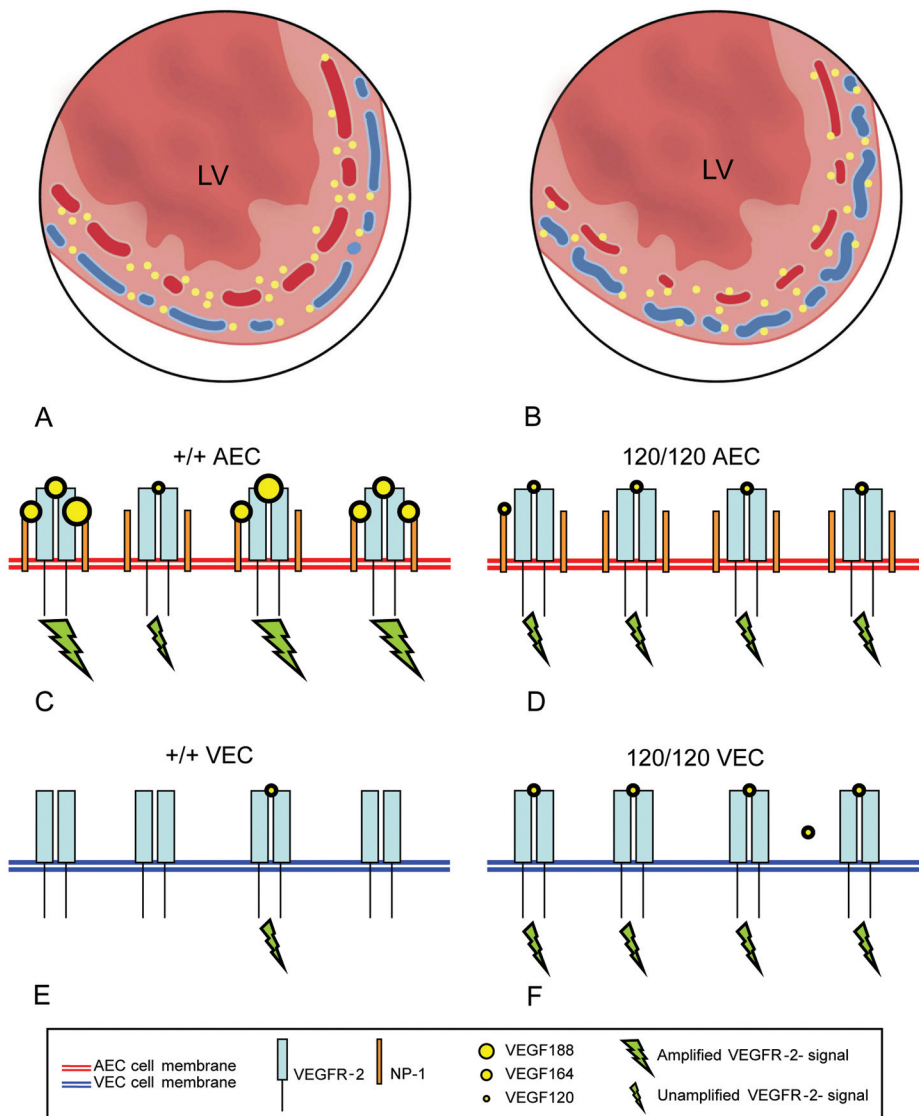
Our *in vitro* data show that the expression of arterial markers in HCAECs varies for the VEGF-isoform applied, with VEGF165 having a more prominent effect than VEGF121. This probably relates to higher levels of VEGF-signaling through VEGFR-2 with VEGF165 due to NP-1-mediated amplification^{9;28;30}. Unfortunately, we could not directly test the effect of VEGF-signaling on coronary venous ECs *in vitro*, as these cells cannot be obtained for culturing. However, earlier published data on HUVEC show that treatment with VEGF induces arterial phenotype of venous ECs^{11;32} as does ectopic VEGF-expression in zebrafish³³.

Total heart volumes are unchanged in mutant embryonic hearts, while a decrease in myocardial/vascular volume-ratio is seen, together with abnormal (dilated) microvascular morphology. This pleads for an increase in vascular volume rather than a decrease in myocardial volume as the underlying cause for the altered myocardial/vascular volume-ratio. This is likely caused by a disturbed VEGF-gradient, as it has been described that loss of a VEGF-gradient leads to alterations in microvascular branching morphogenesis³⁴ and increased availability of VEGF induces hyperfusion of vessels³¹. Furthermore, VEGF is able to induce proliferation of lymphatic ECs³⁵, located subepicardially in the heart. Another function of VEGF as vascular permeability factor³⁶ might additionally lead to the appearance of the increased size of the cardiac lymphatic system in mutant embryos.

Alterations in Vegf120/120 coronary arteriogenesis

We show that incorrect coronary arterial EC-differentiation coincides with impaired development of the media, together with a gain of arterial phenotype in coronary venous ECs and an increased number of venous pericytes. The differentiative state of ECs influences recruitment or proliferation and maturation^{37;38}, suggesting a role for VEGF-

signaling on arteriogenesis via manipulation of endothelial performance. A direct role for VEGF-signaling in arteriogenesis is supported by the described instructive role for NP-1³⁹ and Notch-signaling^{38;40} in differentiation of vSMCs. Concomitantly, we show that the amount of cells expressing α SMA, NP-1, Dll1, Jagged2 and Notch3 in the coronary arterial media and of Notch3-positive microvascular pericytes was impaired in mutant embryos, while an increase in number of cells surrounding the coronary veins positive for these markers was seen. Besides a positive role for Notch-signaling in arteriogenesis, inhibiting roles have been described as well⁴¹. Our data plead for an instructive rather than an inhibiting role. We suggest that lack of larger VEGF-isoforms



leads to a deficient development of the vSMC-layer of the coronary arteries. This can occur either indirectly via altered endothelial differentiation, or directly through a decrease in VEGF-related Notch-signaling in the mutant coronary vSMCs.

Morphological abnormalities in the coronary system of mutant mouse embryos

Congenital coronary anomalies are often correlated with primary cardiac defects. In all *Vegf120/120* mutants with TOF¹⁷ the IVS was supplied by an artery coming from the left sinus, in contrast to normal where the IVS is supplied by a branch of the right coronary artery²⁴. The anomalies specific for TOF (overriding and/or dextroposition of the ascending aorta) might favor the coronary IVS-branch to connect to the left sinus⁴². As in humans with TOF, a single orifice was occasionally encountered in mutant mouse embryos. More often an increased number (3 or 4) of coronary orifices was found, which is regarded to be a rare variation in both humans and mice^{24;43}. Nevertheless, we never saw more than 2 orifices in the 24 wild-type embryos of E15.5 and older.

The presence of VCACs in cardiac anomalies related to pulmonary atresia is not uncommon, even before complete atresia has developed⁴⁴. A substantial part of coronary vSMCs originates from the EPDC-population¹⁵ and EPDC-performance has been suggested to play part in the appearance of VCACs⁴⁴. Abnormal development and/or differentiation of EPDCs due to altered VEGF and/or Notch-signaling might explain the occurrence of VCACs in *Vegf120/120* embryos. Besides VCACs, coronary arterio-venous shunts were observed. Alterations in VEGF and Notch-signaling in *Vegf120/120* embryos may cause arterio-venous shunts, as the presence of such shunts has been described in Notch-mutants⁴⁵. Extracardiac arterio-venous shunts were observed in the aortic arches of perinatal *Vegf120/120* mouse embryos, suggesting that alterations in Notch-signaling are not heart-restricted.

← *Figure 5. VEGF-expression and signaling during embryonic coronary development in normal and Vegf120/120 hearts.* A-B: Schematic drawings of transverse sections of the left ventricle (LV) of wild-type (+/+) and mutant (120/120) embryos of E16.5 are shown. In +/+ embryos, *Vegf*-production mainly occurs at the borderzone between compact and trabecular myocardium (A; see also Figure 1Q), where coronary arteries (red) develop. As this is mainly *Vegf164*, protein distribution (yellow) is expected to give high protein levels around arteries and low around veins (blue). As mutants (B) only produce *Vegf120*, protein distribution is expected to be more dispersed due to lack of heparin-binding domains. This will lead to relative low protein levels around arteries and high levels around veins. C-F: Schemes indicating the expected VEGF-signaling levels in +/+ and 120 coronary arterial endothelial cells (AECs) and venous endothelial cells (VECs) are shown. In a +/+ AEC high VEGF protein-levels combined with neuropilin-1 (NP-1)-mediated amplification leads to high levels of VEGF-signaling (C), while low VEGF-concentrations and lack of NP-1-expression in VECs lead to low levels of VEGF-signaling (E). In mutants, relative low VEGF-levels around the AECs in combination with lack of NP-1-mediated amplification leads to relative low levels of VEGF-signaling in a 120/120 AEC (D), while relative high levels around the VECs inflict high signaling levels (F). NOTE: Due to resolution, in A different VEGF-isoform are indicated with yellow dots of the same size.

We already observed at E11.5, both in wild-type and mutants, two connections of the coronary venous system (in)directly to the right atrium. This is the first report on such early coronary venous drainage in mice. We describe that the connection of the coronary system to the right atrium arises before the coronary connection to the aorta. This is feasible as it enables circulation throughout the coronary system at the onset of systemic flow and pressure, which occurs several days later, without obstruction¹⁴.

Conclusions

We show that loss of *Vegf164* and *Vegf188* in *Vegf120/120* embryos leads to spatiotemporal alterations in VEGF and Notch-signaling in the heart reflected by altered expression of several markers involved in and regulated by these pathways. These alterations coincide with anomalous coronary EC-differentiation and ensuing arteriogenesis. The effect of different VEGF-isoforms on Notch-signaling and coronary EC-differentiation could be confirmed in vitro.

From our study it can be concluded that the spatiotemporal VEGF-distribution as well as specificity of the isoforms are important for proper coronary vascular development. These new insights on instructive roles of VEGF(-isoform) distribution on angiogenesis, endothelial functioning, and arteriogenesis can be of use to improve the efficacy of current therapies targeting VEGF-signaling^{8;46} in tissue revascularization.

Acknowledgements

The authors would like to thank Jan Lens for photographic assistance, Ron Slagter for drawings, Saskia Maas and Conny J. van Munsteren for technical assistance (all Department of Anatomy and Embryology, Leiden University Medical Center, Leiden, The Netherlands) and Sanne Verbruggen (Department of Physiology, Maastricht University, Maastricht, The Netherlands) for assistance with the in vitro experiments.

References

1. Chi JT, Chang HY, Haraldsen G, Jahnsen FL, Troyanskaya OG, Chang DS, Wang Z, Rockson SG, van de RM, Botstein D, Brown PO. Endothelial cell diversity revealed by global expression profiling. *Proc Natl Acad Sci U S A*. 2003;100:10623-10628.
2. Kattan J, Dettman RW, Bristow J. Formation and remodeling of the coronary vascular bed in the embryonic avian heart. *Dev Dyn*. 2004;230:34-43.
3. Casanello P, Escudero C, Sobrevia L. Equilibrative nucleoside (ENTs) and cationic amino acid (CATs) transporters: implications in foetal endothelial dysfunction in human pregnancy diseases. *Curr Vasc Pharmacol*. 2007;5:69-84.
4. Gittenberger-De Groot AC, Van Den Akker NM, Bartelings MM, Webb S, Van Vugt JM, Haak MC. Abnormal lymphatic development in trisomy 16 mouse embryos precedes nuchal edema. *Dev Dyn*. 2004;230:378-384.
5. Carson-Walter EB, Hampton J, Shue E, Geynisman DM, Pillai PK, Sathanoori R, Madden SL, Hamilton RL, Walter KA. Plasmalemmal vesicle associated protein-1 is a novel marker implicated in brain tumor angiogenesis. *Clin Cancer Res*. 2005;11:7643-7650.
6. Deng DX, Tsalenko A, Vailaya A, Ben-Dor A, Kundu R, Estay I, Tabibiazar R, Kincaid R, Yakhini Z, Bruhn L, Quertermous T. Differences in vascular bed disease susceptibility reflect differences in gene expression response to atherogenic stimuli. *Circ Res*. 2006;98:200-208.
7. Lauth M, Cattaruzza M, Hecker M. ACE inhibitor and AT1 antagonist blockade of deformation-induced gene expression in the rabbit jugular vein through B2 receptor activation. *Arterioscler Thromb Vasc Biol*. 2001;21:61-66.
8. Yla-Herttuala S, Rissanen TT, Vajanto I, Hartikainen J. Vascular endothelial growth factors: biology and current status of clinical applications in cardiovascular medicine. *J Am Coll Cardiol*. 2007;49:1015-1026.
9. Soker S, Takashima S, Miao HQ, Neufeld G, Klagsbrun M. Neuropilin-1 is expressed by endothelial and tumor cells as an isoform-specific receptor for vascular endothelial growth factor. *Cell*. 1998;92:735-745.
10. Shawber CJ, Kitajewski J. Notch function in the vasculature: insights from zebrafish, mouse and man. *Bioessays*. 2004;26:225-234.
11. Hainaud P, Contreres JO, Villemain A, Liu LX, Plouet J, Tobelem G, Dupuy E. The Role of the Vascular Endothelial Growth Factor-Delta-like 4 Ligand/Notch4-Ephrin B2 Cascade in Tumor Vessel Remodeling and Endothelial Cell Functions. *Cancer Res*. 2006;66:8501-8510.
12. Villa N, Walker L, Lindsell CE, Gasson J, Iruela-Arispe ML, Weinmaster G. Vascular expression of Notch pathway receptors and ligands is restricted to arterial vessels. *Mech Dev*. 2001;108:161-164.
13. Vrancken Peeters MP, Gittenberger-De Groot AC, Mentink MM, Hungerford JE, Little CD, Poelmann RE. The development of the coronary vessels and their differentiation into arteries and veins in the embryonic quail heart. *Dev Dyn*. 1997;208:338-348.
14. Vrancken Peeters MP, Gittenberger-De Groot AC, Mentink MM, Hungerford JE, Little CD, Poelmann RE. Differences in development of coronary arteries and veins. *Cardiovasc Res*. 1997;36:101-110.

15. Vrancken Peeters MP, Gittenberger-De Groot AC, Mentink MM, Poelmann RE. Smooth muscle cells and fibroblasts of the coronary arteries derive from epithelial-mesenchymal transformation of the epicardium. *Anat Embryol (Berl)*. 1999;199:367-378.
16. Stalmans I, Lambrechts D, De Smet F, Jansen S, Wang J, Maity S, Kneer P, von der OM, Swillen A, Maes C, Gewillig M, Molin DG, Hellings P, Boetel T, Haardt M, Compennolle V, Dewerchin M, Plaisance S, Vlietinck R, Emanuel B, Gittenberger-De Groot AC, Scambler P, Morrow B, Driscoll DA, Moons L, Esguerra CV, Carmeliet G, Behn-Krappa A, Devriendt K, Collen D, Conway SJ, Carmeliet P. VEGF: a modifier of the del22q11 (DiGeorge) syndrome? *Nat Med*. 2003;9:173-182.
17. Van Den Akker NM, Molin DG, Peters PP, Maas S, Wisse LJ, van BR, van Munsteren CJ, Bartelings MM, Poelmann RE, Carmeliet P, Gittenberger-De Groot AC. Tetralogy of fallot and alterations in vascular endothelial growth factor-A signaling and notch signaling in mouse embryos solely expressing the VEGF120 isoform. *Circ Res*. 2007;100:842-849.
18. Carmeliet P, Ng YS, Nuyens D, Theilmeier G, Brusselmans K, Cornelissen I, Ehler E, Kakkar VV, Stalmans I, Mattot V, Perriard JC, Dewerchin M, Flameng W, Nagy A, Lupu F, Moons L, Collen D, D'Amore PA, Shima DT. Impaired myocardial angiogenesis and ischemic cardiomyopathy in mice lacking the vascular endothelial growth factor isoforms VEGF164 and VEGF188. *Nat Med*. 1999;5:495-502.
19. Stalmans I, Ng YS, Rohan R, Fruttiger M, Bouche A, Yuce A, Fujisawa H, Hermans B, Shani M, Jansen S, Hicklin D, Anderson DJ, Gardiner T, Hammes HP, Moons L, Dewerchin M, Collen D, Carmeliet P, D'Amore PA. Arteriolar and venular patterning in retinas of mice selectively expressing VEGF isoforms. *J Clin Invest*. 2002;109:327-336.
20. Gundersen HJ, Jensen EB. The efficiency of systematic sampling in stereology and its prediction. *J Microsc*. 1987;147:229-263.
21. Hellems J, Mortier G, De PA, Speleman F, Vandesompele J. qBase relative quantification framework and software for management and automated analysis of real-time quantitative PCR data. *Genome Biol*. 2007;8:R19.
22. Uyttendaele H, Marazzi G, Wu G, Yan Q, Sassoon D, Kitajewski J. Notch4/int-3, a mammary proto-oncogene, is an endothelial cell-specific mammalian Notch gene. *Development*. 1996;122:2251-2259.
23. Viragh S, Challice CE. Origin and differentiation of cardiac muscle cells in the mouse. *J Ultrastructure Research*. 1973;42:1-24.
24. Kumar D, Hacker TA, Buck J, Whitesell LF, Kaji EH, Douglas PS, Kamp TJ. Distinct mouse coronary anatomy and myocardial infarction consequent to ligation. *Coron Artery Dis*. 2005;16:41-44.
25. Tomanek RJ, Ratajska A, Kitten GT, Yue X, Sandra A. Vascular endothelial growth factor expression coincides with coronary vasculogenesis and angiogenesis. *Dev Dyn*. 1999;215:54-61.
26. Williams CK, Li JL, Murga M, Harris AL, Tosato G. Up-regulation of the Notch ligand Delta-like 4 inhibits VEGF-induced endothelial cell function. *Blood*. 2006;107:931-939.
27. Lawson ND, Vogel AM, Weinstein BM. sonic hedgehog and vascular endothelial growth factor act upstream of the Notch pathway during arterial endothelial differentiation. *Dev Cell*. 2002;3:127-136.
28. You LR, Lin FJ, Lee CT, Demayo FJ, Tsai MJ, Tsai SY. Suppression of Notch signalling by the COUP-TFII transcription factor regulates vein identity. *Nature*. 2005;435:98-104.
29. Houck KA, Leung DW, Rowland AM, Winer J, Ferrara N. Dual regulation of vascular endothelial growth factor bioavailability by genetic and proteolytic mechanisms. *J Biol Chem*. 1992;267:26031-26037.

30. Pan Q, Chanthery Y, Wu Y, Rahtore N, Tong RK, Peale F, Bagri A, Tessier-Lavigne M, Koch AW, Watts RJ. Neuropilin-1 binds to VEGF121 and regulates endothelial cell migration and sprouting. *J Biol Chem.* 2007;282:24049-24056.
31. Drake CJ, Little CD. VEGF and vascular fusion: implications for normal and pathological vessels. *J Histochem Cytochem.* 1999;47:1351-1356.
32. Liu ZJ, Shirakawa T, Li Y, Soma A, Oka M, Dotto GP, Fairman RM, Velazquez OC, Herlyn M. Regulation of Notch1 and Dll4 by vascular endothelial growth factor in arterial endothelial cells: implications for modulating arteriogenesis and angiogenesis. *Mol Cell Biol.* 2003;23:14-25.
33. Lawson ND, Scheer N, Pham VN, Kim CH, Chitnis AB, Campos-Ortega JA, Weinstein BM. Notch signaling is required for arterial-venous differentiation during embryonic vascular development. *Development.* 2001;128:3675-3683.
34. Ruhrberg C, Gerhardt H, Golding M, Watson R, Ioannidou S, Fujisawa H, Betsholtz C, Shima DT. Spatially restricted patterning cues provided by heparin-binding VEGF-A control blood vessel branching morphogenesis. *Genes Dev.* 2002;16:2684-2698.
35. Nagy JA, Vasile E, Feng D, Sundberg C, Brown LF, Detmar MJ, Lawitts JA, Benjamin L, Tan X, Manseau EJ, Dvorak AM, Dvorak HF. Vascular permeability factor/vascular endothelial growth factor induces lymphangiogenesis as well as angiogenesis. *J Exp Med.* 2002;196:1497-1506.
36. Brown LF, Detmar M, Claffey K, Nagy JA, Feng D, Dvorak AM, Dvorak HF. Vascular permeability factor/vascular endothelial growth factor: a multifunctional angiogenic cytokine. *EXS.* 1997;79:233-269.
37. Carmeliet P. Mechanisms of angiogenesis and arteriogenesis. *Nat Med.* 2000;6:389-395.
38. Limbourg A, Ploom M, Elligsen D, Sorensen I, Ziegelhoeffer T, Gossler A, Drexler H, Limbourg FP. Notch ligand Delta-like 1 is essential for postnatal arteriogenesis. *Circ Res.* 2007;100:363-371.
39. Liu W, Parikh AA, Stoeltzing O, Fan F, McCarty MF, Wey J, Hicklin DJ, Ellis LM. Upregulation of neuropilin-1 by basic fibroblast growth factor enhances vascular smooth muscle cell migration in response to VEGF. *Cytokine.* 2005;32:206-212.
40. High FA, Zhang M, Proweller A, Tu L, Parmacek MS, Pear WS, Epstein JA. An essential role for Notch in neural crest cardiovascular development and smooth muscle differentiation. *J Clin Invest.* 2007;117:353-363.
41. Morrow D, Scheller A, Birney YA, Sweeney C, Guha S, Cummins PM, Murphy R, Walls D, Redmond EM, Cahill PA. Notch-mediated CBF-1/RBP-J $\{\kappa\}$ -dependent regulation of human vascular smooth muscle cell phenotype in vitro. *Am J Physiol Cell Physiol.* 2005;289:C1188-C1196.
42. Mawson JB. Congenital heart defects and coronary anatomy. *Tex Heart Inst J.* 2002;29:279-289.
43. Angelini P. Coronary artery anomalies: an entity in search of an identity. *Circulation.* 2007;115:1296-1305.
44. Gittenberger-De Groot AC, Eralp I, Lie-Venema H, Bartelings MM, Poelmann RE. Development of the coronary vasculature and its implications for coronary abnormalities in general and specifically in pulmonary atresia without ventricular septal defect. *Acta Paediatr Suppl.* 2004;93:13-19.
45. Krebs LT, Shutter JR, Tanigaki K, Honjo T, Stark KL, Gridley T. Haploinsufficient lethality and formation of arteriovenous malformations in Notch pathway mutants. *Genes Dev.* 2004;18:2469-2473.
46. Gaffney MM, Hynes SO, Barry F, O'Brien T. Cardiovascular gene therapy: current status and therapeutic potential. *Br J Pharmacol.* 2007;152:175-188.

Appendix

Results

Anomalous coronary morphology in Vegf120/120 mouse embryos

A remarkable observation was that half of the mutant embryos showed abnormalities in the anatomy of the main coronary branches. In all wild-type embryos the main artery supplying the interventricular septum (IVS) originated from the first branch of the right coronary artery (RCA), with sometimes an additional smaller branch coming from the left coronary artery (LCA), which corresponds with earlier observations in normal mice¹. In 8/28 mutant embryos the IVS-supplying branch had its own coronary orifice, which originated in 6 cases from the right and in 2 cases from the left facing sinus. In addition, in 3/28 cases the IVS was solely supplied by a branch that arose from the LCA. All embryos in which the IVS-branch originated (in)directly from the left facing sinus were diagnosed with TOF (5/28)². In contrast to mice, the IVS in humans is normally supplied by the left anterior descending artery and it has been described that patients with TOF often (up to 19%³) present with coronary abnormalities such as bilateral or right-originating anterior descending arteries^{3,4}. The differences between mouse and man, both in normal and pathological coronary morphology might lie in the fact that the angle of the aorta relative to the IVS-axis differ between the two species⁵. Furthermore, in 2/28 *Vegf120/120* cases no major coronary artery could be observed supplying the IVS and in 1/28 cases both a branch splitting from the RCA and from the LCA with the left branch being most prominent was observed.

Table A1. Characteristics of primary antibodies used for immunohistochemistry.

Antigen	Cat. no.	AR	ABC	CSA-II	Reference
VEGFR-2	AF644*	HR	Yes	No	www.rndsystems.com/ihc
LYVE-1	**	P	Yes	No	Mäkinen <i>et al</i> ⁶
cleaved Notch1	2421***	HR	No	Yes	Tanaka <i>et al</i> ⁷
Notch2	Sc-5545†	-	Yes	No	Okuyama <i>et al</i> ⁸
Notch3	Sc-7424†	HR	Yes	No	Karlstöm <i>et al</i> ⁹
Jagged1	Sc-6011†	HR	Yes	No	Sestan <i>et al</i> ¹⁰
Jagged2	Sc-8158†	-	Yes	No	Rivolta <i>et al</i> ¹¹
Dll1	Sc-9102†	HR	Yes	No	Conboy and Rando ¹²
Dll4	AF1389*	HR	Yes	No	www.rndsystems.com
ephrinB2	AF496*	HR	Yes	No	www.rndsystems.com/ihc
EphB4	AF446*	HR	Yes	No	www.rndsystems.com
COUP-TFII	††	HR	Yes	No	You <i>et al</i> ³
NP-1	Sc-7239†	HR	Yes	No	Serini <i>et al</i> ⁴
αSMA (1A4)	A2547†††	HR	No	No	Skalli <i>et al</i> ⁵
Notch4	Sc-8645†	N.A.	N.A.	N.A.	N.A.
Notch4	Sc-5594†	N.A.	N.A.	N.A.	N.A.

Abbreviations; ABC = ABC-kit (Vector) amplification; AR = antigen retrieval; CSA-II = CSA-ii-kit (DAKO) amplification; HR = heat retrieval; N.A. = not applicable; P = pronase treatment.

*= R&D Systems, Minneapolis, USA; **= 103-PABi50: ReliaTech, Braunschweig, Germany; ***= Cell Signaling, Beverly, MA, USA; †= Santa Cruz, Santa Cruz, USA; ††= PP-H7147-00,2ZH7147H: PPMX, Tokyo, Japan; †††= Sig.ma-Adrich, Missouri, USA

Table A3. Overview of alterations in coronary EC-expression patterns in Vegf120/120 mouse embryos.

Marker	Venous ECs	Arterial ECs
VEGFR-2	↑	↑
cleaved Notch1	↑	↓
Notch2	↑	=*
Dll4	↑	↓
Jagged1	=*	↓
ephrinB2	↑	↓
EphB4	↓	↑
COUP-TFII	↓	↑

The protein expression patterns as determined using immunohistochemistry of ECs in *Vegf120/120* mouse embryos are indicated, when compared with wild-type littermates, as shown in Figure 1, 2 and data not shown (*). To indicate a difference, this difference was seen in at least 3 mutant vs 3 wild-type embryos per age-group (E15.5-E19.5). ↑ indicates an increase in expression; ↓ indicates a decrease in expression; = indicates no difference in expression.

Table A2. Primer sequences used for RT-qPCR.

Species	Gene	Forward	Reverse
Homo Sapiens	<i>β-ACTIN</i> (BC002409)	5'-ATCCTCACCCCTGAAGTACCC-3'	5'-GGACTGTGGTCAATGAGTCCT-3'
	<i>GAPDH</i> (NM_002046)	5'-GCCTCAAGATCATCAGCAAT-3'	5'-GGACTGTGGTCAATGAGTCCT-3'
	<i>NP-1</i> (NM_003873)	5'-TGAGCCCTGTGGTTTATTC-3'	5'-CGTACTCCTCTGGCTTCTGG-3'
	<i>NOTCH1</i> (NM_017617)	5'-CTGGAGGACCTCATCAACTC-3'	5'-TTCTTCAGGAGCACAACTGC-3'
	<i>NOTCH4</i> (NM_004557)	5'-GTGGGTATCTCTGCCAGTGT-3'	5'-CTCAGGTTGGGAGTACAG-3'
	<i>DLL4</i> (NM_019074)	5'-ACAACTTGTCGGACTTCCAG-3'	5'-CAGCTCCTTCTTCTGGTTTG-3'
	<i>HES1</i> (NM_005524)	5'-CCAAAGACAGCATCTGAGCA-3'	5'-GCCGGGAGCTATCTTCTT-3'
	<i>EPHRIN2</i> (NM_004093)	5'-GTTCCGAAAGTGGCCTTATT-3'	5'-CTCCGGTACTTCAGCAAGAG-3'
	<i>COUP-TFII</i> (BC014664)	5'-AGCAAGTGGAGAAGCTCAAG-3'	5'-CACATGGGCTACATCAGAGA-3'
	Mus Musculus	<i>β-actin</i> (NM_007393)	5'-actctatgtgggtgacgag-3'
<i>gapdh</i> (BC083149)		5'-aagtggagattgtgccatc-3'	5'-cgtgagtgagtcatactagg-3'
<i>Tie2</i> (X71426)		5'-gccatcaaggagatgaaga-3'	5'-catgctccaagagattgat-3'
<i>Notch1</i> (NM_008714)		5'-agcctccaccataacctt-3'	5'-ggc'tggagc'tgtaagtctg-3'
<i>Notch4</i> (NM_010929)		5'-agaggacgggactacacctt-3'	5'-cctttatccctggctccta-3'
<i>Hes1</i> (NM_008235)		5'-cctctgagcacagaagtca-3'	5'-gccgggagctatcttctta-3'
<i>Ephb4</i> (NM_010144)		5'-gccatcaagatgggaagata-3'	5'-cacatggccaagattttct-3'
<i>Dll4</i> (NM_019454)		5'-actctgtcgaactgtctt-3'	5'-cagcaccagcagaccacta-3'
<i>Hes1</i> (AF232241)		5'-gtaccagtcctttgagaa-3'	5'-tttcagggtgatccacagta-3'

References

1. Kumar D, Hacker TA, Buck J, Whitesell LF, Kaji EH, Douglas PS, Kamp TJ. Distinct mouse coronary anatomy and myocardial infarction consequent to ligation. *Coron Artery Dis.* 2005;16:41-44.
2. Van Den Akker NM, Molin DG, Peters PP, Maas S, Wisse LJ, van BR, van Munsteren CJ, Bartelings MM, Poelmann RE, Carmeliet P, Gittenberger-De Groot AC. Tetralogy of fallot and alterations in vascular endothelial growth factor-A signaling and notch signaling in mouse embryos solely expressing the VEGF120 isoform. *Circ Res.* 2007;100:842-849.
3. Jureidini SB, Appleton RS, Nouri S. Detection of coronary artery abnormalities in tetralogy of Fallot by two-dimensional echocardiography. *J Am Coll Cardiol.* 1989;14:960-967.
4. Mawson JB. Congenital heart defects and coronary anatomy. *Tex Heart Inst J.* 2002;29:279-289.
5. Wessels A, Sedmera D. Developmental anatomy of the heart: a tale of mice and man. *Physiol Genomics.* 2003;15:165-176.
6. Makinen T, Veikkola T, Mustjoki S, Karpanen T, Catimel B, Nice EC, Wise L, Mercer A, Kowalski H, Kerjaschki D, Stacker SA, Achen MG, Alitalo K. Isolated lymphatic endothelial cells transduce growth, survival and migratory signals via the VEGF-C/D receptor VEGFR-3. *EMBO J.* 2001;20:4762-4773.
7. Tanaka M, Marunouchi T. Immunohistochemical localization of Notch receptors and their ligands in the postnatally developing rat cerebellum. *Neurosci Lett.* 2003;353:87-90.
8. Okuyama R, Nguyen BC, Talora C, Ogawa E, Tommasi d, V, Lioumi M, Chiorino G, Tagami H, Woo M, Dotto GP. High commitment of embryonic keratinocytes to terminal differentiation through a Notch1-caspase 3 regulatory mechanism. *Dev Cell.* 2004;6:551-562.
9. Karlstrom H, Beatus P, Dannaeus K, Chapman G, Lendahl U, Lundkvist J. A CADASIL-mutated Notch 3 receptor exhibits impaired intracellular trafficking and maturation but normal ligand-induced signaling. *Proc Natl Acad Sci U S A.* 2002;99:17119-17124.
10. Sestan N, Artavanis-Tsakonas S, Rakic P. Contact-dependent inhibition of cortical neurite growth mediated by notch signaling. *Science.* 1999;286:741-746.
11. Rivolta MN, Halsall A, Johnson CM, Tones MA, Holley MC. Transcript profiling of functionally related groups of genes during conditional differentiation of a mammalian cochlear hair cell line. *Genome Res.* 2002;12:1091-1099.
12. Conboy IM, Rando TA. The regulation of Notch signaling controls satellite cell activation and cell fate determination in postnatal myogenesis. *Dev Cell.* 2002;3:397-409.
13. You LR, Takamoto N, Yu CT, Tanaka T, Kodama T, Demayo FJ, Tsai SY, Tsai MJ. Mouse lacking COUP-TFII as an animal model of Bochdalek-type congenital diaphragmatic hernia. *Proc Natl Acad Sci U S A.* 2005;102:16351-16356.
14. Serini G, Valdembri D, Zanivan S, Morterra G, Burkhardt C, Caccavari F, Zammataro L, Primo L, Tamagnone L, Logan M, Tessier-Lavigne M, Taniguchi M, Puschel AW, Bussolino F. Class 3 semaphorins control vascular morphogenesis by inhibiting integrin function. *Nature.* 2003;424:391-397.
15. Skalli O, Ropraz P, Trzeciak A, Benzonana G, Gillessen D, Gabbiani G. A monoclonal antibody against alpha-smooth muscle actin: a new probe for smooth muscle differentiation. *J Cell Biol.* 1986;103:2787-2796.

Part II

PDGF in Cardiovascular Development

Chapter 4

Platelet-Derived Growth Factors in the Developing Avian Heart and Maturing Coronary Vasculature

Nynke M.S. van den Akker, Heleen Lie-Venema, Saskia Maas, Ismail Eralp, Marco C. DeRuiter, Robert E. Poelmann, Adriana C. Gittenberger-de Groot

Department of Anatomy and Embryology, Leiden University Medical Center, Leiden, The Netherlands

Modified after Developmental Dynamics, 2005;233:1579-1588.

Platelet Derived Growth Factors in the Developing Avian Heart and Maturing Coronary Vasculature

Abstract

Platelet derived growth factors (PDGFs) are important in embryonic development. To elucidate their role in avian heart and coronary development, we investigated protein expression patterns of PDGF-A, PDGF-B and the receptors PDGFR- α and PDGFR- β using immunohistochemistry on sections of pro-epicardial quail-chicken chimeras of HH28-HH35. PDGF-A and PDGFR- α were expressed in the atrial septum, sinus venosus and throughout the myocardium, with PDGFR- α retreating to the trabeculae at later stages. Additionally, PDGF-A and PDGFR- α were present in outflow tract cushion mesenchyme and myocardium, respectively. Small cardiac nerves and (sub)epicardial cells expressed PDGF-B and PDGFR- β . Furthermore, endothelial cells expressed PDGF-B, while vascular smooth muscle cells and interstitial epicardium-derived cells expressed PDGFR- β , indicating a role in coronary maturation. PDGF-B is also present in ventricular septal development, in the absence of any PDGFR. Epicardium-derived cells in the atrioventricular cushions expressed PDGFR- β . We conclude that all four proteins are involved in myocardial development, whereas PDGF-B and PDGFR- β are specifically important in coronary maturation.

Introduction

Normal avian and mammalian coronary development is dependent on correct outgrowth of the epicardium, the outer cell layer of the heart¹⁻⁵. This layer is not derived from cells of the primitive heart itself, but from an extracardiac, cauliflower-like structure, called the pro-epicardial organ (PEO)¹. The PEO is located at the dorsal wall of the embryo near the sinus venosus and the liver. It protrudes in the direction of the heart and after contacting the heart, cells of the PEO start to cover the entire myocardium, thereby forming the epicardium⁶. A subepicardial mesenchyme of epicardium-derived cells (EPDCs)⁵ is formed from the epicardial sheet by epithelial-mesenchymal transformation (EMT)^{3,7}. EPDCs do not only form the subepicardial layer, but are also involved in the formation of the atrioventricular valves^{5,8}. Furthermore, they migrate into the myocardium to form the interstitial fibroblasts⁵ and the smooth muscle cells of the coronary vasculature^{2,5,9}.

The development of the coronary vasculature starts with the formation of a primitive endothelial network^{2,10}, which only stabilizes after recruitment of supporting mural cells, such as vascular smooth muscle cells (vSMCs)^{3,11}. The major cellular source for the developing coronary arterial and venous walls is the EPDC population. Although the processes involved in EMT, migration and differentiation of the epicardium and the EPDCs have been investigated and described^{5,12-18}, many aspects are still unresolved, one of them being the role of Platelet-Derived Growth Factor (PDGF)-signaling molecules.

The PDGF-family is presently thought to consist of four different members, which can form 5 different dimers, namely PDGF-AA, -AB, -BB, -CC and -DD. These ligands are secreted into the extracellular matrix to exert their function. The distance of action depends on the presence of heparin-binding retention motifs in their C-terminus, which is regulated through alternative mRNA splicing in the case of PDGF-A and is thought to be regulated through proteolytical processing in PDGF-B. When such motifs are present, the ligand will not be able to diffuse over a long distance, as it will be caught in the extracellular matrix, due to binding to heparin. When the motifs are not present, the ligand is able to diffuse further from the site of production, thereby increasing the distance of action. Although a developmental role seems to be present for these different variants, their exact role and distribution patterns are not clear¹⁹. Two receptors, PDGF receptor (PDGFR)- α and PDGFR- β , are known. They can form homo- and heterodimers upon ligand binding²⁰. In vitro, PDGFR- α binds PDGF-A, -B and -C and PDGFR- β binds PDGF-B and -D²⁰. In vivo, however, not all of these combinations seem to play a biological role. A role for PDGF-B signaling via PDGFR- α , for example, seems not to exist in mouse embryonic development, because the expression patterns of the ligand and the receptor do not colocalize¹⁹. PDGF-B is described to be expressed solely by endothelial cells and megakaryocytes during mouse embryonic development²¹, whereas PDGFR- β is expressed in non-neuronal neural crest²² and paraxial mesoderm-derived tissues

like the mesenchyme around the vertebrae, the kidneys, the cardiac valves, and the pericardium²³. Similarly, non-overlapping expression patterns have been found for PDGF-A, present in different epithelia²⁴ and PDGFR- β , present in vSMC or pericyte precursors^{21;25;26}. Less is known about the expression and function of the two ligands PDGF-C and PDGF-D^{27;28}, but PDGF-C does not seem to play a role in heart development as it has been described not to be expressed at all in the developing mouse heart²⁹.

Functional roles in embryogenesis for PDGF-A, PDGF-B and the two receptors have been investigated in several null-mutant mouse models. The defects seen in the *Pdgf-b* and *Pdgfr- β* knockout mice are comparable, again suggesting that PDGF-B only has a role in development by signaling via PDGFR- β . The embryos die perinatally^{25;26;30} and present with heart malformations (ventricular septal defect, thin ventricular myocardium), reduction of the number of pericytes in the vessel wall, and overall edema, probably because of microvascular leakage. Based on these observations, PDGF-B and PDGFR- β seem to be involved in maturation and stabilization of several different vascular networks. This idea is further supported by the fact that loss of the heparin-binding domain in the PDGF-B protein leads to structurally abnormal vessels³¹. Knockout mouse embryos for *Pdgf-a* and *Pdgfr- α* show different phenotypes. *Pdgf-a* knockouts either die before embryonic day (E)10 of an unknown cause or die later (several weeks after birth) as a result of lung emphysema²¹. They present with several other malformations, such as intestinal, testicular and hair follicle defects. However, no heart defects have been described²¹. *Pdgfr- α* knockouts, as well as *Patch* mutants (a mutation that involves the *Pdgfr- α* gene), show quite severe heart malformations, including atrial and ventricular septal defects, outflow tract (OFT) malformations, malformed valves and thin myocardium³². They die between E8 and E16²¹. Also, other malformations such as facial cleft, spina bifida and skeletal, lung and gut defects have been found. The OFT and facial abnormalities have been related to abnormalities in neural crest development^{22;32;33}. The large differences between *Pdgf-a* and *Pdgfr- α* knockouts might be explained by functional redundancy of PDGF-B or -C, the other ligands for PDGFR- α . Thus, PDGF-A and PDGFR- α seem to be involved predominantly in the morphogenesis of several organs.

We, therefore, hypothesize that PDGF-B and PDGFR- β , rather than PDGF-A and PDGFR- α , are involved in maturation and stabilization of the coronary vasculature and, thus, are expressed in cells participating in coronary development, such as coronary endothelial cells and EPDCs. To investigate this hypothesis, we describe the protein expression patterns of PDGF-A, PDGF-B and their receptors PDGFR- α and PDGFR- β in the hearts of normal chicken and quail embryos. To elucidate whether EPDCs specifically express these factors, we analyzed expression in quail-chicken chimeras, in which the PEO of the quail was transplanted into the chicken embryo.

Materials and Methods

Embryos

Fertilized eggs of the White Leghorn chicken (*Gallus domesticus*) and of the Japanese quail (*Coturnix coturnix japonica*) were incubated at 37 °C (80% humidity) and staged according to the criteria of Hamburger and Hamilton (HH)⁵³. For normal chicken and quail controls, eggs were incubated for 6-9 days, harvested and staged (HH28-35). The thoraxes were fixed in 20% dimethylsulfoxide and 80% methanol or in 4% paraformaldehyde in PBS for 24 hours. The thoraxes were embedded in paraffin and subsequently sectioned transversely (5 µm).

Chimerization technique

Chimerization was performed as described before². In short, after 3 days of incubation, the quail embryos were removed from the eggs, staged (HH15-18), and the PEO was micro-surgically removed. In the shell of the chicken eggs, a small window was made. The embryos were staged (HH15-18) and a quail PEO was inserted into the pericardial cavity. The eggs were closed with Scotch tape and re-incubated. At 3 to 6 days later (6 to 9 days of incubation), the chimeric embryos were harvested, staged (HH28-35), and processed as the controls. A QCPN (pan-quail nuclear) staining was used to determine the extent of chimerization. A total of 14 chimeras were included in this study.

Western blotting

To confirm the specificity of the polyclonal antibodies against PDGF-A, PDGF-B, PDGFR- α and PDGFR- β in chicken embryonic material, we performed Western blots. In short, total protein was extracted from hearts of normal chicken embryos in ice-cold RIPA buffer (PBS with 1% (v/v) Igepal-CA630, 0.5% (w/v) sodium deoxycholate, and 0.1% sodium dodecyl sulfate) containing phenylmethyl sulfonyl fluoride serine protease inhibitor at a concentration of 1 mMol/L. The total protein content of the extracts was determined using the bicinchronic acid method (BCA kit, Pierce). Western blot analysis of total protein was performed on extracts from 3 independent experiments using the ECL Advance Western Blotting Detection Kit (Amersham). The results of these experiments were that all antibodies, viz. anti-PDGF-A, anti-PDGF-B, anti-PDGFR- α and anti-PDGFR- β , specifically recognized the expected protein. From this finding, we conclude that the antibodies recognize the chicken PDGF-ligands and receptors with adequate specificity.

Immunohistochemistry

Immunohistochemical stainings were performed as described before⁵⁴. Sections were stained for QCPN, QH-1, α -smooth muscle actin (1A4), PDGF-A, PDGF-B and PDGFR- α . Microwave antigen retrieval was applied, except for the QH-1 and the α -smooth muscle actin staining. Endogenous peroxidase activity was quenched by incubation for 15 minutes in 0.3% H₂O₂ in PBS. Sections were incubated overnight

with the primary antibody (anti-QCPN 1:4, anti-QH-1 1:500, anti- α -smooth muscle actin 1:3000, anti-PDGF-A 1:100, anti-PDGF-B 1:50, anti-PDGFR- α 1:50) and incubated with a secondary peroxidase-labeled antibody (QCPN, QH-1 and α -smooth muscle actin staining) or a biotin-labeled (PDGF-A, PDGF-B and PDGFR- α staining) antibody for 1 hour. Sections incubated with a biotin-labeled antibody were then incubated with Vectastain ABC staining kit for 1 hour. Slides were rinsed with PBS and Tris/Maleate (pH 7.6). DAB was used as chromogen and Mayer's hematoxin as counter staining.

Immunofluorescence

The following double-stainings were performed; PDGFR- α /QCPN, PDGFR- α /PDGF-A, PDGFR- α /HHF-35, PDGFR- β /QCPN, PDGFR- β /QH-1, PDGFR- β /PDGF-B and PDGFR- α /PDGF-B. Sections were pretreated as described above and incubated overnight with the first primary antibody (anti-PDGFR- α 1:50, anti-PDGFR- β 1:25). Subsequently, they were incubated with a biotin-labeled secondary antibody for 1 hour, followed by incubation with avidin labeled with FITC (PDGFR- α) or TRITC (PDGFR- β) for 1 hour. Sections were incubated for 2 hours with second primary antibodies (anti-QCPN 1:4, anti-PDGF-A 1:100, anti-HHF-35 1:500, anti-QH-1 1:500 or anti-PDGF-B 1:50) and incubated for 1 hour with secondary TRITC or FITC-labeled antibodies. Finally, sections were mounted with Vectashield containing DAPI to stain the nuclei.

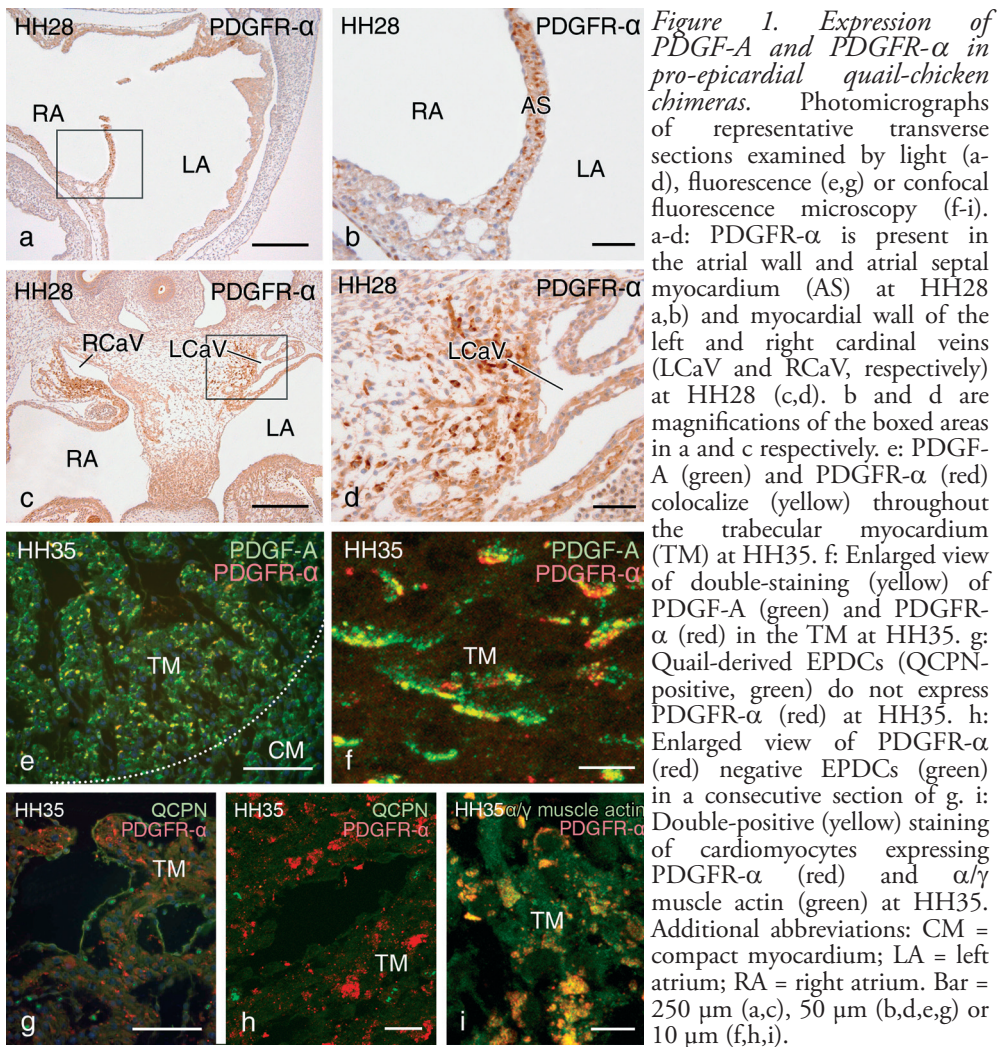
Materials

Primary antibodies used were rabbit-anti-human PDGF-A (SC-128, Santa Cruz), rabbit-anti-human PDGF-B (SC-7878, Santa Cruz), goat-anti-human PDGFR- α (P2110, Sigma-Aldrich), mouse-anti-human α -smooth muscle actin (clone 1A4, A2547, Sigma-Aldrich), mouse-anti-human PDGFR- β (610114, Falcon), mouse-anti-quail QCPN, mouse-anti-quail QH-1 (both Hybridomabank, Iowa City) and mouse-anti-human α/γ -muscle actin (HHF35; M0635, DAKO). Secondary antibodies used were biotin-labeled goat-anti-rabbit, biotin-labeled horse-anti-mouse (BA-2000, Vector Labs), biotin-labeled horse-anti-goat (BA-9500, Vector Labs), FITC-labeled avidin (A-2001, Vector Labs), TRITC-labeled avidin (A-2002, Vector Labs), TRITC-labeled rabbit-anti-mouse (R270, DAKO), FITC-labeled goat-anti-mouse IgG1 (1075-02, Southern Biotechnology Associates), FITC-labeled donkey-anti-rabbit (SC-2090, Santa Cruz) and peroxidase-labeled rabbit-anti-mouse (P0260, DAKO). Furthermore, normal goat serum (S-1000, Vector Labs), normal horse serum (S-2000, Vector Labs), the Vectastain ABC staining kit (PK-6100, Vector Labs), Vectashield (H-1200, Vector Labs), DAB (D5637, Sigma-Aldrich) and Entellan (Merck) were used in the immunohistochemistry and immunofluorescence. Photographs were made using an Olympus AX70 light microscope equipped with an Olympus DP12 digital camera (Olympus), a Leica IRBE fluorescence microscope equipped with a Leica DC350F digital camera (Leica Microsystems) or a Bio-Rad confocal laser scanning microscope. Fluorescent images were analyzed using Leica FW4000 software and confocal images were processed with Image J.

Results

Cardiac protein expression patterns of PDGF-A and PDGFR- α

In the time-span we investigated, PDGF-A was present in several areas of the avian heart during development (Table 1), namely in the myocardial wall of the cardinal veins of the sinus venosus, in the atrial and atrial septal myocardium, in both the compact and the trabecular ventricular myocardium (Figure 1e-f) and in the OFT cushion mesenchyme. The presence of PDGF-A decreased in time in the myocardial wall of the cardinal veins, in the atrial septal myocardium and in the OFT cushion mesenchyme, but stayed constant in the atrial myocardium and in the compact and trabecular ventricular myocardium.



	PDGF-A			PDGFR- α			PDGF-B			PDGFR- β		
	HH28	HH30	HH35	HH28	HH30	HH35	HH28	HH30	HH35	HH28	HH30	HH35
CaV myocardium	■	■	■	■	■	■						
A myocardium	■	■	■	■	■	■						
AS myocardium	■	■	■	■	■	■						
AV valves										■	■	■
VC myocardium	■	■	■	■	■	■						
VT myocardium							■	■	■			
VS myocardium							■	■	■			
OFT myocardium										■	■	■
OFT cushion mesenchyme												
CA-ECs							■	■	■			
C-vSMCs										■	■	■
Epicardium										■	■	■
Subepicardium							■	■	■			
Interstitial cells in VCM										■	■	■

Table 1. Summary of the spatio-temporal protein expression patterns of PDGF-A, PDGFR- α , PDGF-B and PDGFR- β in the avian embryonic heart. This Table reflects alterations in total protein expression per area; for the receptor staining this relates to the number of positive cells per area, whereas for the ligands the overall amount of protein per area is indicated. PDGF-A and PDGFR- α have been observed mainly in myocardial tissues, while PDGF-B and PDGFR- β are mainly expressed in cells related to the developing coronary system. Abbreviations: A = atrial; AS = atrial septal; AV = atrioventricular; CA-ECs = coronary arterial endothelial cells; CaV = cardinal vein; C-vSMCs = coronary vascular smooth muscle cells; OFT = outflow tract; VC = ventricular compact; VCM = ventricular compact myocardium; VS = ventricular septal; VT = ventricular trabecular.

PDGFR- α expression colocalized with PDGF-A staining (Table 1), both in location and in time, in the myocardial wall of the cardinal vein (Figure 1c-d), the atrial myocardium and the atrial septal myocardium (Figure 1a-b). In the ventricular myocardium, PDGFR- α expression decreased in time in the compact myocardium, while increasing in the trabecular myocardium (Figure 1e-i). Furthermore, PDGFR- α was not present in the OFT cushion mesenchyme, but in the adjacent OFT myocardium, where the expression decreased in time.

Cardiac protein expression of PDGF-B and PDGFR- β

Presence of PDGF-B was observed in completely different areas in the heart compared with PDGF-A (Table 1). PDGF-B was present in the ventricular septal myocardium (Figure 2a), in the endothelial cells (Figure 2b) and vSMCs of the coronary arteries, in the subepicardium and in small cardiac nerves (Figure 2c). In the ventricular septal myocardium, PDGF-B was only present during early development of the septum. At HH30, when the ventricular septum was almost completed, presence of PDGF-B was already strongly diminished compared with HH28, and at HH35 PDGF-B was completely absent from the ventricular septum. Furthermore, while the endothelial cells of the coronary arteries already stained with the anti-PDGF-B antibody at HH28, the vSMCs only showed PDGF-B staining from HH30 onward. In addition, the presence of PDGF-B in the subepicardium decreased and the presence in the cardiac nerves stayed constant in time.

With regard to PDGFR- β (Table 1), expression was observed in the atrioventricular valves (Figure 2e), in vSMCs of the coronary arteries (Figure 2f-h), in

the epicardium, in the subepicardium, in interstitial cells located in the myocardium (Figure 2d) and in small cardiac nerves. In the atrioventricular valves and in the vSMCs of the coronary arteries, expression was only seen from HH30 onwards. However, no expression of either PDGFR- α or PDGFR- β in the interventricular septum was observed. The expression of PDGFR- β in the epicardium and subepicardium decreased in time, while the expression stayed constant in the interstitial cells in the myocardium and in the small cardiac nerves.

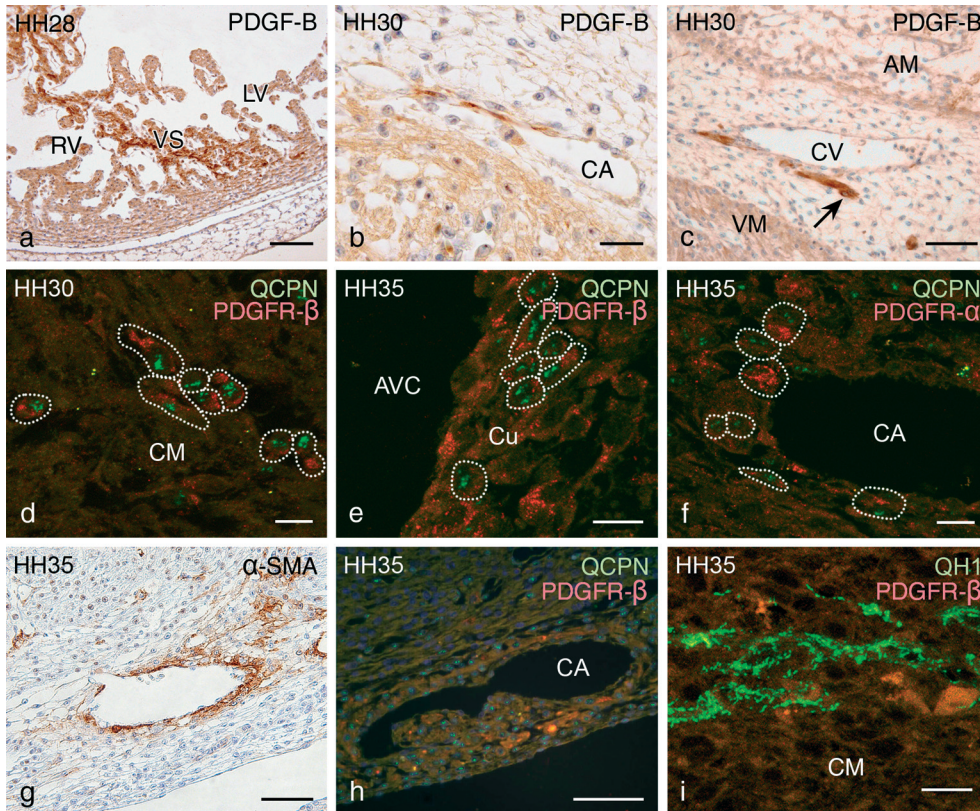


Figure 2. Expression of PDGF-B and PDGFR- β in pro-epicardial quail-chicken chimeras of HH28-35. Photomicrographs of representative transverse sections examined by light (a,b,c,g), fluorescence (h) or confocal fluorescence microscopy (d,e,f,i). a-c: PDGF-B is present in the developing ventricular septum (VS) at HH28 (a), in coronary arterial (CA) endothelial cells (b), and in cardiac nerves (c; arrow) at HH30. d-f: Quail-derived EPDCs (QCPN-positive, green nuclear staining) express PDGFR- β (red membranous staining) located in the compact myocardium (CM) at HH30 (d), in subendocardial cells of the AV-cushions (Cu; e) and in cells around a CA (f) at HH35. g: α -smooth muscle actin (α -SMA) expression around a CA at HH35. h: Consecutive section of g in which PDGFR- β expression (red) is seen in QCPN positive EPDCs (green) around a CA. i: Microvascular strands of quail-derived endothelial cells (QH-1, green) do not express PDGFR- β (red) at HH35. Additional abbreviations: AM = atrial myocardium; AVC = atrioventricular canal; CV = coronary vein; LV = left ventricle; RV = right ventricle; VM = ventricular myocardium;. Bar = 100 μ m (a), 50 μ m (b,c,g,h) or 10 μ m (d,e,f,i).

Expression of the PDGFRs in the EPDCs

The population of PDGFR- β positive cells in the heart closely resembled the spatio-temporal distribution of EPDCs^{2;3;5;8;9}. To analyze the identity of the PDGFR- β positive cells, we used pro-epicardial quail-chicken chimeras, in which quail-derived EPDCs were detected by the QCPN antibody (pan-quail nuclear staining). Double-staining of the QCPN antibody with an antibody against PDGFR- α showed that EPDCs did not express PDGFR- α between HH28 and HH35 (Table 1, Figure 1g,h). PDGFR- β positive EPDCs were present (i.e. in a QCPN/PDGFR- β double-staining cells, these cells showed green nuclear and red membranous staining) in all areas that showed PDGFR- β positive cells (Table 1; Figure 2d-h). The small PDGFR- β positive cardiac nerves are not derived from EPDCs but from neural crest cells³⁴. These results are compiled in the schematic Figure (Figure 3) that represents frontal views of the heart of quail-chicken chimeras at HH28 and HH35.

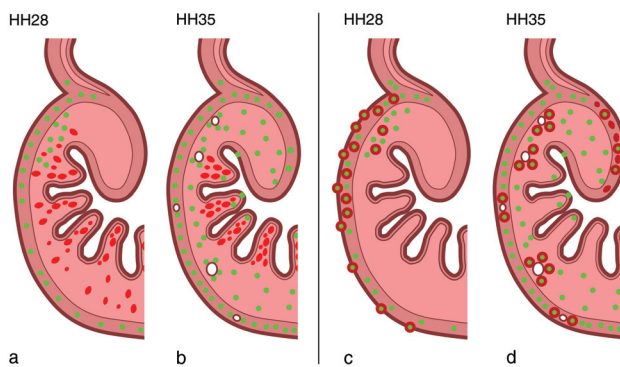


Figure 3. Compilation of PDGFR-expression in EPDCs. a-d: Drawing of a frontal view of a chicken embryonic heart of HH28 (a,c) and HH35 (b,d) in which the white circles represent coronary arteries. Green staining reflects the nuclei of the EPDCs, the red staining reflects PDGFR- α staining in a and b, and PDGFR- β staining in c and d. In a and b, the EPDCs do not express PDGFR- α , therefore no cells with both green and red

staining are visible. In c and d, the green cells represent the PDGFR- β negative EPDCs and the cells with green nuclear and red membranous staining represent PDGFR- β positive EPDCs. These expression patterns suggest that PDGFR- α signaling plays a role in embryonic myocardial development, whereas PDGFR- β signaling is important in the maturation of the coronary vasculature.

PDGFRs in cardiomyocytes, endothelial cells, and vSMCs between HH28 and HH35

To further identify the type of cells that express PDGFR- α or PDGFR- β , double-stainings were performed with either α/γ muscle actin (HHF35; cardiomyocytes and smooth muscle cells) or QH-1 (quail endothelial cells). Consecutive sections were stained for α -smooth muscle actin (1A4; smooth muscle cells), because no double-staining with anti-PDGFR- β antibody could be performed due to identical IgG subunits of the antibodies. Double-staining for PDGFR- α and α/γ muscle actin showed that all ventricular PDGFR- α positive cells from HH28 to HH35 also expressed α/γ muscle actin, implicating these were cardiomyocytes (Figure 1i). Staining for PDGFR- β and α -smooth muscle actin at HH35 showed overlapping expression patterns around the coronary vessels indicating that the epicardium-derived vSMCs in the media of the coronary vessels express PDGFR- β (Figure 2g-h). Furthermore, QH-1 positive endothelial cells were never PDGFR- β positive between HH28 and HH35 (Figure 2i).

Discussion

The present study describes the cardiac expression patterns of PDGF-A, PDGF-B, PDGFR- α and PDGFR- β in the avian embryo, highlighting the later stages of coronary maturation. Here, their possible roles in the development of the avian heart in general, and in that of the coronary system in particular will be discussed.

PDGF-A was found in the atrial and ventricular myocardium, with at HH28 an additional signal in the OFT cushion mesenchyme, while expression of PDGFR- α was seen in the OFT myocardium. It is likely that PDGF-A attracts PDGFR- α positive cells from the myocardium of the outflow tract into the cushion mesenchyme, where these cells lose their PDGFR- α expression. These expression patterns correlate well with OFT-malformations observed in *Patch* mice, harboring a mutated *Pdgfr- α* gene³². At HH28, PDGFR- α is also strongly expressed in the developing atrial septum. A role for PDGFR- α in septal development was also suggested by similar protein expression patterns in mice²³ and by the finding that atrial and ventricular septal defects are often encountered in *Patch* mice³². The presence of PDGF-A and PDGFR- α in the myocardial wall of the cardinal veins of the sinus venosus at HH28 might relate to the still active process of incorporation of the sinus venosus into the atrium. In literature, expression patterns of PDGF-A and PDGFR- α in sinus venosus have never been described. In the ventricular myocardium, the presence of PDGF-A and PDGFR- α was initially observed at low levels in both the compact and the trabecular myocardium. At later stages, PDGF-A remained present in the compact myocardium, but PDGFR- α became restricted to the trabeculae. This finding is in agreement with mRNA expression data of *Pdgfr- α* in mouse embryos³⁵. In the trabeculae, PDGF-A co-localized with, and thus seemed bound to, PDGFR- α , which was expressed by cardiomyocytes, especially in the older embryos (HH30-HH35). The role of PDGF-A/PDGFR- α -signaling in trabecular formation is unknown, although PDGFR- α stimulation by PDGF-A has a role in epithelial-mesenchymal interactions¹⁹. It has been proposed that this signaling is responsible for the formation of a smooth muscle cell layer in newly formed bronchial branches by promoting proliferation and migration of PDGFR- α -positive precursors of alveolar SMCs^{19;36}. Trabecular formation might be a process similar to branching, so it can be hypothesized that PDGF-A might be produced and secreted by the endocardium and promotes the ingrowth of PDGFR- α -expressing cardiomyocytes or cardiomyocyte precursors into the newly formed trabeculae, in a similar way as has been suggested for the bronchi. PDGF-A might have diffused into the myocardium, due to the possible lack of heparin-binding domains¹⁹, thereby explaining the lack of protein expression in the endocardium.

PDGF-B expression has previously only been described in endothelial cells and megakaryocytes during mouse embryonic development^{19;21;25}. However, in our avian model, the PDGF-B protein was highly present in the region of the developing ventricular septum, where neither of these cell types is present at that time, suggesting an additional PDGF-B producing cell type such as the cardiomyocytes. Combined

with observations in *Pdgf-b* and *Pdgfr-β* knockout mouse embryos, which have a higher incidence of ventricular septal defects compared with wild-type mice, these data suggest a role for PDGF-B-signaling in the formation of the ventricular septum. The exact pathways through which PDGF-B exerts its effect during ventricular septal development, however, are unclear as neither PDGFR- α nor PDGFR- β are expressed in the ventricular septum at that time (data not shown). Furthermore, PDGF-B might be involved in embryonic nervous development as well, since staining was observed in (cardiac) nerves. It has been described in rats that PDGF-B might be involved in peripheral nerve regeneration³⁷. With regard to PDGFR- β , its function has mainly been analyzed in vSMCs^{19;25}. Therefore, the presence of PDGFR- β positive EPDCs in AV-cushions, with unknown differentiation characteristics and function is remarkable. These cells might play a role in regulation of endocardial EMT in cushion tissue³⁸, perhaps by means of activation of extracellular matrix degradation. In vitro blockade of PDGFR- β -signaling with antibodies decreases MMP-2 levels³⁹. MMP-2 is an extracellular matrix degrading protein shown to be necessary for EMT in the atrioventricular cushions by facilitating migration⁴⁰⁻⁴². As PDGF-B staining is lacking at this site, PDGF-D might be responsible for activating PDGFR- β in this situation.

In the cells that contribute to the coronary system (epicardial cells, EPDCs, vSMCs and endothelial cells), PDGF-A or PDGFR- α staining was not observed between HH28-35. This finding indicates that PDGF-A signaling via PDGFR- α does not play a crucial role in avian coronary maturation. This is in agreement with data concerning *Pdgf-a* knockout and *Patch* (*Pdgfr-α* mutated) mice, in which no structural coronary malformations were described^{21;32}. However, an indirect role for PDGFR- α in coronary angiogenesis cannot be excluded because, first, *Patch* mice show diminished numbers of blood vessels in the heart³⁵ and second, epicardial PDGFR- α -positivity has been described in E12.5 mouse embryos (comparable with HH25 in avian embryos)²³.

Conversely, PDGF-B and PDGFR- β are present in all cell types of the developing coronary system, at all stages that we investigated. This, and the fact that *Pdgf-b* and *Pdgfr-β* knockout mice have severe coronary defects²⁵, confirm an essential role for PDGF-B and PDGFR- β in coronary maturation. Correct formation of a coronary vasculature with mature and stable vessel walls, depends largely on the properly timed presence and differentiation of EPDCs^{2;3;5;43-45}. We hypothesize that the PDGF-B/R β pathway plays a prominent role at all stages of EPDC formation and differentiation.

This study shows that PDGF-B and its β -receptor are present in the epicardium and subepicardium during the first step in this process: the formation of the subepicardial mesenchyme by EMT. In vitro studies show that this process can be induced by several factors, among which PDGF-B¹¹, FGF-1 and EGF⁷. The expression patterns observed in this study indicate that PDGF-B also contributes to epicardial EMT in vivo. Probably, the role of PDGF-B herein is by means of the upregulation of the expression of the transcription factor *Ets-1*⁴⁶, an intermediate in the PDGF-B signaling cascade that has been shown to be important for the formation of the subepicardial mesenchyme⁴³. Furthermore, stimulation of PDGFR- β might facilitate EMT by increasing MMP-2 levels locally, as has been postulated for endocardial cushion EMT (see above).

Following EMT, EPDCs start to migrate from the subepicardial mesenchyme into the underlying myocardium. We observed PDGFR- β positive, interstitial EPDCs in the myocardium at HH28, interstitial and vessel-related PDGFR- β -positive EPDCs at HH30 and solely vessel-related PDGFR- β -positive EPDCs at HH35. This might reflect the migration of PDGFR- β -positive EPDCs towards the developing coronary system, guided by chemokines such as PDGF-B produced by the endothelial cells. However, because with immunohistochemistry no PDGF-B-gradient, but only strong signal in close proximity to the endothelial cells is seen, this signaling pathway might be specifically responsible for the last part of the guided migration of the EPDCs, whereas other chemokines like PDGF-D or Heparin Binding EGF-like growth factor (HB-EGF)⁴⁷ might be involved in its initiation. PDGF-D is another ligand for PDGFR- β , but its embryonic expression patterns and thus its role in development are yet to be described. HB-EGF recently has been described to be involved in the attraction of vSMCs towards endothelial cells. Therefore, the distribution pattern of PDGFR- β positive cells might not solely be reflecting PDGF-B-dependent migration. Another function of PDGF-B produced by coronary endothelial cells might be stabilization of the structural integrity of the vascular wall³¹, explaining the non-diffuse localization and the increase in expression in the vascular wall in time.

EPDCs have earlier been shown to be the source of the coronary vSMCs^{3;9;14}. At stage HH35, the PDGFR- β -positive EPDCs around the coronary vessels co-localize with cells expressing α -smooth muscle actin, indicating that these EPDCs have differentiated into vSMCs. Since PDGF-B has been shown to induce migration rather than differentiation²⁶, the differentiation of the PDGFR- β -positive cells into vSMCs is probably directed by other factors, such as Transforming Growth Factor β (TGF β)^{48;49} and/or Serum Response Factor (SRF)⁵⁰. The role for PDGFR- β positive cells in the development and stabilization of the coronary vessel wall was demonstrated earlier *in vitro*^{48;51} and in many other vascular beds^{25;26;52}.

In conclusion, the spatiotemporal localization of PDGF-A and -B and their α and β -receptors suggests that PDGF-A signaling via PDGFR- α is important in the remodeling of the myocardium (sinus venosus, OFT, septa, trabeculae). PDGF-B might play a role in ventricular septum formation, however not through interaction with PDGFR- α or PDGFR- β as expression of these receptors is not observed. Furthermore, PDGF-B/PDGFR- β -signaling seems to be predominantly involved in maturation of EPDCs contributing to the coronary system and atrioventricular valves, both processes that start with EMT and are followed by the maturation of epicardium derived cells.

Acknowledgements

The authors would like to thank Jan Lens for photographic assistance, Bas Blankenvoort for the graphics in Figure 3, and Marleen Hessel (Department of Cardiology, LUMC, Leiden, the Netherlands) for technical assistance with the Western blots.

References

1. Viragh S, Gittenberger-De Groot AC, Poelmann RE, Kalman F. Early development of quail heart epicardium and associated vascular and glandular structures. *Anat Embryol (Berl)*. 1993;188:381-393.
2. Poelmann RE, Gittenberger-De Groot AC, Mentink MMT, Bokenkamp R, Hogers B. Development of the Cardiac Coronary Vascular Endothelium, Studied with Antiendothelial Antibodies, in Chicken-Quail Chimeras. *Circ Res*. 1993;73:559-568.
3. Vrancken Peeters MP, Gittenberger-De Groot AC, Mentink MM, Poelmann RE. Smooth muscle cells and fibroblasts of the coronary arteries derive from epithelial-mesenchymal transformation of the epicardium. *Anat Embryol (Berl)*. 1999;199:367-378.
4. Mikawa T, Gourdie RG. Pericardial mesoderm generates a population of coronary smooth muscle cells migrating into the heart along with ingrowth of the epicardial organ. *Dev Biol*. 1996;174:221-232.
5. Gittenberger-De Groot AC, Vrancken Peeters MP, Mentink MM, Gourdie RG, Poelmann RE. Epicardium-derived cells contribute a novel population to the myocardial wall and the atrioventricular cushions. *Circ Res*. 1998;82:1043-1052.
6. Vrancken Peeters MP, Mentink MM, Poelmann RE, Gittenberger-De Groot AC. Cytokeratins as a marker for epicardial formation in the quail embryo. *Anat Embryol (Berl)*. 1995;191:503-508.
7. Morabito CJ, Dettman RW, Kattan J, Collier JM, Bristow J. Positive and negative regulation of epicardial-mesenchymal transformation during avian heart development. *Dev Biol*. 2001;234:204-215.
8. Manner J, Perez-Pomares JM, Macias D, Munoz-Chapuli R. The origin, formation and developmental significance of the epicardium: a review. *Cells Tissues Organs*. 2001;169:89-103.
9. Dettman RW, Denetclaw W, Jr., Ordahl CP, Bristow J. Common epicardial origin of coronary vascular smooth muscle, perivascular fibroblasts, and intermyocardial fibroblasts in the avian heart. *Dev Biol*. 1998;193:169-181.
10. Lie-Venema H, Eralp I, Maas S, Gittenberger-De Groot AC, Poelmann RE, DeRuiter MC. Myocardial heterogeneity in permissiveness for epicardium-derived cells and endothelial precursor cells along the developing heart tube at the onset of coronary vascularization. *Anat Rec A Discov Mol Cell Evol Biol*. 2005;282:120-129.
11. Lu J, Landerholm TE, Wei JS, Dong XR, Wu SP, Liu X, Nagata K, Inagaki M, Majesky MW. Coronary smooth muscle differentiation from proepicardial cells requires rhoA-mediated actin reorganization and p160 rho-kinase activity. *Dev Biol*. 2001;240:404-418.
12. Tomanek RJ. Formation of the coronary vasculature: a brief review. *Cardiovasc Res*. 1996;31 Spec No:E46-E51.
13. Morabito CJ, Kattan J, Bristow J. Mechanisms of embryonic coronary artery development. *Curr Opin Cardiol*. 2002;17:235-241.
14. Munoz-Chapuli R, Macias D, Gonzalez-Iriarte M, Carmona R, Atencia G, Perez-Pomares JM. The epicardium and epicardial-derived cells: multiple functions in cardiac development. *Rev Esp Cardiol*. 2002;55:1070-1082.
15. Perez-Pomares JM, Carmona R, Gonzalez-Iriarte M, Atencia G, Wessels A, Munoz-Chapuli R. Origin of coronary endothelial cells from epicardial mesothelium in avian embryos. *Int J Dev Biol*. 2002;46:1005-1013.

16. Reese DE, Mikawa T, Bader DM. Development of the coronary vessel system. *Circ Res.* 2002;91:761-768.
17. Luttun A, Carmeliet P. De novo vasculogenesis in the heart. *Cardiovasc Res.* 2003;58:378-389.
18. Wessels A, Perez-Pomares JM. The epicardium and epicardially derived cells (EPDCs) as cardiac stem cells. *Anat Rec A Discov Mol Cell Evol Biol.* 2004;276:43-57.
19. Betsholtz C. Biology of platelet-derived growth factors in development. *Birth Defects Res C Embryo Today.* 2003;69:272-285.
20. Heldin CH, Eriksson U, Ostman A. New members of the platelet-derived growth factor family of mitogens. *Arch Biochem Biophys.* 2002;398:284-290.
21. Betsholtz C, Karlsson L, Lindahl P. Developmental roles of platelet-derived growth factors. *Bioessays.* 2001;23:494-507.
22. Morrison-Graham K, Schatteman GC, Bork T, Bowen-Pope DF, Weston JA. A PDGF receptor mutation in the mouse (Patch) perturbs the development of a non-neuronal subset of neural crest-derived cells. *Development.* 1992;115:133-142.
23. Takakura N, Yoshida H, Ogura Y, Kataoka H, Nishikawa S, Nishikawa S. PDGFR alpha expression during mouse embryogenesis: immunolocalization analyzed by whole-mount immunohistochemical staining using the monoclonal anti-mouse PDGFR alpha antibody APA5. *J Histochem Cytochem.* 1997;45:883-893.
24. Orr-Urtreger A, Lonai P. Platelet-derived growth factor-A and its receptor are expressed in separate, but adjacent cell layers of the mouse embryo. *Development.* 1992;115:1045-1058.
25. Lindahl P, Johansson BR, Leveen P, Betsholtz C. Pericyte loss and microaneurysm formation in PDGF-B-deficient mice. *Science.* 1997;277:242-245.
26. Hellstrom M, Kalen M, Lindahl P, Abramsson A, Betsholtz C. Role of PDGF-B and PDGFR-beta in recruitment of vascular smooth muscle cells and pericytes during embryonic blood vessel formation in the mouse. *Development.* 1999;126:3047-3055.
27. Zhuo Y, Hoyle GW, Zhang J, Morris G, Lasky JA. A novel murine PDGF-D splicing variant results in significant differences in peptide expression and function. *Biochem Biophys Res Commun.* 2003;308:126-132.
28. Fang L, Yan Y, Komuves LG, Yonkovich S, Sullivan CM, Stringer B, Galbraith S, Lokker NA, Hwang SS, Nurden P, Phillips DR, Giese NA. PDGF C is a selective alpha platelet-derived growth factor receptor agonist that is highly expressed in platelet alpha granules and vascular smooth muscle. *Arterioscler Thromb Vasc Biol.* 2004;24:787-792.
29. Ding H, Wu X, Kim I, Tam PP, Koh GY, Nagy A. The mouse *Pdgfc* gene: dynamic expression in embryonic tissues during organogenesis. *Mech Dev.* 2000;96:209-213.
30. Bategay EJ, Rupp J, Iruela-Arispe L, Sage EH, Pech M. PDGF-BB modulates endothelial proliferation and angiogenesis in vitro via PDGF beta-receptors. *J Cell Biol.* 1994;125:917-928.
31. Lindblom P, Gerhardt H, Liebner S, Abramsson A, Enge M, Hellstrom M, Backstrom G, Fredriksson S, Landegren U, Nystrom HC, Bergstrom G, Dejana E, Ostman A, Lindahl P, Betsholtz C. Endothelial PDGF-B retention is required for proper investment of pericytes in the microvessel wall. *Genes Dev.* 2003;17:1835-1840.

32. Schatteman GC, Motley ST, Effmann EL, Bowen-Pope DF. Platelet-derived growth factor receptor alpha subunit deleted Patch mouse exhibits severe cardiovascular dysmorphogenesis. *Teratology*. 1995;51:351-366.
33. Soriano P. The PDGF alpha receptor is required for neural crest cell development and for normal patterning of the somites. *Development*. 1997;124:2691-2700.
34. Verberne ME, Gittenberger-De Groot AC, Van IL, Poelmann RE. Distribution of different regions of cardiac neural crest in the extrinsic and the intrinsic cardiac nervous system. *Dev Dyn*. 2000;217:191-204.
35. Schatteman GC, Morrison-Graham K, van Koppen A, Weston JA, Bowen-Pope DF. Regulation and role of PDGF receptor alpha-subunit expression during embryogenesis. *Development*. 1992;115:123-131.
36. Lindahl P, Karlsson L, Hellstrom M, Gebre-Medhin S, Willetts K, Heath JK, Betsholtz C. Alveogenesis failure in PDGF-A-deficient mice is coupled to lack of distal spreading of alveolar smooth muscle cell progenitors during lung development. *Development*. 1997;124:3943-3953.
37. Oya T, Zhao YL, Takagawa K, Kawaguchi M, Shirakawa K, Yamauchi T, Sasahara M. Platelet-derived growth factor-b expression induced after rat peripheral nerve injuries. *Glia*. 2002;38:303-312.
38. Gittenberger-De Groot AC, Bartram U, Oosthoek PW, Bartelings MM, Hogers B, Poelmann RE, Jongewaard IN, Klewer SE. Collagen type VI expression during cardiac development and in human fetuses with trisomy 21. *Anat Rec A Discov Mol Cell Evol Biol*. 2003;275:1109-1116.
39. Kenagy RD, Hart CE, Stedler-Stevenson WG, Clowes AW. Primate smooth muscle cell migration from aortic explants is mediated by endogenous platelet-derived growth factor and basic fibroblast growth factor acting through matrix metalloproteinases 2 and 9. *Circulation*. 1997;96:3555-3560.
40. Alexander SM, Jackson KJ, Bushnell KM, McGuire PG. Spatial and temporal expression of the 72-kDa type IV collagenase (MMP-2) correlates with development and differentiation of valves in the embryonic avian heart. *Dev Dyn*. 1997;209:261-268.
41. Song W, Jackson K, McGuire PG. Degradation of type IV collagen by matrix metalloproteinases is an important step in the epithelial-mesenchymal transformation of the endocardial cushions. *Dev Biol*. 2000;227:606-617.
42. Enciso JM, Gratzinger D, Camenisch TD, Canosa S, Pinter E, Madri JA. Elevated glucose inhibits VEGF-A-mediated endocardial cushion formation: modulation by PECAM-1 and MMP-2. *J Cell Biol*. 2003;160:605-615.
43. Lie-Venema H, Gittenberger-De Groot AC, van Empel LJ, Boot MJ, Kerkdijk H, de Kant E, DeRuiter MC. Ets-1 and Ets-2 transcription factors are essential for normal coronary and myocardial development in chicken embryos. *Circ Res*. 2003;92:749-756.
44. Gittenberger-De Groot AC, Vrancken Peeters MP, Bergwerff M, Mentink MM, Poelmann RE. Epicardial outgrowth inhibition leads to compensatory mesothelial outflow tract collar and abnormal cardiac septation and coronary formation. *Circ Res*. 2000;87:969-971.
45. Eralp I, Lie-Venema H, DeRuiter MC, Van Den Akker NM, Bogers AJ, Mentink MM, Poelmann RE, Gittenberger-De Groot AC. Coronary artery and orifice development is associated with proper timing of epicardial outgrowth and correlated Fas-ligand-associated apoptosis patterns. *Circ Res*. 2005;96:526-534.
46. Naito S, Shimizu S, Maeda S, Wang J, Paul R, Fagin JA. Ets-1 is an early response gene activated by ET-1 and PDGF-BB in vascular smooth muscle cells. *Am J Physiol*. 1998;274:C472-C480.

47. Iivanainen E, Nelimarkka L, Elenius V, Heikkinen SM, Junntila TT, Sihombing L, Sundvall M, Maatta JA, Laine VJ, Yla-Herttuala S, Higashiyama S, Alitalo K, Elenius K. Angiopoietin-regulated recruitment of vascular smooth muscle cells by endothelial-derived heparin binding EGF-like growth factor. *FASEB J*. 2003;17:1609-1621.
48. Hirschi KK, Rohovsky SA, D'Amore PA. PDGF, TGF-beta, and heterotypic cell-cell interactions mediate endothelial cell-induced recruitment of 10T1/2 cells and their differentiation to a smooth muscle fate. *J Cell Biol*. 1998;141:805-814.
49. Nishishita T, Lin PC. Angiopoietin 1, PDGF-B, and TGF-beta gene regulation in endothelial cell and smooth muscle cell interaction. *J Cell Biochem*. 2004;91:584-593.
50. Landerholm TE, Dong XR, Lu J, Belaguli NS, Schwartz RJ, Majesky MW. A role for serum response factor in coronary smooth muscle differentiation from proepicardial cells. *Development*. 1999;126:2053-2062.
51. Zerwes HG, Risau W. Polarized secretion of a platelet-derived growth factor-like chemotactic factor by endothelial cells in vitro. *J Cell Biol*. 1987;105:2037-2041.
52. Hoch RV, Soriano P. Roles of PDGF in animal development. *Development*. 2003;130:4769-4784.
53. Hamburger V, Hamilton HL. A series of normal stages in the development of the chick embryo. *J Morphol*. 1951;88:49-92.
54. Bergwerff M, Gittenberger-De Groot AC, DeRuiter MC, van Iperen L, Meijlink F, Poelmann RE. Patterns of paired-related homeobox genes PRX1 and PRX2 suggest involvement in matrix modulation in the developing chick vascular system. *Dev Dyn*. 1998;213:59-70.

Chapter 5

PDGF-B-signaling is Important for Murine Cardiac Development; Its Role in Developing Atrioventricular Valves, Coronaries, and Cardiac Innervation

Nynke M.S. van den Akker¹, Leah C.J. Winkel¹, Maya H. Nisancioglu², Saskia Maas¹, Lambertus J. Wisse¹, Annika Armulik², Robert E. Poelmann¹, Heleen Lie-Venema¹, Christer Betsholtz² and Adriana C. Gittenberger-de Groot¹

¹Department of Anatomy and Embryology, Leiden University Medical Center, Leiden, The Netherlands; ²The Vascular Biology Laboratory, Division of Matrix Biology, Department of Medical Biochemistry and Biophysics, Karolinska Institutet, Stockholm, Sweden.

Modified after Developmental Dynamics, 2008, In Press.

PDGF-B-signaling is Important for Murine Cardiac Development; Its Role in Developing Atrioventricular Valves, Coronaries, and Cardiac Innervation

Abstract

We hypothesized that PDGF-B/PDGFR- β -signaling is important in the cardiac contribution of epicardium-derived cells and cardiac neural crest, cell lineages crucial for heart development. We analyzed hearts of different embryonic stages of both *Pdgf-b*^{-/-} and *Pdgfr- β* ^{-/-} mouse embryos for structural aberrations with an established causal relation to defective contribution of these cell lineages. Immunohistochemical staining for α SMA, periostin, ephrinB2, EphB4, VEGFR-2, Dll1 and NCAM was performed on wild-type and knockout embryos. We observed that knockout embryos showed perimembranous and muscular ventricular septal defects, maldevelopment of the atrioventricular cushions and valves, impaired coronary arteriogenesis and hypoplasia of the myocardium and cardiac nerves. The abnormalities correspond with models in which epicardial development is impaired and with neuronal neural crest-related innervation deficits. This implies a role for PDGF-B/PDGFR- β -signaling specifically in the contribution of these cell lineages to cardiac development.

Introduction

The development of the heart starts with the formation of the primary heart tube, consisting of a myocardial and an endocardial layer with cardiac jelly in between. Subsequent development into a fully septated heart requires recruitment towards and incorporation within the primitive heart of the cardiac neural crest and the epicardium. Cardiac neural crest cells (cNCCs) are important in development of the aortic arch (AoA), in segmentation of the outflow tract (OFT), in semilunar valve development and in the development of the cardiac conduction system and cardiac innervation¹⁻³. The epicardium develops from the pro-epicardial organ (PEO), which is derived from the dorsal mesoderm⁴. Protrusions of the PEO extend from the sinus venosus towards the naked heart tube. After lateral outgrowth of the epicardium, that eventually covers the complete heart, it gives rise to epicardium-derived cells (EPDCs) via epithelial-to-mesenchymal transformation (EMT)^{5,6}. EPDCs form the subepicardial mesenchyme and numerous EPDCs migrate into the myocardium where they contribute to the interstitial fibroblasts, the coronary vessel wall and to the development of the atrioventricular valves and Purkinje fibers (reviewed in⁷ and⁸).

Platelet-derived growth factors (PDGFs) are important in cardiac development^{9,10}, as ultimately demonstrated in knockout mice for either *Pdgfs* or PDGF-receptors (*Pdgfrs*). For example, loss of PDGFR- α -signaling leads to both AoA and OFT malformations^{11,12}, comparable to the anomalies found in cNCC-ablated chicken embryos¹ and in mouse mutants in which the cNCC-population is affected^{13,14}. The expression patterns of PDGF-B and PDGFR- β during avian cardiogenesis indicate that this pathway is involved in coronary maturation¹⁰. Indeed, knockout mice for either *Pdgf-b* or *Pdgfr- β* show underdeveloped coronary arteries, in addition to dilated hearts and ventricular septal defects (VSDs)^{9,15,16}.

In the current study, we further analyzed the cardiovascular abnormalities in the *Pdgf-b* and *Pdgfr- β* knockout mouse models and discuss how this relates to the cellular biology of PDGF-B/PDGFR- β -signaling within the developing heart. The majority of abnormalities found could be related to abnormal EPDC and/or neuronal cNCC-development, suggesting an important role for PDGF-B/PDGFR- β -signaling in the contribution of these cell lineages to cardiac development.

Materials and Methods

Mouse experiments

Animals were housed in the Scheele Animal Facility at MBB, Karolinska Institute, Stockholm under standard conditions. All procedures were carried out following approval from the animal ethical board of northern Stockholm and in accordance with institutional policies. *Pdgf-b*^{+/-} or *Pdgfr-β*^{+/-} mice were crossed to obtain *Pdgf-b*^{-/-} and *Pdgfr-β*^{-/-} embryos along with wild-type (+/+) littermates. The morning of the vaginal plug was stated embryonic day (E)0.5. Pregnant females were sacrificed by cervical dislocation, embryos were harvested and thoraces were isolated, immersion-fixed in 4% paraformaldehyde/phosphate-buffered saline (0.1 Mol/L, pH 7.4) for 24 hours after which they were dehydrated and embedded in paraffin. *Pdgf-b*^{-/-}, *Pdgfr-β*^{-/-} and wild-type embryos of E13.5, E14.5, E15.5 and E17.5 were transversely sectioned into sections of 5 μm.

Immunohistochemistry and microscopy

Sections were deparaffinated, rehydrated and antigen retrieval was achieved by heating (12 minutes to 98 °C) in citric acid buffer (0.01 Mol/L, pH 6.0). Inhibition of endogenous peroxidase activity was attained by incubation for 20 minutes in 0.3% H₂O₂ in PBS. Incubation with primary antibody (against αSMA, clone 1A4, A2547, Sigma-Adrich, Missouri, USA; periostin, a kind gift from Prof. R.R. Markwald, Charleston, USA; phospho-Histone H3, 06-570, Millipore, Billerica, USA; Dll1, sc-9102, Santa Cruz, Santa Cruz, USA; VEGFR-2, AF644, R&D Systems, Minneapolis, USA; ephrinB2, AF496, R&D Systems; EphB4, AF446, R&D Systems or NCAM, AB5032, Chemicon, Temecula, USA) occurred overnight in a humidified chamber at room temperature. After that, sections were incubated for 1 hour with peroxidase-labeled antibody (in case of αSMA staining; rabbit-anti-mouse; P0260, DAKO, Glostrup, Denmark) or biotin-labeled secondary antibody (all other stainings; goat-anti-rabbit (BA-1000) or horse-anti-goat (BA-9500), both Vector Labs, Burlingame, USA). In all stainings except for the αSMA staining, additional incubation with Vectastain ABC staining kit (PK-6100, Vector Labs) was performed for 45 minutes. Visualization was performed with the DAB-procedure and Mayer's hematoxylin was used as counterstaining. Sections were mounted with Entellan (1.07961.0100, Merck). Micrographs were made using an Olympus AX70-microscope fitted with Olympus UPlanApo-objectives, using an Olympus DP12 camera (Olympus, Tokyo, Japan).

Results

A summary of the observed cardiovascular aberrations in *Pdgf-b*^{-/-} mouse embryos ranging in age from embryonic day (E) 13.5 to E17.5 is provided in Table 1. The abnormalities will be outlined below with respect to their structural, coronary and innervation characteristics and in relation to the *Pdgfr-β*^{-/-} phenotype.

Structural cardiovascular anomalies in Pdgf-b^{-/-} *embryos*

Although the Anlage of the AoA was normal in *Pdgf-b* knockout embryos, ensuing AoA-hypoplasia was encountered in several embryos (Figure 1a,e). In a number of embryos a common pulmonary artery branched off the pulmonary trunk (PT) before splitting in a left and a right artery (Figure 1f). In all wild-type embryos (n=11), the left and right pulmonary artery branched individually from the PT (Figure 1b).

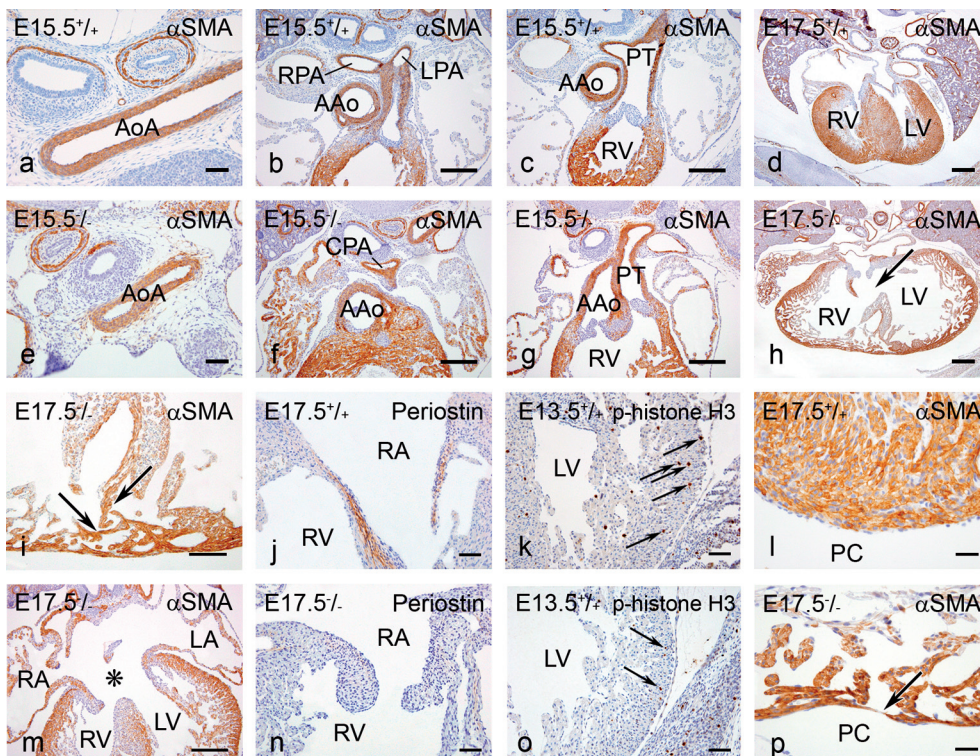
Table 1. Cardiovascular abnormalities in Pdgf-b^{-/-} *embryos of E13.5-E17.5.*

Anomaly	No/Total	%
Hypoplastic aortic arch	4/11	36
Common stem pulmonary arteries	3/11	27
Side-by-side of the AAo and PT	2/11	18
Dextropositioning ascending aorta	6/11	55
VSD	11/11	100
Perimembranous only	1/11	9
Muscular only	2/11	18
Perimembranous + muscular	8/11	73
DORV	6/11	55
AVSD	1/11	9
Underdeveloped AV-valves	9/9*	100
Hypoplastic myocardium	11/11	100
Pinpoint CoO	9/9*	100
>2 CoO	4/9*	44
<2 CoO	1/9*	11
Hypoplastic coronary media	7/9*	78
Wide coronary vessels	11/11	100
Arterial	6/11	55
Venous	5/11	45
Microvascular	6/11	55
VCAC	10/11	91
Hypoplastic nerve plexus PVs	6/8**	75

AAo, ascending aorta; PT, pulmonary trunk; VSD, ventricular septal defect; AVSD, atrioventricular septal defect; DORV, double-outlet right ventricle; AV, atrioventricular; CoO, coronary orifices; VCAC, ventriculo-coronary arterial communications; PVs, pulmonary veins. *could only be scored in embryos of E14.5 and older. **could only be scored in embryos stained for NCAM.

In 9/11 knockout embryos a perimembranous VSD (Figure 1d,h) was found. Furthermore, dextropositioning of the ascending aorta was observed in a subset of embryos, sometimes accompanied by side-by-side positioning of the aorta and PT (Figure 1c,g). All cases with dextropositioning of the ascending aorta also showed a perimembranous VSD, resulting in double-outlet right ventricle (DORV).

In addition to perimembranous VSDs, almost all (10/11) mutant embryos showed discontinuities in the muscular part of the ventricular septum (VS), resulting in muscular VSDs (Figure 1i). In one *Pdgf-b-/-* embryo an atrioventricular septal defect (AVSD) was encountered (Figure 1m). In all knockout embryos of E14.5 and older underdeveloped atrioventricular valves were observed. They showed a short, thick, cushion-like valve-morphology instead of long and slender valves as seen in normal embryos. In addition, a severe decrease in expression of the extracellular matrix-component periostin was observed in *Pdgf-b-/-* atrioventricular valves (Table 1 and Figure 1j,n). Alterations in patterns or levels of periostin-expression were not encountered in other parts of the mutant hearts. Lastly, mutants showed defective establishment of myocardial architecture, with extremely hypoplastic compact myocardium (Table 1 and Figure 1l,p). This was concomitant with decreased levels of myocardial proliferation, mainly observed at earlier developmental stages (E13.5; Figure 1k,o), and with absence of ventricular myocardial apoptosis in both genotypes (data not shown).



Coronary malformations in Pdgf-b^{-/-} embryos

Ingrowth of the coronary system into the aorta normally takes place around E14. Two coronary orifices (CoO) are formed and systemic flow is started, initiating maturation of the coronary vascular bed. Therefore, abnormalities in the CoO and coronary maturation in the *Pdgf-b* knockout model were only scored in embryos of E14.5 and older. Abnormalities in the number of CoO were found with either an increased number (4/9 cases; Figure 2a,e) or a complete absence (1/9 case). Also, pin-point CoO were seen in all of these knockout embryos (Figure 2e,i).

Additionally, the coronary arterial media was maldeveloped as less vascular smooth muscle cells (vSMCs) were seen and the vSMCs were hypoplastic (Figure 2b,f). Normally, Delta-like 1 (Dll1) is expressed by vSMC during coronary maturation (Figure 2c and consecutive α SMA-stained section in 2d). In knockout coronary arteries, however, apparent loss of Dll-1-expression in individual vSMCs was observed (Figure 2g and consecutive α SMA-stained section in 2h).

In nearly all *Pdgf-b^{-/-}* embryos (10/11) ventriculo-coronary artery connections (VCACs) were encountered, in which an open connection was visible between a coronary artery and the ventricular lumen (Figure 2l). In addition, in all mutant embryos one or more types of intracardiac vessels (i.e. coronary arteries, veins and microvessels) were dilated (Figure 2b,f,j,m). In 2 *Pdgf-b^{-/-}* embryos a connection between the coronary venous system and the pericardial cavity was seen (coronary rupture), with in the oldest case (E17.5) an attachment of the pericardium to the epicardium surrounding the rupture (Figure 2k,n).

Although many structural coronary abnormalities were found in this mouse model, differentiation of both coronary arterial and venous endothelial cells (ECs) was normal as observed using immunostainings for arterial and venous EC-specific markers, ephrinB2 and EphB4 respectively (data not shown).

← *Figure 1. Structural cardiac anomalies in Pdgf-b^{-/-} mouse embryos.* Knockout embryos (*-/-*) were compared with wild-types (*+/+*; upper left corner together with embryonic age in days (E)). Indicated upper right are the stainings performed. *Pdgf-b^{-/-}* embryos frequently show abnormalities of the aortic arch (AoA) such as hypoplasia (a,e), a common stem of the pulmonary arteries (CPA; b,f) or a side-by-side positioning of the ascending aorta (AAo) and the pulmonary trunk (PT; c,g). Both perimembranous (arrow in h) and muscular (between arrows in i) ventricular septal defects were seen in most *-/-*, but never in *+/+* embryos (d). Once, an atrioventricular septal defect (AVSD) was seen (asterisk in m). The atrioventricular valves were underdeveloped and showed a severe decrease in periostin-expression (j,n). Decrease in ventricular myocardial proliferation was seen in *-/-* embryos, especially at younger stages (k,o), concomitant with extreme hypoplasia of the compact myocardium, which was observed in all *-/-* embryos (l,p). Abbreviations; L \bar{A} = left atrium; LPA = left pulmonary artery; LV = left ventricle; PC = pericardial cavity; RA = right atrium; RPA = right pulmonary artery and RV = right ventricle. Scale bar: 60 μ m (a,e,j,k,n,o), 200 μ m (b,c,f,g,i,m), 300 μ m (d,h) or 30 μ m (l,p).

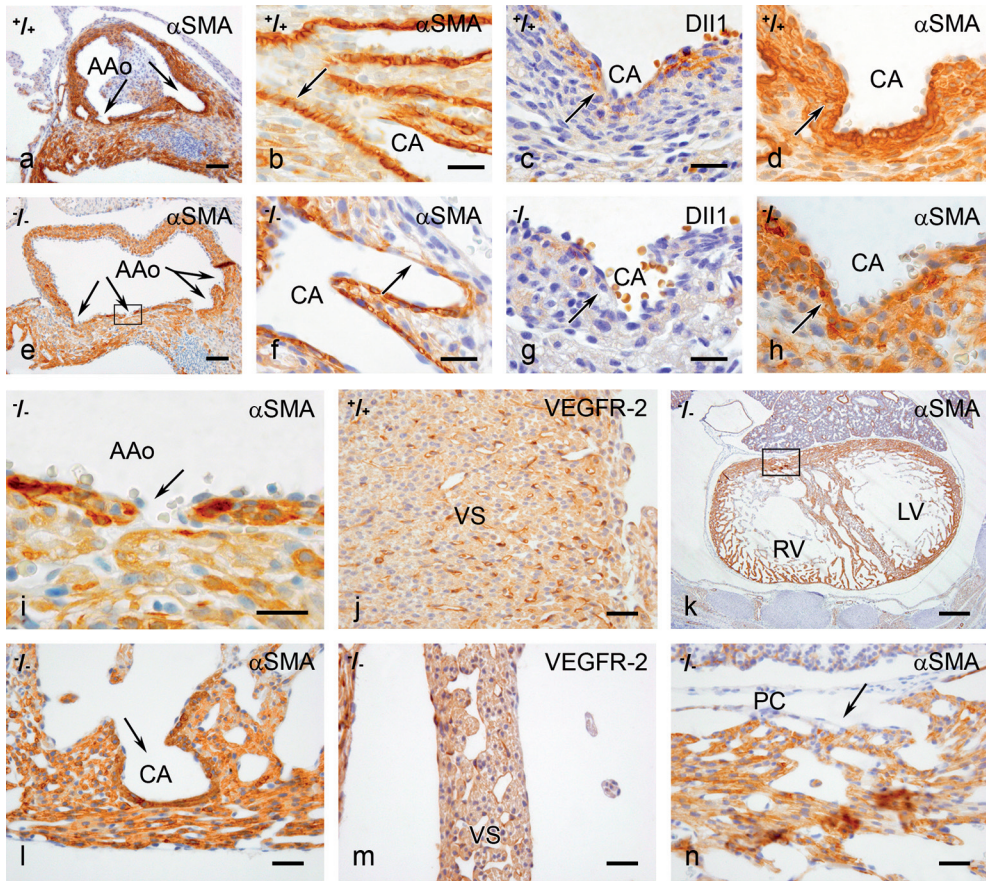


Figure 2. Coronary abnormalities in Pdgf-b-/- embryos. Knockout (-/-) and wild-type (+/+) embryos, as shown in the upper left corner, of embryonic day 17.5 were compared. Stainings performed are indicated in the upper right corner. Knockout embryos show an increase in number of coronary orifices (compare arrows in a with those in e), and pin-point coronary orifices (i; magnification of the boxed area in e). Few, extremely thin, vascular smooth muscle cells cover the arteries (CA; arrows in b and f) and Dll1-expression is downregulated (arrows in c and g). d and h are consecutive α SMA-stained sections of c and g, respectively, showing that vascular smooth muscle cells are present in the -/- embryos, although they lack Dll1-expression. Large microvessels are observed in the hypoplastic ventricular septum (VS; j vs m). Ventriculo-coronary artery connections were often observed in -/- embryos (arrow in l) and occasionally, a connection between the coronary system and the pericardial cavity (PC) was seen (arrow in n; n is a magnification of the boxed area in k). Abbreviations; AAo = ascending aorta; LV = left ventricle and RV = right ventricle. Scale bar: 60 μ m (a,e), 20 μ m (b,c,f,g,i), 30 μ m (j,m,l,n) or 300 μ m (k).

Anomalies in cardiac innervation in Pdgf-b^{-/-} embryos

To investigate cardiac innervation, staining for neural cell adhesion molecule (NCAM) was performed. NCAM is expressed by many cardiac cell types, but at the stages investigated, expression was mainly seen in the cardiac innervation (Figure 3a,d). In 6 out of 8 *Pdgf-b^{-/-}* embryos we observed hypoplasia of the nerves in and surrounding the heart. This was most apparent in the nerve plexus located next to the left cardinal vein and directly caudal from the area where the pulmonary veins enter the left atrium (Figure 3a-b,d-e). The borders of the cardiac nerves could be morphologically determined using high power magnification photos (Figure 3c,f) indicating that the nerves are smaller in size rather than that nervous cells have lost their NCAM-expression. This is also supported by the fact that NCAM-expression per cell is unaltered in mutant cardiac nerves (Figure 3c,f).

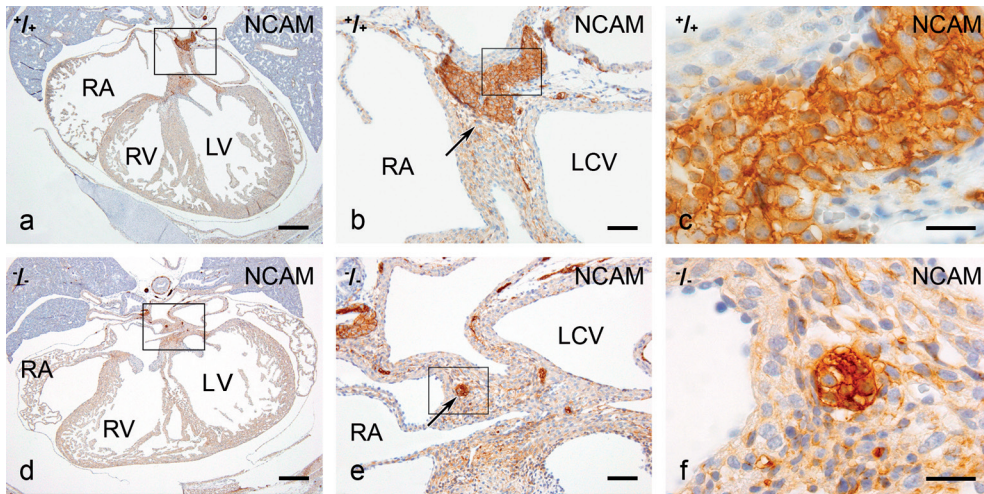


Figure 3. Cardiac innervation in *Pdgf-b^{-/-}* embryos. A nerve-specific marker (NCAM) was used to compare wild-type (+/+) and knockout (-/-) mouse embryos of embryonic day 17.5. In +/+ embryos, a large nerve plexus next to the left cardinal vein (LCV) was seen (a and arrow in b; b is a magnification of the boxed area in a), which is abnormally small in -/- embryos (d and arrow in e; e is a magnification of the boxed area in d). c and f are magnifications of the boxed areas in b and e, respectively, and show that all cells with nerve-morphology are NCAM-positive. Abbreviations; LV = left ventricle; RA = right atrium and RV = right ventricle. Scale bar: 300 μ m (a,d), 60 μ m (b,e) or 20 μ m (c,f).

Anomalies in the Pdgfr-β-/- embryos

When compared with *Pdgf-b-/-* embryos, *Pdgfr-β-/-* embryos showed similar abnormalities, although to a different extent. Of the *Pdgfr-β-/-* embryos investigated (n=6; E15.5 and E17.5), a larger percentage showed hypoplasia of the AoA than in the *Pdgf-b-/-* group (67% vs 36%). All *Pdgfr-β-/-* embryos showed hypoplasia of the compact myocardium, but not as severe as in the *Pdgf-b-/-* embryos (Figure 4a-c). Furthermore, VSDs (perimembranous and/or muscular) were encountered less frequently (67% vs 100%). Abnormalities in the CoO were never encountered in *Pdgfr-β-/-* embryos compared with 100% in the *Pdgf-b-/-* group, although the occurrence of further coronary abnormalities (i.e. impaired arteriogenesis, dilated coronary vessels and VCACs) was comparable between groups (Figure 4d-f and data not shown). The occurrence of hypoplastic cardiac nerves was less frequent in *Pdgfr-β-/-* than in *Pdgf-b-/-* embryos (33% vs 75%).

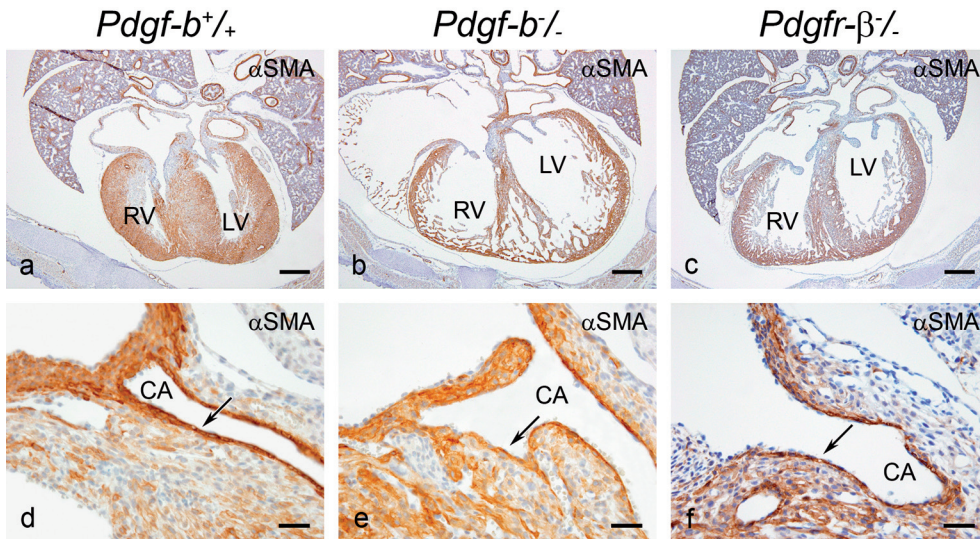


Figure 4. *Abnormalities in Pdgfr-β-/- embryos.* All sections are stained for αSMA. Abnormalities in *Pdgfr-β-/-* (β-/-) are compared with wild-type (+/+) and *Pdgf-b-/-* (-/-) embryos of embryonic day 17.5. Hypoplastic ventricular myocardium is seen in β-/- embryos when compared with +/+ (a vs c), but -/- embryos show more extreme hypoplasia (b). Both β-/- and -/- embryos show wide coronary arteries (CA) with thin, longspread vascular smooth muscle cells (arrows in e and f) when compared with +/+ (d). Abbreviations; LV = left ventricle and RV = right ventricle. Scale bar: 300 μm (a-c) or 30 μm (d-f).

Discussion

*Cardiovascular abnormalities in *Pdgf-b*^{-/-} and *Pdgfr-β*^{-/-} mouse embryos*

The most striking cardiac abnormalities in *Pdgf-b*^{-/-} mouse embryos were perimembranous and muscular VSDs, abnormal AV-valve development, impaired coronary arteriogenesis and hypoplasia of the compact myocardium. Impaired PEO-outgrowth over the heart or defective epicardial EMT leads to comparable malformations¹⁷⁻¹⁹. We suggest that PDGF-B produced by coronary ECs^{10;20} and endocardial cells (unpublished observations) plays a role in epicardial EMT and subsequent recruitment and performance of EPDCs. This is supported by the observation that PDGF-B is able to induce epicardial EMT in vitro²¹, and underscored by in vivo expression patterns of PDGF-B and PDGFR-β during cardiogenesis¹⁰.

Additionally, AoA and OFT-abnormalities were found, reminiscent of neural crest abnormalities. Finally, we show that PDGF-B/PDGFR-β-signaling is important in the development of cardiac nerves, suggesting a role for PDGF-B/PDGFR-β-signaling in (mainly neuronal) cNCC-development.

*Myocardial hypoplasia in *Pdgf-b*^{-/-} and *Pdgfr-β*^{-/-} embryos*

Several genetic and experimental animal models have shown that correct functioning of the epicardium and EPDCs is a prerequisite for development of the compact ventricular myocardium^{18;19;22} (reviewed in⁷). First, EPDCs contribute physically to the myocardial wall as interstitial fibroblasts²², which can make up 70% of the cells of the myocardial wall (reviewed in⁸). Second, EPDC-derived deposition of fibrous tissue that contributes to correct myocardial architecture is important during development of the ventricular wall^{8;23}. This is likely dependent on PDGF-signaling as this pathway is able to promote collagen-production in the infarcted heart²⁴. Third, accurate spatiotemporally regulated myocardial proliferation is essential during cardiac development, a process dependent on EPDC-contribution²⁵. The proliferation-rate in cardiomyocytes of *Pdgf-b*^{-/-} embryos is decreased concomitant with comparable apoptosis-levels pleading for diminished EPDC-dependent induction of cardiomyocyte-proliferation. Therefore, impaired epicardial development in *Pdgf-b*^{-/-} and *Pdgfr-β*^{-/-} embryonic hearts might well explain the hypoplastic myocardium and muscular VSDs through its effect on these three processes.

A direct effect of the loss of PDGF-B/PDGFR-β-signaling on cardiomyocytes is not likely, since embryonic cardiomyocytes do not express PDGFR-β¹⁰. Because PDGF-B can bind PDGFR-α in vitro²⁶, and because most of the embryonic cardiomyocytes express this receptor¹⁰, a PDGFR-β-independent role of PDGF-B on myocardial development can be expected. This is in line with the finding that *Pdgfr-β*^{-/-} embryos show less extreme myocardial hypoplasia than *Pdgf-b*^{-/-} embryos.

*Ventricular septation and AV-valve development in *Pdgf-b/-* mouse embryos*

As proper development of the epicardium and EPDCs is crucial for correct looping and septation of the heart¹⁷, abnormal EPDC-development in *Pdgf-b/-* embryos can additionally explain the occurrence of perimembranous VSD and DORV and of the one AVSD in our dataset.

With regard to normal development of the mitral and tricuspid valves, primitive AV-cushions become populated by endocardial cells through EMT, after which the cushions develop into valves²⁷. Migration of EPDCs into AV-cushions, probably dependent on PDGFR- β -signaling¹⁰, is important in this transition²². One of the extracellular matrix components expressed in AV-valves is periostin²⁸. It is involved in their development through its pro-fibrotic role in remodeling of the extracellular matrix^{28;29}. The failure of AV-cushions transformation towards AV-valves in both *Pdgf-b/-* and *Pdgfr- β /-* mouse embryos coincides with severe decrease in periostin-expression. We recently showed that valvular EPDCs produce periostin during avian atrioventricular valve-development²³. Thus, defective valvular EPDC-recruitment with consequent loss of periostin could explain the valve maturation deficits in our models. In addition, no alterations in periostin-expression were found in other parts of the heart, making a direct effect of PDGF-B/PDGFR- β -signaling on periostin-expression unlikely. This PDGFR- β -dependent role of EPDCs in AV-valve development is further supported by the fact that no abnormalities were found in the OFT-valves, of which development does not rely on EPDCs²².

PDGF-B-signaling and coronary development

A striking observation is the occurrence of dilated coronary vessels in all *Pdgf-b/-* and *Pdgfr- β /-* embryos. It can be hypothesized that the presence of dilated coronary vessels could be induced by lack of physical support to the coronary vessels due to myocardial hypoplasia, thereby proposing an indirect way through which impaired functioning of EPDCs contributes to dilation of the coronary system.

A direct way through which EPDCs influence vascular stability can also be proposed. ECs are the first cells within the coronary system expressing PDGF-B¹⁰. Our results show that endothelial differentiation is normal in the *Pdgf-b/-* mouse model, as ultimately exemplified by ephrinB2 and EphB4 expression³⁰. We confirm that arteriogenesis is severely impaired¹⁶, as only few vSMCs had populated the proximal coronary arteries. We suggest that endothelial function of recruiting and stabilizing vSMCs^{10;20;31} is impaired due to their inability to produce PDGF-B. This can cause impaired recruitment or local expansion and differentiation of EPDCs and thus dilated coronary vessels as seen in the *Pdgf-b/-* embryos. However, other models in which epicardial outgrowth is impaired^{19;32-34} do not markedly show dilation of the coronary system, suggesting that the dilation observed in our models is due to a combination of impaired epicardial development and a direct local effect on vascular stabilization of loss of PDGF-B/PDGFR- β -signaling³¹.

The coronary vSMCs are not only fewer in number, they also show abnormal morphology as revealed using the early-stage vSMC-marker α SMA. Abnormal differentiation can be deduced from aberrant Dll1-expression, involved in later stages of vSMC-development and implicated in arteriogenesis³⁵. Since PDGF-B-signaling is related to pericyte-expression of delta homologue 1 (DLK1)³⁶, a Notch1-binding protein closely related to the Delta proteins³⁷, loss of endothelial PDGF-B-production and PDGFR- β -signaling in the vSMCs may in a similar way lead to impaired Dll1-expression and thus vSMC-differentiation in this setting.

A striking observation in all *Pdgf-b*^{-/-} embryos of E14.5 and older is the presence of pin-point CoO, as has been described in humans to occur in combination with common arterial trunk or pulmonary atresia^{38;39}. Normally, multiple small endothelial strands enter the aorta upon which two become stabilized to form the ultimate CoO⁴⁰, which is an EPDC-dependent process^{18;19}. Impaired EPDC-migration could explain the occurrence of more than two, pin-point, orifices in the *Pdgf-b*^{-/-} embryos. This does not occur in *Pdgfr- β* ^{-/-} embryos, suggesting that PDGF-B-signaling other than through PDGFR- β (possibly through PDGFR- α) is involved in these processes.

Another important finding in the coronary system is the frequent occurrence of VCACs. VCACs have been linked to epicardial and subsequent coronary anomalies rather than to primary myocardial or endocardial abnormalities⁴¹ and are also observed in a chicken model with epicardial impairment¹⁸. This supports altered EPDC-development as an underlying cause for coronary malformations in *Pdgf-b*^{-/-} and *Pdgfr- β* ^{-/-} embryos.

PDGF-B/PDGFR- β -signaling is not crucial in primary OFT-development

PDGFR- α and PDGFR- β -signaling pathways cooperate in modulation of migration and function of cNCCs in OFT-development¹³. Yet, malformations in OFT-septation of *Pdgfr- β* ^{-/-} embryos were not encountered. In contrast, *Pdgfr- α* ^{-/-} embryos show OFT-malformations comparable to cNCC-ablated chicken embryos^{11;12}.

Another population of cells important for OFT-development is the anterior heart field (AHF)⁴². This subpopulation of the second heart field is located in the splanchnic mesoderm. The AHF adds cells to the primitive heart tube at the OFT⁴³, which is thought to be cNCC-dependent⁴⁴. When development of the AHF is impaired, severe OFT-malformation including pulmonary stenosis or even pulmonary atresia arise^{45;46}. Abnormalities found in *Pdgfr- α* ^{-/-} mouse embryos are more reminiscent to these AHF-models than those found in the *Pdgf-b*^{-/-} and *Pdgfr- β* ^{-/-} mouse models.

We describe that both in *Pdgf-b*^{-/-} and *Pdgfr- β* ^{-/-} embryos hypoplasia of the AoA was found. As cNCCs play a role in the remodeling of the AoA and contribute to its medial layer by differentiation into vSMCs^{14;47}, this might implicate an impaired function and/or recruitment of cNCCs in *Pdgf-b*^{-/-} and *Pdgfr- β* ^{-/-} embryos. It should also be noted that vSMCs of the proximal coronary arteries, a population also impaired in our mouse models, are partly recruited from the cNCCs^{3;48}.

Therefore, we agree with Richarte and colleagues¹³ that PDGFR- β -signaling is most likely not crucial for correct cNCC-migration, but plays a modulatory role in regulating function and differentiation of cNCCs towards vSMCs. PDGFR- α -signaling, on the other hand, is crucial in all phases of non-neuronal (i.e. the cardiac neural crest not contributing to developing cardiac nerves) cNCC-development. These pathways can more (in case of PDGFR- α) or less (in case of PDGFR- β) affect the AHF-derived myocardial cells.

Another part of the second heart field, called the posterior heart field (PHF), contributes to the developing heart directly through the inflow tract⁴⁹ and indirectly through providing the PEO⁸. Interestingly, the direct contribution of the PHF seems to be dependent on PDGF-A/PDGFR- α -signaling as we previously showed that these cells express high levels of PDGFR- α before entering the heart¹⁰ and as *Pdgfr- α* mutant mice show inflow tract abnormalities⁵⁰. The indirect contribution of the PHF to heart development through the PEO and subsequent EPDCs, on the other hand, is most likely dependent on PDGF-B/PDGFR- β -signaling¹⁰. This suggests that PDGFR- α and PDGFR- β are both involved in the contribution of the PHF to heart development in a complementary fashion.

The role of PDGF-B in the development of the cardiac nerves

A subpopulation of cNCCs, the neural cNCCs, are the cellular origin of the intracardiac nerves^{2;3}. The intracardiac nerves are severely affected in *Pdgfr-b-/-* and *Pdgfr- β -/-* embryos, indicating an important role of PDGF-B/PDGFR- β -signaling in neural cNCC-development. Its importance in non-neuronal cNCCs-development, however, is less eminent.

Interestingly, the reverse is true for PDGFR- α -signaling, which is mainly important in non-neuronal cNCC-development⁵¹, pleading for complementary roles of PDGFR- α and PDGFR- β signaling in cNCC-development.

Conclusions

We show that loss of PDGF-B/PDGFR- β -signaling during cardiac development leads to malformations related to impaired development of EPDCs and neuronal cNCCs. To conclusively determine the role of PDGF-B/PDGFR- β -signaling in EPDC and cNCC-contribution to the developing heart, it would be valuable to cross our knockout models with mouse models in which these cell lineages can be traced, such as the GATA5-Cre mouse model for tracing EPDCs³² or the Wnt1-Cre mouse model for tracing NCCs^{3;48}.

Impediments in the PDGF-B/PDGFR- β -signaling-pathway might explain congenital heart malformations in humans such as myocardial hypoplasia in ventricular non-compaction⁵², coronary and valvular abnormalities^{53;54} and arrhythmias related to pulmonary vein-innervation^{3;55}. It would be interesting to study patients with, for example, pulmonary valve stenosis and coronary abnormalities including VCAC^{39;41} for possible PDGF-B and PDGFR- β -related mutations.

Acknowledgements

The authors would like to thank Jan Lens (Department of Anatomy and Embryology, LUMC, Leiden, The Netherlands) for excellent photographic assistance.

References

1. Kirby ML, Gale TF, Stewart DE. Neural crest cells contribute to normal aorticopulmonary septation. *Science*. 1983;220:1059-1061.
2. Verberne ME, Gittenberger-De Groot AC, Poelmann RE. Lineage and development of the parasympathetic nervous system of the embryonic chick heart. *Anat Embryol (Berl)*. 1998;198:171-184.
3. Poelmann RE, Jongbloed MR, Molin DG, Fekkes ML, Wang Z, Fishman GI, Doetschman T, Azhar M, Gittenberger-De Groot AC. The neural crest is contiguous with the cardiac conduction system in the mouse embryo: a role in induction? *Anat Embryol (Berl)*. 2004;208:389-393.
4. Viragh S, Gittenberger-De Groot AC, Poelmann RE, Kalman F. Early development of quail heart epicardium and associated vascular and glandular structures. *Anat Embryol (Berl)*. 1993;188:381-393.
5. Vrancken Peeters MP, Gittenberger-De Groot AC, Mentink MM, Poelmann RE. Smooth muscle cells and fibroblasts of the coronary arteries derive from epithelial-mesenchymal transformation of the epicardium. *Anat Embryol (Berl)*. 1999;199:367-378.
6. Morabito CJ, Dettman RW, Kattan J, Collier JM, Bristow J. Positive and negative regulation of epicardial-mesenchymal transformation during avian heart development. *Dev Biol*. 2001;234:204-215.
7. Winter EM, Gittenberger-De Groot AC. Cardiovascular development: towards biomedical applicability : Epicardium-derived cells in cardiogenesis and cardiac regeneration. *Cell Mol Life Sci*. 2007;64:692-703.
8. Lie-Venema H, Van Den Akker NMS, Bax NA, Winter EM, Maas S, Kerkarainen T, Hoeben RC, DeRuiter MC, Poelmann RE, Gittenberger-De Groot AC. Origin, fate and function of epicardium-derived cells (EPDCs) in normal and abnormal cardiac development. *ScientificWorldJournal*. 2007;7:1777-1798.
9. Bjarnegard M, Enge M, Norlin J, Gustafsdottir S, Fredriksson S, Abramsson A, Takemoto M, Gustafsson E, Fassler R, Betsholtz C. Endothelium-specific ablation of PDGFB leads to pericyte loss and glomerular, cardiac and placental abnormalities. *Development*. 2004;131:1847-1857.
10. Van Den Akker NM, Lie-Venema H, Maas S, Eralp I, DeRuiter MC, Poelmann RE, Gittenberger-De Groot AC. Platelet-derived growth factors in the developing avian heart and maturing coronary vasculature. *Dev Dyn*. 2005;233:1579-1588.
11. Soriano P. The PDGF alpha receptor is required for neural crest cell development and for normal patterning of the somites. *Development*. 1997;124:2691-2700.
12. Tallquist MD, Soriano P. Cell autonomous requirement for PDGFRalpha in populations of cranial and cardiac neural crest cells. *Development*. 2003;130:507-518.
13. Richarte AM, Mead HB, Tallquist MD. Cooperation between the PDGF receptors in cardiac neural crest cell migration. *Dev Biol*. 2007;306:785-796.
14. Snider P, Olaopa M, Firulli AB, Conway SJ. Cardiovascular development and the colonizing cardiac neural crest lineage. *ScientificWorldJournal*. 2007;7:1090-1113.
15. Leveen P, Pekny M, Gebre-Medhin S, Swolin B, Larsson E, Betsholtz C. Mice deficient for PDGF B show renal, cardiovascular, and hematological abnormalities. *Genes Dev*. 1994;8:1875-1887.

16. Hellstrom M, Kalen M, Lindahl P, Abramsson A, Betsholtz C. Role of PDGF-B and PDGFR-beta in recruitment of vascular smooth muscle cells and pericytes during embryonic blood vessel formation in the mouse. *Development*. 1999;126:3047-3055.
17. Gittenberger-De Groot AC, Vrancken Peeters MP, Bergwerff M, Mentink MM, Poelmann RE. Epicardial outgrowth inhibition leads to compensatory mesothelial outflow tract collar and abnormal cardiac septation and coronary formation. *Circ Res*. 2000;87:969-971.
18. Lie-Venema H, Gittenberger-De Groot AC, van Empel LJ, Boot MJ, Kerkdijk H, de Kant E, DeRuiter MC. Ets-1 and Ets-2 transcription factors are essential for normal coronary and myocardial development in chicken embryos. *Circ Res*. 2003;92:749-756.
19. Eralp I, Lie-Venema H, DeRuiter MC, Van Den Akker NM, Bogers AJ, Mentink MM, Poelmann RE, Gittenberger-De Groot AC. Coronary artery and orifice development is associated with proper timing of epicardial outgrowth and correlated Fas-ligand-associated apoptosis patterns. *Circ Res*. 2005;96:526-534.
20. Betsholtz C, Karlsson L, Lindahl P. Developmental roles of platelet-derived growth factors. *Bioessays*. 2001;23:494-507.
21. Lu J, Landerholm TE, Wei JS, Dong XR, Wu SP, Liu X, Nagata K, Inagaki M, Majesky MW. Coronary smooth muscle differentiation from proepicardial cells requires rhoA-mediated actin reorganization and p160 rho-kinase activity. *Dev Biol*. 2001;240:404-418.
22. Gittenberger-De Groot AC, Vrancken Peeters MP, Mentink MM, Gourdie RG, Poelmann RE. Epicardium-derived cells contribute a novel population to the myocardial wall and the atrioventricular cushions. *Circ Res*. 1998;82:1043-1052.
23. Lie-Venema H, Eralp I, Markwald RR, Van den Akker NM, Wijffels MC, Kolditz DP, Van der Laarse A, Schalij MJ, Poelmann RE, Bogers AJ, Gittenberger-De Groot AC. Periostin expression by epicardium-derived cells (EPDCs) is involved in the development of the atrioventricular valves and fibrous heart skeleton. *Differentiation*. 2007, In Press.
24. Zymek P, Bujak M, Chatila K, Cieslak A, Thakker G, Entman ML, Frangogiannis NG. The role of platelet-derived growth factor signaling in healing myocardial infarcts. *J Am Coll Cardiol*. 2006;48:2315-2323.
25. Stuckmann I, Evans S, Lassar AB. Erythropoietin and retinoic acid, secreted from the epicardium, are required for cardiac myocyte proliferation. *Dev Biol*. 2003;255:334-349.
26. Heldin CH, Eriksson U, Ostman A. New members of the platelet-derived growth factor family of mitogens. *Arch Biochem Biophys*. 2002;398:284-290.
27. Eisenberg LM, Markwald RR. Molecular regulation of atrioventricular valvuloseptal morphogenesis. *Circ Res*. 1995;77:1-6.
28. Norris RA, Damon B, Mironov V, Kasyanov V, Ramamurthi A, Moreno-Rodriguez R, Trusk T, Potts JD, Goodwin RL, Davis J, Hoffman S, Wen X, Sugi Y, Kern CB, Mjaatvedt CH, Turner DK, Oka T, Conway SJ, Molkentin JD, Forgacs G, Markwald RR. Periostin regulates collagen fibrillogenesis and the biomechanical properties of connective tissues. *J Cell Biochem*. 2007;101:695-711.
29. Kruzynska-Frejtak A, Machnicki M, Rogers R, Markwald RR, Conway SJ. Periostin (an osteoblast-specific factor) is expressed within the embryonic mouse heart during valve formation. *Mech Dev*. 2001;103:183-188.

30. Adams RH, Wilkinson GA, Weiss C, Diella F, Gale NW, Deutsch U, Risau W, Klein R. Roles of ephrinB ligands and EphB receptors in cardiovascular development: demarcation of arterial/venous domains, vascular morphogenesis, and sprouting angiogenesis. *Genes Dev.* 1999;13:295-306.
31. Lindblom P, Gerhardt H, Liebner S, Abramsson A, Enge M, Hellstrom M, Backstrom G, Fredriksson S, Landegren U, Nystrom HC, Bergstrom G, Dejana E, Ostman A, Lindahl P, Betsholtz C. Endothelial PDGF-B retention is required for proper investment of pericytes in the microvessel wall. *Genes Dev.* 2003;17:1835-1840.
32. Merki E, Zamora M, Raya A, Kawakami Y, Wang J, Zhang X, Burch J, Kubalak SW, Kaliman P, Belmonte JC, Chien KR, Ruiz-Lozano P. Epicardial retinoid X receptor alpha is required for myocardial growth and coronary artery formation. *Proc Natl Acad Sci U S A.* 2005;102:18455-18460.
33. van Loo PF, Mahtab EA, Wisse LJ, Hou J, Grosveld F, Suske G, Philipsen S, Gittenberger-De Groot AC. Transcription Factor Sp3 knockout mice display serious cardiac malformations. *Mol Cell Biol.* 2007.
34. Zamora M, Manner J, Ruiz-Lozano P. Epicardium-derived progenitor cells require beta-catenin for coronary artery formation. *Proc Natl Acad Sci U S A.* 2007;104:18109-18114.
35. Limbourg A, Ploom M, Elligsen D, Sorensen I, Ziegelhoeffer T, Gossler A, Drexler H, Limbourg FP. Notch ligand Delta-like 1 is essential for postnatal arteriogenesis. *Circ Res.* 2007;100:363-371.
36. Bondjers C, He L, Takemoto M, Norlin J, Asker N, Hellstrom M, Lindahl P, Betsholtz C. Microarray analysis of blood microvessels from PDGF-B and PDGF-Rbeta mutant mice identifies novel markers for brain pericytes. *FASEB J.* 2006;20:1703-1705.
37. Baladron V, Ruiz-Hidalgo MJ, Nueda ML, az-Guerra MJ, Garcia-Ramirez JJ, Bonvini E, Gubina E, Laborda J. dlk acts as a negative regulator of Notch1 activation through interactions with specific EGF-like repeats. *Exp Cell Res.* 2005;303:343-359.
38. Bogers AJ, Bartelings MM, Bokenkamp R, Stijnen T, van Suylen RJ, Poelmann RE, Gittenberger-De Groot AC. Common arterial trunk, uncommon coronary arterial anatomy. *J Thorac Cardiovasc Surg.* 1993;106:1133-1137.
39. Gittenberger-De Groot AC, Tennstedt C, Chaoui R, Lie-Venema H, Sauer U, Poelmann RE. Ventriculo coronary arterial communications (VCAC) and myocardial sinusoids in hearts with pulmonary atresia with intact ventricular septum: two different diseases. *Progress in Pediatric Cardiology.* 2001;13:157-164.
40. Poelmann RE, Gittenberger-De Groot AC, Mentink MMT, Bokenkamp R, Hogers B. Development of the Cardiac Coronary Vascular Endothelium, Studied with Antiendothelial Antibodies, in Chicken-Quail Chimeras. *Circulation Research.* 1993;73:559-568.
41. Gittenberger-De Groot AC, Eralp I, Lie-Venema H, Bartelings MM, Poelmann RE. Development of the coronary vasculature and its implications for coronary abnormalities in general and specifically in pulmonary atresia without ventricular septal defect. *Acta Paediatr Suppl.* 2004;93:13-19.
42. Kelly RG. Molecular inroads into the anterior heart field. *Trends Cardiovasc Med.* 2005;15:51-56.
43. Mjaatvedt CH, Nakaoka T, Moreno-Rodriguez R, Norris RA, Kern MJ, Eisenberg CA, Turner D, Markwald RR. The outflow tract of the heart is recruited from a novel heart-forming field. *Dev Biol.* 2001;238:97-109.

44. Waldo KL, Hutson MR, Stadt HA, Zdanowicz M, Zdanowicz J, Kirby ML. Cardiac neural crest is necessary for normal addition of the myocardium to the arterial pole from the secondary heart field. *Dev Biol.* 2005;281:66-77.
45. Ward C, Stadt H, Hutson M, Kirby ML. Ablation of the secondary heart field leads to tetralogy of Fallot and pulmonary atresia. *Dev Biol.* 2005;284:72-83.
46. Van Den Akker NM, Molin DG, Peters PP, Maas S, Wisse LJ, van BR, van Munsteren CJ, Bartelings MM, Poelmann RE, Carmeliet P, Gittenberger-De Groot AC. Tetralogy of Fallot and alterations in vascular endothelial growth factor-A signaling and notch signaling in mouse embryos solely expressing the VEGF120 isoform. *Circ Res.* 2007;100:842-849.
47. Molin DG, Poelmann RE, DeRuiter MC, Azhar M, Doetschman T, Gittenberger-De Groot AC. Transforming growth factor beta-SMAD2 signaling regulates aortic arch innervation and development. *Circ Res.* 2004;95:1109-1117.
48. Jiang X, Rowitch DH, Soriano P, McMahon AP, Sucov HM. Fate of the mammalian cardiac neural crest. *Development.* 2000;127:1607-1616.
49. Gittenberger-De Groot AC, Mahtab EA, Hahurij ND, Wisse LJ, DeRuiter MC, Wijffels MC, Poelmann RE. Nkx2.5-negative myocardium of the posterior heart field and its correlation with podoplanin expression in cells from the developing cardiac pacemaking and conduction system. *Anat Rec (Hoboken)*. 2007;290:115-122.
50. Schatteman GC, Motley ST, Effmann EL, Bowen-Pope DF. Platelet-derived growth factor receptor alpha subunit deleted Patch mouse exhibits severe cardiovascular dysmorphism. *Teratology.* 1995;51:351-366.
51. Morrison-Graham K, Schatteman GC, Bork T, Bowen-Pope DF, Weston JA. A PDGF receptor mutation in the mouse (Patch) perturbs the development of a non-neuronal subset of neural crest-derived cells. *Development.* 1992;115:133-142.
52. Pignatelli RH, McMahon CJ, Dreyer WJ, Denfield SW, Price J, Belmont JW, Craigen WJ, Wu J, El SH, Bezold LI, Clunie S, Fernbach S, Bowles NE, Towbin JA. Clinical characterization of left ventricular noncompaction in children: a relatively common form of cardiomyopathy. *Circulation.* 2003;108:2672-2678.
53. Attenhofer Jost CH, Connolly HM, Edwards WD, Hayes D, Warnes CA, Danielson GK. Ebstein's anomaly - review of a multifaceted congenital cardiac condition. *Swiss Med Wkly.* 2005;135:269-281.
54. Angelini P. Coronary artery anomalies: an entity in search of an identity. *Circulation.* 2007;115:1296-1305.
55. Tan AY, Chen PS, Chen LS, Fishbein MC. Autonomic nerves in pulmonary veins. *Heart Rhythm.* 2007;4:S57-S60.

Part III

Nuchal Translucency and Endothelial Differentiation

Chapter 6

Abnormal Lymphatic Development in Trisomy 16 Mouse Embryos Precedes Nuchal Edema

Adriana C. Gittenberger-de Groot¹, Nynke M.S. van den Akker¹, Margot M. Bartelings¹, Sandra Webb², John M.G. Van Vugt³, Monique C. Haak³

¹Department of Anatomy and Embryology, Leiden University Medical Center, Leiden, The Netherlands; ²Department of Biomedical Sciences, Anatomy and Developmental Biology, St. George Hospital Medical School, London, United Kingdom; ³Department of Obstetrics and Gynecology, VU University Medical Center, Amsterdam, The Netherlands

Modified after Developmental Dynamics, 2004;230:378–384.

Abnormal Lymphatic Development in Trisomy 16 Mouse Embryos Precedes Nuchal Edema

Abstract

Ultrasound measurement of increased nuchal translucency is a method of risk assessment for heart malformations and trisomy 21 in human pregnancy. The developmental background of this nuchal edema is still not sufficiently understood. We have studied the process in trisomy 16 (T16) mice that show nuchal edema and heart malformations. We used trisomy 16 and wild-type (WT) embryos from embryonic day (E) 12.5 to E18.5. In WT embryos of E13, bilateral jugular lymphatic sacs were visible that shared a lymphatic-venous membrane with the internal jugular vein. We could not in any case discern a valve between these vessels. At E14 in the T16 embryos, the lymphatic sacs become enlarged showing abnormally thickened endothelium, specifically at the site of the membrane. In these embryos, severe edema develops in the nuchal region. There was a very close colocalisation of the nerves with the vascular structures. The start of reorganization of the jugular lymphatic sac to a lymph node was observed in both wild-type and T16 but was diminished in the latter. In conclusion, abnormal size and structure of the jugular lymphatic sacs coincides with the development of nuchal edema. A disturbance of lymphangiogenesis might be the basis for increased nuchal translucency that is often observed in diseased human fetuses.

Introduction

Nuchal translucency (NT) measurement in human pregnancy is nowadays widely used as risk assessment for trisomy 21. The (patho)morphogenesis of this transient fluid accumulation in the fetal neck region is still unclear. Several hypotheses have been proposed, including temporary cardiac failure¹⁻¹⁰ and the alteration of extracellular matrix components¹¹⁻¹³. These two theories, however, fail to explain the regional accumulation of the fluid in the neck region and the temporary character of the NT enlargement. A more recent finding in both human fetuses and mouse embryos with nuchal edema is the concomitant abnormal enlargement and persistence of the jugular lymphatic sacs (JLSs)¹⁴.

The JLSs are the first part of the lymphatic system to develop, sprouting from the cardinal vein. It is described that, in the primitive lymphatic system, the lymphatic fluid subsequently drains from the JLS into the systemic circulation by secondary formation of valves opening in the internal jugular vein (IJV)¹⁵. The JLS disappears as it is reorganized into a lymphatic node¹⁵.

In this study, the hypothesis that an increased NT is caused by abnormal jugular lymphatic development was further tested by using the trisomy 16 (T16) mouse model. The T16 mouse is an animal model for human trisomy 21 (Down syndrome) as the mouse chromosome 16 contains the syntenic region for the human chromosome band 21q22^{16;17}. That region is considered to be responsible for the pathological features seen in Down syndrome. As in human fetuses, T16 mouse embryos develop a NT-like fluid accumulation in the nuchal region^{12;18}. Immunohistochemistry, using a marker for lymphatic endothelium (LYVE-1), was performed to study the overall morphology of the embryos, and specifically of the lymphatic vessels and the adjoining structures.

Materials and Methods

Embryos

Wild-type (WT) and T16 mouse embryos¹⁹ were collected from gestational age day 10.5 (E10.5) to E18.5 days (Table 1). The embryos were fixed in 4% paraformaldehyde for 24 hours and transported in 70% ethanol. After dehydrating the embryos to xylene, they were embedded in paraffin and sectioned into serial sections of 5 μm (from E10.5 to E16.5 and E18.5) or 7 μm (E17.5). The subsequent sections were mounted on five different slides, so that five different staining procedures could be performed on subsequent sections of the same part of the embryo. The slides were dried at 37 °C for at least 24 hours.

Immunohistochemical Markers

- LYVE-1 Antibody -

The lymphatic vessel endothelial hyaluronan receptor-1 (LYVE-1) is a hyaluronan receptor specific for lymphatic vessels in healthy adult tissue. An immunohistochemical staining using an antibody against LYVE-1, therefore, is considered to stain mainly lymphatics^{20;21}. In early embryonic stages, however, veins also show some LYVE-1-positivity.

- Neural Cell Adhesion Molecule Antibody -

The neural cell adhesion molecule (NCAM) is involved in cell-cell interactions between nerve cells. By using an antibody against NCAM in an immunohistochemical staining, all nervous tissue is stained.

Staining Procedures

First, the slides were deparaffinized. Between all steps, the slides were rinsed twice with phosphate-buffered saline (PBS) and once with PBS/0.05% Tween unless indicated otherwise. An antigen-processing step was performed before the LYVE-1 staining by incubating 5-10 minutes in a pronase E solution (0.4 nU/ml in PBS). For the NCAM staining, the slides were microwave processed by heating them 3 times for 4 minutes to 99°C in a citric acid buffer (0.01 M in aqua-dest, pH 6.0). Then the slides were rinsed twice with PBS and incubated for 15 minutes in a 0.3% H₂O₂ solution to block the endogenous peroxidase activity. The slides were then incubated overnight with the specific antibody against LYVE-1 or NCAM. After that, the sections were incubated for 90 minutes with the second antibody GAR-Ig. Then, incubation with R-PAP took place for 90 min. The slides were rinsed twice with PBS and once with Tris/Maleate (pH 7.6) before 3-3'-diaminobenzidin tetrahydrochloride was used as chromogen. Counterstaining was performed by dipping the slides for 10 seconds in Mayer's hematoxylin. The slides were rinsed for 10 minutes in tap water, dehydrated to xylene, and mounted with Entellan.

3D-reconstructions

Unilateral three-dimensional reconstructions were made from the JLS and the internal jugular vein, selecting one WT and one T16 mouse embryo of E14. Drawings were made of sections stained with the LYVE-1 antibody, using a drawing microscope. As one in five sections of the investigated area were used for the reconstruction the distance between two sections, i.e., one level, was 25 μm . For the left JLS of the WT mouse embryo, 40 levels were drawn from the cranial blind beginning till the ending at the internal jugular vein. Sixty levels were drawn of the right JLS of the T16 mouse. The drawings were scanned and analyzed in the same magnification and converted to a three-dimensional image by using Amira software.

Table 1. Number of mouse embryos examined per embryonic day

Embryonic day	Wild-type (no.)	T16 (no.)
10.5	1	1
11	1	0
11.5	2	1
12	1	2
12.5	0	1
13	2	3
14	4	4
15.5	1	1
16.5	1	1
17.5	1	1
18.5	1	1

Results

Normal Development

The earliest stage that was investigated was E10.5. At this stage, no positive cells were observed in LYVE-1-stained sections, except for the myocardium and liver tissue, both of which always show some background staining (data not shown).

At E11, some large veins showed partly positive staining at the locations where small veins sprout from these larger veins as well as at the lateral part of the cardinal vein, just above the heart (Figure 1A). Also, some LYVE-1-positive vessels were seen adjacent to this vein at day E11.5 and E12 (Figure 1C). These vessels appeared to be the first indication of the formation of the JLS.

At E13, a clear LYVE-1-positive JLS, located lateral to the internal jugular vein, was observed (Figure 2A). This JLS started blindly at about the level of the developing eye, then following it caudally, it dilates to its maximal diameter of approximately 1-2 times the size of the diameter of the internal jugular vein. More caudally, the JLS became very closely located to the internal jugular vein until they were only separated by a bilayered endothelial membrane being approximately 200 μm in length (cranial-caudal). This lymphatic-venous membrane (LVM) was seen in all wild-type embryos of E13 (Figure 2E). No valve was ever seen between the JLS and the internal jugular vein. The JLS ended blunt at approximately the level where the internal jugular vein fused with the left caval vein. Furthermore, at the level of the LVM, the left superior caval vein became positive for LYVE-1 and stayed positive until it entered the heart.

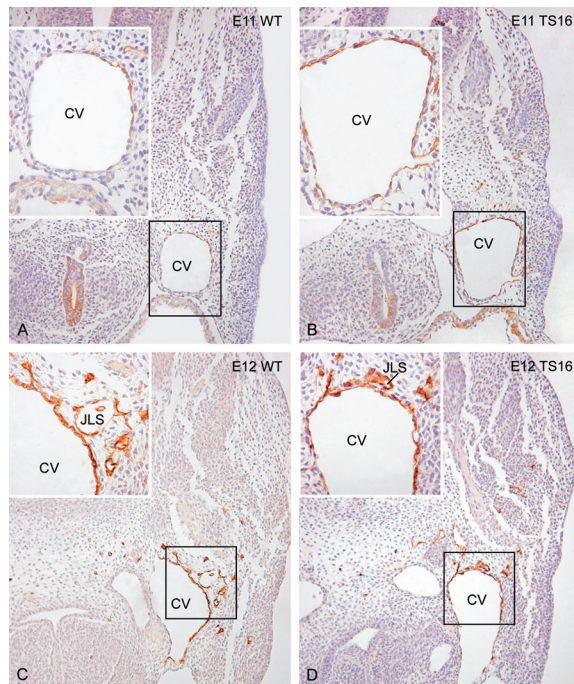


Figure 1. Early formation of the jugular lymphatic system. A: Transverse section of a wild-type (WT) embryo at embryonic day (E)11. The endothelium of the cardinal vein (CV) is partly positive for LYVE-1 (see insert for detail). *B:* Section at a similar level in a trisomy 16 (TS16) embryo of the same age. The CV is almost completely positive for LYVE-1. *C:* At E12, there is sprouting and budding from the CV of LYVE-1-positive vessels, indicating the first formation of the jugular lymphatic sac (JLS). *D:* This finding is identical in WT and TS16 (D).

At E14, the situation was comparable to E13 (Figure 2A,C). The maximal diameter of the jugular lymphatic sac was 2-3 times larger than that of the internal jugular vein (Figure 3A,B). It was perforated by a large cervical nerve surrounded by mesenchyme (Figure 3C).

The start of reorganization of the jugular lymphatic sac into a jugular lymph node was observed for the first time at E15.5 (Figure 4A,B). Furthermore, the LVM had become much smaller in size (maximum length from cranial to caudal, 25 μm). The situation at E16.5 was comparable to E15.5, except that the LVM could no longer be seen in the jugular area. The size of the jugular lymphatic sac at E17.5 had decreased further, the LVM being no longer visible. At E18.5, reorganization has led to almost complete disappearance of the JLS.

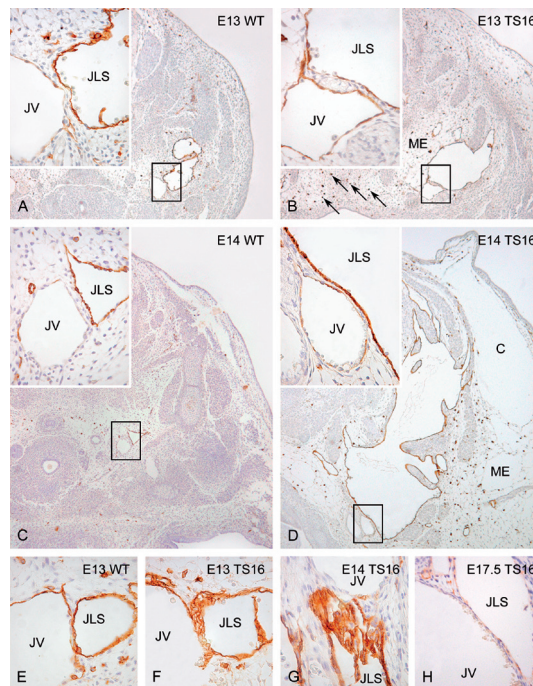


Figure 2. Transverse sections through the nuchal region of a wild-type (WT) and trisomy 16 (TS16) embryo stained with LYVE-1 at embryonic day (E)13 and E14. A: In the WT embryo, the internal jugular vein (JV) is now negative for LYVE-1. The JV runs parallel and close to the LYVE-1 positive jugular lymphatic sac (JLS). B: In the TS16 embryo, both the JV and the JLS are positive for LYVE-1 and the latter is larger as compared with the WT. There are more scattered LYVE-1-positive cells (arrows), and there is more generalized nuchal mesenchymal edema (ME) compared with the WT. C: The size of the JV and the JLS almost identical at E14 in the WT embryo (see insert for difference in LYVE-1 positivity). D: In the TS16 embryo, at E14 the JLS is very large compared with the JV, and shows more LYVE-1 positivity compared with the WT. There are many scattered LYVE-1-positive cells, and severe ME. This fluid has accumulated in a cavity (C) lined by mesenchymal cells. E shows the lymphatic-venous membrane (LVM) in a WT mouse of E13. Both the JV and the JLS are LYVE-1-positive at this site. F,G: Details of the thickened lymphatic endothelium of the LVM at E13 and E14 in the TS16. H: The LVM is still present in T16 at E17.5 in contrast to WT.

Abnormal Development

As in the WT embryos, no positive structures or cells were present in the T16 embryo of E10.5, except for the myocardium and liver tissue (not shown). At E11.5, the situation was similar to the WT embryos with a slightly positive staining of the notochord. The LYVE-1 staining was more extensive in the large veins at branching points, and the complete cardinal vein just above the heart was positive (Figure 1B).

At stages E12 and E12.5, comparable to the WT embryo, small LYVE-1-positive vessels sprouting from the lateral wall of the caval vein (Figure 1D) could be observed. This finding appeared to be the first indication of formation of the JLS.

At E13, a clear JLS was visible (Figure 2B) starting more cranially compared with the WT embryos (about the level of the forebrain). It was approximately 5-6 times the diameter of the internal jugular vein and had many branches (Figure 3D,E). It ended at the same level as in WT mouse embryos at this age. The region where the JLS and the internal jugular vein were closely related to each other was larger (Figure 2B), but the LVM appeared to be of the same length compared with the WT. The morphology of the LVM was altered, the lymphatic endothelium was thickened and more folded compared with normal (Figure 2F). In the nuchal region, the mesenchyme was very edematous (Figure 2B).

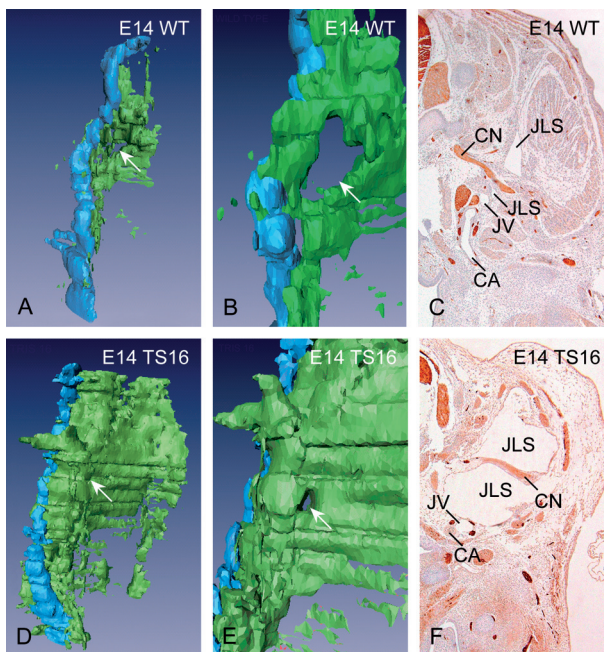


Figure 3. Unilateral 3D-reconstructions of the internal jugular vein (JV; blue) and the laterally located jugular lymphatic sac (JLS; green) at embryonic day (E)14. A,B: The complete sac of a wild-type (WT) embryo is depicted (A), showing a penetration (arrow in B) through which the cervical nerve crosses surrounded by mesenchymal tissue. C: Transverse section stained with NCAM at the site of the cervical nerve (CN) crossing. D: The sac in the trisomy 16 (TS16) embryo is very large, even without the cranial part which could not be reconstructed. E: Magnification of D showing the nerve penetrating site (arrow) that is much smaller compared with the WT. F: Section through this level comparable to C, showing the much larger JLS compared with normal, whereas the JV and the carotid artery (CA) are of identical size in WT and TS16. The CN in TS16 is not surrounded by mesenchyme explaining the smaller penetration site.

At E14, the difference between the JLS in the WT and the T16 mouse embryos was even more obvious (Figure 2C,D). In T16 embryos, the JLS sac was approximately 8-10 times the diameter of the internal jugular vein (Figure 3D,E), had numerous branches and was crossed by several cervical nerves that showed no surrounding mesenchyme (Figure 3F). The lymphatic endothelium seemed thickened at many locations, including the LVM (Figure 2G). Many more isolated positive cells around JLS were found in the T16 embryos compared with WT embryos of E14 (Figure 2C,D). As in WT embryos, the superior caval vein became LYVE-1-positive caudally from the blind ending of the JLS. No reorganization into lymphatic nodes was observed. Furthermore, the edematous region in the neck had increased and contained a large edematous cavity that was not lined by any specific endothelium or epithelium (Figure 2D).

As in WT embryos, reorganization of the JLS was first visible at E15.5 (Figure 4D). The decrease in JLS-size that was observed in the WT embryo of E15.5 (Figure 4A), however, was not present in the T16 embryo (Figure 4C). The LVM had decreased in size and the abnormal morphology of the endothelium as seen at E14 had disappeared. At E16.5 and E17.5, the JLS was still enlarged compared with the WT embryos. The size of the membrane was very small, but, in contrast to the WT embryos, it was still present at this age (Figure 2H). The size of the JLS was still enlarged but the LVM had totally disappeared at E18.5. At these stages (E16.5–E18.5), reorganization of the wall into lymph node tissue was present but diminished compared with WT embryos.

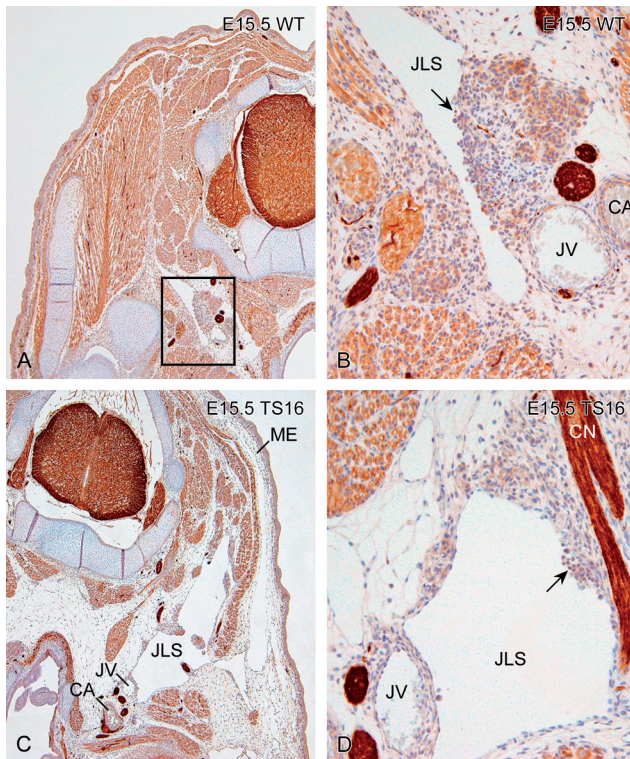


Figure 4. Transverse sections through wildtype (WT) and trisomy 16 (TS16) embryos at embryonic day (E)15.5 stained for NCAM. A,B: Right lateral side of a WT embryo (A) with start of reorganization of the wall of the jugular lymphatic sac (JLS) into lymph node tissue (arrow in B). C: Left lateral side of a TS16 embryo, showing the still much larger JLS and the nuchal mesenchymal edema (ME). D: Reorganization site (arrow) is found but much less pronounced as compared with the WT. Abbreviations: CA = carotid artery; JV = internal jugular vein.

Discussion

Normal and abnormal jugular lymphatic development was investigated in mouse embryos to study the hypothesis that an increased subcutaneous accumulation of fluid in the nuchal region might relate to a developmental problem of the JLS. A discrepancy between formation and drainage of lymphatic fluid could result in subcutaneous edema in the neck, which can be visualized in human pregnancy as an increased nuchal translucency^{18;22}.

The JLS is the first part of the lymphatic system to develop. It has been described previously^{15;23;24} that bilaterally, the anterior cardinal veins give rise to vascular buds, which fuse and form the JLS. In our study, we observed lateral positivity for LYVE-1 of the cardinal vein; the positivity at branching points at E11, and the budding and sprout formation from the cardinal vein at E12 were similar in WT and T16 mouse embryos. Therefore, we presume that the jugular lymphatic malformations, found in older T16 mouse embryos, are not the result of an abnormal Prox-1-dependent budding and sprouting process of the lymphatics²².

Other characteristic differences of the JLS between the normal mouse and the T16 mouse were investigated. The JLS was easily distinguished microscopically, running parallel and lateral from the internal jugular vein. It starts and ends blunt, but at the caudal end, there is a region where the JLS and the internal jugular vein are only separated by two layers of endothelium, the so-called LVM. This LVM was seen in all WT embryos between E13 and E15.5. In the T16 mouse embryos, the LVM was present between E13 and E17.5, which is 2 days longer than normal. Also the lymphatic endothelium at this site was abnormally folded and thickened. It seems likely that, at the LVM, diffusion of fluid from the lymphatic system into the venous system takes place, because we were not able to find a valve between the JLS and the internal jugular vein at any stage during development. This finding is in contrast with the data from the literature where the drainage of the lymphatic fluid from the JLS is described in both the human¹⁵ and the mouse fetus²⁵ to take place through a valve between the internal jugular vein and the JLS. A lack of this valve was described in T16 mouse embryos of E14²⁵. We can only confirm the latter finding.

The formation of the lymphatic system in humans is completed by the ingrowth of the right thoracic duct into the left JLS, thereby connecting several lymphatic vessels²⁴. After the subsequent reorganization of the JLS into lymphatic nodes, this connection of the thoracic duct to the internal jugular vein is the main site where drainage of lymphatic fluid into the systemic circulation takes place. We assume that early embryonic drainage of the lymphatic fluid is through the LVM in our mouse model. The reorganization of the JLS into a lymph node will nullify the function of the LVM. This process is completed by E17.5 in the WT mouse. In the T16 mouse, the LVM is, after an initial abnormal thickening at E14, a time at which the JLS is at its largest size, still present at E17.5 albeit in again a thin form. It might be possible that, like in the T16 embryos, this process of disappearance of the LVM and the

reorganization of the JLS into lymph nodes is delayed in human fetuses with trisomy 21 (Down syndrome), thereby explaining the transient nature of NT. Support for this hypothesis is found in the fact that, in human NT, the JLS is still present at week 14 of gestation, which is normally not the case¹⁸. Further study of human fetal material is necessary to prove this supposition.

An interesting observation was the thickening and folding of the lymphatic endothelium in the T16 mouse embryos, most pronounced at E14, which could be the result of an abnormal differentiation of the lymphatic and/or venous endothelium. The shift of LYVE-1 expression in both WT and T16 embryos from some large veins at E11, to both veins and lymphatic vessels at E12, and then to an almost exclusive expression of LYVE-1 in the lymphatics at E13 with exception of the site of the LVM, suggests a differentiation of venous into lymphatic endothelium. Abnormalities in this lymphatic endothelial development, exemplified by the more extensive LYVE-1 expression in the large veins and the thickened lymphatic endothelium, could possibly affect the transport of lymphatic fluid into the lymphatics or the drainage of lymphatic fluid into the venous circulation. An imbalance between formation and drainage of lymphatic fluid could result in the formation of mesenchymal edema in the nuchal region.

As LYVE-1 is a transmembrane hyaluronan (HA) receptor, this endothelial differentiation pattern suggests a shift of HA sensitivity from venous to lymphatic endothelium. HA is an extracellular matrix glycosaminoglycan with a high affinity for water and plays an important role in embryonic morphogenesis by facilitating cell migration²⁰. HA is mobilized by lymphatic vessels and mostly degraded in lymph nodes. It has been suggested that it enters the lymphatic system by LYVE-1-mediated internalization²⁰. In the absence of a functional lymphatic system in early embryonic development, HA might be internalized by the LYVE-1-positive venous endothelium into the venous system to be degraded in the liver. At the time the JLSs are being formed, the LYVE-1-positivity shifts from the venous to the lymphatic endothelium, enabling HA uptake into the jugular lymphatic sac. We observed the presence of HA in the jugular lymphatic sacs (data not shown). It is likely that HA is degraded in the lymphatic sac in the period between the moment that the veins become LYVE-1-negative and the formation of lymphatic nodes. An increased accumulation of lymphatic fluid in the jugular lymphatic sacs in T16 mouse embryos could be the result of a disturbance of degradation of HA. In combination with a malfunctioning LVM, this could result in a distention of the lymphatic sac. The imbalance between formation and degradation of lymphatic fluid will, as described above, result in subcutaneous edema in the nuchal region. With formation of the lymphatic nodes, the HA will be degraded in these nodes²⁰ and the lymphatic fluid disappears. This process is delayed in the T16 mouse and could explain the transient aspect of the nuchal edema in addition to the above described disturbed transportation of fluid through the LVM.

In both WT and T16 embryos, we found a close correlation between the JLS and the cervical nerves, which passed through the sac. In the T16 embryos, the nerves following the vascular neck structures had a somewhat different position but

this finding might be caused by the mechanics of the enlarged JLS. It remains to be investigated whether there is a mutual influence of nerves and vessels in the development of nuchal edema as both endothelium and nerves share many genes²⁶. Genes of interest involved in this interaction between nerves and endothelial differentiation are VEGF and its coreceptors, Neuropilin-1 (NP-1) and NP-2. NPs are known to mediate axonal guidance in the developing nervous system, but recently they are also found to play a role in angiogenesis.

In conclusion, our observations of the normal development of the lymphatic system in the WT mouse embryos correlates with previous studies^{15;23;24;27}. However, the opening, or valve, of the JLS into the internal jugular vein was not observed. Instead, an LVM consisting of one layer of venous and one layer of lymphatic endothelium was observed. Lymphatic malformations and abnormal lymphatic endothelium were markedly present in T16 mouse embryos. The findings correlate with our recent observations with ultrasound study of the nuchal region in the human fetus, where a temporary persistence of the JLS accompanies increased NT in a high number of cases¹⁸. Further studies are necessary to elucidate the (patho)morphogenesis of these lymphatic abnormalities to understand the development and the clinical impact of the transient nuchal edema¹⁴ seen in human fetuses with chromosomal and cardiac abnormalities.

Acknowledgements

The authors thank David Jackson for providing the antibody against LYVE-1 and Stanley Hoffman for providing the antibody against NCAM.

References

1. Hyett J, Moscoso G, Nicolaides K. Increased nuchal translucency in trisomy 21 fetuses: relationship to narrowing of the aortic isthmus. *Hum Reprod.* 1995;10:3049-3051.
2. Hyett J, Moscoso G, Papapanagiotou G, Perdu M, Nicolaides KH. Abnormalities of the heart and great arteries in chromosomally normal fetuses with increased nuchal translucency thickness at 11-13 weeks of gestation. *Ultrasound Obstet Gynecol.* 1996;7:245-250.
3. Hyett JA, Brizot ML, von Kaisenberg CS, McKie AT, Farzaneh F, Nicolaides KH. Cardiac gene expression of atrial natriuretic peptide and brain natriuretic peptide in trisomic fetuses. *Obstet Gynecol.* 1996;87:506-510.
4. Hyett JA, Noble PL, Snijders RJ, Montenegro N, Nicolaides KH. Fetal heart rate in trisomy 21 and other chromosomal abnormalities at 10-14 weeks of gestation. *Ultrasound Obstet Gynecol.* 1996;7:239-244.
5. Hyett J, Moscoso G, Nicolaides K. Abnormalities of the heart and great arteries in first trimester chromosomally abnormal fetuses. *Am J Med Genet.* 1997;69:207-216.
6. Hyett JA, Perdu M, Sharland GK, Snijders RS, Nicolaides KH. Increased nuchal translucency at 10-14 weeks of gestation as a marker for major cardiac defects. *Ultrasound Obstet Gynecol.* 1997;10:242-246.
7. Montenegro N, Matias A, Areias JC, Castedo S, Barros H. Increased fetal nuchal translucency: possible involvement of early cardiac failure. *Ultrasound Obstet Gynecol.* 1997;10:265-268.
8. Matias A, Gomes C, Flack N, Montenegro N, Nicolaides KH. Screening for chromosomal abnormalities at 10-14 weeks: the role of ductus venosus blood flow. *Ultrasound Obstet Gynecol.* 1998;12:380-384.
9. Matias A, Montenegro N, Areias JC, Brandao O. Anomalous fetal venous return associated with major chromosomopathies in the late first trimester of pregnancy. *Ultrasound Obstet Gynecol.* 1998;11:209-213.
10. Matias A, Huggon I, Areias JC, Montenegro N, Nicolaides KH. Cardiac defects in chromosomally normal fetuses with abnormal ductus venosus blood flow at 10-14 weeks. *Ultrasound Obstet Gynecol.* 1999;14:307-310.
11. von Kaisenberg CS, Brand-Saberi B, Christ B, Vallian S, Farzaneh F, Nicolaides KH. Collagen type VI gene expression in the skin of trisomy 21 fetuses. *Obstet Gynecol.* 1998;91:319-323.
12. von Kaisenberg CS, Krenn V, Ludwig M, Nicolaides KH, Brand-Saberi B. Morphological classification of nuchal skin in human fetuses with trisomy 21, 18, and 13 at 12-18 weeks and in a trisomy 16 mouse. *Anat Embryol (Berl).* 1998;197:105-124.
13. Bohlandt S, von Kaisenberg CS, Wewetzer K, Christ B, Nicolaides KH, Brand-Saberi B. Hyaluronan in the nuchal skin of chromosomally abnormal fetuses. *Hum Reprod.* 2000;15:1155-1158.
14. Haak MC, Bartelings MM, Jackson DG, Webb S, Van Vugt JM, Gittenberger-De Groot AC. Increased nuchal translucency is associated with jugular lymphatic distension. *Hum Reprod.* 2002;17:1086-1092.
15. Sabin FR. The lymphatic system in human embryos, with a consideration of the morphology of the system as a whole. *Am J Anat.* 1909;9:43-91.

16. Miyabara S, Gropp A, Winking H. Trisomy 16 in the mouse fetus associated with generalized edema and cardiovascular and urinary tract anomalies. *Teratology*. 1982;25:369-380.
17. Veikkola T, Jussila L, Makinen T, Karpanen T, Jeltsch M, Petrova TV, Kubo H, Thurston G, McDonald DM, Achen MG, Stacker SA, Alitalo K. Signalling via vascular endothelial growth factor receptor-3 is sufficient for lymphangiogenesis in transgenic mice. *EMBO J*. 2001;20:1223-1231.
18. Haak MC, Bartelings MM, Gittenberger-De Groot AC, Van Vugt JM. Cardiac malformations in first-trimester fetuses with increased nuchal translucency: ultrasound diagnosis and postmortem morphology. *Ultrasound Obstet Gynecol*. 2002;20:14-21.
19. Webb S, Brown NA, Anderson RH. Cardiac morphology at late fetal stages in the mouse with trisomy 16: consequences for different formation of the atrioventricular junction when compared to humans with trisomy 21. *Cardiovasc Res*. 1997;34:515-524.
20. Banerji S, Ni J, Wang SX, Clasper S, Su J, Tammi R, Jones M, Jackson DG. LYVE-1, a new homologue of the CD44 glycoprotein, is a lymph-specific receptor for hyaluronan. *J Cell Biol*. 1999;144:789-801.
21. Prevo R, Banerji S, Ferguson DJ, Clasper S, Jackson DG. Mouse LYVE-1 is an endocytic receptor for hyaluronan in lymphatic endothelium. *J Biol Chem*. 2001;276:19420-19430.
22. Wigle JT, Oliver G. Prox1 function is required for the development of the murine lymphatic system. *Cell*. 1999;98:769-778.
23. van der Putte SC. The development of the lymphatic system in man. *Adv Anat Embryol Cell Biol*. 1975;51:3-60.
24. van der Putte SC, van LJ. The embryonic development of the main lymphatics in man. *Acta Morphol Neerl Scand*. 1980;18:323-335.
25. Miyabara S. Animal model for congenital anomalies induced by chromosome aberrations. *Congen Anom*. 1990;30:49-68.
26. Carmeliet P. Blood vessels and nerves: common signals, pathways and diseases. *Nat Rev Genet*. 2003;4:710-720.
27. Wilting J, Neeff H, Christ B. Embryonic lymphangiogenesis. *Cell Tissue Res*. 1999;297:1-11.

Chapter 7

Jugular Lymphatic Maldevelopment in Turner Syndrome and Trisomy 21: Different Anomalies Leading to Nuchal Edema

Nynke M.S. van den Akker^{1*}, Mireille N. Bekker^{1,2*}, Yolanda M. de Mooij^{1,2}, Margot M. Bartelings¹, John M.G. van Vugt², Adriana C. Gittenberger-de Groot¹

¹Department of Anatomy and Embryology, Leiden University Medical Center, Leiden, the Netherlands; ²Department of Obstetrics and Gynecology, VU University Medical Center, Amsterdam, the Netherlands.

* These authors contributed equally to this work

Modified after Reproductive Sciences, 2008, In Press.

Jugular Lymphatic Maldevelopment in Turner Syndrome and Trisomy 21: Different Anomalies Leading to Nuchal Edema

Abstract

Increased nuchal translucency (NT) is an ultrasound marker for trisomy 21 and other aneuploidies. Nuchal edema is the morphological equivalent of increased NT. Turner syndrome usually presents with a massively increased NT, referred to as cystic hygroma. There are conflicting data on the question whether or not cystic hygroma and increased NT are to be considered as different entities. Both have been associated with jugular lymphatic distension. In this study the jugular lymphatic system of human fetuses with trisomy 21, Turner syndrome and normal karyotype were compared. Fourteen fetuses (trisomy 21 n=5, Turner n=5, control n=4) of 12 to 20 weeks of gestation were investigated by immunohistochemistry using the lymphatic endothelial markers Prox-1, Podoplanin, LYVE-1, the blood vessel endothelial markers NP-1 and VEGF and additional endothelial markers vWF, VEGFR-2 and ephrinB2. α -Smooth muscle actin was used as smooth muscle cell marker. The trisomy 21 fetuses showed cavities in the area of the nuchal edema that were not lined by an endothelial layer. These mesenchymal nuchal cavities were extremely large in the Turner fetuses, showing similar characteristics. The subepidermal skin showed numerous dilated lymph vessels in trisomy 21 and scanty small lymph vessels in case of Turner syndrome. A jugular lymphatic sac was present in both control and trisomy 21 fetuses, being markedly enlarged and showing an abnormal venous-lymphatic phenotype in the trisomy 21 cases. In the Turner fetuses we could not identify a jugular lymphatic sac. Our data suggest that nuchal edema in trisomy 21 and Turner syndrome are similar entities that are caused by different abnormalities of the jugular lymphatic system.

Introduction

Nuchal translucency (NT) is a translucent area in the neck region of the fetus, which is visible between 9 to 14 weeks of gestational age (GA). The size of the NT is measured by ultrasound and is part of the first-trimester screening for aneuploidy. Increased NT is defined as >95th percentile. The most frequently encountered chromosomal defects in case of increased NT are trisomy 21, trisomy 18, trisomy 13 and Turner syndrome (monosomy X or 45,X)¹. Nuchal edema (NE) is the morphological equivalent of increased NT and represents mesenchymal edema².

In case of Turner syndrome the NT is usually massively increased and is also referred to as cystic hygroma and considered the outcome of anomalous lymphatic development. In about 75% of fetuses with cystic hygromas, there is a chromosomal abnormality, and in about 95% of these cases, the abnormality is Turner syndrome³. Conflicting data exists in literature regarding the nomenclature and origin of this so-called cystic hygroma³⁻⁵.

Ultrasonographically, cystic hygroma has been described as the appearance of large bilateral translucencies in the fetal occipito-cervical region, which are separated by a septum in the posterior midline. This septum represents the nuchal ligament, which extends from the external occipital protuberance and median nuchal line to the spinous process of the seventh cervical vertebra. In the bilateral cavities several septa can be present^{6,7}. The bilateral spaces are suggested to be distended and hyperplastic jugular lymphatic sacs (JLS), which fail to connect to the venous system^{3,8,9}. Conversely, other studies describe an absence or hypoplasia of the lymph vessels in the skin of Turner fetuses as cause for the edema^{10,11}.

A recent study of Molina et al has shown that increased NT can also contain several septa and, consequently, first-trimester ultrasound cannot distinguish a large NT from a "cystic hygroma"³. The question remains whether a cystic hygroma must be seen as a severe and persistent form of increased NT or whether this is a different entity, specifically since recent ultrasound and morphological studies show that increased NT is also associated with bilateral JLS distension^{2,12,13}. A delayed or disturbed jugular lymphatic development is even suggested as a common cause for NE in the wide spectrum of associated anomalies¹⁴.

The lymphatic system starts to develop by the formation of the JLS. The lymphatic endothelial cells (LEC) of the JLS develop by budding and differentiation from the anterior cardinal veins, which is controlled by the homeobox transcription factor Prox-1. The peripheral lymphatic system is thought to develop by sprouting of the JLS in surrounding structures and through lymphangiogenesis from superficial local lymphangioblasts¹⁵. In a previous study we showed a disturbed venous-lymphatic phenotype in fetuses with trisomy 21 and 18, which was characterized by a diminished expression of lymphatic markers Prox-1 and its target gene Podoplanin in the LEC of the JLS. Furthermore, the LEC showed an upregulation of the blood vessel markers vascular endothelial growth factor-A (VEGF-A or VEGF) and its coreceptor neuropilin-

1 (NP-1)¹⁴. Also, the JLS contained blood cells and was surrounded by a layer of smooth muscle cells.

The aim of the current study was to compare the jugular lymphatic system of fetuses with Turner syndrome, trisomy 21 and normal karyotype. A morphological study was performed using lymphatic endothelial cell specific markers (Prox-1, Podoplanin, vascular endothelial growth factor-C (VEGF-C), lymphatic vessel endothelial hyaluronan receptor-1 (LYVE-1)) and blood endothelial cell specific markers (VEGF and NP-1, von Willebrand Factor (vWF)¹⁶). Antibodies against vascular endothelial growth factor receptor-2 (VEGFR-2) and ephrinB2 were included as additional endothelial markers. VEGFR-2 is expressed by all types of endothelium¹⁷⁻²⁰, while ephrinB2 is expressed specifically by arterial and lymphatic endothelium^{21;22}. α -Smooth muscle actin (α SMA) was included as marker indicative for the presence of smooth muscle cells.

Table 1: Characteristics of the 14 fetuses included in the study.

	GA	CRL	Karyotype	NT	Cardiac Morphology
Control (n=4)	12 ⁺¹	49	46XX	1.2	normal
	13 ⁺³	75	46XX	1.0	normal
	13 ⁺³	81	46XX	1.4	normal
	14 ⁺³	84	46XY	1.2	normal
Trisomy 21 (n=5)	13 ⁺²	87	47XX+21	3.3	normal
	14 ⁺¹	90	47XY+21	4.0	AVSD
	14 ⁺²	82	47XX+21	3.8	ASD, narrowing of aortic isthmus
	15 ⁺⁰	108	47 XY+21	5.0	normal
	18 ⁺²	134	47XY+21	3.6	AVSD
Turner (n=5)	13 ⁺⁴	78	45X	10.0	HLHS
	14 ⁺³	85	45X	7.8	HLHS
	15 ⁺³	72	45X	7.1	ARSA
	17 ⁺⁰	117	45X	9.0	unknown
	20 ⁺⁵	140	45X	ND	ARSA; dilation of right atrium, ventricle, pulmonary trunk

Gestational age (GA) in weeks and crown-rump length (CRL) in mm are measured at birth, nuchal translucency (NT) in mm at the NT ultrasound scan, performed in the first trimester of pregnancy. ND: not determined; nuchal translucency measurement was not possible as the first ultrasound scan was at 16 weeks' gestation. The fetus showed a cystic hygroma of 21.9 mm (anterior-posterior). ASD = atrial septal defect; ARSA: aberrant right subclavian artery (aortic arch anomaly); AVSD = atrioventricular septal defect; HLHS = hypoplastic left heart syndrome.

Materials and Methods

Fourteen fetuses were investigated (normal karyotype n=4, trisomy 21 n=5, Turner syndrome n=5). All fetuses were prenatally examined by ultrasound and diagnosed with normal or increased nuchal translucency. The NT measurement was performed between 11 and 14 weeks' gestation according to the guidelines of the Fetal Medical Foundation^{3;23}. One fetus with Turner syndrome was examined for the first time by ultrasound at 16 weeks' gestation. Therefore, an official nuchal translucency measurement was not possible anymore^{3;23}. The fetus showed two large bilateral translucencies in the nuchal region, defined as second-trimester cystic hygroma^{3;23} (Table 1). This fetus died at GA 20⁺⁴ weeks after development of fetal hydrops.

The fetuses were karyotyped by chorion villus sampling or amniocentesis. The medical ethical committee of the VU University Medical Center approved the study. All patients received information and gave written informed consent. Fetal tissue was obtained after termination of pregnancy either by spontaneous abortion (due to cervical insufficiency) or abdominal hysterectomy (for oncological reasons) in case of the control fetuses or by misoprostol induction in case of aneuploidy. The fetal tissue was fixed in 4% paraformaldehyde, embedded in paraffin and transversely sectioned into serial sections of 8 μm . Analysis of the transverse sections was performed from eye level to the aortic arch.

Antibodies and staining procedures

We used antibodies against LYVE-1 (ReliaTech), Prox-1 (ReliaTech), Podoplanin (provided by V. Schacht²⁴), NP-1 (Santa Cruz Biotechnology), VEGF (Santa Cruz Biotechnology), VEGF-C (Santa Cruz Biotechnology), α -smooth muscle actin (α SMA) (clone 1A4, Sigma-Aldrich), vWF (DAKO), VEGFR-2 (R&D Systems) and ephrinB2 (R&D Systems). The sections for different staining procedures were incubated for 20 minutes in a solution of 0.3% H_2O_2 to inhibit the endogenous peroxidase activity. When staining for Prox-1, Podoplanin, vWF or ephrinB2, the sections were incubated for 12 minutes in 0.01 M citric buffer of pH 6.0 at 97 °C. Subsequently, sections were incubated overnight with the primary antibody. Next day the sections were incubated for 1 hour with the secondary antibody. For Prox-1, LYVE-1, VEGF and vWF this was a biotinylated goat-anti-rabbit antibody (Vector Labs), for Podoplanin a biotinylated horse-anti-mouse antibody (Vector Labs), for NP-1, VEGFR-2 and ephrinB2 a biotinylated horse-anti-goat-biotin antibody (Vector Labs) and for α SMA a horseradish peroxidase-conjugated rabbit-anti-mouse antibody (DAKO). All sections, except those following the staining procedure for α SMA, were incubated with ABC-reagent (Vector Labs) for 45 minutes. Visualisation was performed using 3-3'-diaminobenzidin tetrahydrochlorid (DAB). Finally, the sections were counterstained with Mayer's hematoxylin (Sigma-Aldrich) for 10 seconds, rinsed for 10 minutes in tap water and dehydrated to xylene. The sections were mounted with Entellan (Merck).

Results

The characteristics of the 14 fetuses included in the study are listed in Table 1. Morphological examination of the control fetuses revealed no abnormalities (n=4). All fetuses with trisomy 21 showed NE (n=5). Two fetuses (of GA 13⁺² and 15⁺⁰ weeks) showed no structural cardiac anomalies. The heart of the fetus of GA 14⁺¹ weeks was difficult to diagnose due to severe artefacts, but this heart likely showed an atrioventricular septal defect (AVSD). The fetus of GA 14⁺² weeks showed a narrowing of the aortic arch isthmus and a large atrial septal defect. The fetus of GA 18⁺² weeks showed a complete, balanced AVSD.

Table 2: Results of the morphological and immunohistochemical examinations of the neck region of the fourteen fetuses.

	Control (n=4)	Trisomy 21 (n=5)	Turner (n=5)
Morphology			
Nuchal skin	Some lymph vessels; not dilated	Edematous; numerous dilated lymph vessels; small subcutaneous cavities	Edematous; scanty small lymph vessels; large bilateral subcutaneous cavities
JLSs	Normal	Enlarged and abnormal	Absent
Immunohistochemistry of the LECs*			
LYVE-1	+	+	+
Prox-1	+	-	+ [†]
Podoplanin	+	-	+
VEGF-C	+/-	+/-	+/-
VEGF-A	+/-	++	+/-
VEGFR-2	+/-	+/-	+/-
NP-1	+/-	++	+/-
ephrinB2	+/-	+/-	+/-
vWF	-	+	-
SMA	-	+	-

JLSs jugular lymphatic sacs; - absent staining; +/- lightly positive staining; + positive staining; ++ strong positive staining. * of the lymph vessels in the nuchal skin and (if present) the jugular lymphatic sacs; [†]cytoplasmic staining

All fetuses with Turner syndrome (n=5) showed an extremely large NE. Cardiac examination of the fetus of GA 13⁺⁴ weeks revealed a hypoplastic left heart syndrome. The aortic valve was bicuspid and the left ventricle was underdeveloped. Furthermore, the ascending aorta and aortic arch were hypoplastic, from which an aberrant right subclavian artery originated. The dorsal aorta was also hypoplastic. The fetus with Turner syndrome of GA 14⁺³ weeks showed a heart with a dysplastic bicuspid aortic valve and slight hypoplasia of the left ventricle, the ascending aorta and tubular hypoplasia of the aortic arch between the left carotid artery and the left subclavian artery. The fetuses with Turner syndrome of GA 15⁺³ and 20⁺⁵ weeks both showed bicuspid aortic valves and an aortic arch from which an aberrant right subclavian artery originated.

The fetus of GA 20⁺⁵ weeks showed in addition dilation of the right atrium, ventricle and pulmonary trunk. The heart of the Turner fetus of GA 17⁺⁰ weeks could not be investigated due to parental informed consent for neck-restricted diagnosis. The results of the morphological examinations are described below and summarized in Table 2.

Lymphatic vascular endothelium

Normal karyotype

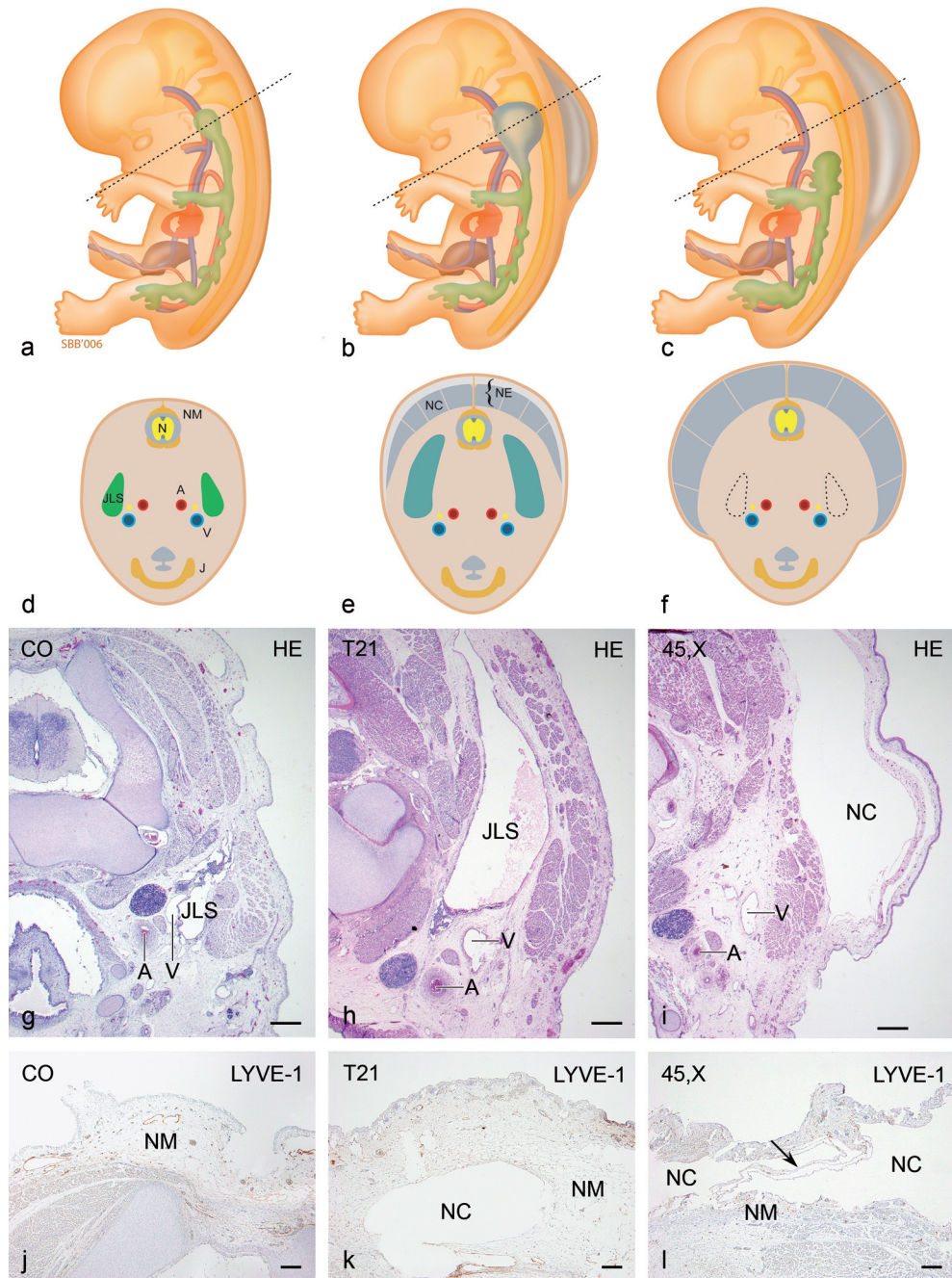
In the control fetuses (Figure 1a,d,g,j) the layer of subcutaneous nuchal mesenchyme was thin and showed no subcutaneous edema, while some lymph vessels were observed. The JLSs were positioned directly lateral to the jugular vein and the carotid artery (Figure 1d,g). The control fetus of GA 12⁺¹ weeks showed some lymph node tissue in the JLS, indicating the start of reorganization of the sac into lymph nodes. The two fetuses of GA 13⁺³ weeks showed somewhat more reorganization and the JLS were still present. In the control fetus of 14 weeks the reorganization was nearly completed. This was indicated by the smaller JLSs, which were almost filled with lymph node tissue.

The LECs were clearly positive for the lymphatic markers LYVE-1 (Figure 2a), Prox-1 and Podoplanin, whereas the LECs were slightly positive for VEGF (Figure 2e), NP-1, VEGFR-2, VEGF-C and ephrinB2. The LECs stained negative for vWF (Figure 2i). There was no difference in staining intensities between the LECs of the JLS and subcutaneous lymph vessels. No α SMA-positive cells were observed surrounding the LECs of the JLS. The staining characteristics did not differ between the control fetuses.

Trisomy 21

The fetuses with trisomy 21 showed subcutaneous mesenchymal edema (i.e. NE) and bilaterally distended JLSs (Figure 1b,e,h,k), which were still present in the trisomy 21 fetuses older than 14 weeks of gestation. The posterior part of the neck showed cavities within the NE that were surrounded by mesenchymal cells (Figure 1e,k). Also, in the edematous nuchal subepidermis several hyperplastic lymph vessels were observed. The large and distended JLS showed a small amount of lymph node tissue in the corner of the JLS close to the jugular vein (Figure 1h). The JLSs were positioned directly lateral to the jugular vein and carotid artery, as was the case in the control fetuses (Figure 1e,h). As described previously¹⁴, the LECs of the JLS showed a diminished Prox-1 and Podoplanin staining as compared with the control fetuses, while LYVE-1 (Figure 2b), VEGF-C, VEGFR-2 and ephrinB2 staining-intensities were similar. The VEGF and NP-1 (Figure 2f) protein expression was increased compared with the control fetuses. Also, the LEC were positive for vWF in contrast to the control fetuses (Figure 2j). A strong α SMA positivity was observed in the cell layers surrounding the JLS. Furthermore, the JLS contained blood cells. The LECs of the subcutaneous lymph vessels showed a similar staining pattern as the LECs of the JLSs for all endothelial markers. Some of the lymph vessels were surrounded by a smooth muscle cell layer and contained blood cells, just as the JLS.

The cells lining the nuchal cavity showed a weak VEGF (Figure 2g) and NP-1-positivity and stained negative for all other markers (LYVE-1 (Figure 1k and 2c), vWF (Figure 2k), VEGFR-2, ephrinB2, Prox-1, Podoplanin and VEGF-C). The staining characteristics did not differ between the trisomy 21 fetuses.



Turner syndrome

In the posterior neck region of the Turner fetuses (Figure c,f,i,l) two large subcutaneous nuchal cavities were observed, extending to anterior and positioned bilaterally but distant from the jugular vein and carotid artery. The cavities were encased within the mesenchyme and lined by mesenchymal cells, just as in the fetuses with trisomy 21 (Figure 1f,i,l). The size of the cavities, however, was approximately 10 times larger than the nuchal cavities of the trisomy 21 fetuses. In the posterior midline the nuchal ligament was clearly visible as a septum between the cavities (arrow in Figure 1l). Within the cavities some septa were present. The amount of remaining subcutaneous mesenchymal tissue between the upper dermis and the cavities was small and sporadically showed a small lymph vessel (Figure 1l).

The cells lining the cavities were negative for the lymphatic markers Prox-1, Podoplanin and LYVE-1 (Figure 1l and 2d) and showed a strong VEGF (Figure 2h) and NP-1-expression. Moreover, the lining of the cavities stained negative for vWF (Figure 2l), VEGFR-2 and ephrinB2. In addition, smooth muscle cells did not surround the cavities, further excluding a vacular origin. More caudally the position of the bilateral cavities shifted towards the jugular vein. The wall remained negative for all lymphatic markers. Next to the jugular vein and carotid artery several veins were present but no JLS or other lymph vessels could be observed. The LECs of the very few lymphatic vessels that were present in the nuchal subepidermis stained similar as the control fetuses for all markers. In two of the fetuses with Turner syndrome (GA 15⁺³ and 20⁺⁵ weeks) no subepidermal lymph vessels could be observed at all. The staining characteristics did not differ between fetuses with Turner syndrome.

← *Figure 1. Schematic illustrations and micrographs of the nuchal area of an euploid human fetus (CO), a trisomy 21 fetus (T21) and a monosomy X fetus (45,X).* The dashed line in the sagittal view in a-c indicate the transverse plane of d-f. (a,d) The jugular lymphatic sac (JLS) in the control fetus is positioned laterally and directly next to the jugular vein (V) and carotid artery (A). The subcutis contains a thin layer of nuchal mesenchyme (NM). (b,e) The JLS in the trisomy 21 fetus is abnormally differentiated and enlarged. The JLS is positioned next to V and A. The NM is edematous and contains small nuchal cavities (NC) and nuchal edema (NE) is present. (c,f) In the Turner fetus no JLS is visible next to V and A. The dashed lines indicate where the JLS was expected. More distant and lateral large NC are visible. The NC extend from posterior to the antero-lateral part of the neck and contain septa. (g-l) Transverse sections of the antero-lateral (g-i) and posterior (j-l) nuchal neck region of an euploid control fetus, a trisomy 21 fetus and a fetus with Turner syndrome of 14 weeks' gestation, stained with hematoxylin and eosin (HE) or LYVE-1. (g) The JLS in the control fetus is positioned directly next to V and A. Lymph node tissue can be observed within the JLS. (h) In a fetus with trisomy 21 the enlarged JLS is positioned directly next to V and A. The JLS shows a small amount of lymph node tissue in the corner next to the V. (i) In the fetus with Turner syndrome no JLS is present next to the V and A. More distant and lateral from the V and A a subcutaneous NC is visible. (j) The NM of the control fetus is thin and shows some LYVE-1 positive lymph vessels. (k) The NM of the trisomy 21 fetus is edematous and contains numerous LYVE-1 positive lymph vessels. Within the NM a LYVE-1 negative NC is present. (l) In the fetus with Turner syndrome large NCs are present, which are separated by the nuchal ligament (arrow) in the posterior midline. The NC stains negative for LYVE-1. The small amount of NM between the NC and the upper dermis contains scanty small LYVE-1 positive lymph vessels. Abbreviations: N = neural tube and J = jaw. Scale bars: (g-i) 600 µm; (j-l) 300 µm.

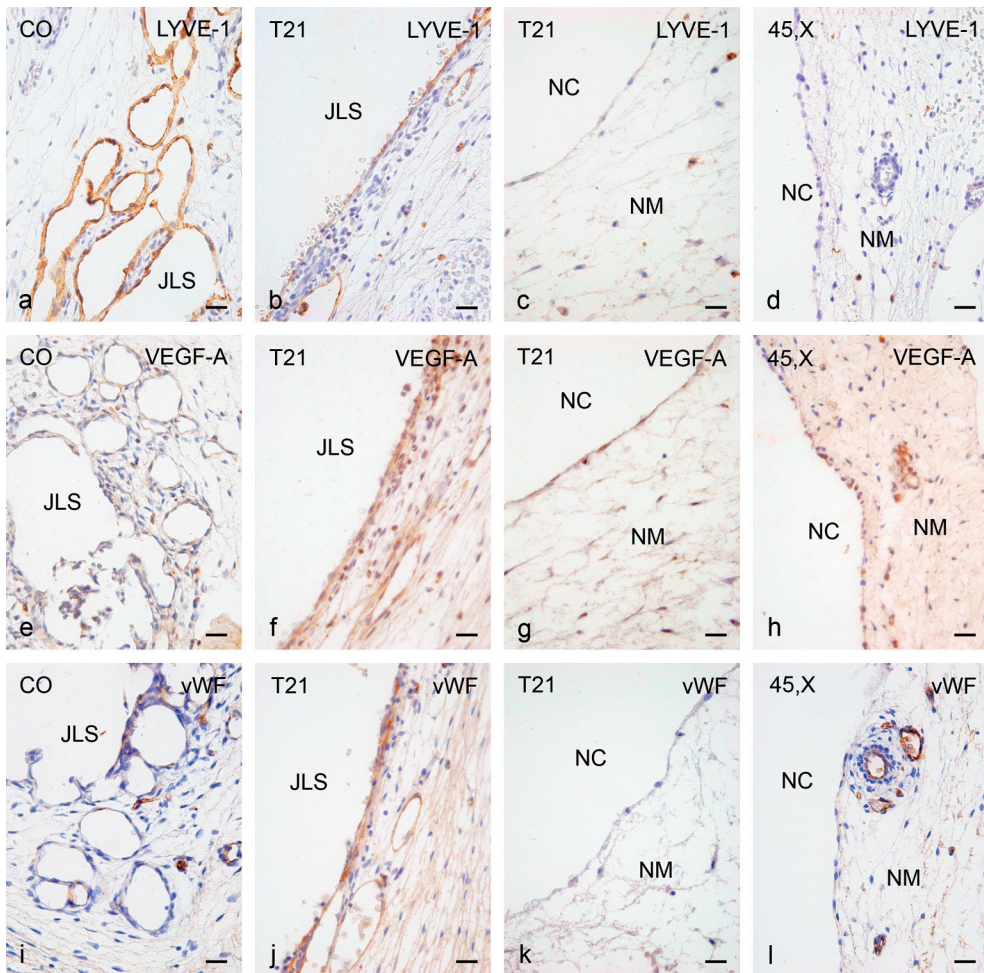


Figure 2. Immunohistochemical analysis of the lymphatic endothelial cells (LEC) of the jugular lymphatic sac (JLS) of a control (CO) and trisomy 21 (T21) fetus and the mesenchymal cells lining the nuchal cavities (NC) of a T21 and Turner syndrome (45,X) fetus. The LECs of the JLS stain positive with LYVE-1 in the CO (a) and the T21 fetus (b). The cells lining the NC stain negative for LYVE-1 in both the T21 (c) and the 45,X fetus (d). The LEC of the JLS shows a slightly positive VEGF (VEGF-A)-staining in the CO fetus (e) and a strong VEGF staining in the T21 fetus (f). The cells lining the NC in the T21 (g) and the 45,X fetus (h) are positive for VEGF. The LECs of the JLS stain negative for vWF in the CO fetus (i), in contrast to a positive vWF-staining in the T21 fetus (j). The cells surrounding the NC are negative for vWF in both the T21 (k) and 45,X fetus (l). Scale bars: a-l 30 μ m.

Discussion

In this study we investigated the jugular lymphatic system of fetuses with Turner syndrome, trisomy 21 and euploid controls, using LEC and BEC specific markers. Our data suggest that NE in Turner syndrome and trisomy 21 are similar entities, that is mesenchymal edema containing nuchal cavities, but are the result of different lymphatic anomalies. Turner syndrome was associated with an absence of the JLS and subcutaneous lymphatic hypoplasia or even aplasia, whereas the trisomy 21 fetuses demonstrated subcutaneous lymphatic hyperplasia with a marked JLS distension.

In the fetuses with trisomy 21 we observed a diminished expression of the LEC-markers Prox-1 and Podoplanin, together with the increase of blood vessel characteristics in the endothelium of the JLS, which also contained blood cells. This was reported previously by our group in a larger dataset of aneuploid human fetuses (trisomy 21 and 18) and trisomy 16 mouse embryos¹⁴. It indicates a disturbed venous-lymphatic differentiation of the endothelial cells budding from the cardinal vein and forming the JLS. Prox-1, master control transcription factor in lymphangiogenesis, is likely to play a crucial role in the disturbed lymphatic development, as it induces the expression of LEC-specific genes and suppresses BEC-specific genes under normal circumstances²⁵. The nuchal cavities of the trisomy 21 fetuses are probably a consequence of the fluid accumulation in the neck. They were described before in human fetuses and trisomy 16 mouse embryos with NE^{2;12}.

The fetuses with Turner syndrome showed two large bilateral subcutaneous cavities, extending in the neck from posterior to anterior and containing a large amount of fluid. These cavities were first described in 1828 by Radenbacher and were later thought to present immensely distended JLS, which failed to connect with the venous system. Several studies have since reported these bilateral cavities^{6;8;9;26}. However, we found an absence of staining of the LEC-specific markers Prox-1, Podoplanin and LYVE-1 and also of the other endothelial markers vWF, VEGFR-2 and ephrinB2 in the lining of these cavities. Also, the cavities were not positioned in the typical JLS location, directly adjacent to the jugular vein.

To our knowledge other reports of the expression of LEC-specific markers in the cystic hygroma of fetuses with Turner syndrome do not exist. In general, studies of lymphatic development in normal and abnormal human fetuses are relatively scarce. In most reports, series were small and the fetuses were often in poor condition, since lymphatic tissue has no support as it is positioned in loose connective tissue and lacks a smooth muscle cell media. Moreover, only recently, highly specific LEC-markers such as Prox-1, Podoplanin and LYVE-1 have been identified. Prox-1 has shown to be a stable and specific marker in normal and diseased human tissues^{15;27;28}.

We show by the lack of staining with LEC and BEC-specific markers that these cavities are neither the JLS nor of other vascular identity. We conclude that in case of Turner syndrome there is a failure of JLS-development (aplasia) and the cavities are formed by accumulation of fluid in the intercellular spaces of the connective tissue. The

latter also explains the septated and cystic appearance of the hygroma. Also, it clarifies the lack of an endothelial lining of the cavities. The cavities are comparable with the nuchal cavities seen in human trisomy 21 fetuses and trisomy 16 mouse embryos with NE^{2;12}. In fetuses with NE, the nuchal cavities, as well as the JLS usually resolve when the jugular lymphatic development proceeds and are therefore a transient phenomenon. In case of cystic hygroma, on the other hand, the edema cavities typically persist and can become extremely enlarged. This can be attributed to an aplasia or complete loss of lymphatic identity of the JLS, which is a more severe and permanent form of lymphatic maldevelopment. The massive NE is associated with hydrops and intrauterine demise or can persist as cystic hygroma or a webbed neck after birth. The overall prognosis in fetuses with cystic hygromas is poor, and the survival rate is less than 5%⁷.

The hypoplasia of the subcutaneous nuchal lymphatic vessels in the Turner fetuses in this study is in agreement with previous studies of fetuses with Turner syndrome^{8;10;29}. On the other hand, Van der Putte observed both lymphatic hyperplasia with distension of the JLS as well as lymphatic hypoplasia in a morphological study of seven human fetuses with cystic hygroma⁹. No consistent abnormality could be determined in the examined fetuses. In some of the fetuses he observed cavities in the nuchal region as well as next to the jugular vein, while in other fetuses solely cavities in the nuchal skin we seen. Interestingly, he described that the walls of these isolated cavities in the nuchal region were surrounded by connective tissue. He concluded that the fact that no endothelial cells in the lining of the cavities could be seen was probably a result of maceration. Although he speculated about the possibility of aplasia of the JLS in some of the fetuses, he finally concluded that cystic hygromas present enlarged JLS, which have failed to connect with the venous system. As karyotyping was not performed in the study of Van der Putte it is tempting to speculate that both trisomy 21 fetuses with enlarged JLS as well as Turner syndrome fetuses with a lymphatic hypoplasia and absent JLS were examined. The fact that Van der Putte did not observe endothelial cells is in agreement with our findings in the nuchal cavities.

In another study, Chitayat et al compared the neck region of Turner (n=4) and non-Turner fetuses (n=2 trisomy 21; n=1 trisomy 13; n=2 euploidy) with NE⁸. Their findings of an absence of lymphatic vessels in the nuchal skin of the Turner fetuses and numerous dilated lymphatic vessels in the non-Turner fetuses are in agreement with our findings. Chitayat et al found nuchal cavities in both groups. In the non-Turner fetuses the cavities were smaller and surrounded by a wall of connective tissue. In the Turner fetuses the cavities were described to be lined by endothelial cells and were therefore assumed to be the JLS. This is in contrast with our results. However, Chitayat et al did not use LEC specific markers and did not investigate the antero-lateral neck region. Therefore, the relation of the cavities with anatomical landmarks such as the jugular vein and carotid artery are unknown. Furthermore, Chitayat et al used vWF as an endothelial marker, which is normally not expressed in the LEC¹⁶. In contrast, we did not observe vWF in the lining of the nuchal cavities, or any other endothelial marker, which fits with the designation of the nuchal cavity as an

interstitial cavity. As the number of fetuses examined is limited in both studies further research is warranted.

In our study the NE of both the trisomy 21 and the Turner fetuses correlated with an increased VEGF-expression. The fetuses with Turner syndrome presented with an overall increased VEGF-expression, while in the trisomy 21 fetuses the increased VEGF-expression was solely observed in the LECs and in the wall of the nuchal cavities. VEGF-expression can be induced by tissue expansion causing mechanical stretch, by shear stress due to altered haemodynamics, and by hypoxia^{30;31}. It is likely that the edema, in trisomy 21 possibly caused by abnormal endothelial functioning of the JLS¹⁴ and in Turner syndrome by aplasia or extreme hypoplasia of the lymphatic system, leads to overexpression of VEGF through tissue expansion. This can also explain the fact that in trisomy 21, where lymphatic malformations transiently arise in the neck region¹⁴, overexpression of VEGF is only seen in the nuchal area, while Turner fetuses, in which lymphatic anomalies throughout the body are common^{8;11;32}, show an overall increased VEGF-expression. Moreover, overexpression of VEGF, also known as vascular permeability factor, has been shown to cause severe edema. For instance, it is reported in the cardiac tissues of human fetuses with hydrops³³⁻³⁵. In addition, it is associated with vascular and lymphatic anomalies³⁶. Therefore, we hypothesize that the increased VEGF-expression might, subsequently, further augment the edema.

Our data show that increased NT and cystic hygroma are comparable entities with marked difference in size, but which are most probably caused by different mechanisms. Discrimination by ultrasound is in our opinion not feasible. Nuchal cavities and septa can be present in both increased NT as well as in cystic hygroma. Also, the nuchal ligament can be observed in both cases, when there is sufficient edema. The larger the NT the more it presumably resembles the massive edema of a cystic hygroma. Identification of the JLS adjacent to the jugular vein in the antero-lateral neck region facilitates the diagnosis of increased NT, since in a Turner fetus with cystic hygroma marked JLSs are missing. Therefore, we agree with Molina et al that the clinical diagnosis of cystic hygroma should be preserved for the second trimester, in which the NT resolves or becomes a thickened nuchal skin while the cystic hygroma remains as transonic cavities in the posterior neck region³.

In conclusion, our data indicate that NE in trisomy 21 and Turner syndrome are most probably caused by different mechanisms. The Turner fetuses in this study showed an absence of the JLSs and lymphatic hypoplasia, whereas the fetuses with trisomy 21 presented with enlarged JLS and numerous dilated lymph vessels in the nuchal skin. Furthermore, while the trisomy 21 fetuses showed a disturbed LEC-differentiation resulting in an abnormal phenotype, the Turner fetuses showed a total lack of LEC-differentiation towards a JLS. A relation between NT-size and the extent of aberrant lymphatic morphology or endothelial differentiation could not be established due to the limited number of cases. Research in larger data sets should be performed and the possible relation between lymphatic and cardiovascular anomalies should be further investigated.

References

1. Nicolaides KH, Brizot ML, Snijders RJ. Fetal nuchal translucency: ultrasound screening for fetal trisomy in the first trimester of pregnancy. *Br J Obstet Gynaecol.* 1994;101:782-786.
2. Haak MC, Bartelings MM, Jackson DG, Webb S, Van Vugt JM, Gittenberger-De Groot AC. Increased nuchal translucency is associated with jugular lymphatic distension. *Hum Reprod.* 2002;17:1086-1092.
3. Molina FS, Avgidou K, Kagan KO, Poggi S, Nicolaides KH. Cystic hygromas, nuchal edema, and nuchal translucency at 11-14 weeks of gestation. *Obstet Gynecol.* 2006;107:678-683.
4. Bronshtein M, Zimmer EZ, Blazer S. A characteristic cluster of fetal sonographic markers that are predictive of fetal Turner syndrome in early pregnancy. *Am J Obstet Gynecol.* 2003;188:1016-1020.
5. Malone FD, Ball RH, Nyberg DA, Comstock CH, Saade GR, Berkowitz RL, Gross SJ, Dugoff L, Craigo SD, Timor-Tritsch IE, Carr SR, Wolfe HM, Dukes K, Canick JA, Bianchi DW, D'Alton ME. First-trimester septated cystic hygroma: prevalence, natural history, and pediatric outcome. *Obstet Gynecol.* 2005;106:288-294.
6. Chervenak FA, Isaacson G, Blakemore KJ, Breg WR, Hobbins JC, Berkowitz RL, Tortora M, Mayden K, Mahoney MJ. Fetal cystic hygroma. Cause and natural history. *N Engl J Med.* 1983;309:822-825.
7. Azar GB, Snijders RJ, Gosden C, Nicolaides KH. Fetal nuchal cystic hygromata: associated malformations and chromosomal defects. *Fetal Diagn Ther.* 1991;6:46-57.
8. Chitayat D, Kalousek DK, Bamforth JS. Lymphatic abnormalities in fetuses with posterior cervical cystic hygroma. *Am J Med Genet.* 1989;33:352-356.
9. van der Putte SC. Lymphatic malformation in human fetuses. A study of fetuses with Turner's syndrome or status Bonnevie-Ullrich. *Virchows Arch A Pathol Anat Histol.* 1977;376:233-246.
10. von Kaisenberg CS, Nicolaides KH, Brand-Saberi B. Lymphatic vessel hypoplasia in fetuses with Turner syndrome. *Hum Reprod.* 1999;14:823-826.
11. Vittay P, Bosze P, Gaal M, Laszlo J. Lymph vessel defects in patients with ovarian dysgenesis. *Clin Genet.* 1980;18:387-391.
12. Gittenberger-De Groot AC, Van Den Akker NM, Bartelings MM, Webb S, Van Vugt JM, Haak MC. Abnormal lymphatic development in trisomy 16 mouse embryos precedes nuchal edema. *Dev Dyn.* 2004;230:378-384.
13. Bekker MN, Haak MC, Rekoert-Hollander M, Twisk J, Van Vugt JM. Increased nuchal translucency and distended jugular lymphatic sacs on first-trimester ultrasound. *Ultrasound Obstet Gynecol.* 2005;25:239-245.
14. Bekker MN, Van Den Akker NM, Bartelings MM, Arkesteijn JB, Fischer SG, Polman JA, Haak MC, Webb S, Poelmann RE, Van Vugt JM, Gittenberger-De Groot AC. Nuchal edema and venous-lymphatic phenotype disturbance in human fetuses and mouse embryos with aneuploidy. *J Soc Gynecol Investig.* 2006;13:209-216.
15. Wilting J, Aref Y, Huang R, Tomarev SI, Schweigerer L, Christ B, Valasek P, Papoutsis M. Dual origin of avian lymphatics. *Dev Biol.* 2006;292:165-173.

16. Lymboussaki A, Partanen TA, Olofsson B, Thomas-Crusells J, Fletcher CD, de Waal RM, Kaipainen A, Alitalo K. Expression of the vascular endothelial growth factor C receptor VEGFR-3 in lymphatic endothelium of the skin and in vascular tumors. *Am J Pathol.* 1998;153:395-403.
17. Paavonen K, Mandelin J, Partanen T, Jussila L, Li TF, Ristimäki A, Alitalo K, Kontinen YT. Vascular endothelial growth factors C and D and their VEGFR-2 and 3 receptors in blood and lymphatic vessels in healthy and arthritic synovium. *J Rheumatol.* 2002;29:39-45.
18. Partanen TA, Mäkinen T, Arola J, Suda T, Weich HA, Alitalo K. Endothelial growth factor receptors in human fetal heart. *Circulation.* 1999;100:583-586.
19. Saaristo A, Veikkola T, Enholm B, Hytonen M, Arola J, Pajusola K, Turunen P, Jeltsch M, Karkkainen MJ, Kerjaschki D, Bueler H, Ylä-Herttuala S, Alitalo K. Adenoviral VEGF-C overexpression induces blood vessel enlargement, tortuosity, and leakiness but no sprouting angiogenesis in the skin or mucous membranes. *FASEB J.* 2002;16:1041-1049.
20. Soker S, Miao HQ, Nomi M, Takashima S, Klagsbrun M. VEGF165 mediates formation of complexes containing VEGFR-2 and neuropilin-1 that enhance VEGF165-receptor binding. *J Cell Biochem.* 2002;85:357-368.
21. le Noble F, Moyon D, Pardanaud L, Yuan L, Djonov V, Matthijsen R, Breant C, Fleury V, Eichmann A. Flow regulates arterial-venous differentiation in the chick embryo yolk sac. *Development.* 2004;131:361-375.
22. Mäkinen T, Adams RH, Bailey J, Lu Q, Ziemiecki A, Alitalo K, Klein R, Wilkinson GA. PDZ interaction site in ephrinB2 is required for the remodeling of lymphatic vasculature. *Genes Dev.* 2005;19:397-410.
23. Pandya PP, Snijders RJ, Johnson SP, De Lourdes BM, Nicolaides KH. Screening for fetal trisomies by maternal age and fetal nuchal translucency thickness at 10 to 14 weeks of gestation. *Br J Obstet Gynaecol.* 1995;102:957-962.
24. Schacht V, Ramirez MI, Hong YK, Hirakawa S, Feng D, Harvey N, Williams M, Dvorak AM, Dvorak HF, Oliver G, Detmar M. T1alpha/Podoplanin deficiency disrupts normal lymphatic vasculature formation and causes lymphedema. *EMBO J.* 2003;22:3546-3556.
25. Petrova TV, Mäkinen T, Makela TP, Saarela J, Virtanen I, Ferrell RE, Finegold DN, Kerjaschki D, Ylä-Herttuala S, Alitalo K. Lymphatic endothelial reprogramming of vascular endothelial cells by the Prox-1 homeobox transcription factor. *EMBO J.* 2002;21:4593-4599.
26. Sabin FR. The lymphatic system in human embryos, with a consideration of the morphology of the system as a whole. *Am J Anat.* 1909;9:43-91.
27. Wigle JT, Harvey N, Detmar M, Lagutina I, Grosveld G, Gunn MD, Jackson DG, Oliver G. An essential role for Prox1 in the induction of the lymphatic endothelial cell phenotype. *EMBO J.* 2002;21:1505-1513.
28. Wilting J, Papoutsis M, Christ B, Nicolaides KH, von Kaisenberg CS, Borges J, Stark GB, Alitalo K, Tomarev SI, Niemeyer C, Rossler J. The transcription factor Prox1 is a marker for lymphatic endothelial cells in normal and diseased human tissues. *FASEB J.* 2002;16:1271-1273.
29. Miyabara S, Sugihara H, Maehara N, Shouno H, Tasaki H, Yoshida K, Saito N, Kayama F, Ibara S, Suzumori K. Significance of cardiovascular malformations in cystic hygroma: a new interpretation of the pathogenesis. *Am J Med Genet.* 1989;34:489-501.

30. Gruden G, Thomas S, Burt D, Lane S, Chusney G, Sacks S, Viberti G. Mechanical stretch induces vascular permeability factor in human mesangial cells: mechanisms of signal transduction. *Proc Natl Acad Sci U S A*. 1997;94:12112-12116.
31. Lantieri LA, Martin-Garcia N, Wechsler J, Mitrofanoff M, Raulo Y, Baruch JP. Vascular endothelial growth factor expression in expanded tissue: a possible mechanism of angiogenesis in tissue expansion. *Plast Reconstr Surg*. 1998;101:392-398.
32. Kalousek DK, Seller MJ. Differential diagnosis of posterior cervical hygroma in preivable fetuses. *Am J Med Genet Suppl*. 1987;3:83-92.
33. Larcher F, Murillas R, Bolontrade M, Conti CJ, Jorcano JL. VEGF/VPF overexpression in skin of transgenic mice induces angiogenesis, vascular hyperpermeability and accelerated tumor development. *Oncogene*. 1998;17:303-311.
34. Flamme I, von RM, Drexler HC, Syed-Ali S, Risau W. Overexpression of vascular endothelial growth factor in the avian embryo induces hypervascularization and increased vascular permeability without alterations of embryonic pattern formation. *Dev Biol*. 1995;171:399-414.
35. Brandenburg H, Bartelings MM, Wisse LJ, Steegers EA, Gittenberger-De Groot AC. Increased expression of vascular endothelial growth factor in cardiac structures of fetus with hydrops as compared to nonhydropic controls. *Fetal Diagn Ther*. 2006;21:84-91.
36. Nagy JA, Vasile E, Feng D, Sundberg C, Brown LF, Detmar MJ, Lawitts JA, Benjamin L, Tan X, Manseau EJ, Dvorak AM, Dvorak HF. Vascular permeability factor/vascular endothelial growth factor induces lymphangiogenesis as well as angiogenesis. *J Exp Med*. 2002;196:1497-1506.

Chapter 8

Nuchal Edema and Venous-lymphatic Phenotype Disturbance in Human Fetuses and Mouse Embryos with Aneuploidy

Mireille N. Bekker^{1,2}, Nynke M.S. van den Akker², Margot M. Bartelings², Jenny B. Arkesteijn², Sigrid G.L. Fischer², Japke A.E. Polman², Monique C. Haak¹, Sandra Webb³, Robert E. Poelmann², John M.G. van Vugt¹, Adriana C. Gittenberger-de Groot²

¹Department of Obstetrics and Gynecology, VU University Medical Center, Amsterdam, the Netherlands; ²Department of Anatomy and Embryology, Leiden University Medical Center, Leiden, the Netherlands; ³Division of Basic Medical Sciences, Anatomy and Developmental Biology, St. George Hospital Medical School, London, United Kingdom.

Modified after Journal of the Society for Gynecologic Investigation, 2006;13:209-216.

Nuchal Edema and Venous-lymphatic Phenotype Disturbance in Human Fetuses and Mouse Embryos with Aneuploidy

Abstract

Nuchal translucency is a clinical indicator for aneuploidy, cardiovascular anomalies and several genetic syndromes. Its etiology, however, is unknown. In the nuchal area the endothelium of the jugular lymphatic sacs develops by budding from the blood vascular endothelium of the cardinal veins. Abnormal distension of these jugular sacs is associated with nuchal edema (NE), the morphological equivalent of nuchal translucency. We hypothesize that a disturbed lymphatic endothelial differentiation and sac formation causes nuchal edema. We investigated endothelial differentiation of the jugular lymphatic system in human fetuses and mouse embryos with NE. Aneuploid human fetuses (trisomy 21; trisomy 18) were compared with euploid controls (gestational age 12 to 18 weeks). Trisomy 16 mouse embryos were compared with wild-type controls (embryonic day 10 to 18). Trisomy 16 mice are considered an animal model for human trisomy 21. Endothelial differentiation was investigated by immunohistochemistry using lymphatic markers Prox-1, Podoplanin, lymphatic vessel endothelial hyaluronan receptor-1 and blood vessel markers Neuropilin-1 (NP-1) and ligand vascular endothelial growth factor-A (VEGF). α -Smooth muscle actin was included as a smooth muscle cell marker. We report a disturbed venous-lymphatic phenotype in aneuploid human fetuses and mouse embryos concomitant with enlarged jugular sacs and NE. Our results show absent or diminished expression of the lymphatic markers Prox-1 and Podoplanin in the enlarged jugular sac, while LYVE-1 expression was normal. Additionally, the enlarged jugular lymphatic sacs showed blood vessel characteristics, including increased NP-1 and VEGF expression. The lumen contained blood cells and smooth muscle cells surrounded the endothelium. A loss of lymphatic identity seems to be the underlying cause for NE. Also, abnormal endothelial differentiation provides a link to the cardiovascular anomalies associated with NE.

Introduction

The lymphatic endothelial cells (LEC) in the neck bud from the anterior cardinal veins, forming the jugular lymphatic sacs (JLSs). The bilateral peripheral lymphatic system then develops by sprouting from the JLS into the surrounding tissues^{1,2}. The process of budding and differentiating of a subpopulation of cardinal vein-derived primitive blood vascular endothelial cells (BEC) into LEC is controlled by the homeobox transcription factor Prox-1². Prox-1 promotes the expression of LEC-specific genes, including Podoplanin, vascular endothelial growth factor receptor receptor-3 (VEGFR-3) and suppresses the expression of BEC-specific genes, such as Neuropilin-1 (NP-1) and VEGFR-2³.

Abnormal persistence and enlargement of the JLS coincides with nuchal edema (NE), and has been described in both human fetuses and trisomy 16 mouse embryos⁴⁻⁶. NE in human fetuses is associated with aneuploidy, such as trisomy 13, 18 and 21, Turner syndrome, several structural, mainly isolated cardiovascular, defects, and various genetic syndromes⁶. The trisomy 16 mouse is considered an animal model for human trisomy 21 as the mouse chromosome 16 contains the syntenic region for the human chromosome band 21q22⁷. In these mice with NE, the reorganization of the JLS into lymph nodes is diminished and/or delayed⁵. Although NE, clinically referred to as nuchal translucency, assessment by ultrasound in the first-trimester of pregnancy is a common used screening method, the pathogenic mechanisms underlying this phenomenon are unknown.

We hypothesize that a disturbed lymphatic endothelial differentiation and sac formation causes NE. Impaired signaling of Prox-1, which is considered a master control transcription factor in LEC differentiation, and subsequent altered expression levels of its target genes could be part of this process.

Podoplanin is normally involved in lymphatic cell adhesion, migration and tube formation⁸. The vascular endothelial growth factor (VEGF)-family, including VEGF-A (or VEGF), placental growth factor, VEGF-B, VEGF-C and VEGF-D, comprises of key modulators of angiogenesis and lymphangiogenesis. VEGF-C and VEGF-D have been shown to induce lymphangiogenesis through their receptor VEGFR-3^{9,10}. VEGF is primarily involved in angiogenesis through its receptors VEGFR-1 and VEGFR-2 and coreceptors NP-1 and NP-2¹¹. Overexpression of VEGF leads to hypervascularization, increased vascular permeability and edema^{12,13}. VEGF has been shown to induce lymphangiogenesis as well¹⁴. NP-1 and NP-2 have been described as being specifically expressed in arteries and veins, respectively¹⁵.

Here we have evaluated these LEC and BEC specific markers in trisomy 16 mice and human aneuploid fetuses (trisomy 21 and 18) with NE and enlarged JLS. Lymphatic vessel endothelial hyaluronan receptor-1 (LYVE-1) was included as additional LEC marker and α -smooth muscle actin (α SMA) as marker for smooth muscle cell differentiation.

Materials and Methods

Mouse embryos

Wild-type (WT) mouse embryos from embryonic day 10 (E10) to E18 were compared with trisomy 16 mouse embryos (n=22) of a similar age range. Generation and genotyping have been described previously⁷. The commission for animal experiments of St. George Hospital Medical School approved the study. The embryos were fixed in 4% paraformaldehyde at 4°C overnight. After dehydrating the embryos through an ethanol series to xylene, the whole mouse embryos were embedded in paraffin and sectioned into transverse sections of 5 µm. The neck region of the mouse embryos was analyzed from the cranial to the caudal end of the JLS.

Human fetuses

The medical ethical committee of the VU University Medical Center approved the study. All patients received information and gave written informed consent. Fetal tissue was obtained after termination of pregnancy or spontaneous miscarriage. Termination of the pregnancy was performed at request of the parents for medical or psychosocial reasons, either by an operative or a misoprostol procedure. The fetal neck was removed from below eye level to diaphragm level.

The fetal tissue was fixed in buffered 4% paraformaldehyde, embedded in paraffin and transversely sectioned into serial sections of 8 µm. The neck region of the human fetuses was analyzed from the cranial to the caudal end of the JLS.

Characteristics of the human fetuses included in the study are listed in Table 1. All fetuses were prenatally examined by ultrasound and diagnosed with normal or increased nuchal translucency, referred to in this study as NE. The fetuses were karyotyped by chorion villus sampling or amniocentesis.

Antibodies and staining procedures

We used antibodies against LYVE-1¹⁶, Prox-1 (Relia-Tech), Podoplanin⁸, NP-1 (Santa Cruz Biotechnology), NP-2 (Santa Cruz Biotechnology), VEGF (Santa Cruz Biotechnology), VEGF-C (Santa Cruz Biotechnology) and α SMA (Sigma-Aldrich).

The sections were incubated for 20 minutes in a solution of 0.3% H₂O₂ to inhibit endogenous peroxidase activity. In case of Prox-1, Podoplanin and NP-2 stainings, the sections were additionally incubated for 12 minutes in 0.01 M citric acid buffer of pH 6.0 in the microwave at a temperature of 97 °C for recruitments of epitopes. After incubation, all sections were rinsed consecutively in PBS, PBS and PBS/0.05% Tween. Subsequently, they were incubated overnight with the first specific antibody. Next day rinsing was performed consecutively in PBS, PBS and PBS/0.05% Tween, followed by incubation of the sections during 40 minutes with the second antibody. This second antibody differed per staining procedure. For Prox-1, LYVE-1, NP-2 and VEGF this was a biotinylated goat-anti-rabbit antibody, for Podoplanin a biotinylated horse-anti-

mouse antibody, for NP-1 a biotinylated rabbit-anti-goat antibody and for α SMA a horseradish a peroxidase-conjugated rabbit-anti-mouse antibody. In case of LYVE-1 a third incubating step was performed with rabbit peroxidase-anti-peroxidase complex (R/PAP), with which the slides were incubated for 90 minutes. Thereafter, rinsing in PBS, PBS and PBS/0.05% Tween, took place. All sections, except those following the staining procedure for LYVE-1 and α SMA, were incubated with ABC-reagens (Vector) for 40 minutes. All sections were rinsed consecutively with PBS, PBS and tris/maleate pH 7.6, followed by a 10 minutes incubation with 3-3'diaminobenzidin tetrahydrochlorid (DAB) for visualisation. Finally the sections were counterstained with Mayer's hematoxylin for 10 seconds, rinsed for 10 minutes in tap water and dehydrated to xylene. The sections were mounted with Entellan (Merck).

Table 1: Overview of the human fetuses included in the study

Human fetus	Gestational age (wk)	N	Karyotype
Control	12	1	Normal
	14	2	Normal
Nuchal edema	13	1	Trisomy 21
	14	2	Trisomy 21
	15	1	Trisomy 21
		1	Trisomy 18
	16	1	Trisomy 21
		1	Trisomy 18
	17	1	Trisomy 21
	18	1	Trisomy 21

Results

Mouse embryos

Nuchal morphology.

Trisomy 16 mouse embryos with NE were compared with WT littermates. At E11, the first indication of the formation of the JLS was the formation of small vessels adjacent to the cardinal vein. The part of the endothelium of the cardinal vein proximal to these lymphatic sprouts is the budding site of the vessel wall². From E12 onwards the JLS was located laterally and caudally from the jugular vein (formerly the cardinal vein) and carotid artery in all embryos. Lymph node formation was first observed in WT embryos of E15. Thereafter, the volume of the sacs decreased. At E18 the sacs had almost disappeared and were reorganized into lymph nodes in the WT embryos.

As described previously⁵, the JLSs of the NE embryos were enlarged when compared with WT (Figure 1a,g), and remained present until E18. The JLS contained blood cells in 6/18 embryos examined at stages E12 through E18. The start of lymph node formation was first seen at E15 like in WT embryos, but the amount of recognizable lymph node tissue in the JLS was diminished in the NE embryos.

Blood vascular endothelium.

The BEC of WT and NE embryos showed similar staining patterns with all our markers. The BEC of the arteries and veins were negative for the lymphatic marker VEGF-C in all embryos. At E11 to 12 the cardinal and jugular veins showed endothelial positivity for LYVE-1, Prox-1 and Podoplanin at the site of budding of the LEC. From E14.5 on the jugular vein was negative for LYVE-1, Prox-1 and Podoplanin. Other veins and arteries were also negative for these markers at all embryonic stages. NP-1 staining was negative in veins and positive in the carotid artery and small subcutaneous arteries. Conversely, NP-2 staining was positive in veins and negative in arteries. VEGF was not observed in the BEC of the embryos. The smooth muscle cells of the carotid artery showed some VEGF positivity. α SMA was positive in smooth muscle cells surrounding the endothelium of arteries (four cell layers) and veins (one cell layer).

Lymphatic vascular endothelium.

From E11 onwards, the LECs of WT embryos stained clearly positive for Prox-1 (Figure 1b), Podoplanin (Figure 1c) and LYVE-1 (data not shown), whereas the endothelium showed no or only slight positivity for NP-1 (Figure 1d), VEGF (Figure 1e), VEGF-C and NP-2 (data not shown). No α SMA was observed in the region surrounding the JLS (Figure 1f).

The LECs of the NE mice showed markedly diminished Prox-1 (Figure 1h) and diminished or even absent Podoplanin protein expression (E11 through 18) (Figure 1i). LYVE-1 expression, however, was similar to that in WT embryos (data not shown).

Furthermore, a strong and overlapping expression of NP-1 and VEGF (Figure 1j,k) was observed in the LEC of the JLS, in contrast to the WT embryos (E12 through 18). Unlike WT embryos, smooth muscle cells, positive for α SMA, were observed in the subendothelial mesenchyme of the JLS of NE embryos (E13-E18) (Figure 1l). No difference in LYVE-1, VEGF-C and NP-2 staining was observed between NE and WT mice (data not shown).

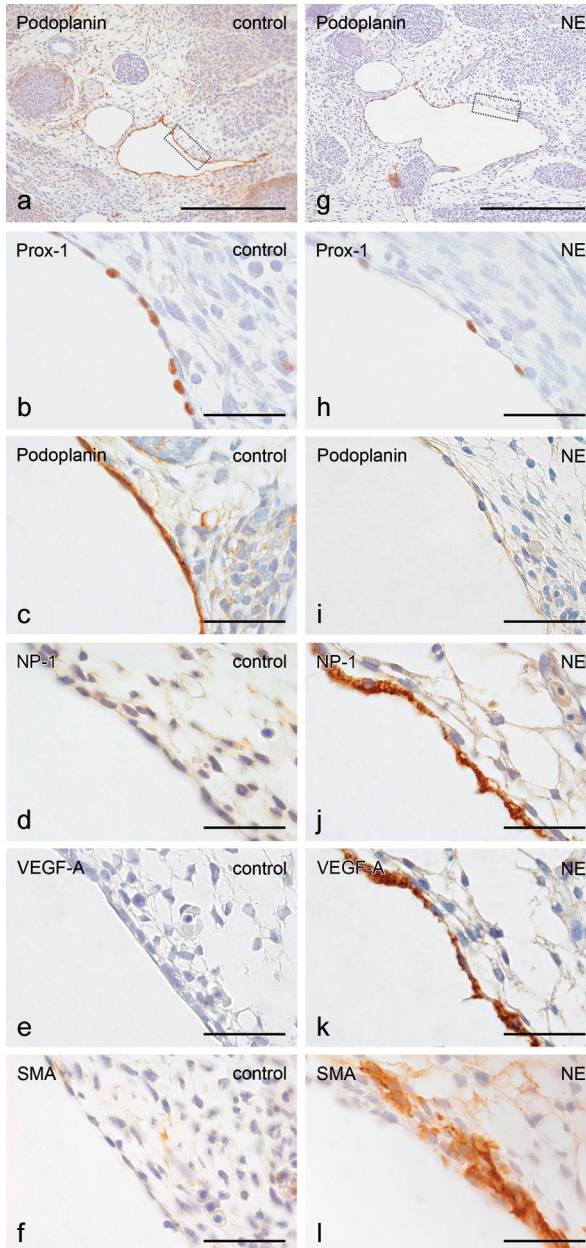


Figure 1. Immunohistochemical analysis of jugular lymphatic sacs (JLS), positioned next to the jugular vein (V). (a) Transverse section of the neck of a wild-type mouse embryo of E13 with normal nuchal skin (control) and Podoplanin staining in the JLS. (b-f) Magnification of consecutive sections of the boxed area in (a) showing the staining results of the lymphatic endothelium with different antibodies: positive Prox-1 (b) and Podoplanin (c) staining; negative NP-1 (d), VEGF (e) and α SMA (SMA; f) staining. (g) Transverse section of the neck of a trisomy 16 mouse embryo of E13 with nuchal edema (NE) and a diminished Podoplanin staining in the enlarged JLS. (h-l) Magnification of consecutive sections of the boxed area in (g) showing the staining results of the lymphatic endothelium with different antibodies: diminished Prox-1 (h) and Podoplanin (i) staining; increased staining of NP-1 (j) and VEGF (k); SMA positive cells are present in the subendothelial mesenchyme of the JLS (l). Scale bars: (a,g) 250 μ m; (b-f,h-l) 50 μ m.

Human fetuses

Nuchal morphology.

Fetuses with NE (n=9) were compared with controls (n=3) (Table 1). Fetuses with NE included fetuses with trisomy 21 (n=7) or trisomy 18 (n=2). All fetuses with NE showed enlarged JLSs, in contrast to controls. The size of the JLS differed but was maximal at 13 to 15 weeks gestational age (GA). Both normal (GA 12, 14 weeks) and NE fetuses (GA 13 to 18 weeks) showed lymph node tissue in the JLS indicating reorganization of the JLS into lymph nodes. In the control fetuses of GA 14 weeks the reorganization was almost completed (Figure 2a, 3a). In contrast, there was still a JLS present in the fetuses with NE at GA 14 to 18 weeks (Figure 2b, 3b). Blood cells were demonstrated in the JLS of 3/9 NE fetuses (Figure 2b, 3g).

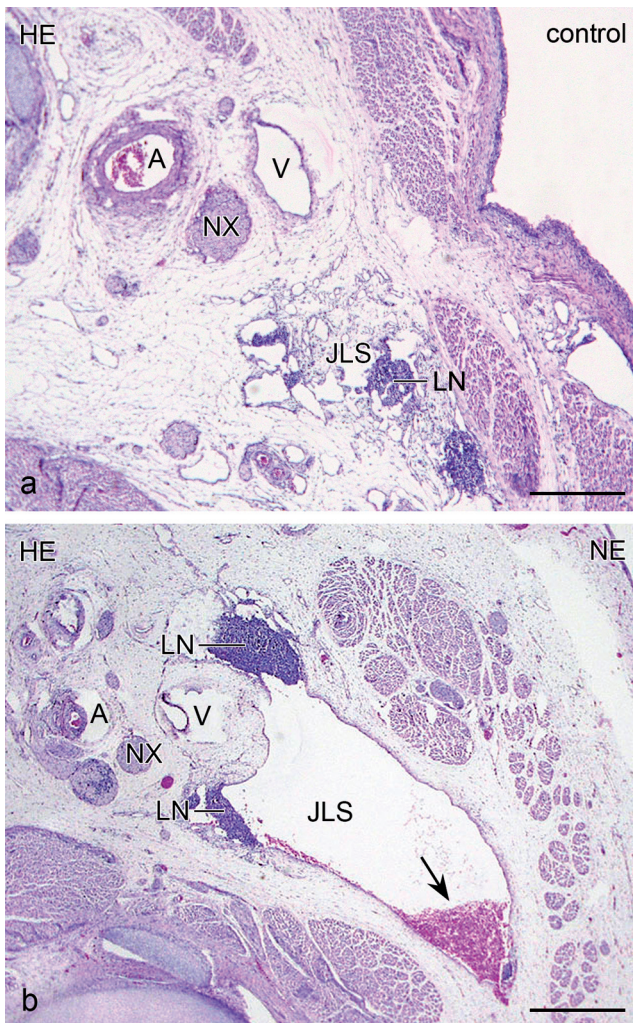


Figure 2. Transverse sections of the neck of a human fetus with normal nuchal skin (control) and a trisomy 21 human fetus with nuchal edema (NE) at 14 weeks of gestation, stained with hematoxylin and eosin (HE). (a) The reorganization of the jugular lymphatic sac (JLS) into lymph node (LN) tissue is almost completed in the control fetus. Next to the lymph node tissue some remnants of the JLS are visible. (b) The JLS of the NE fetus is still present and contains blood (arrow). Some lymph node tissue is present in the corners of the JLS. In both control (a) and NE fetus (b) the JLS is located close to the jugular vein (V), carotid artery (A) and vagal nerve (NX). Scale bars: (a-b) 250 μ m.

Blood vascular endothelium.

The BEC of veins and arteries were negative for VEGF-C, LYVE-1 and Podoplanin both in controls and in fetuses with NE. NP-1 was present in arteries and not present in veins. Conversely, NP-2 was present in veins and not present in arteries. VEGF-staining was negative in arteries and veins in all fetuses. α SMA was positive in smooth muscle cells surrounding the endothelium of arteries and veins, as in the mouse embryos. There was no difference in the staining intensity between control and NE fetuses.

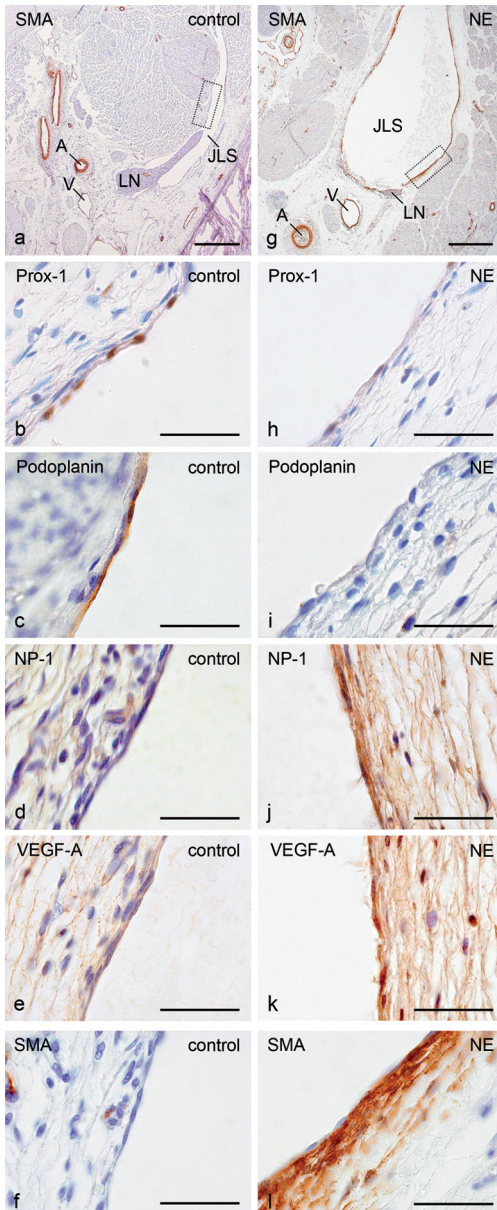


Figure 3. Immunohistochemical analysis of jugular lymphatic sacs (JLS). (a) Transverse section of the neck of a human fetus at GA 14 weeks with normal nuchal skin (control) and JLS. The JLS is filled with lymph node (LN) tissue. α SMA (SMA) positive smooth muscle cells are present in the wall of the carotid artery (A) and jugular vein (V). (b-f) Magnification of consecutive sections of the boxed area in (a) showing the staining results of the lymphatic endothelium with different antibodies: positive Prox-1 (b) and Podoplanin (c) staining; negative NP-1 (d), VEGF (e) and SMA (f) staining. (g) Transverse section of the neck of a human trisomy 21 fetus at GA 14 weeks with nuchal edema (NE). Smooth muscle cells, positive for SMA, are in the wall of carotid artery and jugular vein and in the subendothelial mesenchyme of the JLS. The JLS is enlarged and contains blood. A small amount of lymph node tissue is present in the JLS. (h-l) Magnification of consecutive sections of the boxed area in (g) showing the staining results of the lymphatic endothelium with different antibodies: diminished Prox-1 (h) and Podoplanin (i) staining; increased staining of NP-1 (j) and VEGF (k); SMA positive cells are present in the subendothelial mesenchyme of the JLS (l). Scale bars: (a,g) 500 μ m; (b-f,h-l) 50 μ m.

Lymphatic vascular endothelium.

The LECs of the JLS were clearly positive for LYVE-1, Prox-1 (Figure 3b) and Podoplanin (Figure 3c), whereas the endothelium was negative or slightly positive for NP-1 (Figure 3d), VEGF (Figure 3e), VEGF-C and NP-2 (data not shown). No α SMA positive cells were observed surrounding the LECs of the JLS (Figure 3a,f).

In contrast to the LECs of control fetuses, Prox-1 was diminished (n=9) (Figure 3h) and Podoplanin protein expression was absent (n=7) (Figure 3i) in the largest JLSs or diminished (n=2) in the somewhat smaller JLS of NE fetuses, while LYVE-1 expression was not affected (data not shown). The NP-1 and VEGF protein expression was increased compared with controls, at overlapping sites of the endothelial lining of the JLS (Figure 3j,k). In addition, strong α SMA-positivity was observed in cells surrounding the JLS, similar to NE mouse embryos (Figure 3g,l). No difference in VEGF-C and NP-2 staining between NE and control fetuses was observed (data not shown).

Within the examined fetuses with nuchal edema we did not observe differences in staining between trisomy 21 and trisomy 18.

In conclusion, the same aberrant pattern of staining was seen in the LEC of both human fetuses and mouse embryos with NE, as compared controls (summarized in Table 2). The staining profile of BEC, in addition, was the same in human fetuses and mouse embryos, both with and without NE.

Table 2 : Staining results in the lymphatic endothelial cells in trisomy 16 mouse embryos and human fetuses with nuchal edema (NE) compared with controls with normal nuchal skin.

	LEC		
	Trisomy 16 mice	Human NE fetuses	
Prox-1	↓	↓	↓, ↑ indicates decreased or increased expression compared with controls, respectively; = indicates similar expression as controls, + indicates smooth muscle cells are present in the subendothelial mesenchyme in contrast to controls.
Podoplanin	↓	↓	
LYVE-1	=	=	
VEGF	↑	↑	
VEGF-C	=	=	
NP-1	↑	↑	
NP-2	=	=	
α SMA	+	+	

Discussion

This study describes the phenotype of disturbed lymphatic vasculature in mouse embryos and human fetuses with NE and enlarged JLSs. We demonstrated absent or strongly diminished Prox-1 and Podoplanin-expression in the LECs of the JLSs, while the lymphatic marker LYVE-1 was still present. The abnormally large JLSs therefore exhibited a loss of lymphatic identity and, in contrast to a normal JLS, showed blood vascular characteristics, such as endothelial VEGF/NP-1-expression and a gain of α SMA-positive cells in the subendothelial mesenchyme. The blood vessel-identity was also confirmed by the presence of red blood cells, which are under normal circumstances absent in lymphatic vessels (Figure 4).

Our findings of Prox-1-expression in WT mice confirms previous studies, which have identified *Prox-1* as master control gene for induction of the lymphatic development^{2;3}. In the severely edematous *Prox-1*^{-/-} mouse embryos lymphatic sprout formation from the anterior cardinal vein is arrested at E11. However, the mouse embryos and interestingly also the human fetuses with NE in our study differ from the *Prox-1*^{-/-} embryos in that JLS-formation is present, although with abnormal LEC-differentiation and with severe distension of the JLS. It can, therefore, be concluded that either absence of JLS-formation or distension of JLS, as a consequence of either absent or diminished Prox-1-expression, can lead to NE.

It has been reported that Prox-1 upregulates the expression of the lymphatic-endothelial cell-specific markers Podoplanin-1, VEGFR-3 and desmoplakin I/II³. Conversely, it suppresses, the expression of the blood endothelial cell-specific markers, NP-1 and VEGFR-2³. Our findings of a decreased expression of Podoplanin with a concomitant increase in NP-1-expression in the LEC in the NE model are, therefore, most likely caused by diminished Prox-1-activity.

Podoplanin promotes LEC-adhesion, migration and tube formation, which is demonstrated by the fact that RNA-mediated inhibition of Podoplanin-expression decreased LEC adhesion⁸. *Podoplanin*^{-/-} mice die at birth due to respiratory failure and have defects in lymphatic, but not blood vessel, patterning, similar to our NE model⁸. These defects are associated with diminished lymphatic transport, congenital lymph edema and dilation of lymphatic vessels. Interestingly, these mice have subcutaneous neck edema, known as NE. Therefore, a diminished Podoplanin-expression presumably contributes to the formation of edema in our NE model.

Co-expression of NP-1 and VEGF was anticipated, as NP-1 is a coreceptor for VEGF and enhances binding of VEGF to VEGFR-2, thereby increasing VEGFR-2 activity^{17;19}. Also, positive feedback mechanisms between VEGF and NP-1 and VEGFR-2 exist^{20;21}. Overexpression of VEGF, also known as vascular permeability factor, leads to hypervascularization, increased vascular permeability and edema^{12;13}. Therefore, we hypothesize that the NE in our model is partially caused by an increased permeability and decreased cell adhesion due to VEGF-overexpression in the LEC, together with a diminished Podoplanin-expression. In addition, VEGF is known for its key role in angiogenesis and also stimulates lymphangiogenesis^{12;14}.

Venous-Lymphatic endothelial differentiation

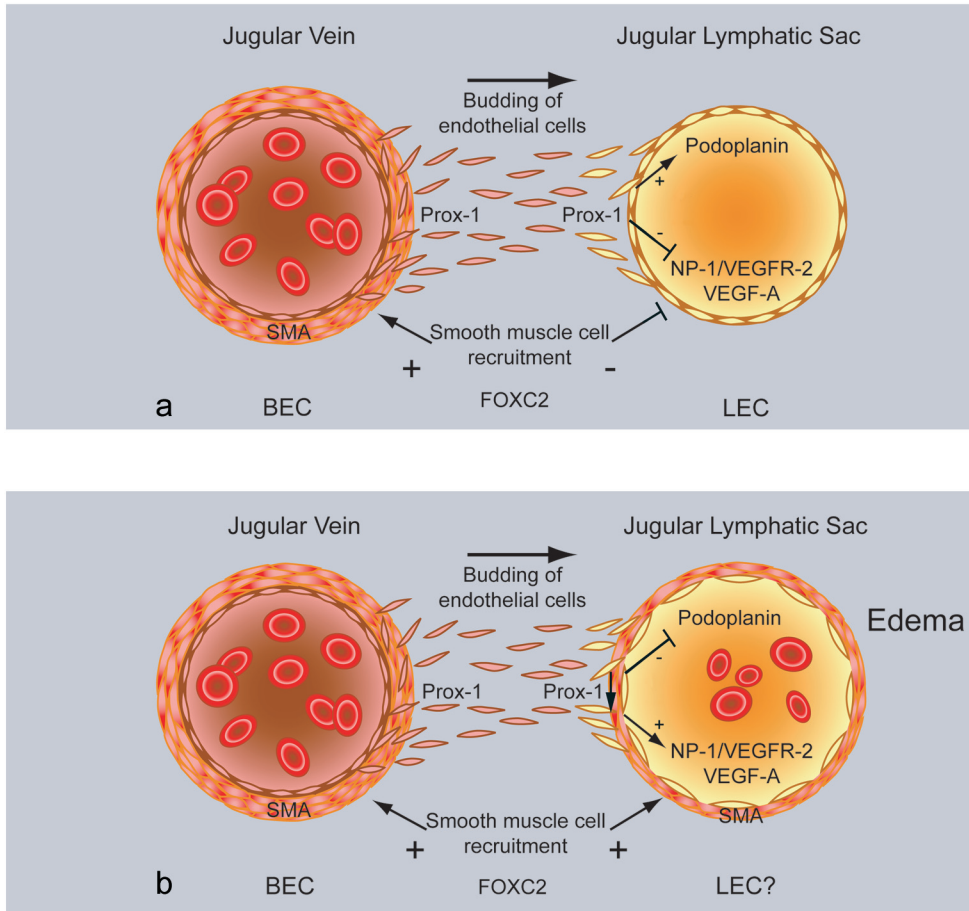


Figure 4. Schematic overview of venous-lymphatic differentiation. (a) Normal venous-lymphatic differentiation from the jugular vein with normal Prox-1 and Podoplanin-expression and suppression of NP-1, VEGF and expected FOXC2 expression in the lymphatic endothelium of the JLS (b) Disrupted venous-lymphatic differentiation from the jugular vein with diminished Prox-1, Podoplanin-expression and concomitant increased NP-1, VEGF in the endothelium of the enlarged JLS. The vascular permeability of the abnormal endothelium is increased which causes edema. The JLS is surrounded by smooth muscle cells, possibly due to impaired FOXC2 expression. The presence of red blood cells in the lumen further indicates a loss of lymphatic identity as this is specific for arteries and veins.

It has been described that overexpression of VEGF induces the formation of enlarged lymphatics²². Notably, the abnormal vessels in that study also contained red blood cells, like the abnormal JLS in our study, which is an abnormal finding in lymphatic vessels. As no difference in VEGF-C staining between mouse embryos and fetuses with NE compared with controls was observed, we assume that VEGF-C does not play a prominent role in our models.

Another important finding was the presence of smooth muscle cells around the LEC of the enlarged JLS (Figure 4), which are normally only present around BEC of arteries and veins and the large collecting lymph vessels²³. The presence of smooth muscle cells, combined with diminished expression of lymphatic markers Prox-1 and Podoplanin, indicate a disturbance of the venous-lymphatic differentiation and suggest a loss of lymphatic identity. This is further supported by the presence of blood cells in the JLS in several cases and the increased expression of the artery-specific NP-1. The positive staining of the lymphatic-specific marker LYVE-1 in the LEC of all NE embryos does not contradict a disrupted venous-lymphatic differentiation, since LYVE-1 is known to stain positive in the venous endothelium at the budding site of the cardinal vein²⁴, as was observed in this study.

Abnormal smooth muscle cells surrounding enlarged lymph vessels have recently been reported in *Foxc2*^{-/-} mice as well²³. Mutation of the *FOXC2*-gene in humans is associated with defective lymph valves and familial lymph edema. Under normal circumstances, FOXC2 blocks smooth muscle cell recruitment in lymphatic vessels, most likely by inhibition of platelet-derived growth factor (PDGF)-B and endoglin, which are essential for smooth muscle cell recruitment in blood vessels²³. Since we have not studied FOXC2-expression in our models we do not know whether abnormalities herein are involved in the abnormal smooth muscle cell recruitment as observed. Further investigation is necessary to solve this question.

Our study demonstrates an abnormal venous-lymphatic phenotype in mouse embryos as well as human fetuses with NE. The question arises what sets the sequence of events into motion. First of all, NE in the human fetus is known to be associated with a broad spectrum of genetic and structural anomalies with a variable extent of severity²⁵. Therefore, we assume that there is not one single cause for NE but that several genetic origins and epigenetic influences, linked to a common developmental process, may lead to NE.

Our study suggests that disturbances in the process of (endothelial) venous-lymphatic differentiation lie at the base of NE-development, as it was observed in all the examined NE-fetuses, regardless of karyotype. The various mechanisms leading to this common disturbed lymphatic-vascular phenotype are most likely linked to either Prox-1-inhibition, VEGF/NP-1-overexpression and, possibly, FOXC2-inhibition.

We postulate that one possible cause for the described phenotype is a disturbed signaling of neural crest cells. This is suggested by a former study in trisomy 16 mice, showing an upregulation of neural cell adhesion molecule-1 (NCAM-1) in neuronal and cardiovascular structures²⁶. NCAM is a cell adhesion molecule, which influences neural crest cell migration, neuronal differentiation and axon guidance^{27,28}. Interestingly, the NCAM-1 upregulation is present in the vagal nerve, which is located close to the JLS, jugular vein, carotid artery, as well as the aortic arch. Impaired signaling from the neural crest cell derived vagal nerve could also influence the development of the surrounding lymphatic structures. An impaired neural crest signaling is further indicated by the altered expression of NP-1 and Prox-1 in the LEC. NP-1 is, besides in

endothelial development, involved in neuronal development and migration of neural crest cells as well^{29;30}. Prox-1 is upregulated by mammalian achaete-scute homolog-1 (MASH-1), which induces neural crest cell differentiation and *Mash-1*^{-/-} mice show loss of Prox-1-expression³¹. Abnormal neural crest-development towards smooth muscle cells and vagal nerve fibers surrounding the aortic arch could also explain outflow tract anomalies often seen in human fetuses with NE^{32;33}. Abnormal development of neural crest cells is thought to play a role in the development of aortic arch anomalies (type B interruption) in trisomy 16 and several other mouse models^{26;34;35}. Perturbation of neural crest cell-development has also been proposed in the pathomorphogenesis of several cardiovascular anomalies associated with human trisomy 21³⁶.

Finally, NE-assessment through NT-measurements in the human fetus is a worldwide used screening method in the first trimester of pregnancy, even though its pathophysiology is not fully understood. This is the first report on a disturbed lymphatic-vascular phenotype associated with NE and enlarged JLS. Further research is necessary to investigate the lymphatic phenotype and underlying mechanisms in other NE fetuses with different chromosomal and/or structural anomalies.

Acknowledgements

We thank Jan Lens and Bas Blankevoort for the graphics and layout and Bert Wisse for his technical assistance.

References

1. Sabin FR. The lymphatic system in human embryos, with a consideration of the morphology of the system as a whole. *Am J Anat.* 1909;9:43-91.
2. Wigle JT, Oliver G. Prox1 function is required for the development of the murine lymphatic system. *Cell.* 1999;98:769-778.
3. Petrova TV, Makinen T, Makela TP, Saarela J, Virtanen I, Ferrell RE, Finegold DN, Kerjaschki D, Yla-Herttua S, Alitalo K. Lymphatic endothelial reprogramming of vascular endothelial cells by the Prox-1 homeobox transcription factor. *EMBO J.* 2002;21:4593-4599.
4. Haak MC, Bartelings MM, Jackson DG, Webb S, Van Vugt JM, Gittenberger-De Groot AC. Increased nuchal translucency is associated with jugular lymphatic distension. *Hum Reprod.* 2002;17:1086-1092.
5. Gittenberger-De Groot AC, Van Den Akker NM, Bartelings MM, Webb S, Van Vugt JM, Haak MC. Abnormal lymphatic development in trisomy 16 mouse embryos precedes nuchal edema. *Dev Dyn.* 2004;230:378-384.
6. Bekker MN, Haak MC, Rekoert-Hollander M, Twisk J, Van Vugt JM. Increased nuchal translucency and distended jugular lymphatic sacs on first-trimester ultrasound. *Ultrasound Obstet Gynecol.* 2005;25:239-245.
7. Webb S, Brown NA, Anderson RH. Cardiac morphology at late fetal stages in the mouse with trisomy 16: consequences for different formation of the atrioventricular junction when compared with humans with trisomy 21. *Cardiovasc Res.* 1997;34:515-524.
8. Schacht V, Ramirez MI, Hong YK, Hirakawa S, Feng D, Harvey N, Williams M, Dvorak AM, Dvorak HF, Oliver G, Detmar M. T1alpha/Podoplanin deficiency disrupts normal lymphatic vasculature formation and causes lymphedema. *EMBO J.* 2003;22:3546-3556.
9. Karkkainen MJ, Alitalo K. Lymphatic endothelial regulation, lymphoedema, and lymph node metastasis. *Semin Cell Dev Biol.* 2002;13:9-18.
10. Lymboussaki A, Olofsson B, Eriksson U, Alitalo K. Vascular endothelial growth factor (VEGF) and VEGF-C show overlapping binding sites in embryonic endothelia and distinct sites in differentiated adult endothelia. *Circ Res.* 1999;85:992-999.
11. Yuan L, Moyon D, Pardanaud L, Breant C, Karkkainen MJ, Alitalo K, Eichmann A. Abnormal lymphatic vessel development in neuropilin 2 mutant mice. *Development.* 2002;129:4797-4806.
12. Flamme I, von RM, Drexler HC, Syed-Ali S, Risau W. Overexpression of vascular endothelial growth factor in the avian embryo induces hypervascularization and increased vascular permeability without alterations of embryonic pattern formation. *Dev Biol.* 1995;171:399-414.
13. Larcher F, Murillas R, Bolontrade M, Conti CJ, Jorcano JL. VEGF/VPF overexpression in skin of transgenic mice induces angiogenesis, vascular hyperpermeability and accelerated tumor development. *Oncogene.* 1998;17:303-311.
14. Nagy JA, Vasile E, Feng D, Sundberg C, Brown LF, Detmar MJ, Lawitts JA, Benjamin L, Tan X, Manseau EJ, Dvorak AM, Dvorak HF. Vascular permeability factor/vascular endothelial growth factor induces lymphangiogenesis as well as angiogenesis. *J Exp Med.* 2002;196:1497-1506.
15. Martyn U, Schulte-Merker S. Zebrafish neuropilins are differentially expressed and interact with vascular endothelial growth factor during embryonic vascular development. *Dev Dyn.* 2004;231:33-42.

16. Jackson DG. Biology of the lymphatic marker LYVE-1 and applications in research into lymphatic trafficking and lymphangiogenesis. *APMIS*. 2004;112:526-538.
17. Soker S, Miao HQ, Nomi M, Takashima S, Klagsbrun M. VEGF165 mediates formation of complexes containing VEGFR-2 and neuropilin-1 that enhance VEGF165-receptor binding. *J Cell Biochem*. 2002;85:357-368.
18. Kawasaki T, Kitsukawa T, Bekku Y, Matsuda Y, Sanbo M, Yagi T, Fujisawa H. A requirement for neuropilin-1 in embryonic vessel formation. *Development*. 1999;126:4895-4902.
19. Yamada Y, Takakura N, Yasue H, Ogawa H, Fujisawa H, Suda T. Exogenous clustered neuropilin 1 enhances vasculogenesis and angiogenesis. *Blood*. 2001;97:1671-1678.
20. Bates DO, Harper SJ. Regulation of vascular permeability by vascular endothelial growth factors. *Vascul Pharmacol*. 2002;39:225-237.
21. Hattori M, Fujiyama A, Taylor TD, Watanabe H, Yada T, Park HS, Toyoda A, Ishii K, Totoki Y, Choi DK, Groner Y, Soeda E, Ohki M, Takagi T, Sakaki Y, Taudien S, Blechschmidt K, Polley A, Menzel U, Delabar J, Kumpf K, Lehmann R, Patterson D, Reichwald K, Rump A, Schillhabel M, Schudy A, Zimmermann W, Rosenthal A, Kudoh J, Schibuya K, Kawasaki K, Asakawa S, Shintani A, Sasaki T, Nagamine K, Mitsuyama S, Antonarakis SE, Minoshima S, Shimizu N, Nordsiek G, Hornischer K, Brant P, Scharfe M, Schon O, Desario A, Reichelt J, Kauer G, Blocker H, Ramser J, Beck A, Klages S, Hennig S, Riesselmann L, Dagand E, Haaf T, Wehrmeyer S, Borzym K, Gardiner K, Nizetic D, Francis F, Lehrach H, Reinhardt R, Yaspo ML. The DNA sequence of human chromosome 21. *Nature*. 2000;405:311-319.
22. Nagy JA, Vasile E, Feng D, Sundberg C, Brown LF, Manseau EJ, Dvorak AM, Dvorak HF. VEGF induces angiogenesis, arteriogenesis, lymphangiogenesis, and vascular malformations. *Cold Spring Harb Symp Quant Biol*. 2002;67:227-237.
23. Petrova TV, Karpanen T, Norrmen C, Mellor R, Tamakoshi T, Finegold D, Ferrell R, Kerjaschi D, Mortimer P, Yla-Herttuala S, Miura N, Alitalo K. Defective valves and abnormal mural cell recruitment underlie lymphatic vascular failure in lymphedema distichiasis. *Nat Med*. 2004;10:974-981.
24. Wigle JT, Harvey N, Detmar M, Lagutina I, Grosveld G, Gunn MD, Jackson DG, Oliver G. An essential role for Prox1 in the induction of the lymphatic endothelial cell phenotype. *EMBO J*. 2002;21:1505-1513.
25. Pandya PP, Snijders RJ, Johnson SP, De Lourdes BM, Nicolaidis KH. Screening for fetal trisomies by maternal age and fetal nuchal translucency thickness at 10 to 14 weeks of gestation. *Br J Obstet Gynaecol*. 1995;102:957-962.
26. Bekker MN, Arkesteijn JB, Van Den Akker NM, Hoffman S, Webb S, Van Vugt JM, Gittenberger-De Groot AC. Increased NCAM expression and vascular development in trisomy 16 mouse embryos: relationship with nuchal translucency. *Pediatr Res*. 2005;58:1222-1227.
27. Akitaya T, Bronner-Fraser M. Expression of cell adhesion molecules during initiation and cessation of neural crest cell migration. *Dev Dyn*. 1992;194:12-20.
28. Walsh FS, Doherty P. Neural cell adhesion molecules of the immunoglobulin superfamily: role in axon growth and guidance. *Annu Rev Cell Dev Biol*. 1997;13:425-456.
29. Osborne NJ, Begbie J, Chilton JK, Schmidt H, Eickholt BJ. Semaphorin/neuropilin signaling influences the positioning of migratory neural crest cells within the hindbrain region of the chick. *Dev Dyn*. 2005;232:939-949.

30. Mukoyama YS, Gerber HP, Ferrara N, Gu C, Anderson DJ. Peripheral nerve-derived VEGF promotes arterial differentiation via neuropilin 1-mediated positive feedback. *Development*. 2005;132:941-952.
31. Torii M, Matsuzaki F, Osumi N, Kaibuchi K, Nakamura S, Casarosa S, Guillemot F, Nakafuku M. Transcription factors Mash-1 and Prox-1 delineate early steps in differentiation of neural stem cells in the developing central nervous system. *Development*. 1999;126:443-456.
32. Hyett J, Moscoso G, Papanagioutou G, Perdu M, Nicolaides KH. Abnormalities of the heart and great arteries in chromosomally normal fetuses with increased nuchal translucency thickness at 11-13 weeks of gestation. *Ultrasound Obstet Gynecol*. 1996;7:245-250.
33. Hyett J, Moscoso G, Nicolaides K. Abnormalities of the heart and great arteries in first trimester chromosomally abnormal fetuses. *Am J Med Genet*. 1997;69:207-216.
34. Waller BR, III, McQuinn T, Phelps AL, Markwald RR, Lo CW, Thompson RP, Wessels A. Conotruncal anomalies in the trisomy 16 mouse: an immunohistochemical analysis with emphasis on the involvement of the neural crest. *Anat Rec*. 2000;260:279-293.
35. Bergwerff M, DeRuiter MC, Hall S, Poelmann RE, Gittenberger-De Groot AC. Unique vascular morphology of the fourth aortic arches: possible implications for pathogenesis of type-B aortic arch interruption and anomalous right subclavian artery. *Cardiovasc Res*. 1999;44:185-196.
36. Kirby ML. Neural crest and the morphogenesis of Down syndrome with special emphasis on cardiovascular development. *Prog Clin Biol Res*. 1991;373:215-225.

Chapter 9

General Discussion

General Discussion

Introduction

VEGF, Notch and PDGF in heart development

Cardiac neural crest

The epicardium and cardiomyocyte-development

Endocardial cushion development

The contribution of the second heart field

Clinical implications

VEGF, Notch and PDGF in coronary development

The primitive endothelial network

Endothelial differentiation

Arteriogenesis and patterning

Clinical implications

Signaling pathways in cardiovascular development

VEGF-signaling

Notch-signaling

PDGF-signaling

Nuchal translucency and lymphatic development

Phenotypes, genotypes and karyotypes

Endothelial differentiation and lymphatic performance

Development of lymph nodes

Ultrasound and microscopy

Conclusions

Introduction

In this thesis the influence of VEGF, Notch and PDGF on cardiovascularogenesis has been studied. Using several mouse models in which VEGF or PDGF-signaling was altered, we show that tight spatiotemporal control of these signaling pathways is crucial. First, the effect of alterations in these pathways with regard to cell lineages contributing to heart development is discussed. Second, the role of these three factors on specifically coronary endothelial differentiation and coronary maturation is addressed, focusing on different stages of coronary development. Third, the function of (aberrant) VEGF, Notch and PDGF-signaling on cardiovascular development is recapitalized. Fourth, the impact of normal and anomalous lymphatic endothelial differentiation on normal and increased nuchal translucency (NT) and the link with nuchal edema (NE) is discussed.

VEGF, Notch and PDGF in heart development

The effect of spatiotemporal alterations in the VEGF, Notch and PDGF-signaling pathways on specific developmental processes and stages within cardiogenesis using *Vegf120/120*, *Pdgf-b*^{-/-} and *Pdgfr-β*^{-/-} embryos has been explored in this thesis and will be discussed below. Special emphasis is given to the effect of these alterations on performance of different cell types contributing to heart development.

Cardiac neural crest

Vegf120/120 mouse embryos develop aortic arch and outflow tract (OFT)-anomalies indicative for altered cardiac neural crest cell (cNCC)-performance¹. Unpublished data of our group in this model (Van den Akker and Gittenberger-de Groot, 2007) additionally show abnormalities in the organization of the condensed mesenchyme. This is a compact collection of predominantly cNCCs within the developing aortopulmonary septum²⁻⁴ and essential for septation of the OFT⁵ and myocardialization of the OFT-septum⁶. In *Vegf120/120* embryos, however, these cells are scattered. It is known that, besides cNCC-ablation leading total to disruption of NCC migration and development^{7;8}, also a combination of normal cNCCs-migration into the heart and local malfunctioning can give rise to cardiac anomalies⁹⁻¹¹. cNCC-migration patterns into the heart are unaltered in the *Vegf120/120* our mouse model¹, proposing the latter is the case. As Notch-signaling is important for cNCC-differentiation¹² rather than for cNCC-migration and as Notch-expression and signaling is altered in many cell types of *Vegf120/120* embryos, this implies that impairments in this pathway in mutant cNCCs could provide the basis for their aberrant performance.

The cardiac nerves in both the *Pdgf-b*^{-/-} and *Pdgfr-β*^{-/-} embryos are extremely hypoplastic, suggesting an important role for PDGFR-β-signaling in the neuronal subpopulation of cNCCs. PDGF-B is expressed in the cardiac nerves during avian heart development and PDGFR-β-signaling plays a role in the development and recovery of nerves in other circumstances¹³⁻¹⁵, further implying involvement of this pathway in the development of the cardiac nerves. We suggest that PDGF-B/PDGFR-β-signaling is involved in neurogenesis besides its well-known role in vascular smooth muscle cell (vSMC)-development. It would be valuable if this role could be further explored in future research, e.g. by using conditional nerve-specific *Pdgf-b* and/or *Pdgfr-β*-mutants.

Both *Pdgf-b*^{-/-} and *Pdgfr-β*^{-/-} embryos additionally show hypoplasia of the aortic arch, implying impaired functioning of non-neuronal cNCCs in these models. However, PDGFR-α rather than PDGFR-β-signaling has been implied in non-neuronal neural crest-function¹⁶⁻¹⁸. We propose that PDGFR-α and PDGFR-β-signaling play complementary roles in the development of the cardiac neural crest, in which PDGFR-α is mainly involved in the non-neuronal and PDGFR-β in the neuronal subpopulation.

The epicardium and cardiomyocyte-development

One of the functions of epicardium-derived cells (EPDCs) is regulation of myocardial proliferation¹⁹⁻²², of which spatiotemporal instruction is essential for heart development²⁰. Hypoplasia of the ventricular walls is seen in post-septational *Vegf120/120* mouse embryos could be related to a lower EPDC-number due to impaired epicardial epithelial-to-mesenchymal transformation (EMT). This is supported by roles for VEGF²³ and (subsequent) Notch-signaling²⁴ in the process of EMT. Expression of VEGFR-2 and several members of the Delta/Jagged/Notch-family are noted in the epicardium at the time of epicardial EMT, but no (sub)epicardial changes in expression could be observed in mutant mouse embryos (unpublished observations; Van den Akker and Gittenberger-de Groot, 2007). A normal amount of subepicardial cells in mutant embryos further pleads against alterations in epicardial EMT, although impaired functioning of these cells could still be involved. In vitro culture experiments or tracing of EPDCs using transgenic mouse lines²⁵ should be performed to solve this question.

Small, malformed coronary arteries are prominent in *Vegf120/120* embryos. Subsequent decreased coronary flow could reduce nutrients and oxygen, provoking growth retardation and, eventually, myocardial hypoplasia²⁶. As reduction in proliferating cells is not apparent in these embryos (unpublished observations; Van den Akker and Gittenberger-de Groot, 2007), we assume that this is not a major cause for myocardial hypoplasia in this model. Interestingly, direct endothelial-cardiomyocyte interactions are important in survival and organization of cardiomyocytes²⁷, suggesting a way in which abnormal coronary endothelial development, obvious in this model, could be a cause for the aberrant myocardial development.

A direct effect of altered VEGF or Notch-signaling on cardiomyocytes could cause myocardial abnormalities as well. Cardiomyocytes can express VEGFR-2²⁸ and VEGF is necessary for differentiation of stem cells into cardiomyocytes^{29;30}. Cardiac myofibroblasts (i.e. EPDCs) produce VEGF^{31;32}, suggesting a VEGF-mediated paracrine effect. Spatiotemporal alterations in VEGF-signaling in cardiomyocytes might lead to distorted Notch-signaling in the *Vegf120/120* myocardium. This can contribute to abnormal cardiomyocyte differentiation as observed in *Vegf120/120* mouse embryos (unpublished observations; Van den Akker and Gittenberger-de Groot, 2007)³³.

The *Pdgf-b-/-* and the *Pdgfr-β-/-* mouse embryos show more severe myocardial hypoplasia than the *Vegf120/120* embryos, with the *Pdgf-b-/-* model being the most extreme. It is likely that diminished epicardial EMT in these cases does strongly contribute to the impaired development of the compact myocardium -through diminished physical contribution and through impairing myocardial proliferation- as PDGF-B is able to induce epicardial EMT in vitro³⁴ and we have described that EPDCs express PDGFR-β. Also, the *Pdgf-b-/-* and *Pdgfr-β-/-* embryos show malformations in other structures of the heart in which the role of EPDCs is crucial, such as the atrioventricular valves and the coronary arteries.

An effect of depletion of PDGF-B-signaling in cardiomyocytes should also be considered as a cause for the myocardial hypoplasia observed in these models. We describe that embryonic cardiomyocytes express PDGFR- α while they lack PDGFR- β . PDGF-B can bind to PDGFR- α in vitro³⁵, suggesting that during cardiac development, binding of PDGF-B to PDGFR- α present on cardiomyocytes plays a role in the development of the compact myocardium. This could also explain the more extreme hypoplasia in *Pdgf-b*^{-/-} compared with *Pdgfr- β* ^{-/-} embryos.

Endocardial cushion development

As for VEGF both stimulating^{36;37} and inhibiting^{38;39} roles on endocardial EMT have been described, we propose that spatiotemporal VEGF-distribution and the cell types producing and reacting on VEGF⁴⁰ define the ultimate effect. For example, VEGF expressed by the myocardium surrounding the atrioventricular cushions is described to inhibit endocardial EMT³⁸. In contrast, we see increase of VEGF and subsequent Notch-signaling levels in the endocardial and cushion mesenchymal cells as well as in specifically the subpulmonary myocardium (discussed below) concomitant with hyperplasia of the right ventricular OFT-cushions in the *Vegf120/120* mouse model, implying a stimulating role of VEGF on cushion-EMT in this setting.

Both expression patterns as well as normal initial cushion development in *Pdgf-b*^{-/-} and *Pdgfr- β* ^{-/-} embryos plead against a role for this growth factor in endocardial EMT, in contrast to its probable role in epicardial EMT³⁴. The transition of atrioventricular cushions into the mitral and tricuspid valves, in which the subpopulation of EPDCs seems crucial¹⁹, is, however, obviously impaired (exemplified by thick, short valves). This could be either explained by depletion of the EPDC-population, due to impairment in epicardial EMT, or by reduced chemoattractivity for EPDCs of the atrioventricular cushions. We expect PDGF-B/PDGFR- β -signaling to play a role in both processes, as can be deduced from expression patterns of these proteins during valve development.

The contribution of the second heart field

The OFT-subset of the second heart field (SHF) is called the anterior heart field (AHF). Development of the AHF-derived myocardium depends on several factors, such as interaction with cNCCs⁴¹ and spatiotemporal orchestration of various proteins (reviewed in^{42;43}). Contribution of the AHF is essential for positioning of the large OFT vessels⁴⁴. This is exemplified by experiments in a chicken embryonic model, in which ablation of the anterior part of the SHF resulted in development of Tetralogy of Fallot (TOF) or pulmonary atresia in a large percentage of embryos⁴⁵.

During normal OFT-development, hypoxia-triggered apoptosis of a small subset of (AHF-derived) OFT-cardiomyocytes is involved in OFT-remodeling⁴⁶⁻⁴⁸. Hypoxia induces VEGF-expression, which is assumed to have a protective effect on survival of cardiomyocytes in this process^{47;49}. In our *Vegf120/120* mouse embryos, an abnormally large area of apoptotic cells related to the AHF-derived subpulmonary

myocardium is seen, concomitant with locally increased VEGF and Notch-signaling, suggesting a negative rather than a positive effect of VEGF-signaling on cardiomyocyte-survival⁴⁷. As Notch-signaling through the ligand Jagged2 is able to induce apoptosis during embryonic limb development^{50;51}, increases in expression-levels of these proteins, as seen in this model, could explain the high levels of apoptosis. It is likely that the ultimate effect of VEGF on cardiomyocyte-survival is concentration-dependent with a protective effect at a relative low concentration and an induction of Notch and Jagged2-expression and, secondarily, apoptosis at an extremely high concentration (as seen in mutant embryos). The question remains what triggers the initial increase in VEGF-expression. Alterations in initial VEGF-signaling levels due to lack of coreceptor-binding isoforms could lead to alterations in (Notch-mediated) feedback mechanisms and thus to increase in VEGF-levels⁵².

Increased subpulmonary myocardial apoptosis combined with hyperplasia of the right ventricular OFT-cushions (see above), could explain the large percentage (29%) of embryos in post-septational stages that shows TOF. Impaired (instructive) contribution of cNCCs to the developing AHF⁴¹, due to alterations in VEGF-signaling affecting cNCC-performance, could contribute to the development of TOF as well.

With regard to PDGF, both the *Pdgf-b*^{-/-} and *Pdgfr-β*^{-/-} mouse models show low frequency of malformations pointing towards altered AHF-development. PDGF-B/PDGFR-β-signaling is furthermore unlikely to play a substantial role in cardiomyocyte and non-neuronal cNCC-development (see above) and is presumably dispensable in the development of the AHF-derived subset of myocardium. PDGF-A/PDGFR-α-signaling, on the other hand, is most likely involved in AHF-development as *Pdgfr-α* mutant mice show OFT-abnormalities⁵³ and the role of PDGF-A/PDGFR-α in cNCC-development is clear¹⁸.

The development of the posterior heart field (PHF) can be divided in the direct contribution of the PHF through the inflow tract (IFT) and through the pro-epicardial organ (PEO) and subsequent EPDCs. PDGF-B/PDGFR-β-signaling most likely plays a role in the PEO/EPDC-dependent contribution, as *Pdgf-b*^{-/-} and *Pdgfr-β*^{-/-} mouse embryos develop abnormalities that can be attributed to impaired contribution of this subset of the PHF. The direct contribution of the PHF to heart development is likely mainly dependent on PDGF-A/PDGFR-α-signaling, as *Pdgfr-α* mutant mice develop IFT-abnormalities and as PDGFR-α-expression is obvious in this subset of the SHF⁵³.

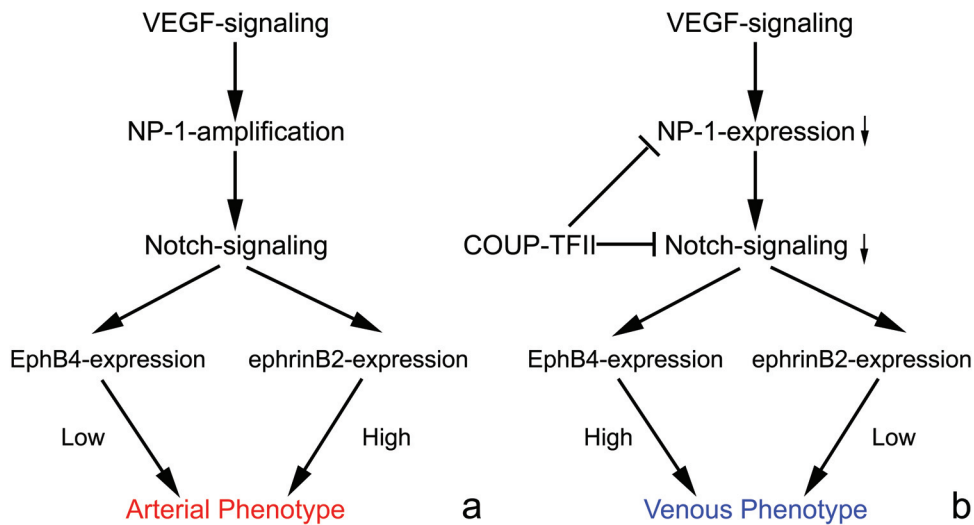
Clinical implications

We have shown that alterations in VEGF and Notch-signaling in the endocardium of the OFT-cushions and subpulmonary cardiomyocytes during their development lead to structural cardiac OFT-abnormalities (TOF and isolated pulmonary stenosis) reminiscent to those found in humans with mutations in *VEGF* or *NOTCH*-related genes⁵⁴⁻⁵⁶. Our data imply that these signaling pathways are highly spatiotemporally controlled and essential for cardiogenesis. Further research regarding association of in utero conditions (such as circulating maternal VEGF-levels or, in mouse, location in

the uterus horn) and the penetrance of the phenotype could give us a starting point for development of therapies. Knowledge regarding the genes and mutations associated with OFT-anomalies could improve our preconceptional and prenatal screening methods or be the topic of pharmacokinetic intervention.

No mutations in the human *PDGF-B* or *PDGFR-β*-genes have been related to congenital heart malformations yet. We describe that knockout of one of these genes in mice leads to cardiac malformations such as myocardial hypoplasia, immature atrioventricular valves and hypoplasia of the cardiac nerves. Our observations warrant genetic screening for *PDGF-B* and *PDGFR-β*-mutations and/or polymorphisms in patients with ventricular non-compaction⁵⁷, valvular abnormalities⁵⁸ and/or arrhythmias related to anomalies in pulmonary vein-innervation⁵⁹.

Table 1. Role of VEGF-signaling in arterio-venous endothelial differentiation.



Adapted from You et al, Nature 2005

(a) High levels of VEGF-signaling, partly due to arterial endothelial cell (EC)-specific NP-1-expression, lead to high levels of Notch-signaling. Notch-signaling can induce expression of the arterial EC-specific marker ephrinB2 and inhibit expression of vein-specific EphB4, leading to an arterial phenotype of the EC. (b) When COUP-TFII, a vein-specific transcription factor, is introduced, NP-1-expression is decreased, leading to lower levels of VEGF-signaling and thus of Notch-signaling. Also, COUP-TFII directly negatively influences Notch-expression and thus signaling. This gives rise to lower levels of ephrinB2 and higher levels of EphB4, concomitant with a venous phenotype of the EC.

VEGF, Notch and PDGF in coronary development

VEGF, Notch and PDGF are -besides their role in heart development- important in vascular development. In this thesis, the development of the coronary system in the *Vegf120/120*, the *Pdgf-b-/-* and the *Pdgfr-β-/-* mouse models with emphasis on vascular patterning, endothelial differentiation and medial development was explored.

The primitive endothelial network

As VEGF is crucial for vasculogenesis and angiogenesis in general^{60;61}, we anticipated that alterations in VEGF-expression and signaling, as present in the *Vegf120/120* mouse embryos, would lead to aberrant initial coronary development. Yet, this was not a marked phenomenon. The sole difference in early coronary development between wild-type and *Vegf120/120* embryos is that mutant coronary veins are markedly enlarged, which can partly be explained by hyperfusion of vessels due to altered VEGF-signaling levels⁶². An effect of (alterations in) Notch-signaling in these early processes of coronary development is not anticipated, as Notch-signaling is mainly involved in later stages of vascular development⁵².

PDGF-B/PDGFR-β-signaling, similar to Notch-signaling, is mainly known for its role in later processes of vascular development (see below). Recent data, however, also point towards a role for PDGF-B in vasculogenesis⁶³ and angiogenesis⁶⁴ but this is not supported by our observations in *Pdgf-b-/-* and *Pdgfr-β-/-* embryos. Either this signaling pathway is dispensable in these processes or redundancy of other PDGF(R)-family members suffices.

Endothelial differentiation

Many markers, several belonging to the Notch-family⁶⁵, have been identified to be specifically expressed by arterial ECs, while relatively few vein-specific markers are currently known (reviewed in⁶⁶). Recently, a mechanism has been proposed through which arteriovenous endothelial differentiation is regulated (Table 1 and⁶⁷) with VEGF-signaling playing a central role.

In our *Vegf120/120* mouse model, anomalous coronary endothelial differentiation is obvious. The arterial ECs show a diminished protein-expression of the arterial markers Notch1, Delta-like (Dll)4, Jagged1 and ephrinB2 concomitant with an increase in expression of the vein-specific markers COUP-TFII and EphB4. The coronary venous ECs showed exactly the opposite with an increase in arterial and a decrease in venous markers. These alterations coincide with a prolonged endothelial expression (both arterial and venous) of VEGFR-2. We postulate that in the normal situation, a high VEGFR-2-signaling level is present in the coronary arterial ECs, due to i) neuropilin (NP)-1-mediated amplification of the VEGFR-2-signaling level (as NP-1 is specifically expressed by arterial ECs)^{68;69} and ii) a high level of VEGF due to heparin-binding of the larger isoforms⁶⁸ (as the area where the

coronary arteries develop overlaps spatiotemporally with the area of cardiac VEGF-production). Correspondingly, a lower level of VEGFR-2-signaling is expected in the subepicardially located coronary veins. As the *Vegf120/120* mouse embryos only express the VEGF120-isoforms, which lacks both the capacity of amplifying VEGFR-2-signaling through NP-1 and of binding to heparin^{68;69}, diminished arterial and increased venous EC signaling levels are expected in the mutant embryos. These data imply that regulation of VEGF-signaling is not only crucial for vasculogenesis and angiogenesis, but also for endothelial differentiation.

In contrast, PDGF-B/PDGFR- β -signaling seems to be less crucial for coronary endothelial differentiation. In both the *Pdgf-b-/-* and *Pdgfr- β -/-* mouse embryos, endothelial differentiation is normal, as exemplified by normal expression levels of ephrinB2 (artery-specific) and of EphB4 (vein-specific).

Arteriogenesis and patterning

Diminished arteriogenesis is obvious in the coronary arteries of *Vegf120/120* embryos, but reduced availability of either EPDCs or cNCCs is unexpected (see above). The coronary veins showed a gain in pericytes/vSMCs. Alterations in recruitment and in local differentiation of vSMCs rather than diminished availability of vSMC-progenitor cells are thus probable. Aberrant endothelial function, expected to be due to distorted endothelial differentiation, could be the underlying cause for the abnormalities in coronary arteriogenesis in the *Vegf120/120* mouse model. As Notch-signaling has been implicated in vSMC-development^{70;71}, we propose that alterations in this pathway, caused by distorted VEGF-signaling in ECs, and perhaps also in vSMCs⁷², contribute to aberrant arteriogenesis. This is further supported by alterations in Notch3, Dll1 and Jagged2-expression in coronary vSMCs in *Vegf120/120* mouse embryos.

Malformations in patterning of the main coronary branches are seen in a large percentage of *Vegf120/120* mouse embryos. In mice, the ventricular septum is normally supplied by an artery branching from the right coronary artery. However, in several *Vegf120/120* mouse embryos the ventricular septum received a coronary artery branching from the left coronary artery. All these embryos could be diagnosed with TOF. Apparently, the OFT-malformations specific for TOF favor the coronary vasculature supplying the ventricular septum to connect to the left side.

In *Pdgf-b-/-* and *Pdgfr- β -/-* mouse embryos coronary arteriogenesis is impaired as demonstrated by dilated coronary vessels throughout the coronary system. In the more distal coronary arteries, this can be explained by lack of sufficient numbers of EPDCs. In the most proximal coronary arteries non-neuronal cNCCs contribute to the medial wall, but no clues are present that less of these are available. The impaired coronary arteriogenesis is probably caused both by i) impaired recruitment, local expansion and differentiation of vSMCs due to absence of EC-derived PDGF-B and ii) by, mainly distally, diminished numbers of EPDCs due to reduced epicardial EMT. Additionally, ventriculo-coronary artery communications (VCACs) were often found in these mouse models. As these have been linked to distorted epicardial and subsequent

coronary development⁷³, they are most likely also caused by impaired performance or presence of EPDCs.

Clinical implications

In humans, congenital coronary malformations are often correlated with primary heart defects⁷⁴. In the *Vegf120/120* mouse model, we show that although alterations in VEGF-signaling are obvious, the abnormalities in coronary patterning are more likely related to structural cardiac defects than to a direct effect of altered VEGF-signaling on coronary patterning. Alterations in the VEGF and, subsequently, the Notch-signaling pathway during coronary development do have a high impact on the maturation, morphology and, as a consequence, on coronary performance. This could explain that in humans, polymorphisms in the *VEGF* and *VEGFR-2*-genes are associated with Kawasaki Disease⁷⁵, in which children can develop coronary aneurysms upon inflammation⁷⁶, and with coronary heart disease⁷⁷. Our findings regarding the instructive roles of VEGF(-isoform) distribution on coronary development can be used in optimizing revascularization therapies targeting VEGF-signaling⁷⁸.

As is the case for congenital heart malformations, no human *PDGF-B* or *PDGFR-β*-mutations are known to be involved in either congenital or acquired coronary malformations yet. It would be interesting to investigate whether the occurrence of VCACs⁷⁹, with or without other congenital heart defects, is associated with mutations or polymorphisms in one of these genes.

Signaling pathways in cardiovascular development

Many ways in which VEGF, Notch and PDGF (might) contribute to (ab)normal cardiovascular development have been discussed so far. To reduce complexity, detailed description on alterations in signaling levels and pathways was minimized. A somewhat more extensive description on changes in signaling pathways is provided below.

VEGF-signaling

In case of VEGF-signaling, many isoforms⁸⁰, two receptors (VEGFR-1 and VEGFR-2) and several coreceptors (NP-1, NP-2, heparin/heparan sulphate) are responsible for high complexity of the ultimate signal⁷⁸. Activation of, or signaling through, VEGFR-2 can be amplified by (one of) the coreceptors^{68;81}, but whether amplification takes place depends on the specific VEGF-isoform involved. The VEGF120-isoform in the mouse (or VEGF121 in humans) is unable to induce this amplification^{69;81}. Additionally, the presence of VEGFR-1 can regulate VEGF-signaling levels through VEGFR-2 by trapping of VEGF⁸². To complicate the matter, feedback-mechanisms regulating VEGF or VEGFR-expression levels also mediate the ultimate effect of VEGF-signaling⁵².

In this thesis it is shown that sole expression of the VEGF120-isoform leads to numerous developmental cardiovascular malformations in mouse embryos, related to alterations in VEGF and downstream Notch-signaling. In what way the alterations in spatiotemporal distribution of VEGF and the lack of larger VEGF-isoforms lead to distorted VEGF-signaling on a cellular level remains unclear. First, lack of heparin-binding isoforms is expected to result in altered distribution of VEGF. This will produce changes in spatiotemporal ligand availability and locally increased or decreased levels of binding of VEGF to its receptor. Second, the VEGF120-isoform is unable to induce coreceptor-mediated amplification of the VEGFR-2-induced signal, thereby decreasing signaling levels, especially in cells that normally rely on (NP-1-dependent) amplification such as arterial ECs. Third, it is unclear whether different isoforms can induce divergent intracellular pathways with differing effects. We postulate that mainly protein distribution, VEGFR-2 and NP-1-levels per cell and presence/absence of amplification, resulting in altered signaling levels rather than changes in signaling characteristics, play a role in VEGF-related congenital cardiovascular malformations. Fourth, VEGF-signaling is involved in regulation of Notch-expression and signaling. Notch-signaling in its turn can downregulate VEGFR-2 expression. As in our *Vegf120/120* mouse model prolonged arterial endothelial and myocardial VEGFR-2-expression is observed concomitant with decreased Notch-signaling (unpublished observations; Van den Akker and Gittenberger-de Groot, 2007), we propose that this feedback-mechanism plays an important role in regulating developmental cardiac VEGF-signaling.

VEGF can also bind and phosphorylate PDGFR- β ⁸³. This adds another possibility through which VEGF could be involved in arteriogenesis; by regulating chemoattractance of PDGFR- β -positive vSMC(-precursors) to the primitive vascular bed. Impairment of the VEGF-protein gradient in the *Vegf120/120* mouse model

due to lack of heparin-binding isoforms could disturb this mechanism and impair arteriogenesis.

Notch-signaling

The Notch-family constitutes of four transmembrane receptors and five membrane-bound ligands and all ligands can bind to all receptors, although evidence exists that not all combinations indeed result in signaling^{52;84}. Recent data indicate that upon binding to its receptor, some of the ligands also induce an intracellular signaling pathway⁸⁵⁻⁸⁸. As all possible combinations and their individual signaling characteristics have yet to be fully investigated, it can be anticipated that seemingly controversial findings in literature concerning Notch-signaling (such as both stimulating^{70;71} and inhibiting⁸⁹ functions on vSMC-development) will be elucidated in the near future.

It is interesting to note that PDGF-signaling can downregulate Notch-receptor and ligand expression in vSMCs^{90;91}, implying that Notch-signaling is particularly involved in specific phases of vSMC-development and differentiation.

PDGF-signaling

Within cardiovascular development, PDGF-A/PDGFR- α and PDGF-B/PDGFR- β -signaling pathways have distinct cellular and developmental properties^{92;93}. PDGF-B is able to bind to PDGFR- α in vitro and it is expected that this interaction could also fulfill a biological function during development. *Pdgf-b*^{-/-} mouse embryos show more severe cardiac malformations when compared with the *Pdgfr- β* ^{-/-} mouse embryos demonstrating that the PDGF-B/PDGFR- α combination can probably play a partly redundant role. Two other recently discovered members of the PDGF-family, PDGF-C and PDGF-D, are less extensively investigated and limited information regarding developmental function and/or expression patterns is currently present. Information regarding signaling characteristics of every individual combination could be important in therapies involved in revascularization and subsequent therapeutic options on stabilization of primitive vessels.

In chicken-quail chimeras, PDGF-B is highly expressed in the top of the growing interventricular septum in the absence of either PDGFR- α or PDGFR- β and *Pdgf-b*^{-/-} mouse embryos develop more frequently and more severe ventricular septal defects when compared with *Pdgfr- β* ^{-/-} mouse embryos. This implies that PDGFR- β -independent PDGF-B-signaling is involved in the development of the interventricular septum. However, PDGFR- α expression is also lacking in this area. We propose that during cardiovascular development, a third PDGF-B-binding receptor is involved. Interestingly, a *PDGFR-like* gene is present in the genome of several mammals, including rat, mouse and human. This gene is found to be expressed during kidney development⁹⁴ and in breast cancer⁹⁵, and also in heart tissue (www.genecards.org). It is interesting to investigate developmental expression patterns of this gene and explore its possible role in cardiovascular development.

Nuchal translucency and lymphatic development

Increased nuchal translucency (NT), and its morphological equivalent nuchal edema (NE), are associated with enlargement of the embryonic jugular lymphatic sacs (JLSs), however, an exact description of the etiology is still lacking. In this thesis differences in morphology and endothelial differentiation between normal, trisomy 21 (T21; Down syndrome), trisomy 18 (T18; Edward syndrome⁹⁶) and monosomy X (45,X; Turner syndrome) human fetuses were examined, combined with data on the murine trisomy 16 (T16) model, in order to further elucidate developmental alterations underlying increased NT.

Phenotypes, genotypes and karyotypes

To give an accurate spatiotemporal description of the correlation between lymphatic development and NE the T16 mouse model was used. Compared with wild-type littermates, alterations in nuchal morphology are apparent in T16 embryos, including dilated JLSs and NE. In both wild-type and T16 embryos, all phases of JLS-development, i.e. budding of lymphatic ECs from internal jugular vein (IJV), bilateral formation of the JLS, and reorganization of the JLSs into lymphatic nodes^{97;98}, could be observed. The valves described to be present between the JLS and the IJV to enable embryonic lymphatic drainage⁹⁷ were, however, not encountered in any of our embryos, either wild-type or T16, and were also not found in human fetuses (unpublished observations; Van den Akker and Gittenberger-de Groot, 2007). Instead, a transient area in which the endothelium of the JLS and the IJV adjoined is seen, which we call the lymphatic-venous membrane (LVM). We suggest that, during early embryonic phases, the LVM facilitates lymphatic drainage but later disappears as the ingrowth of the thoracic duct provides the definitive lymphatic drainage and the JLS remodels into a lymphatic node.

The morphology of the LVM is altered in T16 mouse embryos. It is thickened and folded and is prolonged present. The abnormal morphology of the LVM probably affects lymphatic drainage in T16 mouse embryos, explaining the occurrence of dilated JLSs and NE. Drainage is probably restored after ingrowth of the thoracic duct, explaining the transient appearance of increased NT. The observations made in T16 mouse embryos could likely explain the etiology of increased NT in case of T21 in human development⁹⁹.

To evaluate this assumption, and to determine whether comparable developmental abnormalities could provide the basis of increased NT in other chromosomal abnormalities, morphology of control human fetuses was compared with that of T21, T18 and 45,X fetuses. T21 and T18 human fetuses, as well as the T16 mouse embryos, present with strongly enlarged JLSs and NE, suggesting that the abnormalities seen in the T16 mouse embryos are reminiscent to the human T21 cases. In extreme T21 cases even nuchal cavities (NCs; cyst-like structures that develop in cases of extreme NE) within the mesenchyme have been observed. The 45,X-fetuses

show a complete absence of the JLSs, implying a different developmental deficit from the T21 and T18 fetuses. This was associated with more extreme NE than in T21 fetuses, including large NCs and accentuated visibility of the nuchal ligament, a structure consisting of highly arranged connective tissue probably serving as a fortification between the head and neck¹⁰⁰. 45,X fetuses, and also girls and women with Turner syndrome, often present with cystic hygroma, or webbed neck, which is described to be a 'bilateral, septated, cystic structure, located in the occipitocervical region'¹⁰¹. These structures were regarded to be extremely enlarged JLSs¹⁰², but our morphological data in 45,X fetuses suggest that JLSs are absent, whereas the cystic hygromas indicate an extreme variant of NE/NC. These structures are not of vascular origin which is supported by the absence of any endothelial marker in the cell lining of the NCs. The NCs found in T21 likely develop in a similar, although less extreme way, as the large cystic structures characteristic for cystic hygroma. Although the induction of NE is likely different between karyotypes, i.e. deficient lymphatic drainage in T21/T18 and aplasia of JLSs in 45,X, the increased NT comprises in both cases of massive NE.

Endothelial differentiation and lymphatic performance

To investigate the mechanism underlying abnormal lymphatic development, and subsequent NE, endothelial differentiation characteristics were investigated as it is known that in blood vessels, alterations in endothelial differentiation can result in impaired endothelial performance and subsequent pathology¹⁰³.

In T16 mouse embryos, T21 and T18 human fetuses, differentiation of lymphatic ECs (LECs) of the JLSs was extremely distorted. While expression of the lymphatic marker LYVE-1 was unaltered, expression of Prox-1 and Podoplanin, two other lymphatic markers, was strongly diminished. Prox-1 normally induces expression of the lymphatic marker VEGFR-3 and inhibits NP-1-expression, which is specifically expressed in arterial ECs within the endothelial lineage¹⁰⁴. Its role in developmental lymphogenesis is demonstrated by the phenotype of *Prox-1*^{-/-} mouse embryos, in which JLS-development is arrested after the initial budding-phase⁹⁸. Loss of Podoplanin in *Podoplanin*^{-/-} mouse embryos is associated with congenital lymphedema and dilation of lymphatic vessels¹⁰⁵. We propose that the loss of LEC-characteristics results in impaired LEC-performance, and as such is partly responsible for the development of NE and dilation of the JLSs.

Concomitant with the loss of lymphatic characteristics, increase of VEGF and NP-1 was seen, suggesting -besides a loss of lymphatic characteristics- a gain of (arterial) blood vascular EC (BEC)-characteristics. This is further supported by the presence of von Willebrand factor in T21/T18-LECs, which is normally solely expressed by BEC¹⁰⁶. The increase of VEGF could be caused by NE-induced tissue expansion, as this upregulates VEGF-expression¹⁰⁷. Subsequently, as VEGF can induce vascular permeability¹⁰⁸, its overexpression could further augment NE.

Overexpression of VEGF could, additionally, cause abnormal LEC-differentiation in T16 mouse embryos and T21 fetuses, as VEGF-signaling is involved

in EC-differentiation^{109;110}. The *Vegf120/120* mouse model, however, does not show altered LEC-differentiation in the JLSs, while these embryos do present an increase of *Vegf* mRNA in the LECs and hyperplasia of the JLSs (unpublished observations; Van den Akker and Gittenberger-de Groot, 2007). Therefore, we suggest that VEGF is mainly involved in the differentiation between arterial and venous ECs, but less between venous and lymphatic ECs (Table 2). The combination of loss of lymphatic and induction of arterial characteristics in T16 mouse embryos and T21/T18 human fetuses is probably caused by another pathway. Candidates are COUP-TFII or members of the Notch-pathway, as these proteins are known to be involved in endothelial differentiation (Table 1 and^{52;67}). Further research regarding the exact mechanisms of abnormal LEC-differentiation in T21/T18 is necessary to solve this question.

Another possible consequence of aberrations in LEC-differentiation is the gain of α SMA-expressing cells surrounding the JLSs in T16 mouse embryos, and in T21 and T18 human fetuses. A mouse model deficient for *Foxc2* shows a comparable increase in pericyte-investment in lymphatic vessels and mutations in the human *FOXC2*-gene have been related with multiple lymphedema syndromes¹¹¹. During normal LEC-development FOXC2 inhibits PDGF-B-expression, which is involved in recruitment and differentiation of vSMCs in the embryonic systemic vascular system¹¹¹. Recent data from our group show that FOXC2 is downregulated together with an increase in PDGF-B-expression in the LEC of the JLSs in human T21 fetuses (unpublished observations; De Mooij et al, 2007). The gain of a vSMC-layer around the JLS will impair the transport of lymphatic fluid from the extracellular mesenchyme into the JLS, enhancing NE. It might also abrogate lymphatic drainage of the JLS into the IJV, explaining dilation of the JLSs.

In the 45,X fetuses, the JLSs are not formed. As *Prox-1*^{-/-} mouse embryos show an arrest of formation of the JLS after initial budding, alterations in Prox-1-signaling could be involved in the development of the abnormalities seen in 45,X fetuses. Prox-1 is a transcription factor and therefore must be translocated to the nucleus to exert its function. In the ECs of the IJV in 45,X fetuses this translocation seems to be impaired as only high levels of cytoplasmic staining concomitant with lack of nuclear expression are seen (unpublished observations; Van den Akker and Gittenberger-de Groot, 2007). This suggests that in 45,X fetuses, lack of Prox-1-signaling in the lateral ECs of the IJV leads to failure of JLS-development and as such to extreme NE.

Development of lymph nodes

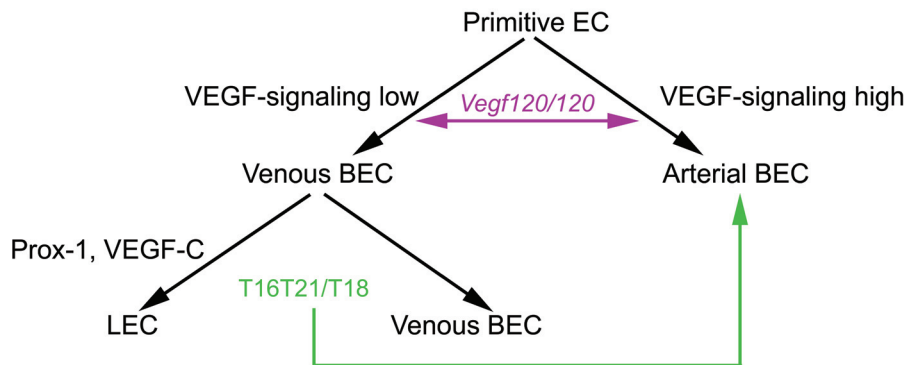
Following abnormal JLS-development, aberrant lymph node-development is observed in T16 mouse embryos as well as in T21 and T18 human fetuses. Normally, lymphocytes start to populate the JLS until it is totally transformed into a lymph node⁹⁷. This process was impaired in all murine and human trisomy cases, resulting in smaller lymph nodes and delayed disappearance of the JLSs. Both T21 and T18 are associated with impaired lymphocyte-development, although differences in affected subpopulations have been reported¹¹². Lymphohematopoietic ECs could be isolated from murine embryos¹¹³, and

we propose that one of the areas where this process could emerge in the embryo is the endothelium of the JLSs.

Ultrasound and microscopy

In this thesis the hypothesis that aberrant lymphatic development is the cause of increased NT⁹⁹ as measured by ultrasound was explored. We show that increased NT represents NE and is associated with distended JLSs in T21 and T18 fetuses. Unexpectedly, we found that in 45,X fetuses JLSs were absent, concomitant with cyst-like structures in the nuchal mesenchyme referred to as nuchal cavities (NCs). NCs could also be encountered in T21 fetuses, although these were usually smaller. Using ultrasound it is currently impossible to distinguish NE from NCs and thus T21/T18 from 45,X. Specific identification of the JLS using ultrasound could facilitate the identification, although this should preferably occur in a transversal plane while for NT-measurements usually sagittal planes are used. Moreover, numerous NCs can be present in either T21/T18 or 45,X and JLSs normally regress (although in T21/T18 likely at later stages than normal fetuses). Therefore, this discernment should only be made with extreme care leading to the proposition that ultrasound is currently not sufficient to distinguish between dilated (in case of T21/T18) and absent (in case of 45,X) JLSs.

Table 2. Arterio-venous and lymphatic differentiation of endothelial cells.



A primitive endothelial cells (EC) can differentiate into either an arterial blood vascular EC (BEC) or a venous BEC. This process is partially regulated by VEGF-signaling, as is exemplified by alterations in both arterial and venous BEC-differentiation in *Vegf120/120* mouse embryos, indicated in purple. Subsequently, a venous BEC can either stay committed to the venous BEC-lineage or differentiate into a lymphatic EC (LEC). The latter process is regulated, amongst others, by Prox-1 and VEGF-C-signaling. In T16 mouse embryos, T21 and T18 human fetuses, this process is altered with loss of LEC and gain of (arterial) BEC-characteristics in the endothelium lining the jugular lymphatic sac (shown in green).

Conclusions

As outlined above, the central cell type within vascular development is the EC. It forms during (lymph)vasculogenesis, proliferates during angiogenesis and instructs the medial cells during arteriogenesis. The venous population also gives rise to a subset of the lymphatic endothelium and the endocardium is instructive in the formation of the primitive heart.

In this thesis we show that endothelial plasticity is very high in the developing embryo/fetus and that its outcome is dependent on the VEGF, Notch and PDGF-signaling pathways. We show that alterations in VEGF and Notch-signaling abrogate endocardial and endothelial differentiation and, subsequently, cardiac OFT-cushion development and coronary maturation. Alterations in these pathways are most likely also involved in the abnormal lymphatic development as seen in fetuses with increased NT and might even additionally the occurrence of NE. In the part of this thesis concerning lymphatic development, endothelial plasticity is particularly underscored, as lymphatic ECs even gain arterial characteristics. Additionally, we show that impaired VEGF, Notch and PDGF-B/PDGFR- β -signaling in ECs and/or vSMCs severely impairs coronary arteriogenesis.

In conclusion, many growth factors either influencing the EC (such as VEGF) or produced by the EC (such as PDGF) play a role in regulating and fine-tuning these processes. Therefore, increasing our knowledge on how these factors influence (ab)normal vascular development will improve our understanding of many pathological conditions and might increase therapeutic approaches.

References

1. Stalmans I, Lambrechts D, De Smet F, Jansen S, Wang J, Maity S, Kneer P, von der OM, Swillen A, Maes C, Gewillig M, Molin DG, Hellings P, Boetel T, Haardt M, Compernelle V, Dewerchin M, Plaisance S, Vlietinck R, Emanuel B, Gittenberger-De Groot AC, Scambler P, Morrow B, Driscoll DA, Moons L, Esguerra CV, Carmeliet G, Behn-Krappa A, Devriendt K, Collen D, Conway SJ, Carmeliet P. VEGF: a modifier of the del22q11 (DiGeorge) syndrome? *Nat Med*. 2003;9:173-182.
2. Bartelings MM, Wenink AC, Gittenberger-De Groot AC, Oppenheimer-Dekker A. Contribution of the aortopulmonary septum to the muscular outlet septum in the human heart. *Acta Morphol Neerl Scand*. 1986;24:181-192.
3. Waldo K, Miyagawa-Tomita S, Kumiski D, Kirby ML. Cardiac neural crest cells provide new insight into septation of the cardiac outflow tract: aortic sac to ventricular septal closure. *Dev Biol*. 1998;196:129-144.
4. Boot MJ, Gittenberger-De Groot AC, Van IL, Hierck BP, Poelmann RE. Spatiotemporally separated cardiac neural crest subpopulations that target the outflow tract septum and pharyngeal arch arteries. *Anat Rec A Discov Mol Cell Evol Biol*. 2003;275:1009-1018.
5. Laane HM, Roest-Wagenaar JA. Development and fusion of endocardial structures in the arterial pole of the heart of chick, rat and human embryos. *Perspectives in Cardiovascular Research*. 1981;5:267-277.
6. Poelmann RE, Mikawa T, Gittenberger-De Groot AC. Neural crest cells in outflow tract septation of the embryonic chicken heart: Differentiation and apoptosis. *Developmental Dynamics*. 1998;212:373-384.
7. Kirby ML, Gale TF, Stewart DE. Neural crest cells contribute to normal aorticopulmonary septation. *Science*. 1983;220:1059-1061.
8. Gittenberger-De Groot AC, Bartelings MM, Bogers AJ, Boot MJ, Poelmann RE. The embryology of the common arterial trunk. *Progress in Pediatric Cardiology*. 2002;15:1-8.
9. Molin DG, Poelmann RE, DeRuiter MC, Azhar M, Doetschman T, Gittenberger-De Groot AC. Transforming growth factor beta-SMAD2 signaling regulates aortic arch innervation and development. *Circ Res*. 2004;95:1109-1117.
10. Jiang X, Choudhary B, Merki E, Chien KR, Maxson RE, Sucov HM. Normal fate and altered function of the cardiac neural crest cell lineage in retinoic acid receptor mutant embryos. *Mech Dev*. 2002;117:115-122.
11. Epstein JA, Li J, Lang D, Chen F, Brown CB, Jin F, Lu MM, Thomas M, Liu E, Wessels A, Lo CW. Migration of cardiac neural crest cells in Splotch embryos. *Development*. 2000;127:1869-1878.
12. Cornell RA, Eisen JS. Notch in the pathway: the roles of Notch signaling in neural crest development. *Semin Cell Dev Biol*. 2005;16:663-672.
13. Sasahara M, Sato H, Iihara K, Wang J, Chue CH, Takayama S, Hayase Y, Hazama F. Expression of platelet-derived growth factor B-chain in the mature rat brain and pituitary gland. *Brain Res Mol Brain Res*. 1995;32:63-74.
14. Oya T, Zhao YL, Takagawa K, Kawaguchi M, Shirakawa K, Yamauchi T, Sasahara M. Platelet-derived growth factor-b expression induced after rat peripheral nerve injuries. *Glia*. 2002;38:303-312.

15. Ishii Y, Oya T, Zheng L, Gao Z, Kawaguchi M, Sabit H, Matsushima T, Tokunaga A, Ishizawa S, Hori E, Nabeshima Y, Sasaoka T, Fujimori T, Mori H, Sasahara M. Mouse brains deficient in neuronal PDGF receptor-beta develop normally but are vulnerable to injury. *J Neurochem.* 2006;98:588-600.
16. Soriano P. The PDGF alpha receptor is required for neural crest cell development and for normal patterning of the somites. *Development.* 1997;124:2691-2700.
17. Tallquist MD, Soriano P. Cell autonomous requirement for PDGFRalpha in populations of cranial and cardiac neural crest cells. *Development.* 2003;130:507-518.
18. Morrison-Graham K, Schatteman GC, Bork T, Bowen-Pope DF, Weston JA. A PDGF receptor mutation in the mouse (Patch) perturbs the development of a non-neuronal subset of neural crest-derived cells. *Development.* 1992;115:133-142.
19. Gittenberger-De Groot AC, Vrancken Peeters MP, Mentink MM, Gourdie RG, Poelmann RE. Epicardium-derived cells contribute a novel population to the myocardial wall and the atrioventricular cushions. *Circ Res.* 1998;82:1043-1052.
20. Stuckmann I, Evans S, Lassar AB. Erythropoietin and retinoic acid, secreted from the epicardium, are required for cardiac myocyte proliferation. *Dev Biol.* 2003;255:334-349.
21. Eralp I, Lie-Venema H, DeRuiter MC, Van Den Akker NM, Bogers AJ, Mentink MM, Poelmann RE, Gittenberger-De Groot AC. Coronary artery and orifice development is associated with proper timing of epicardial outgrowth and correlated Fas-ligand-associated apoptosis patterns. *Circ Res.* 2005;96:526-534.
22. Kang JO, Sucov HM. Convergent proliferative response and divergent morphogenic pathways induced by epicardial and endocardial signaling in fetal heart development. *Mech Dev.* 2005;122:57-65.
23. Morabito CJ, Dettman RW, Kattan J, Collier JM, Bristow J. Positive and negative regulation of epicardial-mesenchymal transformation during avian heart development. *Dev Biol.* 2001;234:204-215.
24. Loomes KM, Taichman DB, Glover CL, Williams PT, Markowitz JE, Piccoli DA, Baldwin HS, Oakey RJ. Characterization of Notch receptor expression in the developing mammalian heart and liver. *Am J Med Genet.* 2002;112:181-189.
25. Merki E, Zamora M, Raya A, Kawakami Y, Wang J, Zhang X, Burch J, Kubalak SW, Kaliman P, Belmonte JC, Chien KR, Ruiz-Lozano P. Epicardial retinoid X receptor alpha is required for myocardial growth and coronary artery formation. *Proc Natl Acad Sci U S A.* 2005;102:18455-18460.
26. Tomanek RJ, Ratajska A, Kitten GT, Yue X, Sandra A. Vascular endothelial growth factor expression coincides with coronary vasculogenesis and angiogenesis. *Dev Dyn.* 1999;215:54-61.
27. Narmoneva DA, Vukmirovic R, Davis ME, Kamm RD, Lee RT. Endothelial cells promote cardiac myocyte survival and spatial reorganization: implications for cardiac regeneration. *Circulation.* 2004;110:962-968.
28. Sugishita Y, Takahashi T, Shimizu T, Yao A, Kinugawa K, Sugishita K, Harada K, Matsui H, Nagai R. Expression of genes encoding vascular endothelial growth factor and its Flk-1 receptor in the chick embryonic heart. *J Mol Cell Cardiol.* 2000;32:1039-1051.
29. Chen Y, Amende I, Hampton TG, Yang Y, Ke Q, Min JY, Xiao YF, Morgan JP. Vascular endothelial growth factor promotes cardiomyocyte differentiation of embryonic stem cells. *Am J Physiol Heart Circ Physiol.* 2006;291:H1653-H1658.

30. Song YH, Gehmert S, Sadat S, Pinkernell K, Bai X, Matthias N, Alt E. VEGF is critical for spontaneous differentiation of stem cells into cardiomyocytes. *Biochem Biophys Res Commun.* 2007;354:999-1003.
31. Chintalgattu V, Nair DM, Katwa LC. Cardiac myofibroblasts: a novel source of vascular endothelial growth factor (VEGF) and its receptors Flt-1 and KDR. *J Mol Cell Cardiol.* 2003;35:277-286.
32. LaFramboise WA, Scalise D, Stoodley P, Graner SR, Guthrie RD, Magovern JA, Becich MJ. Cardiac fibroblasts influence cardiomyocyte phenotype in vitro. *Am J Physiol Cell Physiol.* 2007;292:C1799-C1808.
33. Pedrazzini T. Control of cardiogenesis by the notch pathway. *Trends Cardiovasc Med.* 2007;17:83-90.
34. Lu J, Landerholm TE, Wei JS, Dong XR, Wu SP, Liu X, Nagata K, Inagaki M, Majesky MW. Coronary smooth muscle differentiation from proepicardial cells requires rhoA-mediated actin reorganization and p160 rho-kinase activity. *Dev Biol.* 2001;240:404-418.
35. Heldin CH, Eriksson U, Ostman A. New members of the platelet-derived growth factor family of mitogens. *Arch Biochem Biophys.* 2002;398:284-290.
36. Enciso JM, Gratzinger D, Camenisch TD, Canosa S, Pinter E, Madri JA. Elevated glucose inhibits VEGF-A-mediated endocardial cushion formation: modulation by PECAM-1 and MMP-2. *J Cell Biol.* 2003;160:605-615.
37. Lee YM, Cope JJ, Ackermann GE, Goishi K, Armstrong EJ, Paw BH, Bischoff J. Vascular endothelial growth factor receptor signaling is required for cardiac valve formation in zebrafish. *Dev Dyn.* 2006;235:29-37.
38. Dor Y, Camenisch TD, Itin A, Fishman GI, McDonald JA, Carmeliet P, Keshet E. A novel role for VEGF in endocardial cushion formation and its potential contribution to congenital heart defects. *Development.* 2001;128:1531-1538.
39. Dor Y, Klewer SE, McDonald JA, Keshet E, Camenisch TD. VEGF modulates early heart valve formation. *Anat Rec A Discov Mol Cell Evol Biol.* 2003;271:202-208.
40. Armstrong EJ, Bischoff J. Heart valve development: endothelial cell signaling and differentiation. *Circ Res.* 2004;95:459-470.
41. Waldo KL, Hutson MR, Stadt HA, Zdanowicz M, Zdanowicz J, Kirby ML. Cardiac neural crest is necessary for normal addition of the myocardium to the arterial pole from the secondary heart field. *Dev Biol.* 2005;281:66-77.
42. Kelly RG. Molecular inroads into the anterior heart field. *Trends Cardiovasc Med.* 2005;15:51-56.
43. Black BL. Transcriptional pathways in second heart field development. *Semin Cell Dev Biol.* 2007;18:67-76.
44. Bajolle F, Zaffran S, Kelly RG, Hadchouel J, Bonnet D, Brown NA, Buckingham ME. Rotation of the myocardial wall of the outflow tract is implicated in the normal positioning of the great arteries. *Circ Res.* 2006;98:421-428.
45. Ward C, Stadt H, Hutson M, Kirby ML. Ablation of the secondary heart field leads to tetralogy of Fallot and pulmonary atresia. *Dev Biol.* 2005;284:72-83.

46. Watanabe M, Choudhry A, Berlan M, Singal A, Siwik E, Mohr S, Fisher SA. Developmental remodeling and shortening of the cardiac outflow tract involves myocyte programmed cell death. *Development*. 1998;125:3809-3820.
47. Sugishita Y, Leifer DW, Agani F, Watanabe M, Fisher SA. Hypoxia-responsive signaling regulates the apoptosis-dependent remodeling of the embryonic avian cardiac outflow tract. *Dev Biol*. 2004;273:285-296.
48. Sharma PR, Anderson RH, Copp AJ, Henderson DJ. Spatiotemporal analysis of programmed cell death during mouse cardiac septation. *Anat Rec A Discov Mol Cell Evol Biol*. 2004;277:355-369.
49. Sugishita Y, Watanabe M, Fisher SA. Role of myocardial hypoxia in the remodeling of the embryonic avian cardiac outflow tract. *Dev Biol*. 2004;267:294-308.
50. Francis JC, Radtke F, Logan MP. Notch1 signals through Jagged2 to regulate apoptosis in the apical ectodermal ridge of the developing limb bud. *Dev Dyn*. 2005;234:1006-1015.
51. Pan Y, Liu Z, Shen J, Kopan R. Notch1 and 2 cooperate in limb ectoderm to receive an early Jagged2 signal regulating interdigital apoptosis. *Dev Biol*. 2005;286:472-482.
52. Hofmann JJ, Iruela-Arispe ML. Notch signaling in blood vessels - Who is talking to whom about what? *Circulation Research*. 2007;100:1556-1568.
53. Schatteman GC, Motley ST, Effmann EL, Bowen-Pope DF. Platelet-derived growth factor receptor alpha subunit deleted Patch mouse exhibits severe cardiovascular dysmorphism. *Teratology*. 1995;51:351-366.
54. Eldadah ZA, Hamosh A, Biery NJ, Montgomery RA, Duke M, Elkins R, Dietz HC. Familial Tetralogy of Fallot caused by mutation in the jagged1 gene. *Hum Mol Genet*. 2001;10:163-169.
55. McElhinney DB, Krantz ID, Bason L, Piccoli DA, Emerick KM, Spinner NB, Goldmuntz E. Analysis of cardiovascular phenotype and genotype-phenotype correlation in individuals with a JAG1 mutation and/or Alagille syndrome. *Circulation*. 2002;106:2567-2574.
56. Le Caignec C, Lefevre M, Schott JJ, Chaventre A, Gayet M, Calais C, Moisan JP. Familial deafness, congenital heart defects, and posterior embryotoxon caused by cysteine substitution in the first epidermal-growth-factor-like domain of jagged 1. *Am J Hum Genet*. 2002;71:180-186.
57. Pignatelli RH, McMahon CJ, Dreyer WJ, Denfield SW, Price J, Belmont JW, Craigen WJ, Wu J, El SH, Bezold LI, Clunie S, Fernbach S, Bowles NE, Towbin JA. Clinical characterization of left ventricular noncompaction in children: a relatively common form of cardiomyopathy. *Circulation*. 2003;108:2672-2678.
58. Attenhofer Jost CH, Connolly HM, Edwards WD, Hayes D, Warnes CA, Danielson GK. Ebstein's anomaly - review of a multifaceted congenital cardiac condition. *Swiss Med Wkly*. 2005;135:269-281.
59. Tan AY, Chen PS, Chen LS, Fishbein MC. Autonomic nerves in pulmonary veins. *Heart Rhythm*. 2007;4:S57-S60.
60. Ferrara N, Gerber HP, LeCouter J. The biology of VEGF and its receptors. *Nat Med*. 2003;9:669-676.
61. Carmeliet P. Mechanisms of angiogenesis and arteriogenesis. *Nat Med*. 2000;6:389-395.
62. Drake CJ, Little CD. VEGF and vascular fusion: implications for normal and pathological vessels. *J Histochem Cytochem*. 1999;47:1351-1356.

63. Rolny C, Nilsson I, Magnusson P, Armulik A, Jakobsson L, Wentzel P, Lindblom P, Norlin J, Betsholtz C, Heuchel R, Welsh M, Claesson-Welsh L. Platelet-derived growth factor receptor-beta promotes early endothelial cell differentiation. *Blood*. 2006;108:1877-1886.
64. Ulrica MP, Looman C, Ahgren A, Wu Y, Claesson-Welsh L, Heuchel RL. Platelet-Derived Growth Factor Receptor- β Constitutive Activity Promotes Angiogenesis In Vivo and In Vitro. *Arterioscler Thromb Vasc Biol*. 2007.
65. Villa N, Walker L, Lindsell CE, Gasson J, Iruela-Arispe ML, Weinmaster G. Vascular expression of Notch pathway receptors and ligands is restricted to arterial vessels. *Mech Dev*. 2001;108:161-164.
66. Hirashima M, Suda T. Differentiation of arterial and venous endothelial cells and vascular morphogenesis. *Endothelium*. 2006;13:137-145.
67. You LR, Lin FJ, Lee CT, Demayo FJ, Tsai MJ, Tsai SY. Suppression of Notch signalling by the COUP-TFII transcription factor regulates vein identity. *Nature*. 2005;435:98-104.
68. Soker S, Takashima S, Miao HQ, Neufeld G, Klagsbrun M. Neuropilin-1 is expressed by endothelial and tumor cells as an isoform-specific receptor for vascular endothelial growth factor. *Cell*. 1998;92:735-745.
69. Pan Q, Chanthery Y, Wu Y, Rahtore N, Tong RK, Peale F, Bagri A, Tessier-Lavigne M, Koch AW, Watts RJ. Neuropilin-1 binds to VEGF121 and regulates endothelial cell migration and sprouting. *J Biol Chem*. 2007;282:24049-24056.
70. Limbourg A, Ploom M, Elligsen D, Sorensen I, Ziegelhoeffer T, Gossler A, Drexler H, Limbourg FP. Notch ligand Delta-like 1 is essential for postnatal arteriogenesis. *Circ Res*. 2007;100:363-371.
71. High FA, Zhang M, Proweller A, Tu L, Parmacek MS, Pear WS, Epstein JA. An essential role for Notch in neural crest during cardiovascular development and smooth muscle differentiation. *J Clin Invest*. 2007;117:353-363.
72. Liu W, Parikh AA, Stoeltzing O, Fan F, McCarty MF, Wey J, Hicklin DJ, Ellis LM. Upregulation of neuropilin-1 by basic fibroblast growth factor enhances vascular smooth muscle cell migration in response to VEGF. *Cytokine*. 2005;32:206-212.
73. Gittenberger-De Groot AC, Eralp I, Lie-Venema H, Bartelings MM, Poelmann RE. Development of the coronary vasculature and its implications for coronary abnormalities in general and specifically in pulmonary atresia without ventricular septal defect. *Acta Paediatr Suppl*. 2004;93:13-19.
74. Jureidini SB, Appleton RS, Nouri S. Detection of coronary artery abnormalities in tetralogy of Fallot by two-dimensional echocardiography. *J Am Coll Cardiol*. 1989;14:960-967.
75. Kariyazono H, Ohno T, Khajoev V, Ihara K, Kusuhara K, Kinukawa N, Mizuno Y, Hara T. Association of vascular endothelial growth factor (VEGF) and VEGF receptor gene polymorphisms with coronary artery lesions of Kawasaki disease. *Pediatr Res*. 2004;56:953-959.
76. Freeman AF, Shulman ST. Recent developments in Kawasaki disease. *Curr Opin Infect Dis*. 2001;14:357-361.
77. Wang Y, Zheng Y, Zhang W, Yu H, Lou K, Zhang Y, Qin Q, Zhao B, Yang Y, Hui R. Polymorphisms of KDR gene are associated with coronary heart disease. *J Am Coll Cardiol*. 2007;50:760-767.

78. Yla-Herttuala S, Rissanen TT, Vajanto I, Hartikainen J. Vascular endothelial growth factors: biology and current status of clinical applications in cardiovascular medicine. *J Am Coll Cardiol*. 2007;49:1015-1026.
79. Luo L, Kebede S, Wu S, Stouffer GA. Coronary artery fistulae. *Am J Med Sci*. 2006;332:79-84.
80. Robinson CJ, Stringer SE. The splice variants of vascular endothelial growth factor (VEGF) and their receptors. *J Cell Sci*. 2001;114:853-865.
81. Houck KA, Leung DW, Rowland AM, Winer J, Ferrara N. Dual regulation of vascular endothelial growth factor bioavailability by genetic and proteolytic mechanisms. *J Biol Chem*. 1992;267:26031-26037.
82. Shibuya M, Claesson-Welsh L. Signal transduction by VEGF receptors in regulation of angiogenesis and lymphangiogenesis. *Exp Cell Res*. 2006;312:549-560.
83. Ball SG, Shuttleworth CA, Kielty CM. Vascular endothelial growth factor can signal through platelet-derived growth factor receptors. *J Cell Biol*. 2007;177:489-500.
84. Ladi E, Nichols JT, Ge W, Miyamoto A, Yao C, Yang LT, Boulter J, Sun YE, Kintner C, Weinmaster G. The divergent DSL ligand DLL3 does not activate Notch signaling but cell autonomously attenuates signaling induced by other DSL ligands. *J Cell Biol*. 2005;170:983-992.
85. Ascano JM, Beverly LJ, Capobianco AJ. The C-terminal PDZ-ligand of JAGGED1 is essential for cellular transformation. *J Biol Chem*. 2003;278:8771-8779.
86. Bland CE, Kimberly P, Rand MD. Notch-induced proteolysis and nuclear localization of the Delta ligand. *J Biol Chem*. 2003;278:13607-13610.
87. Kolev V, Kacer D, Trifonova R, Small D, Duarte M, Soldi R, Graziani I, Sideleva O, Larman B, Maciag T, Prudovsky I. The intracellular domain of Notch ligand Delta1 induces cell growth arrest. *FEBS Lett*. 2005;579:5798-5802.
88. Hiratochi M, Nagase H, Kuramochi Y, Koh CS, Ohkawara T, Nakayama K. The Delta intracellular domain mediates TGF-beta/Activin signaling through binding to Smads and has an important bidirectional function in the Notch-Delta signaling pathway. *Nucleic Acids Res*. 2007;35:912-922.
89. Morrow D, Scheller A, Birney YA, Sweeney C, Guha S, Cummins PM, Murphy R, Walls D, Redmond EM, Cahill PA. Notch-mediated CBF-1/RBP-J{kappa}-dependent regulation of human vascular smooth muscle cell phenotype in vitro. *Am J Physiol Cell Physiol*. 2005;289:C1188-C1196.
90. Campos AH, Wang W, Pollman MJ, Gibbons GH. Determinants of Notch-3 receptor expression and signaling in vascular smooth muscle cells: implications in cell-cycle regulation. *Circ Res*. 2002;91:999-1006.
91. Wang W, Campos AH, Prince CZ, Mou Y, Pollman MJ. Coordinate Notch3-hairy-related transcription factor pathway regulation in response to arterial injury. Mediator role of platelet-derived growth factor and ERK. *J Biol Chem*. 2002;277:23165-23171.
92. Hoch RV, Soriano P. Roles of PDGF in animal development. *Development*. 2003;130:4769-4784.
93. Betsholtz C. Biology of platelet-derived growth factors in development. *Birth Defects Res C Embryo Today*. 2003;69:272-285.

94. Potter SS, Hartman HA, Kwan KM, Behringer RR, Patterson LT. Laser capture-microarray analysis of Lim1 mutant kidney development. *Genesis*. 2007;45:432-439.
95. Seitz S, Korsching E, Weimer J, Jacobsen A, Arnold N, Meindl A, Arnold W, Gustavus D, Klebig C, Petersen I, Scherneck S. Genetic background of different cancer cell lines influences the gene set involved in chromosome 8 mediated breast tumor suppression. *Genes Chromosomes Cancer*. 2006;45:612-627.
96. Tucker ME, Garringer HJ, Weaver DD. Phenotypic spectrum of mosaic trisomy 18: two new patients, a literature review, and counseling issues. *Am J Med Genet A*. 2007;143:505-517.
97. Sabin FR. The lymphatic system in human embryos, with a consideration of the morphology of the system as a whole. *Am J Anat*. 1909;9:43-91.
98. Wigle JT, Oliver G. Prox1 function is required for the development of the murine lymphatic system. *Cell*. 1999;98:769-778.
99. Haak MC, Bartelings MM, Jackson DG, Webb S, Van Vugt JM, Gittenberger-De Groot AC. Increased nuchal translucency is associated with jugular lymphatic distension. *Hum Reprod*. 2002;17:1086-1092.
100. Dean NA, Mitchell BS. Anatomic relation between the nuchal ligament (ligamentum nuchae) and the spinal dura mater in the craniocervical region. *Clin Anat*. 2002;15:182-185.
101. Molina FS, Avgidou K, Kagan KO, Poggi S, Nicolaidis KH. Cystic hygromas, nuchal edema, and nuchal translucency at 11-14 weeks of gestation. *Obstet Gynecol*. 2006;107:678-683.
102. Chitayat D, Kalousek DK, Bamforth JS. Lymphatic abnormalities in fetuses with posterior cervical cystic hygroma. *Am J Med Genet*. 1989;33:352-356.
103. Deng DX, Tsalenko A, Vailaya A, Ben-Dor A, Kundu R, Estay I, Tabibiazar R, Kincaid R, Yakhini Z, Bruhn L, Quertermous T. Differences in vascular bed disease susceptibility reflect differences in gene expression response to atherogenic stimuli. *Circ Res*. 2006;98:200-208.
104. Petrova TV, Mäkinen T, Mäkelä TP, Saarela J, Virtanen I, Ferrell RE, Finegold DN, Kerjaschki D, Ylä-Herttua S, Alitalo K. Lymphatic endothelial reprogramming of vascular endothelial cells by the Prox-1 homeobox transcription factor. *EMBO J*. 2002;21:4593-4599.
105. Schacht V, Ramirez MI, Hong YK, Hirakawa S, Feng D, Harvey N, Williams M, Dvorak AM, Dvorak HF, Oliver G, Detmar M. T1alpha/podoplanin deficiency disrupts normal lymphatic vasculature formation and causes lymphedema. *EMBO J*. 2003;22:3546-3556.
106. Lymboussaki A, Partanen TA, Olofsson B, Thomas-Crusells J, Fletcher CD, de Waal RM, Kaipainen A, Alitalo K. Expression of the vascular endothelial growth factor C receptor VEGFR-3 in lymphatic endothelium of the skin and in vascular tumors. *Am J Pathol*. 1998;153:395-403.
107. Lantieri LA, Martin-Garcia N, Wechsler J, Mitrofanoff M, Raulo Y, Baruch JP. Vascular endothelial growth factor expression in expanded tissue: a possible mechanism of angiogenesis in tissue expansion. *Plast Reconstr Surg*. 1998;101:392-398.
108. Brown LF, Detmar M, Claffey K, Nagy JA, Feng D, Dvorak AM, Dvorak HF. Vascular permeability factor/vascular endothelial growth factor: a multifunctional angiogenic cytokine. *EXS*. 1997;79:233-269.

109. Hainaud P, Contreres JO, Villemain A, Liu LX, Plouet J, Tobelem G, Dupuy E. The Role of the Vascular Endothelial Growth Factor-Delta-like 4 Ligand/Notch4-Ephrin B2 Cascade in Tumor Vessel Remodeling and Endothelial Cell Functions. *Cancer Res.* 2006;66:8501-8510.
110. Lawson ND, Vogel AM, Weinstein BM. sonic hedgehog and vascular endothelial growth factor act upstream of the Notch pathway during arterial endothelial differentiation. *Dev Cell.* 2002;3:127-136.
111. Petrova TV, Karpanen T, Norrmen C, Mellor R, Tamakoshi T, Finegold D, Ferrell R, Kerjaschki D, Mortimer P, Yla-Herttuala S, Miura N, Alitalo K. Defective valves and abnormal mural cell recruitment underlie lymphatic vascular failure in lymphedema distichiasis. *Nat Med.* 2004;10:974-981.
112. Zizka Z, Calda P, Fait T, Haakova L, Kvasnicka J, Viskova H. Prenatally diagnosable differences in the cellular immunity of fetuses with Down's and Edwards' syndrome. *Fetal Diagn Ther.* 2006;21:510-514.
113. Nishikawa SI, Nishikawa S, Kawamoto H, Yoshida H, Kizumoto M, Kataoka H, Katsura Y. In vitro generation of lymphohematopoietic cells from endothelial cells purified from murine embryos. *Immunity.* 1998;8:761-769.

List of Abbreviations

α SMA	α -smooth muscle actin
α/γ MA	α/γ muscle actin
AAo	ascending aorta
AEC	arterial endothelial cell
AHF	anterior heart field
AM	atrial myocardium
AoA	aortic arch
ARSA	aberrant right subclavian artery
ASD	atrial septal defect
AV	atrioventricular
AVC	atrioventricular canal
AVSD	atrioventricular septal defect
BEC	blood vascular endothelial cell
bFGF	basic fibroblast growth factor
β -HCG	β -human chorionic gonadotropin
CA	coronary artery
CL	cardiac lymphatics
CM	compact myocardium
cNCC	cardiac neural crest cell
CoO	coronary orifice
CO	control
COUP-TFII	chicken ovalbumin upstream promoter transcription factor II
CV	coronary vein
DA	ductus arteriosus
DAB	3-3' diaminobenzidine tetrahydrochloride
DAO	dorsal aorta
DAPI	4'6-diamidino-2-phenylidole-dihydrochloride
DII	delta-like
DLK	delta homologue
DNA	deoxyribonucleic acid
DORV	double outlet right ventricle
E	embryonic day
EC	endothelial cell
EDTA	ethylenediaminetetraacetic acid
EGF	epidermal growth factor
EMT	epithelial-mesenchymal transformation
EPDC	epicardium-derived cell
Eph	ephrin receptor
FGF	fibroblast growth factor
FITC	fluorescein isothiocyanate

FOXC2	forkhead box C2
GA	gestational age
GAPDH	glyceraldehyde 3-phosphate dehydrogenase
HA	hyaluronan
HCAEC	human coronary arterial endothelial cell
HE	Hematoxylin/Eosin
HERP	hairy enhancer of split-related repressor protein
Hes	hairy enhancer of split
HH	Hamburger and Hamilton
HLHS	hypoplastic left heart syndrome
HR	heat retrieval
IFT	inflow tract
IJV	internal jugular vein
ISH	in situ hybridisation
IVS	interventricular septum
JLS	jugular lymphatic sac
LA	left atrium
LCA	left coronary artery
LEC	lymphatic endothelial cell
LV	left ventricle
LVM	lymphatic-venous membrane
LYVE	lymphatic vessel endothelial hyaluronan receptor
MASH	mammalian achaete-scute complex homologue
MMP	matrix metalloproteinase
mRNA	messenger ribonucleic acid
NC	nuchal cavity
NCAM	neural cell adhesion molecule
NE	nuchal edema
NICD	intracellular domain of Notch
NIH	National Institute of Health
NP	neuropilin
NT	nuchal translucency
NVB	noten-vruchtenbol
OFT	outflow tract
PA	pulmonary artery
PAPP-A	pregnancy-associated plasma protein-A
PBS	phosphate-buffered saline
PC	pericardial cavity
PCR	polymerase chain reaction
PDGF	platelet-derived growth factor
PDGFR	platelet-derived growth factor receptor
PEO	proepicardial organ

PFA	paraformaldehyde
PHF	posterior heart field
PIGF	placenta growth factor
PT	pulmonary trunk
PV	pulmonary vein
p-value	probability value
p-VEGFR-2	phosphorylated vascular endothelial growth factor receptor-2
qPCR	quantitative polymerase chain reaction
RA	right atrium
RCA	right coronary artery
RNA	ribonucleic acid
RT	reverse transcriptase
RV	right ventricle
SHF	second heart field
T16	trisomy 16
T18	trisomy 18
T21	trisomy 21
TGF β	transforming growth factor β
TM	trabecular myocardium
TOF	tetralogy of Fallot
TRITC	tetrahodamine isothiocyanate
TUNEL	terminal deoxynucleotidyl transferase biotin dUTP nick-end labeling
VCAC	ventriculo-coronary artery connections
VEC	venous endothelial cell
VEGF	vascular endothelial growth factor
VEGFR	vascular endothelial growth factor receptor
VM	ventricular myocardium
VSD	ventricular septal defect
vSMC	vascular smooth muscle cell
vWF	Von Willebrand factor
WT	wild type

Summary

In this thesis, the influence of Vascular Endothelial Growth Factor (VEGF) and Platelet-derived Growth Factor (PDGF)-signaling on cardiovascular development has been explored. Additionally, the relation between abnormal development of the embryonic lymphatic system and increased nuchal translucency (NT) has been investigated.

In Chapter 1, a general introduction of this thesis is provided. The development of the cardiovascular and the lymphatic system are described, together with the role of VEGF, Notch and PDGF-signaling pathways, showing involvement of VEGF and PDGF.

In Chapter 2, the effect of the murine *Vegf120/120* genotype on spatiotemporal *Vegf* mRNA expression and on cardiac development has been explored. The *Vegf120/120* genotype leads to sole expression of the VEGF120 isoform that is unable to bind to heparin present in the extracellular matrix and is therefore highly diffuse. Furthermore, VEGF120 is, in contrast to the larger VEGF-isoforms, unable to induce the high signaling potent VEGFR-2/NP-1 complexes. Therefore, both altered VEGF protein gradients and alterations in local signaling levels are expected in *Vegf120/120* mouse embryos. During normal cardiac development, the subpulmonary myocardium transiently (i.e. during the stages in which cardiac septation takes place) expressed relatively high *Vegf* mRNA levels when compared to the remainder of the heart. This area showed large amounts of apoptotic cardiomyocytes in mutant embryos, concomitant with extremely high levels of *Vegf* mRNA, activated VEGFR-2, Jagged 2 and cleaved (activated) Notch1. Additionally, the endocardial cells, as well as cushion mesenchymal cells, of the outflow tract cushions showed prolonged expression of VEGF, VEGFR-2 and activated Notch1 concomitant with outflow tract cushion hyperplasia, indicative for prolonged endocardial epithelial-to-mesenchymal transformation. These two pathological, highly spatiotemporally regulated, processes can lead to hypoplasia of the pulmonary trunk, dextropositioning of the aorta and to a subaortic ventricular septal defect, which are the three embryological/fetal characteristics of Tetralogy of Fallot.

Chapter 3 also concerns the *Vegf120/120* mouse model, only here the development of the coronary system is described. In mutant mouse embryos, the endothelial cells of the coronary arteries failed to gain proper arterial characteristics (i.e. high levels of activated Notch1, Jagged1, Dll4 and ephrinB2 and low levels of VEGFR-2, EphB4 and COUP-TFII), while the endothelial cells of the coronary veins showed ectopic expression of the arterial markers together with low expression of the venous markers. Also, the mutant coronary arteries showed an underdeveloped medial layer, while the coronary veins are surrounded by an increased number of pericytes. As *Vegf* mRNA expression was mainly seen close to the area where the coronary arteries develop (i.e. close to the trabeculae) in normal mouse embryos, this part of the coronary system is expected to be subjected to high levels of VEGF-signaling due to retention of the larger

VEGF-isoforms in the heparin-containing extracellular matrix and to NP-1-mediated amplification. In the subepicardially located coronary veins, therefore, low VEGF-signaling levels are expected. Due to lack of retention of VEGF120 in the extracellular matrix and lack of NP-1-mediated amplification in *Vegf120/120* mouse embryos, the inverse is likely the case, leading to the coronary pathologies as observed.

Chapter 4 describes the expression patterns of PDGF-A, PDGF-B, PDGFR- α and PDGFR- β during the developing avian heart. We showed that their patterns were linked to epicardial cells and epicardium-derived cells (EPDCs) by making use of pro-epicardial quail-chicken chimeras. A quail pro-epicardial organ (from which the epicardium and EPDCs arise) was placed in the pericardial cavity of a chicken embryo, giving a way to trace the epicardium and EPDCs and determine expression patterns. During cardiac development, PDGF-B and PDGFR- β were expressed by cells contributing to the coronary system (endothelial cells and EPDCs/vascular smooth muscle cells, respectively), while PDGF-A and PDGFR- α -expression was restricted to cardiomyocytes within the heart. In addition, PDGF-B and PDGFR- β were expressed by cardiac nerves and PDGFR- α -expression was obvious in the dorsal mesoderm surrounding the cardinal veins. This implies that PDGF-B/PDGFR- β -signaling is important in epicardial/EPDC and nervous development, while PDGF-A/PDGFR- α -signaling is involved in (posterior heart field-derived) myocardial development.

In Chapter 5, the role of PDGF-B/PDGFR- β -signaling in cardiovascular development is further explored using *Pdgf-b*^{-/-} and *Pdgfr- β* ^{-/-} (knockout) mouse models. *Pdgf-b*^{-/-} mouse embryos showed cardiac malformations, such as underdeveloped atrioventricular valves, hypoplasia of the myocardium and coronary abnormalities, that can be traced back to impaired development of the epicardium/EPDCs. Also, extreme hypoplasia of the cardiac nerves was seen, implying that PDGF-B/PDGFR- β -signaling is important in the neuronal contribution of cardiac neural crest cells to heart development. The *Pdgfr- β* ^{-/-} mouse embryos showed comparable, but less extreme, cardiac malformations, suggesting that partial redundancy of another PDGFR (possibly PDGFR- α) took place. These data, combined with data from literature on *Pdgf-a* and *Pdgfr- α* mutant mouse models, suggest that PDGF-A/PDGFR- α and PDGF-B/PDGFR- β -signaling pathways play complementary roles in 1) cardiac neural crest-contribution to the heart, where PDGF-A/PDGFR- α -signaling is involved in the non-neuronal and PDGF-B/PDGFR- β -signaling in the neuronal contribution, and in 2) posterior heart field contribution, where PDGF-A/PDGFR- α -signaling is involved in the direct contribution of the dorsal mesoderm through the inflow tract of the heart, while PDGF-B/PDGFR- β -signaling indirectly influences posterior heart field-development through its effect on the pro-epicardial organ.

Chapter 6 contains a description of early embryonic lymphatic development in normal and trisomy 16 mouse embryos, which is a mouse model for human trisomy 21, or

Down syndrome. Normally, two jugular lymphatic sacs (JLSs) arise laterally from the internal jugular veins. An area where the abluminal sides of the endothelial layers connect (the lymphatic-venous membrane) is thought to serve as primitive lymphatic drainage site before ingrowth of the thoracic duct. After ingrowth of the thoracic duct, the JLSs reorganize into lymphatic nodes. In trisomy 16 mouse embryos, the JLSs were extremely enlarged and the lymphatic-venous membrane was tortuous and thickened and reorganization of the JLSs was delayed. Also, nuchal edema was observed. The abnormal lymphatic development in trisomy 16 mouse embryos could in a similar way in human trisomy 21 cases lead to nuchal edema which can ultrasonographically be seen as an increased nuchal translucency.

In Chapter 7, the hypothesis that in human fetuses abnormal lymphatic development lies at the base of increased nuchal translucency is further substantiated. In human fetuses with trisomy 21, which showed a substantially increased nuchal translucency, a morphology highly comparable to that of trisomy 16 mouse embryos was seen, including increased size of the JLSs and nuchal edema. In human fetuses with monosomy X, or Turner syndrome, in contrast, no JLSs could be observed at all concomitant with extremely increased nuchal translucency and profuse nuchal edema. Thus, it seems that although both trisomy 21 and monosomy X ultrasonographically present with increased nuchal translucency (which represents nuchal edema), the underlying cause seems to be different, with lack of JLS-development in monosomy X and development of dysfunctional JLSs in case of trisomy 21.

Chapter 8 further explores the underlying causes of dysfunction of the JLSs in both murine trisomy 16 embryos and human trisomy 21 fetuses. Endothelial differentiation-characteristics were investigated and this showed that JLSs of murine trisomy 16 embryos as well as those of human trisomy 21 fetuses lose expression of the lymphatic markers Prox-1 and podoplanin, while they gained (arterial) blood vessel characteristics such as high expression of VEGF and NP-1. In addition, the JLSs gained an abnormally large medial layer and erythrocytes were seen in the lumen of the JLSs in the absence of any open connection between the systemic circulation and the JLSs. The abnormal endothelial characteristics, in combination with the gain of a vascular smooth muscle cell-layer could result in deficit interstitial fluid uptake and impaired lymphatic drainage through the lymphatic-venous membrane, which could lead to nuchal edema. Nuchal edema can subsequently be seen as increased nuchal translucency using ultrasound.

Chapter 9 provides a general discussion of the data presented in this thesis. The role of the VEGF, Notch and PDGF-signaling pathways in several aspects of cardiovascular development is discussed and, where possible, a link with human pathologies is made. Additionally, the correlation between the data on (ab)normal lymphatic development and the current use of ultrasound for prenatal screening for chromosomal abnormalities is discussed.

Samenvatting

In dit proefschrift wordt het effect van Vascular Endothelial Growth Factor (VEGF)- en Platelet-derived Growth Factor (PDGF)-signalering in de embryonale ontwikkeling van het cardiovasculaire systeem onderzocht. Ook is gekeken naar de relatie tussen abnormale lymfatische ontwikkeling en het ontstaan van een verdikte nekplooi, beiden gerelateerd aan VEGF en PDGF.

In Hoofdstuk 1 wordt een algemene introductie gegeven. De embryonale ontwikkeling van de bloedvaten, het hart en de lymfevaten wordt uitgelegd. Het effect van VEGF-, Notch- en PDGF-signalering op deze processen wordt, voor zover momenteel bekend, beschreven.

In Hoofdstuk 2 is het effect van het *Vegf120/120*-genotype in een muismodel op spatiotemporele expressie van *Vegf* mRNA en op hartontwikkeling onderzocht. Dit genotype leidt ertoe dat van het *Vegf*-gen slechts 1 isovorm, namelijk de VEGF120-isovorm, kan worden aangemaakt. Deze isovorm kan niet binden aan de heparine in de extracellulaire matrix en heeft hierdoor een grotere diffusie-capaciteit. Ook kan deze isovorm, in tegenstelling tot de andere (grotere) VEGF-isovormen, niet de krachtige VEGFR-2/NP-1-signaleringscomplexen induceren. Wegens deze specifieke karakteristieken worden in de *Vegf120/120* muizenembryo's een veranderde eiwitgradiënt en veranderingen in lokale VEGF-signaleringsniveaus verwacht. Tijdens de septatiefases van de normale hartontwikkeling werd aangetoond dat het subpulmonale myocard hogere *Vegf* mRNA-niveaus liet zien in vergelijking met de rest van het hart. In mutante muizenembryo's werd een groot aantal apoptotische cardiomyocyten samen met een nog hoger niveau van *Vegf* mRNA, geactiveerde VEGFR-2, Jagged2 en geactiveerde Notch1 in dit gebied gezien. Ook vertoonden de endocard- en mesenchymcellen van de uitstroomkussens een vertraagde afname in expressie van VEGF, VEGFR-2 en geactiveerde Notch1. Tegelijkertijd werd er hyperplasie van de uitstroomkussens gezien, wat een indicatie is voor een verlengde epitheel-mesenchymtransformatie van het endocard van de uitstroomkussens. Deze twee, zeer spatiotemporeel gereguleerde, pathologische processen kunnen leiden tot hypoplasie van de truncus pulmonalis, dextropositie van de aorta en tot een subaortaal ventriculair septumdefect. Deze drie afwijkingen zijn kenmerkend voor de foetale fase van Tetralogie van Fallot.

Hoofdstuk 3 heeft eveneens betrekking op het *Vegf120/120*-muismodel. In dit hoofdstuk wordt de coronairontwikkeling beschreven. In mutante muizenembryo's lieten de endotheelcellen van de coronairarteriën onvoldoende arteriële kenmerken (zoals hoge expressieniveaus van geactiveerd Notch1, Jagged1, Dll4 en ephrinB2 samen met lage expressieniveaus van VEGFR-2, EphB4 en COUP-TFII) zien, terwijl het endotheel van de coronairvenen juist een meer arterieel expressiepatroon vertoonde. Ook hadden de mutante coronairarteriën een onderontwikkelde gladde spiercellaag,

terwijl de coronairvenen omringd waren door een verhoogd aantal pericyten. Omdat *Vegf* mRNA-expressie met name gezien werd in dat deel van het hart waar ook de coronairarteriën zich ontwikkelen (vlakbij de trabeculae) is het te verwachten dat dit deel van het coronairsysteem in normale muizenembryo's een hoge VEGF-signalering vertoont omdat de grote VEGF-isovormen aan de extracellulaire matrix binden en zo zorgen voor een lokaal hoge concentratie VEGF. Ook wordt de signalering versterkt door de vorming van VEGFR-2/NP-1-signaleringscomplexen. In de coronairvenen, die subepicardiaal gelegen zijn, wordt dus een lage VEGF-signalering verwacht. Omdat in de *Vegf120/120* muizenembryo's geen retentie van het eiwit in de extracellulaire matrix plaatsvindt, en omdat de VEGF120-isovorm de VEGFR-2/NP-1-signaleringscomplexen niet kan vormen is het waarschijnlijk dat in deze embryo's het omgekeerde plaatsvindt wat ten grondslag kan liggen aan de coronairafwijkingen die in dit muismodel gevonden worden.

In Hoofdstuk 4 worden de expressiepatronen van PDGF-A, PDGF-B, PDGFR- α en PDGFR- β tijdens hartontwikkeling van de kip beschreven. Door gebruik te maken van pro-epicardiale kip-kwartel-chimeren worden deze patronen gerelateerd aan het epicard en de epicardium-derived cells (EPDCs). Hiervoor werd een pro-epicardorgaan (waarvan het epicard en de EPDCs afgeleid zijn) van een kwartelembryo in de pericardholte van een kippenembryo geplaatst. Op deze manier konden in het kippenembryo de cellen afgeleid van het pro-epicardorgaan gevolgd worden en hiervan expressiepatronen worden beoordeeld. Tijdens de hartontwikkeling werden PDGF-B en PDGFR- β tot expressie gebracht door cellen die bijdragen aan het coronairsysteem (respectievelijk endotheelcellen en EPDCs/gladde spiercellen), terwijl de PDGF-A- en PDGFR- α -expressie in het hart beperkt was tot de cardiomyocyten. PDGF-B en PDGFR- β werden verder ook tot expressie gebracht door de zenuwen in het hart en PDGFR- α -expressie werd ook gezien in het dorsale mesoderm dat grenst aan de cardinaalvenen. Dit suggereert dat PDGF-B/PDGFR- β -signalering belangrijk is in de ontwikkeling van het epicard/EPDCs en de zenuwen, terwijl PDGF-A/PDGFR- α -signalering betrokken is bij (posterior heart field-afgeleide) myocardontwikkeling.

In Hoofdstuk 5 wordt de rol van PDGF-B/PDGFR- β -signalering in hart- en vaatontwikkeling verder onderzocht. Hiervoor werd gebruik gemaakt van *Pdgf-b/-* en *Pdgfr- β -/-* (knockout) muizenembryo's. *Pdgf-b/-* muizenembryo's vertoonden hartafwijkingen, zoals onderontwikkelde atrioventriculaire kleppen, myocardiale hypoplasie en coronairafwijkingen, die gerelateerd kunnen worden aan abnormale ontwikkeling van het epicard en EPDCs. Ook werd een extreme hypoplasie van de zenuwen in het hart gezien, wat impliceert dat PDGF-B/PDGFR- β -signalering ook betrokken is bij de neuronale bijdrage van de cardiale neurale lijstcellen. De *Pdgfr- β -/-* muizenembryo's lieten vergelijkbare hartafwijkingen, maar in ernstigere mate, zien. Dit suggereert dat een andere PDGFR (bijvoorbeeld PDGFR- α) de rol van PDGFR- β tijdens hartontwikkeling deels kan overnemen. Deze data, gecombineerd

met data uit de literatuur over muismodellen die een mutatie in het *Pdgf-a*- of *Pdgfr- α* -gen vertonen, suggereren dat PDGF-A/PDGFR- α - en PDGF-B/PDGFR- β -signalering een complementaire rol vervullen in 1) de bijdrage van cardiale neurale lijst aan hartontwikkeling, waarbij PDGF-A/PDGFR- α -signalering betrokken is bij de niet-neuronale en PDGF-B/PDGFR- β -signalering bij de neuronale bijdrage, en in 2) de bijdrage van het posterior heart field, waarbij PDGF-A/PDGFR- α -signalering betrokken is bij directe bijdrage van het dorsale mesoderm aan de instroomzijde van het hart en PDGF-B/PDGFR- β -signalering bij de indirecte bijdrage door de ontwikkeling van het pro-epicardorgaan te beïnvloeden.

Hoofdstuk 6 bevat een beschrijving van de vroeg-embryonale ontwikkeling van het lymfesysteem in normale en trisomie 16 muizenembryo's. Trisomie 16 in de muis is een model voor humane trisomie 21 (of Down syndroom). Tijdens normale lymfeontwikkeling ontstaan er twee jugular lymphatic sacs (JLSs) lateraal van de venae jugularis interna. Het gebied waar de abluminale zijden van de respectievelijke endotheellagen met elkaar in contact staan (het lymfatisch-veneuze membraan) wordt beschouwd te functioneren als primitieve lymfatische drainage voordat de ductus thoracicus is ingegroeid. Na ingroei van de ductus thoracicus reorganiseren de JLSs naar lymfeknopen. In trisomie 16 muizenembryo's waren de JLS extreem vergroot en was het lymfatisch-veneuze membraan grillig en verdikt. Ook was reorganisatie van de JLSs naar lymfeknopen vertraagd en werd oedeem in de nekregio gezien. De abnormale lymfe-ontwikkeling in trisomie 16 muizenembryo's zou op een vergelijkbare manier in gevallen van humane trisomie 21 kunnen leiden tot oedeem in de nekregio. Dit oedeem kan echoscopisch als een verdikte nekplooi gezien worden.

In Hoofdstuk 7 wordt de hypothese dat abnormale lymfeontwikkeling in humane foetussen ten grondslag kan liggen aan een verdikte nekplooi verder uitgewerkt. In humane foetussen met trisomie 21, die een substantieel verdikte nekplooi laten zien, werd een morfologie gezien die sterk vergelijkbaar is met de morfologie van de trisomie 16 muizenembryo's. Zo werden ook bij de humane trisomie 21 foetussen vergrote JLSs en oedeem in de nekregio aangetroffen. In humane foetussen met monosomie X (Turner syndroom) konden helemaal geen JLSs worden aangetroffen terwijl wel een extreem verdikte nekplooi en zeer veel oedeem in de nekregio gezien werden. Het lijkt er dus op dat, ondanks dat zowel trisomie 21 als monosomie X echoscopisch een verdikte nekplooi (die oedeem in de nekregio representeert) laten zien, de afwijkingen die hieraan ten grondslag liggen anders zijn. De verdikte nekplooi in gevallen met monosomie X kunnen waarschijnlijk verklaard worden door de afwezigheid van JLSs, terwijl in gevallen met trisomie 21 disfunctie van de JLS waarschijnlijk de verdikte nekplooi veroorzaakt.

In Hoofdstuk 8 worden de oorzaken van de disfunctionele JLSs zowel in trisomie 16 in de muis als in trisomie 21 in de mens verder beschreven. De karakteristieken

van endotheeldifferentiatie werden bestudeerd en hieruit kon worden afgeleid dat de JLSs van zowel trisomie 16 muizenembryo's als van humane foetussen met trisomie 21 een verlies van expressie van de lymfatische markers Prox-1 en podoplanin samen met ectopische expressie van (arteriële) bloedvatmarkers VEGF en NP-1 lieten zien. Ook verkregen de JLSs een abnormaal dikke gladde spiercellaag en waren erythrocyten aanwezig in het lumen van de JLSs, terwijl geen verbinding tussen de systeemcirculatie en de JLSs aanwezig was. De abnormale kenmerken van het endotheel, in combinatie met de dikke gladde spiercellaag om de JLSs zou kunnen leiden tot abnormale opname van het interstitiële lymfevocht en tot verstoorde drainage van het lymfevocht door het lymfatische-veneuze membraan. Deze afwijkingen kunnen leiden tot oedeem in de nekregio, wat echoscopisch gezien wordt als een verdikte nekplooi.

Hoofdstuk 9 bediscussieert de data die in dit proefschrift gepresenteerd worden. De rol van VEGF-, Notch- en PDGF-signalering in verschillende aspecten van cardiovasculaire ontwikkeling wordt besproken en er wordt, waar mogelijk, een link naar de humane pathologie gelegd. Ook wordt de correlatie tussen de data over (ab)normale lymfeontwikkeling en het huidige gebruik van echoscopie voor prenatale diagnostiek van chromosomale afwijkingen behandeld.

Curriculum Vitae

Nynke Margaretha Sophie van den Akker was born in Zoeterwoude, The Netherlands, at March 10th 1981. She graduated from the 'Stedelijke Scholengemeenschap Nehalennia Middelburg' in Middelburg in 1998 (Gymnasium). After that, she started her study Biomedical Sciences at the Leiden University Medical Center. During her study, she performed three training periods. The first was carried out at the Department of Nephrology of the Leiden University Medical Center, under supervision of Dr. Cees van Kooten and Dr. Andrea M. Woltman, and was entitled 'Detection of dendritic cells in human renal tissue and the role of GM-CSF produced by proximal tubular epithelial cells on survival and differentiation of dendritic cells in vitro'. Her second training period was performed at the Department of Anatomy and Embryology of the Leiden University Medical Center under the supervision of Prof. Dr. Adriana C. Gittenberger-de Groot and Dr. Monique C. Haak (Department of Gynaecology and Obstetry of the Vrije Universiteit Medical Center, Amsterdam). This training period was entitled 'Lymphatic development in normal and trisomy 16 mouse embryos: relationship with increased nuchal translucency'. She performed her graduation training period, entitled 'Signal transduction of CXC Chemokine Receptor 3 (CXCR3) in human T-lymphocytes', in the Department of Dermatology of the Leiden University Medical Center under supervision of Dr. Cees P. Tensen. She received her Master's degree *cum laude* in January 2003.

Also in January 2003, she started her PhD-project at the Department of Anatomy and Embryology of the Leiden University Medical Center on the role of PDGF in avian cardiovascular development. Due to an outbreak of bird flu in The Netherlands, she started to work with the *Vegf120/120* mouse model, thereby expanding the focus of this thesis. Additionally, she continued to participate in the research on nuchal translucency started during her second training period. The results of these studies are presented in this thesis.

Currently, she is working as a post-doc at the Department of Cardiology of the University Maastricht in the Vascular and Molecular Cardiology Laboratory of Prof. Dr. Johannes Waltenberger.

Rynke

Acknowledgements

Mijn promotietijd was een zeer leerzame en waardevolle tijd. De ondersteuning van veel mensen heeft het gemaakt tot wat het was. Een aantal hiervan wil ik hier in het bijzonder uitlichten.

Ten eerste wil ik mijn collega's van de afdeling Anatomie en Embryologie noemen. Saskia, Conny, Liesbeth vI en Bert wil ik speciaal noemen voor alle hulp op praktisch vlak en Bert nog extra voor het altijd klaarstaan met (on)gevraagd advies. Al mijn mede-AIO's (Marit, Shirin, Bianca, Ismail, Robert, Kim, Fanneke, Liesbeth W, Nathan, Edris, Anton, Noortje, Rebecca en Brigit) waren hoogst belangrijk voor alle wetenschappelijke discussies en support. Ook Leah, Annelies en Sanneke wil ik noemen voor hun inzet in de projecten. Verder een speciale vermelding voor mijn kamergenoot-vanaf-het-begin Heleen; voor het altijd klaarstaan met advies.

For their support in the development of the papers that can be found in this thesis I would like to acknowledge our collaborators Peter Carmeliet (Center for Transgene Technology and Gene Therapy, Leuven, Belgium), Vincenza Caolo, Sanne Verbruggen and Patricia Peters (Department of Physiology, Maastricht, The Netherlands), Maya Nisancioglu, Annika Armulik and Christer Betsholtz (The Vascular Biology Laboratory, Stockholm, Sweden), and Monique Haak, Mireille Bekker, Yolanda de Mooij and John van Vugt (Department of Obstetrics and Gynecology, Amsterdam, The Netherlands).

Mijn paranimfen Eline en Liesbeth: ik waardeer zeer dat jullie me op deze manier willen steunen. Eline, dat jij ook in Leiden woonde tijdens mijn promotie was heel waardevol. Liesbeth, aan de avonden samen schrijven heb ik hele goede herinneringen; heel veel succes met het afronden van jouw promotie met de nodige NVB's.

Elsemieke, Evelien en Linda waren voor mij tijdens mijn studie- en promotietijd heel belangrijk dankzij onze vele (al dan niet) wetenschappelijke gesprekken. Nynke, Catherine, Iris en Anne-Mary noem ik voor hun zachte dwang zoveel mogelijk woensdagavonden vrij te houden. Pauline, de adviezen van een ervaringsdeskundige waren zeer nuttig. Annemarie, jouw diergeneeskundige visie op mijn bezigheden op het lab was vaak onverwacht verhelderend.

Ik zou dit proefschrift niet voltooid kunnen hebben zonder back-up van mijn (schoon)familie en ik wil in het bijzonder mijn ouders bedanken. Mam, jouw kracht van de afgelopen jaren is een groot voorbeeld voor mij. Heel erg bedankt voor alle steun en vertrouwen.

Daniël, alle dingen die wij samen de afgelopen jaren meegemaakt en voor elkaar gekregen hebben zijn niet niks en ik ben heel blij dat ik bij alles jou naast me heb gehad. Dat er maar veel moois samen mag volgen!

List of Publications

Mahtab EA, Wijffels MC, Van den Akker NM, Hahurij ND, Lie-Venema H, Wisse LJ, DeRuiter MC, Uhrin P, Zaujec J, Binder BR, Schalij MJ, Poelmann RE, Gittenberger-de Groot AC. Cardiac malformations and myocardial abnormalities in podoplanin knockout mouse embryos: Correlation with abnormal epicardial development. *Dev Dyn*. 2008, In Press.

Bekker MN, Van den Akker NM, De Mooij YM, Bartelings MM, Van Vugt JM, Gittenberger-de Groot AC. Jugular lymphatic maldevelopment in Turner syndrome and trisomy 21: Different anomalies leading to nuchal edema. *Reprod Sci*. 2008, In Press.

Van den Akker NM, Caolo V, Wisse LJ, Peters PP, Poelmann RE, Carmeliet P, Molin DG, Gittenberger-de Groot AC. Developmental coronary maturation is disturbed by aberrant cardiac VEGF-expression and Notch-signaling. *Cardiovasc Res*. 2008, In Press.

Van den Akker NM, Winkel LC, Nisancioglu MH, Maas S, Wisse LJ, Armulik A, Poelmann RE, Lie-Venema H, Betsholtz C, Gittenberger-de Groot AC. PDGF-B signaling is important for murine cardiac development; Role in developing atrioventricular valves, coronaries and cardiac innervation. *Dev Dyn*. 2008, In Press.

Lie-Venema H, Eralp I, Markwald RR, Van den Akker NM, Wijffels MC, Kolditz DP, Van der Laarse A, Schalij MJ, Poelmann RE, Bogers AJ, Gittenberger-de Groot AC. Periostin expression by epicardium-derived cells (EPDCs) is involved in the development of the atrioventricular valves and fibrous heart skeleton. *Differentiation*. 2008, In Press.

Lie-Venema H, Van den Akker NM, Bax NA, Winter EM, Maas S, Kekarainen T, Hoeben RC, DeRuiter MC, Poelmann RE, Gittenberger-de Groot AC. Origin, fate and function of epicardium-derived cells (EPDCs) in normal and abnormal cardiac development. *ScientificWorldJournal*. 2007;7:1777-1798.

Van den Akker NM, Molin DG, Peters PP, Maas S, Wisse LJ, Van Brempt R, Van Munsteren CJ, Bartelings MM, Poelmann RE, Carmeliet P, Gittenberger-De Groot AC. Tetralogy of fallot and alterations in vascular endothelial growth factor-A signaling and notch signaling in mouse embryos solely expressing the VEGF120 isoform. *Circ Res*. 2007;100:842-849.

Eralp I, Lie-Venema H, Bax NA, Wijffels MC, Van Der Laarse A, DeRuiter MC, Bogers AJ, Van Den Akker NM, Gourdie RG, Schalij MJ, Poelmann RE, Gittenberger-de Groot AC. Epicardium-derived cells (EPDCs) are important for correct development of the Purkinje fibers in the avian heart. *Anat Rec A Discov Mol Cell Evol Biol*. 2006;288:1272-1280.

Bekker MN, Van Den Akker NM, Bartelings MM, Arkesteijn JB, Fischer SG, Polman JA, Haak MC, Webb S, Poelmann RE, Van Vugt JM, Gittenberger-De Groot AC. Nuchal edema and venous-lymphatic phenotype disturbance in human fetuses and mouse embryos with aneuploidy. *J Soc Gynecol Investig*. 2006;13:209-216.

Bekker MN, Arkesteijn JB, Van Den Akker NM, Hoffman S, Webb S, Van Vugt JM, Gittenberger-De Groot AC. Increased NCAM expression and vascular development in trisomy 16 mouse embryos: relationship with nuchal translucency. *Pediatr Res*. 2005;58:1222-1227.

Van den Akker NM, Lie-Venema H, Maas S, Eralp I, DeRuiter MC, Poelmann RE, Gittenberger-De Groot AC. Platelet-derived growth factors in the developing avian heart and maturing coronary vasculature. *Dev Dyn*. 2005;233:1579-1588.

Eralp I, Lie-Venema H, DeRuiter MC, Van Den Akker NM, Bogers AJ, Mentink MM, Poelmann RE, Gittenberger-De Groot AC. Coronary artery and orifice development is associated with proper timing of epicardial outgrowth and correlated Fas-ligand-associated apoptosis patterns. *Circ Res*. 2005;96:526-534.

Gittenberger-De Groot AC, Van Den Akker NM, Bartelings MM, Webb S, Van Vugt JM, Haak MC. Abnormal lymphatic development in trisomy 16 mouse embryos precedes nuchal edema. *Dev Dyn*. 2004;230:378-384.

